Kinetic Studies of Carotenoid Degradation

David Han Yen Wong-Pascua

A thesis submitted in partial fulfilment of the requirements for the degree of Doctor of Philosophy

Department of Chemistry

Durham University

March 2017

Declaration

The work described in this thesis was carried out at the Department of Chemistry, Durham University, between October 2012 and March 2017, under the supervision of Dr. AnnMarie O'Donoghue. The material contained has not been previously submitted for a degree at this or any other university. All work has been carried out by the author unless otherwise indicated.

Statement of Copyright

Abstract

Carotenoids are a diverse family of naturally occurring pigments that are produced by plants, photosynthetic bacteria and certain fungi. Their biological roles within these organisms include the quenching of reactive oxygen species, acting as accessory pigments in photosystems and the colouration of flowers and fruits. Although mammals do not produce carotenoids, they may be obtained through the diet. Numerous health benefits in humans have been found to be associated with carotenoid containing diets, such as the maintenance of cardiovascular health and protection against degenerative eye diseases. These discoveries have led to an interest in ways to increase the stability of carotenoids within foodstuffs. Contrary to the vast majority of studies involving carotenoids, the detergency industry is interested in finding solutions to decolourise carotenoid containing stains. Carotenoid stains are usually composed of oily hydrophobic soils that adhere strongly to fabrics and sequester away from water. Due to the difficulty in complete removal of carotenoid stain material from fabric and the strong colouration of carotenoids, the detergency industry has adopted the approach of making the stain less perceivable through bleaching rather than attempting to eliminate all stain material.

Although processes involved in the oxidative degradation of carotenoids are well established and there are numerous investigations of carotenoid decomposition in foodstuffs, quantitative studies of factors influencing the bleaching of carotenoids under conditions relevant to an aqueous washing environment are scarce. We have performed a quantitative study of the effect of fatty acid, surfactant and pH on the bleaching of β-carotene in oil-in-water emulsions. Experiments were monitored using UV-Vis spectrophotometry and focussed on quantifying initial rates of oxidation of fatty acid (a process closely related to carotenoid oxidative degradation) and the bleaching of β-carotene. Linoleic acid was found to autoxidise faster at lower pH while the bleaching of β-carotene in the presence of linoleic acid was found to proceed more faster at neutral pH. Experiments were performed in the absence and presence of lipoxygenases (LOXs) from soybean. These enzymes promote the bleaching of carotenoids by accelerating the formation of hydroperoxide bleaching species from polyunsaturated fatty acids. LOXs are known to be relatively slow, however, a study in

the literature has reported that a bleaching synergy exists between two isozymes, LOX1 and LOX3. The activities of LOX1 and LOX3 linoleic acid oxidation and β-carotene degradation were quantified and found to be pH and surfactant dependent. Combinations of these enzymes were used to quantified this synergy under a range of conditions.

To complement bleaching experiments in microemulsion solutions, work was performed at P&G Newcastle to investigate factors influencing the bleaching of carotenoid stains on fabrics. Stain decolourisation was quantified by stain removal index (SRI) values obtained by DigiEye. The effect of concentration of linoleic acid and α-tocopherol (a powerful antioxidant) in stain material was found to show correlation with results obtained from solution bleaching experiments and confirmed that the majority of fatty acid dependent bleaching of carotenoids on fabric is reliant on a radical mechanism. A study of the effect of fabric type and treatment discovered that stain removal in the wash was more facile on hydrophilic fabric, however, bleaching of carotenoid stain material after the wash appeared to be faster on hydrophobic materials. In experiments monitoring the bleaching of carotenoid containing microemulsions in the presence of fabric, cotton and polycotton were found to strongly inhibit the bleaching process while polyester slowed the rate but not the extent of bleaching.

A side project, involved the preliminary study of the hydrolysis of triethyloxonium tetrafluoroborate, a commercially available alkylating agent, usually restricted to use in dry organic solvents. Preliminary results showed a pH independent region from pH 2 to 10. A pH dependent region was discovered above pH 10, however, reactions proceeded too rapidly to quantify rate constants. Hydrolysis rate constants were also measured in 50% acetonitrile with rate constants almost identical to those in 100% water.

Table of Contents

Abbreviations

°C	Degree Celsius
µmol	Micromole
Abs	Absorbance
ACO	Apocarotenoid oxygenase
AE	Alcohol ethoxylate
Ala	Alanine
APX	Ascorbate peroxidase
Arg	Arginine
Asn	Asparagine
Asp	Aspartate
CAR	Carotenoids
CCD	Carotenoid cleavage dioxygenases
CCO	Carotenoid cleavage oxygenases
CCP	Cytochrome *c* peroxida
cm	Centimetre
CMC	Critical micelle concentration
CTAB	Cationic Surfactant Hexadecyltrimethylammonium Bromide
DDM	Dodecyl maltoside
DMF	Dimethylformamide
EDTA	Ethylenediaminetetraacetic acid
EPR	Electron paramagnetic resonance
ESR	Erythrocyte sedimentation rate
ATP	Adenosine triphosphate
FB	Free base
g	Gram
Gln	Glutamine
Gly	Glycine
h	Hour(s)
HDL	High density lipoprotein
HeLa	Henrietta Lacks
HGC	Human gastric carcinoma
HI	Hydrophilicity index
His	Histidine
HLB	Hydrophilicity-lipophilicity balance
HPLC	High performance liquid Chromatography
HRPC	Horseradish isozymes C
I	Ionic strength
Ile	Isoleucine
K	Kelvin
Kcal	Kilocalories
kDa	Kilodalton
kg	Kilogram
KIE	Kinetic isotope effect
K_m	Michaelis constant - substrate concentration; rate is half of V_{max}
k_{obs}	Observed-rate constant
LDL	Low density lipoprotein
Leu	Leucine
LIP	Lignin peroxidase
LOX	Lipoxygenase
M	Molar
MCF-7	Michigan Cancer Foundation-7
mg	Milligram
min	Minute
mL	Millilitre
mM	Millimolar
mmol	Millimole
mol	Mole
MW	Molecular weight
nm	Nanometre
PANC	Pancreatic
PCB-150	Peltier Controlled Cryobath
PDB	Protein Data Bank
Phe	Phenylalanine
pK_a	Negative log of acid dissociation constant
PNP	Peanut peroxidase
s	Seconds
SAXS	Small angle X-ray scattering
SCC-25	Squamous cell carcinoma
SD	Standard deviation
SDS	Sodium dodecyl sulphate
Ser	Serine
SRI	Stain removal index
Thr	Threonine
Trp	Tryptophan
Tyr	Tyrosine
UV-vis	Ultraviolet-Visible
v/v	Volume per volume
Val	Valine
VLX	Vegetative Isoform of LOX
V_{max}	Maximal velocity. Rate of enzyme catalysed reaction when system is saturated with substrate
w/w	Weight per weight
ε	Extinction Coefficient
λ_{max}	Wavelengths of maximum absorbance
µg	Microgram
µM	Micromolar
υ	Initial rate

THESIS PART I

CHAPTER 1

Introduction

1.0 Foreword

Pasta sauce, curry, paprika and any other foodstuffs containing derivatives of tomatoes or red peppers are found in the diets of many cultures around the world. A notable component of these foods is a group of highly coloured, natural pigments known as carotenoids such as β-carotene **1**. The presence of carotenoids confers vivid red, orange and yellow shades, a feature exploited by many flora and fauna in Nature and a significant problem when handling carotenoid containing foods. Greasy carotenoid stains are known to penetrate and adhere strongly to materials (especially fabrics and plastics) leaving a constant blemish even after several wash cycles. Owing to the difficulty in complete removal of these stains, the detergent industry has become interested in strategies to selectively bleach the coloured carotenoid pigments within the stain. This pragmatic approach aims to make the stain imperceivable without requiring elimination of stain material.

The aims of this thesis are to quantitatively study the oxidation and subsequent bleaching of carotenoids under a range of conditions including non-enzymatic autoxidation associated with polyunsaturated fatty acids and enzymatic oxidation catalysed by lipoxygenases. This chapter introduces carotenoids, details their important chemical reactions with respect to this project and reviews several existing bleaching strategies.

1.1 Carotenoid structure and properties

At present there are over 700 carotenoid structures that have been discovered.[1, 2] Carotenoids are a subgroup belonging to the isoprenoid class of biological molecules; compounds formed from units of the C5 molecule isoprene. Almost all carotenoids are derived from the colourless compound phytoene, a C40 linear tetraterpene.[3] Successive desaturation steps of phytoene transforms the colourless compound into lycopene **2**, a deep red pigment with 13 double bonds, 11 of which are conjugated. This large conjugated system of alternate carbon-carbon double bonds is the primary feature of carotenoids and confers their characteristic vivid colouration. Hydroxylases, ketolases and cyclases act on the linear backbone to produce a wide variety of compounds typically with ring systems at the termini as found in the carotene and xanthophylls sub-groups. Other common functional groups include hydroxyls and ketones.[4]

Figure 1.1 shows the chemical structures of some common, naturally occurring carotenoids and some UV-vis spectrophotometric data demonstrating the highly coloured property of these molecules.1 Carotenoids are responsible for the colouration of many organisms in Nature: β-carotene **1** is the orange pigment found in carrot, sponges and crustaceans. Lycopene **2** is a red carotenoid found mainly in tomatoes while the red pigmentation of peppers and their derivative paprika is a result of capsanthin **3**. The yellow tint of flour is caused by the carotenoid lutein **4**. Astaxanthin **5** colours salmon, shrimp and algae while canthaxanthin is the pigment found in flamingo plumage and moths. The unusually water soluble carotenoid crocin **6** is found in the flowers of crocus and gardenia.[4] The carotenoids of particular interest in the project are β-carotene **1**, lycopene **2** and capsanthin **3** as β-carotene and lycopene are the predominant carotenoids found in tomato (*Solanum lycopersicum*) based foods while capsanthin is the main carotenoid from red pepper (*Capsicum anuum*) derivatives (Table 1.1). These carotenoids appear as deep red/orange pigments depending on concentration.

Another property of carotenoids, caused by the long unsaturated hydrocarbon backbone, is the extreme hydrophobicity (the terminal sugar groups of crocin **6** make this molecule one of the few water soluble carotenoids). This aspect of carotenoids is significant with respect to stain removal as hydrophobic molecules tend to aggregate with similar molecules such as fats and adsorb more strongly to hydrophobic materials. This results in separation water, the medium that carries cleaning additives and detergents.

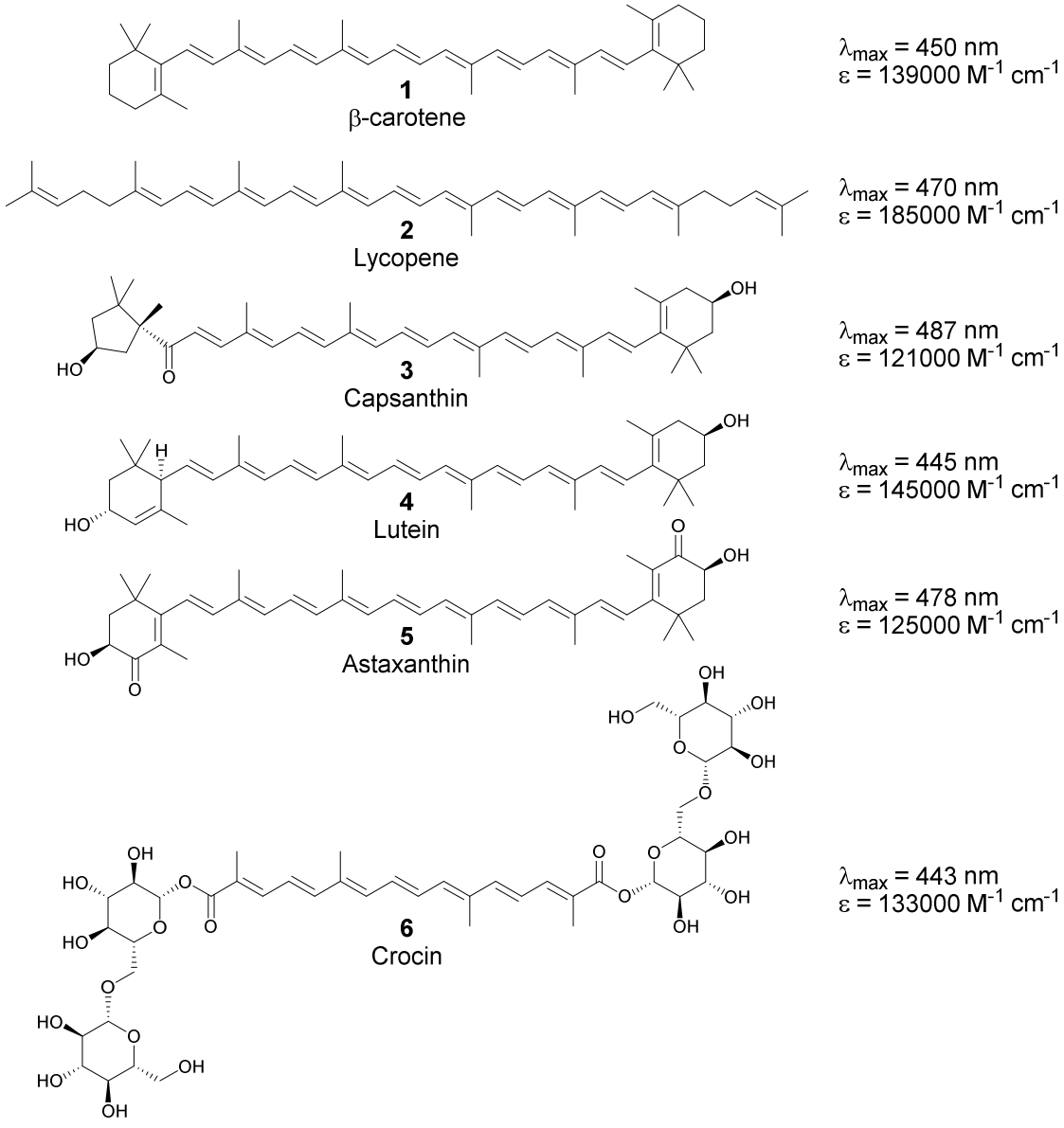

Figure 1.1 Chemical structures and UV-visible spectral data for common carotenoid molecules

Table 1.1 Data tables from analytical studies of carotenoid contents of common foods.[5,6]

Quantity of carotenoid pigments extracted from tomato based foods (mg carotenoid per 100 g food)

	Lycopene	α-Carotene	β-Carotene	γ-Carotene	Neurosporene	ζ-Carotene	Phytofluene	Phytoene	Lutein
Tomato Paste	55.45	-	1.27	9.98	6.95	0.84	3.63	8.36	0.34
Tomato Sauce	17.98	-	0.45	3.17	2.48	0.29	1.27	2.95	trace
Ketchup	17.23	-	0.59	3.03	2.63	0.33	1.54	3.39	-
Tomato Puree	16.67	-	0.41	2.94	2.11	0.25	1.08	2.40	0.09
Spaghetti Sauce	15.99	-	0.44	3.02	3.15	0.34	1.56	2.77	0.16
Tomato Juice	10.77	-	0.27	1.74	1.23	0.18	0.83	1.90	0.06
Vegetable Juice	9.66	0.21	0.83	-	ND	-	0.69	1.71	0.08
Tomato	9.27	-	0.23	1.50	1.11	0.21	0.82	1.86	0.08

Distribution of carotenoid pigments in paprika determined by HPLC (% of total carotenoids)

Capsanthin	β-Carotene	Violaxanthin	Cryptoxanthin	Capsorubin	Cryptocapsin	Zeaxanthin	Antheraxanthin	Capsanthin epoxide
31.7-38.1	11.6-18.6	7.1-9.9	4.2-12.3	6.4-10.3	1.8-5.1	2.3-6.5	1.6-9.2	0.9-4.2

1.2 Carotenoid function in Nature

Carotenoids are present in a wide range of organisms, generated via biosynthetic pathways in many phototrophic and in some non-phototrophic species.[4] Carotenoids are not usually produced by animals, however, they are frequently obtained through the diet leading to the coloration seen in salmon muscle and bird plumage.[7] While pigmentation is possibly the most noticeable feature of the carotenoid family, there are several other important functions that carotenoids provide to organisms. These include structural modification of phospholipid membranes and protection from excess light energy in phototrophic organisms as quenching agents for reactive oxygen species. This protective role is extended to non-phototrophic organisms that may benefit from the chain-breaking antioxidant properties of carotenoids. As a result there has been significant interest in studying the impact of carotenoid containing diets on human health. The various roles of carotenoids in organisms will be discussed further within this section.

1.2.1 Modification of lipid bilayers

The original role of carotenoids has been speculated to involve the control of membrane rigidity.[4] Carotenoids are well suited to this role as the conjugated double-bond backbone is hydrophobic and stiff allowing integration within and reducing the fluidity of phospholipid bilayers. However, more recent studies have suggested more complex carotenoid-membrane interactions arising from the structure of the integrated carotenoid, particularly the presence and position of polar groups, and the orientation of the carotenoid within the lipid membrane.

A spin-label study by Subczynski *et al.* demonstrated that polar carotenoids (dihydroxycarotenoids, zeaxanthin and violaxanthin) increase the ordering and decrease the fluidity of the alkyl chains of membrane lipids helping to maintain membrane structural integrity at higher temperatures. [8] Additionally, regions with carotenoid incorporation possessed greater mobility in polar head groups and increased water

accessibility, decreasing the interaction between charged head groups such as in dimyristoylphosphatidylcholine. The authors suggested that carotenoid function within membranes was to modulate fluidity in prokaryotes, analogous to the function of cholesterol in eukaryotes. Notably, while prokaryotes lack cholesterol in cell membranes, carotenoids have been discovered within the cell membranes of a diverse range of eukaryote animal tissues, prominently in skin and eye, but also nerves and liver.

A study of carotenoids in aquatic mollusc cell membranes by Vershinin, concluded that the primary function was also stabilisation of membrane fluidity.[9] Additional functions of membrane carotenoids were discovered by Mishra *et al.*: carotenoids were found to influence cell membrane rigidity and reduce the interaction with cationic antimicrobial peptides in strains of methicillin susceptible *Staphylococcus aureus*, conferring greater survivability.[10] Studies of the orientation of carotenoids within lipid bilayers of nerve cells have discovered that polar carotenoids such as xanthophylls generally span membranes with polar terminal groups anchored at both external surfaces and influence adjacent acyl chains to adopt similar orientations/tilt leading to local ordering.[11,12] Carotenoid orientation was found to be affected by the membrane potential and extracellular ATP[11] and has been suggested to influence membrane reordering, an effect that may modify the excitability of nerve fibres.[12]

1.2.2 Role in photosynthetic systems

Carotenoids have been discovered to possess two functions within photosynthetic organisms: accessory pigments and photoprotection. As described earlier, the large conjugated system of the carotenoid backbone absorbs light in the range of 450 to 570 nm, a region only weakly absorbed by chlorophylls, the primary photosynthetic pigments. Consequently, many phototrophic organisms utilise carotenoids as accessory pigments in antenna systems to augment light harvesting.[3,13]

Carotenoids are also present in the photosystem reaction centre where they provide protection from excess energy – the low energy triplet state is ideal for quenching singlet oxygen and triplet chlorophyll. [14] Experiments by Foote and Denny employing photosensitised generation of singlet oxygen demonstrated the oxidative protection mechanism of carotenoids.[15]

$$^1O_2 + CAR \rightarrow {}^3O_2 + {}^3CAR \qquad (1)$$

$$^3CAR \rightarrow CAR + heat \qquad (2)$$

The mechanism involves electron exchange energy transfer between singlet oxygen and carotenoid, which generates triplet oxygen and the excited state triplet carotenoid (eq. 1). The triplet state carotenoid is then able to dissipate energy by vibrational and rotational interactions with solvent molecules to reform the ground state carotenoid (eq. 2). Notably, while carotenoids may act as potent quenching agents of reactive oxygen species there is the possibility of chemical reaction, resulting in oxidised carotenoid products.[16] These products are typically less intense in colouration and will be discussed in later sections of this chapter.

In higher plants another key pathway involved in the dissipation of excess light energy are the xanthophyll cycles (Fig. 1.2). One of the known xanthophyll cycles contains three carotenoid pigments that are enzymatically interconverted depending on light conditions. De-epoxidation occurs during light stress to quench excess energy and prevent damage to photosystems while violaxanthin is regenerated by epoxidation in low light conditions.[14]

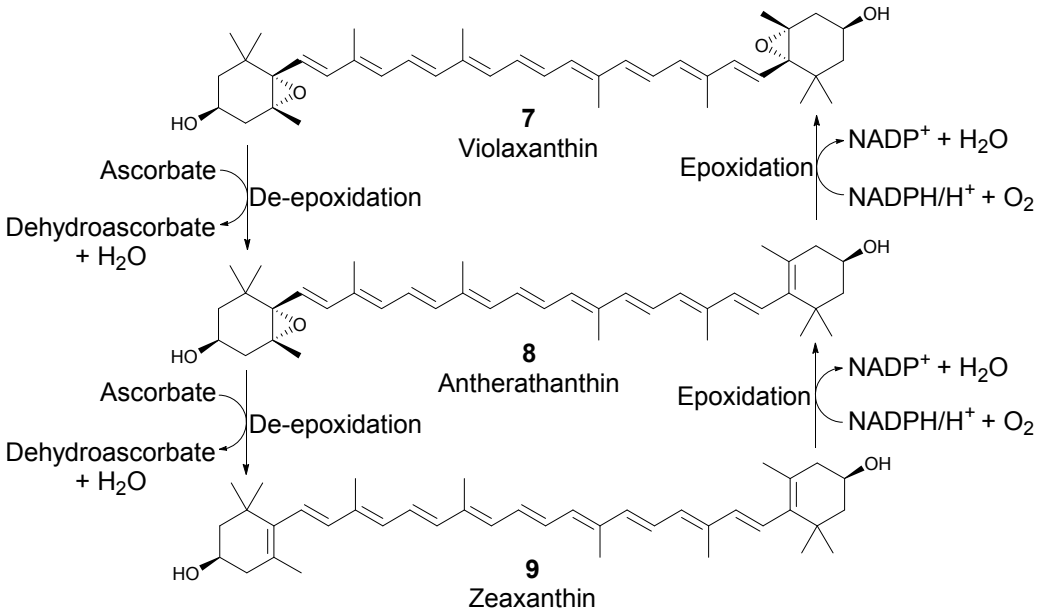

Figure 1.2 The xanthophyll cycle – a core pathway in higher plants allowing for dissipation of high energy during light stress.[14]

In addition to this mechanism, carotenoids have a low oxidation potential allowing them to act as good electron donors. The large conjugated system also stabilises radicals derived from carotenoids. This property facilitates quenching of singlet oxygen and triplet state chlorophyll.[17,18] Recent reviews detail the reactions of carotenoid radicals and their role as accessory pigments and antioxidants.[19,20]

1.2.3 Antioxidant activity and effect on human health

The protective role of carotenoids extends to many non-phototrophic organisms. Many bacteria and other organisms benefit from the photoprotective property of carotenoids possibly accounting for the wide range of caratogenic organisms.[21] Human health benefits of carotenoids are also well-documented in humans, although damaging proxidant (acceleration of oxidation reactions) behaviour, has also been observed in those exposed to cigarette smoke and asbestos.[22] The main health areas that dietary carotenoids are

documented to impact include cancer prevention, maintenance of cardiovascular health and inhibition of certain degenerative eye diseases.

Cancer prevention is an interesting topic as carotenoids have been discovered to have significant influence over the growth patterns of cells. There are numerous papers demonstrating the ability of carotenoids to selectively inhibit or induce apoptosis in tumour cell lines *in vitro* with an implication that dietary carotenoids may act as anti cancer agents *in vivo*. Table 1.2 presents a summary of the findings of several *in vitro* studies on the effect of carotenoids on cell growth.

Table 1.2 Effect of carotenoid treatment on cell growth pattern (summary of results from various studies).

Cell Lines	Carotenoid Treatment	Effect on Cells
		Cell proliferation inhibition (%)
SK-MES lung carcinoma[23]	70 μM β-carotene	70
SCC-25 oral carcinoma		80
Normal human keratinocytes		-10
SK-MES lung carcinoma	300 μM β-carotene	84
SCC-25 oral carcinoma		79
Normal human keratinocytes		-10
GOTO (neuroblastoma), PANC-1 (pancreatic cancer), HGC27 (stomach cancer) and HeLa (cervical cancer) [24]	15 μM palm oil carotenoids (60% β-carotene, 30% α-carotene and 10% other carotenoid	Up to 50% growth inhibition
GOTO (neuroblastoma)	5 μM α-carotene	82% decrease in N-myc mRNA expression and induction of temporary quiescent state
MCF-7 mammary cancer cells[25]	0.75 μM lycopene	Substantial decreases in insulin-like growth factor stimulated proliferation
Primary normal human mammary epithelial cells	7 μM lutein	No significant decrease in cell viability relative to control and reduced apoptosis in the presence of etoposide and cisplatin
MCF-7 human mammary carcinoma cells[26]		Significant decrease in cell viability and no protection against etoposide and cisplatin

The relation of carotenoids to a healthy cardiovascular system is believed to be derived from antioxidant activity[27] as other dietary antioxidants such as vitamins C, E and A have similar effects, such as reductions in high blood pressure, lowered risk of impaired glucose/lipid profile and decreased low density lipoprotein (LDL) oxidation.[28,29] Protection of LDL from oxidation is thought to be a major mechanism by which carotenoids prevent cardiovascular disease. Foam cells within the vascular endothelium have been discovered to more readily uptake oxidised LDL contributing to the development of atherosclerosis lesions.[30] The antioxidant property of carotenoids is expected to be a significant influence in this pathway as LDL is the major transporter of β-carotene and lycopene in the circulatory system.[31] Another related factor in the prevention of atherosclerosis is that carotenoids have been observed to decrease LDL and increase high density lipoprotein (HDL) levels in human and transgenic mice studies.[32,33]

Dietary intake of specifically lutein **4** has been shown to affect macular degeneration and cataracts. These are the only carotenoids found in the human retina[34] and lens.[35] Lutein and zeaxanthin may confer protection against these eye diseases by reducing the amount of damaging light wavelengths to the cells (both carotenoids strongly absorb blue light) and/or by quenching reactive oxygen or hydroperoxide species formed by photo-oxidation of cell lipids.

Due to the health benefits of dietary carotenoids and their ability to inhibit oxidation of other compounds in food such as lipids, food industries strive to incorporate greater amounts of carotenoids into food and ensure their stability.[36] As a result of the greater prevalence of carotenoid foodstuffs, detergency industries have become more interested in strategies to remove stains caused by these foods.

1.3 Carotenoid reaction with radicals

Reactions with radicals are an aspect of carotenoid chemistry important for their role as antioxidants as well as for bleaching studies. Carotenoids are classified as chain-breaking antioxidants – a term derived from their ability to react with radical species and form stable radicals/radical adducts that prevent the propagation of new reactive radicals. Although there are several proposed mechanisms for carotenoid-radical reactions, stabilization of radical products is attributed to resonance effects through the conjugated carotenoid backbone. Reactions with radicals generally involve hydrogen abstraction from the carotenoid (CAR) by the radical species ($R^{\bullet}$) resulting in the formation of a resonance stabilised radical ($CAR^{\bullet}$) (eq. 3). Subsequently, this species ($CAR^{\bullet}$) may terminate by reaction with another radical or reform the original carotenoid (CAR) by reaction with another antioxidant. Reactions of carotenoids with radicals vary depending on conditions as well as the structures of the carotenoid and radical involved.[37] The main mechanisms include electron transfer (eq. 4) forming the radical cation, hydrogen abstraction (eq. 5) affording the neutral radical and addition (eq. 6) generating the neutral adduct.[38] In particular, the hydroperoxyl radicals ($ROO^{\bullet}$) formed as a result of fatty acid or lipid oxidation are common radical species that react with carotenoids.

$$R^{\bullet} + CAR \rightarrow CAR^{\bullet} + RH \quad (3)$$

$$CAR + ROO^{\bullet} \rightarrow CAR^{\bullet+} + ROO^{-} \quad (4)$$

$$CAR + ROO^{\bullet} \rightarrow CAR^{\bullet} + ROOH \quad (5)$$

$$CAR + ROO^{\bullet} \rightarrow ROO\text{-}CAR^{\bullet} \quad (6)$$

Work by Burton and Ingold suggest the reaction of β-carotene with hydroperoxyl radical to be an addition mechanism with the formation of a carbon-centred peroxy-carotenoid radical stabilised by the conjugated double bonds of the carotenoid. Additionally the authors found that β-carotene became a less potent chain-breaking antioxidant at higher

oxygen pressure, thought to be the result of auto-oxidative processes.[39] In peroxidation systems, analysis of products has supported the existence of addition radical intermediates[40,41] as well as neutral carotenoid radicals.[42,43] The suggestion that all three mechanisms occurred in peroxidation systems was made by Woodall *et al.* in their study of various carotenoid structures.[44]

More recent studies using laser flash photolysis or pulse radiolysis coupled with kinetic absorption spectroscopy have suggested that the carotenoid and radical structures and the homogeneity/heterogeneity and polarity of the reaction medium affect the mechanism. Reaction with β-carotene and $CCl_3O_2^{\bullet}$ in a polar medium has been shown to form the carotenoid radical cation and addition radical in a 1:1 ratio while reaction formation of the radical cation was less likely in non-polar medium.[45] The same reaction conducted in water:*tert*-butanol (1:1) studied using pulse radiolysis suggests a cation radical intermediate[46] while later studies performed in micelles detected two species, identified as the cation radical and the CCl_3O_2-β-carotene$^{\bullet}$ adduct.[47]

1.4 Carotenoid oxidative degradation and bleaching

In carotenoid-containing materials, oxidative degradation as a result of interaction with oxidised fatty acid components is well documented.[48,49] The initial step is oxidation of polyunsaturated fatty acid to hydroperoxide radical which may occur through the process of autoxidation (shown in Fig. 1.3 for linoleic acid **10**).[50]

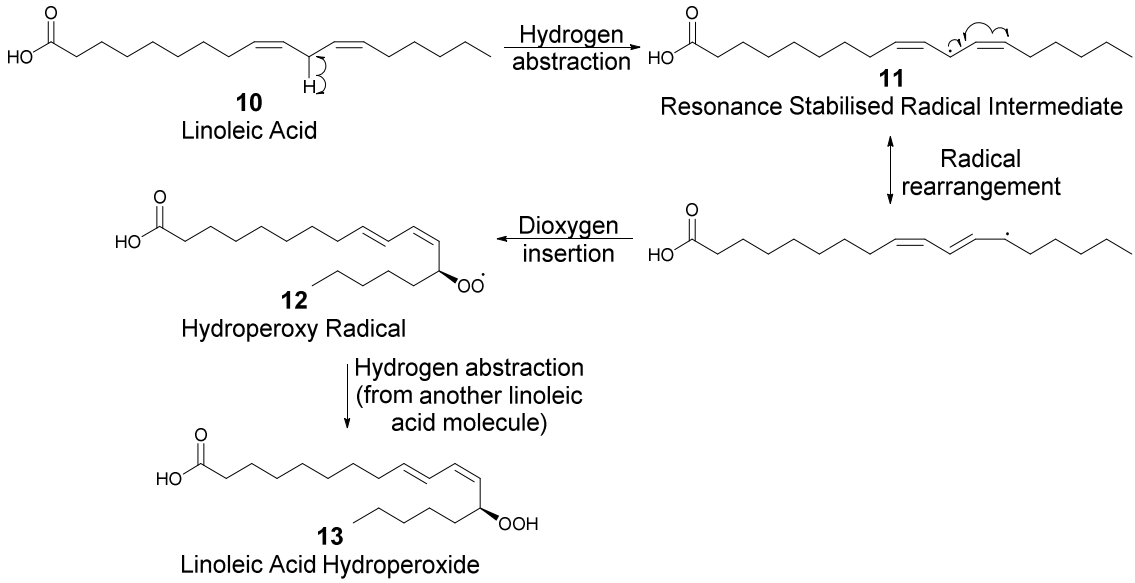

Figure 1.3 Autoxidation of linoleic acid **10** to hydroperoxide **13**

The radical hydroperoxide species is the active bleaching compound and initially reacts with carotenoid as described in the previous section. A subsequent oxidative cleavage reaction occurs that truncates the carotenoid molecule into smaller apo-carotenoids and epoxy products (Fig. 1.4). The mechanisms involved in oxidative degradation of carotenoids are yet to be determined, however products of this reaction with β-carotene and linoleic acid were thoroughly examined in a study by Wu *et al.* showing a wide range of cleavage products at early stages of the reaction, followed by conversion to smaller cleavage products and carotenoid bleaching as time progressed.[51] The authors suggested that fatty acid hydroperoxide radicals attack randomly along the carotenoid chain forming smaller apo-products (species **14-16** for example) that may react further with radical species. The result of successive reactions of oxidative cleavage is that the original, highly

conjugated carotenoid molecule is converted to smaller less conjugated cleavage products. The reduction in conjugation leads to less absorbance in the visible region effectively causing bleaching.

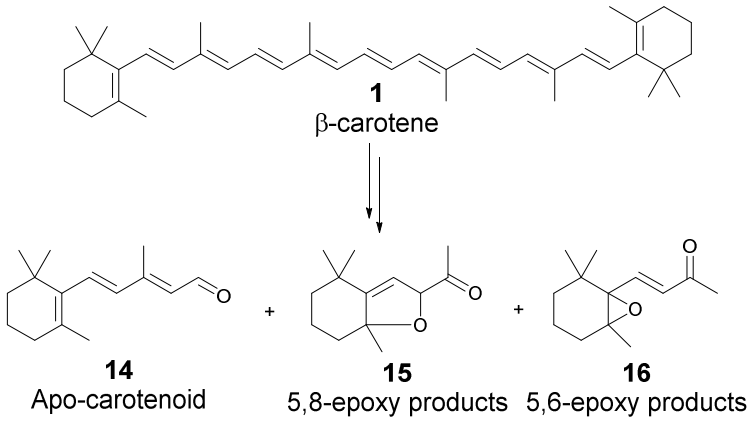

Figure 1.4 Oxidative cleavage of β-carotene **1** to representative degradation products **14-16** resulting in bleaching.

Investigation into the oxidative conversion of polyunsaturated fatty acids to hydroperoxides and the subsequent oxidative cleavage of carotenoid could provide a potentially elegant solution to carotenoid bleaching. Carotenoid containing foods, especially oily foods, typically contain appreciable amounts of polyunsaturated fatty acid which could be oxidised to carotenoid bleaching species.[52,53] Conveniently, both fatty acids and carotenoids are hydrophobic molecules meaning they will localise in the same areas of the stain/fabric, allowing for selective bleaching. Another aspect is that polyunsaturated fatty acids are the substrate for the oxidative enzymes lipoxygenases, presenting the possibility for enzyme catalysed formation of bleaching agent.

1.5 Carotenoid bleaching enzymes

While autoxidation may be a concern for long term storage of carotenoid containing foods, the process is likely to be too slow to completely bleach carotenoid stains over the duration of a wash and dry laundry cycle. A possible solution is the application of enzymes to increase rates of bleaching. Reaction schemes of several enzymes (lipoxygenases, peroxidases laccases and carotenoid cleavage dioxygenases) that produce carotenoid bleaching agents or directly catalyse carotenoid degradation are shown in Fig. 1.5.

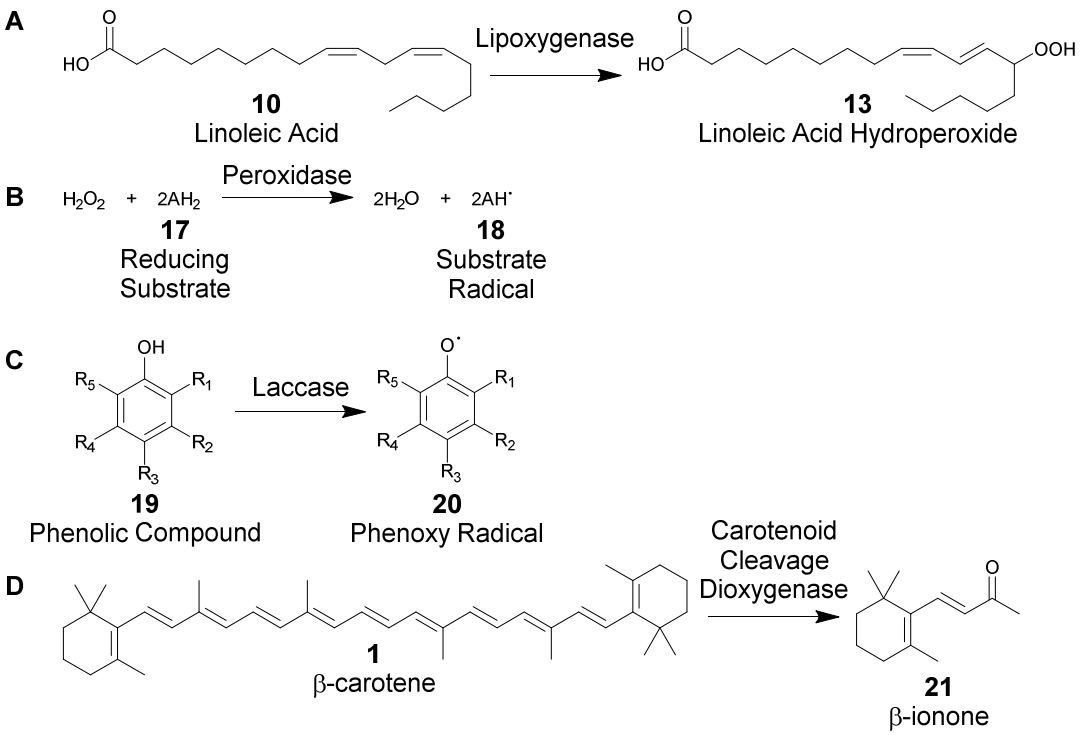

Figure 1.5 Enzyme catalysed generation of radical bleaching species by lipoxygenases, peroxidase and laccase, and representative direct carotenoid oxidative cleavage by carotenoid cleavage dioxygenase.

1.5.1 Lipoxygenases

Lipoxygenases (Fig. 1.5 A) are dioxygenase enzymes that catalyse the conversion of polyunsaturated fatty acids, such as linoleic acid, to hydroperoxides by insertion of molecular oxygen at the terminal end of a 1,4-pentadiene system.[54] These hydroperoxides subsequently react with carotenoids to form oxidative cleavage products. The mechanisms and reaction pathways of lipoxygenase catalysed carotenoid degradation are similar to autoxidation with the lipoxygenase system benefitting from an accelerated formation of bleaching species. Surprisingly, lipoxygenases from soybean flour have been utilised in baking for more than a century to bleach lutein within dough to obtain whiter bread, however these enzymes have yet to be applied in detergency. Additionally, while linoleic acid hydroperoxidation and carotenoid cooxidation activity measurements of lipoxygenases in aqueous solutions exist in the literature[55,56,57] there are few quantitative studies of the effect of surfactant, pH and presence of multiple isoforms. A possible limitation of lipoxygenases is that enzymatic bleaching rate constants are only a few orders of magnitude larger than those for background autoxidation. One solution to this restriction may be the exploitation of a reported bleaching synergy between two isozymes of lipoxygenase from soybean – lipoxygenase 1 (LOX1) and lipoxygenase 3 (LOX3).[58] These two enzymes are the main focus of enzymatic bleaching studies in the project and will be discussed in further detail in Chapter 3.

1.5.2 Peroxidases

Peroxidases are enzymes that catalyse the oxidation of a variety of organic substrates and dyes utilising hydrogen peroxide or an equivalent compound such as fatty acid hydroperoxide (Fig. 1.5 B).[59] Oxidation of particular substrates can result in striking changes in colour and is the basis of peroxidase markers in biochemical applications.[60] Peroxidases have been discovered to be involved in a wide range of physiological pathways including lignifications, cell wall cross-linking, pathogen resistance and plant hormone metabolism.[61]

Horseradish peroxidase, the most well studied peroxidase, features a haem iron prosthetic group and utilises hydrogen peroxide as the final electron acceptor in oxidation reactions of substrates (the overall reaction is shown in eq. 7).

$$2ROH \quad + H_2O_2 \rightarrow 2RO\bullet + 2H_2O \qquad (7)$$

The catalytic cycle of haem peroxidase is shown in eq. 8-10 and Fig. 1.6. The initial step of the peroxidase cycle is oxidation of the ferric haem group by peroxide to form an oxyferryl centre and porphyrin π-cation radical known as compound I ($Fe^{4+}OP\bullet^{+}$). The resting ferric state is regenerated by two successive single electron reduction steps with substrate. The porphyrin radical is reduced first, yielding compound II ($Fe^{4+}OP$), followed by the oxyferryl centre.[62]

$$Fe^{3+}P + H_2O_2 \rightarrow Fe^{4+}OP\bullet^{+} + H_2O \qquad (8)$$

$$Fe^{4+}OP\bullet^{+} + ROH \rightarrow Fe^{4+}OP + RO\bullet \qquad (9)$$

$$Fe^{4+}OP + ROH \rightarrow Fe^{3+}P + RO\bullet + H_2O \qquad (10)$$

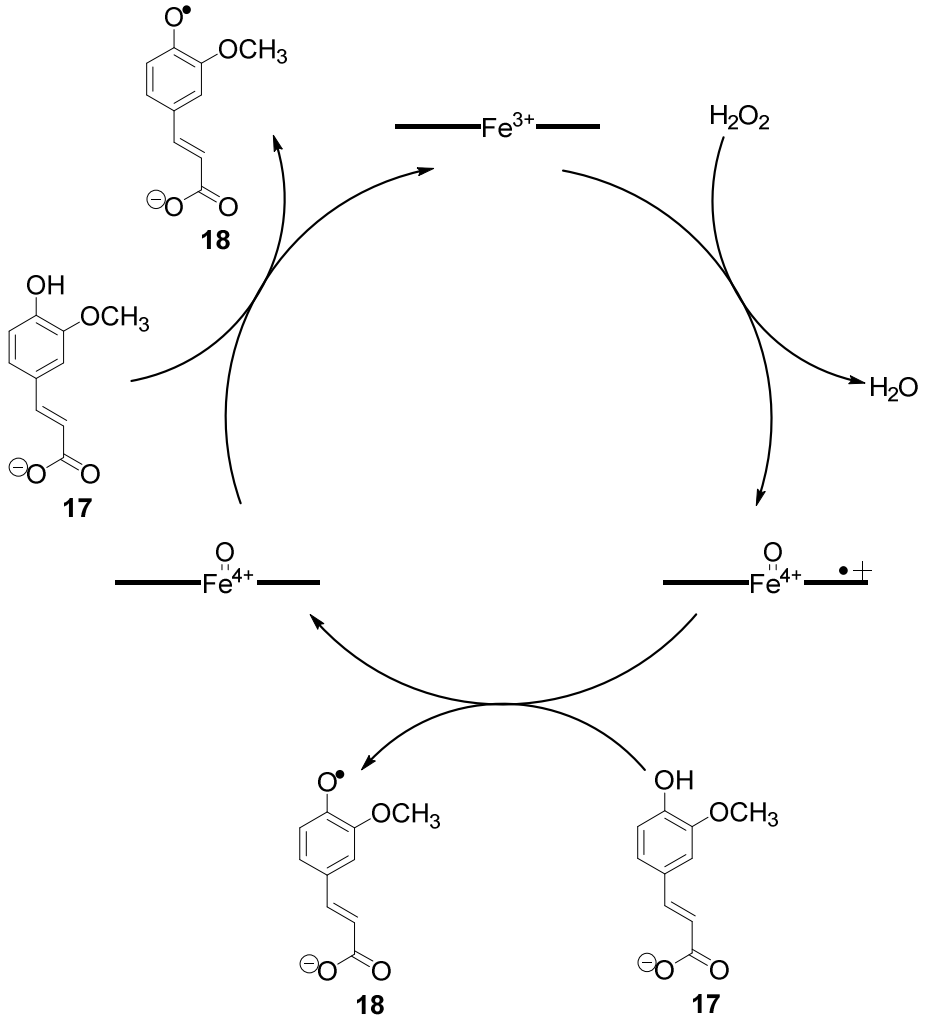

Figure 1.6 Heme peroxidase catalytic cycle [61]

The haem peroxidase family is subdivided into three categories: class I feature intracellular peroxidases found in the cytosol (or chloroplasts) of plant, fungi and bacteria; class II are secretory fungal peroxidases; and class III are secretory plant peroxidases. Most haem peroxidases possess a single non-covalently bound haem and constitute a single polypeptide chain of approximately 300 residues. The crystal structures of several peroxidases have been solved including yeast cytochrome *c* peroxidase (CCP) and pea cytosolic ascorbate peroxidase (APX) class I peroxidases, four fungal peroxidases from class II, and horseradish isozymes C (HRPC) and peanut peroxidase (PNP) of class III.

Haem peroxidases are predominantly alpha-helical proteins of similar fold. Structural comparisons of peroxidases between classes revealed that the ten helices, A-J, are found in similar positions and there are thirteen structurally conserved regions.[63,64] Key differences between class III peroxidases and the other classes are the addition of helices D', F' and F'' to the core peroxidase fold and a long insertion between helices F and G. A disulfide bridge maintains the structure of this additional insertion. Fig. 1.7 shows cartoon diagram structures of class I (CCP), class II (LIP) and class III (PNP) peroxidases with alpha helical structures highlighted in either blue or green and ligands in red. Alpha helices A-J are highlighted in blue in all diagrams. Alpha helix B' (top of both CCP and LIP) is also coloured blue. The characteristic additional class III peroxidase helices, D', F' and F'' are highlighted in green in PNP. The haem prosthetic group is shown as the red ball and stick model located near the centre of each

CCP (4A71)

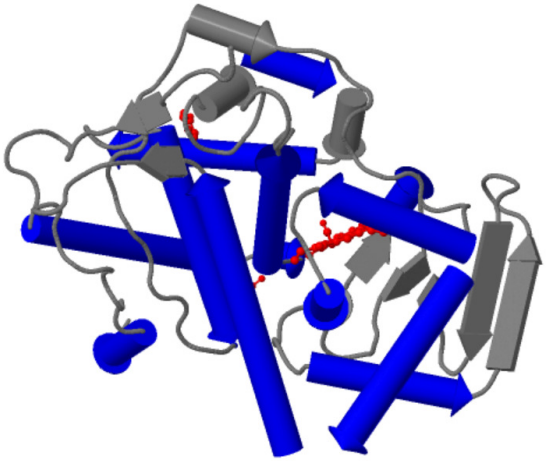

LIP (3M5Q)

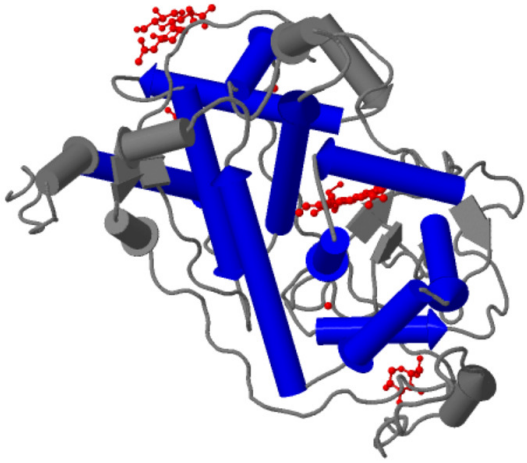

PNP (1SCH)

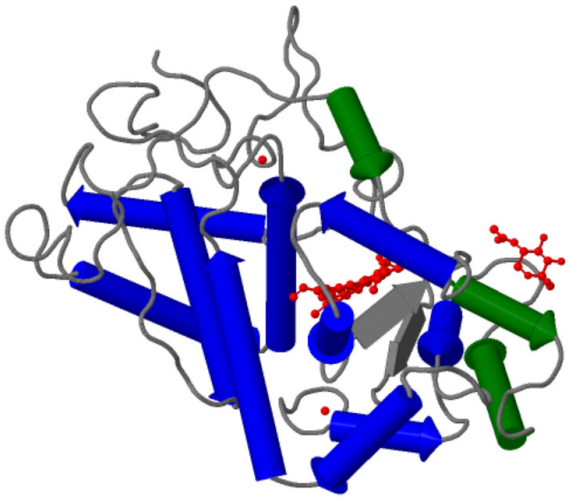

Figure 1.7 Cartoon rocket diagrams of yeast cytochrome c peroxidase (CCP), lignin peroxidase from *P. chrysosporium* (LIP) and peanut peroxidase (PNP). Alpha helical structures are coloured blue or green (blue = helices A-J and B', green = D', F' and F'') and ligands in red ball and stick models. The haem group is located in the centre of each diagram. Diagrams created using JSmol and PDB entries (accession codes in brackets).

The key features of the haem environment appear to be mostly conserved between the different classes. In HRPC, His 170 is the proximal haem ligand and is covalently bonded to the haem iron as found in the crystal structures of haem peroxidases. His 170 is hydrogen bonded to Asp 247 through the Nδ1 atom resulting in an increased basicity relative to the globins.[63] This is a characteristic feature of the peroxidase haem site and aids in the stability of the high oxidation intermediates and maintenance of the five-coordinated haem state. The propionate moieties of the haem unit are directly hydrogen bonded to residues Gln 176, Ser 73, Ser 35 and Arg 31.

An analysis of haem containing oxygenases and peroxidases, including cytochrome P450, highlights the importance of protein structural environment that gives rise to the differing oxidation reactions.[65] Horseradish peroxidase was noted to possess features that facilitate O-O bond cleavage of peroxide such as a charged, polar haem environment and an axial imidazole ligand. Electron transfer reactions are also promoted by the presence of an exposed haem edge while oxo transfer reactions are inhibited by the relatively low accessibility of the haem iron. These features are in marked contrast with the haem iron of cytochrome P450: a highly non-polar environment with a buried haem edge but accessible haem iron. Cytochrome P450 enzymes instead catalyse oxo transfer rather than peroxidase electron transfer reactions.

The substrate access channel of HRPC possesses a flexible, hydrophobic region accessible to solvent that acts as an aromatic donor binding region. Hydrophobic residues (Phe 68, Phe 142 and Phe 179) are also present at the exposed haem edge.[66] The external section of the substrate channel of class III peroxidases are thought to have a hydrophobic nature for interaction with aromatic substrates, however peroxidases have been recognised to perhaps be lacking a conventional binding site for specific substrates: the substrate channel of CCP, APX and PNP are wide open and peroxidase substrates exhibit poor Michaelis-Menten kinetics, suggesting that a typical, tight enzyme-substrate complex is not formed.[64]

In industry, peroxidases have found an application in the removal of phenol from aqueous solution by conversion to the phenoxy radical followed by polymerisation and precipitation.[67] In addition to this peroxidases may have greater roles in the treatment of water supplies in the future. Degradation of dyes from the effluent discharge of textile and dye industries by microbial treatment is currently ongoing and includes studies of several peroxidase producing fungi and the effectiveness of immobilised peroxidases.[68,69]

Several studies have also reported the involvement of peroxidases in carotenoid degradation. Decomposition of lutein in senescent plant leaves[70] and the cleavage of β-carotene and other carotenoids to flavour compounds (**21, 22, 23 and 24**) by fungal peroxidases[71,72] are a few examples (Fig. 1.8). Notably, these studies do not have rate measurements for the degradation of carotenoids. While peroxidases may be effective at degrading carotenoids in their host systems a significant difficulty that may be encountered when utilising these enzymes *in vitro* is a source of hydrogen peroxide. Hydrogen peroxide or equivalent compounds are not stable in liquid formulations and may also act as non-specific bleaching agents. Furthermore, the bleaching activity of peroxidases may not be specific to carotenoids.

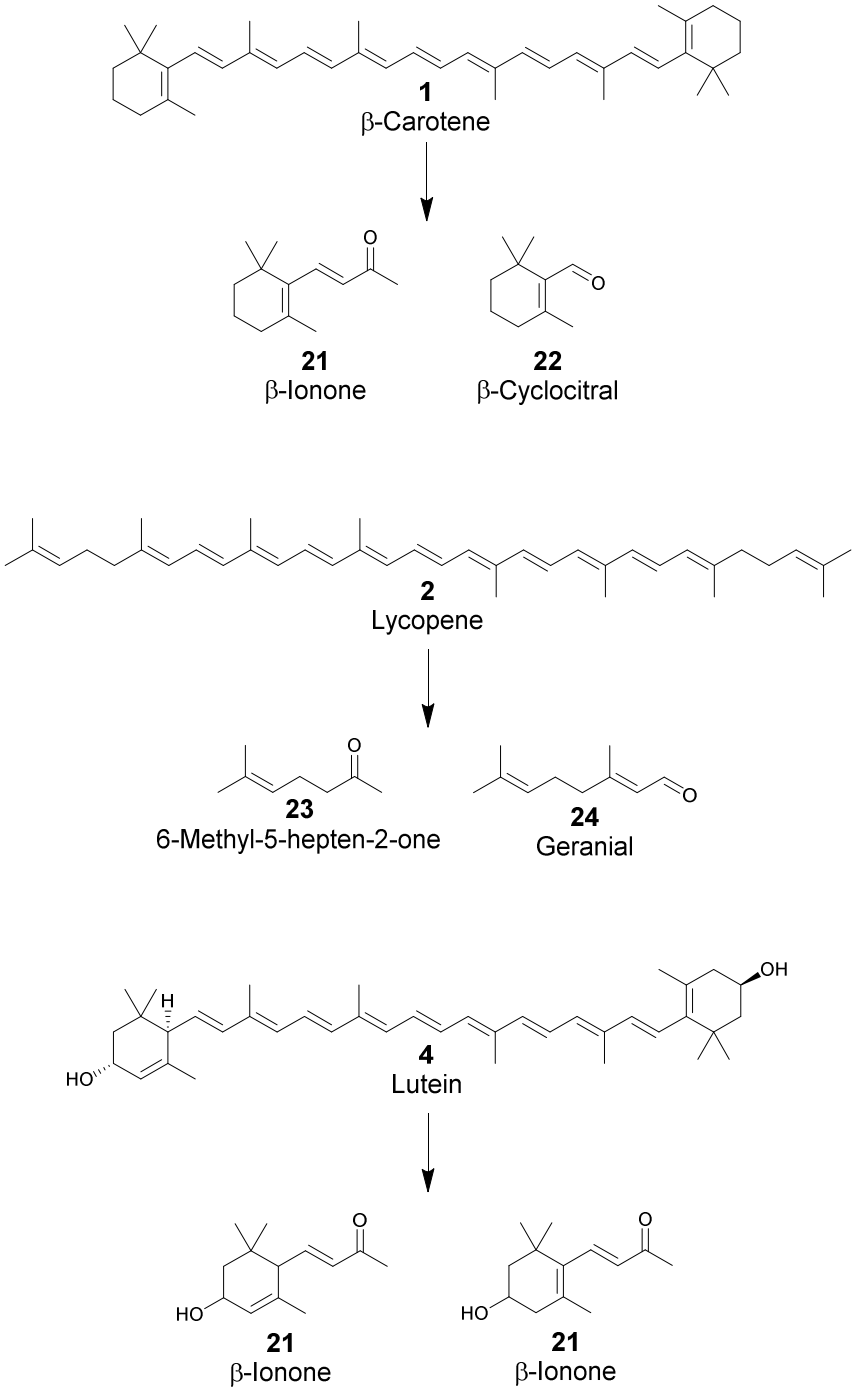

Figure 1.8 Oxidative cleaveage of carotenoids to flavour compounds catalysed by *M. scorodonius* peroxidase.[71]

1.5.3 Laccases

Laccases are multicopper oxidase enzymes that catalyse the conversion of specific phenol compounds to phenoxy radicals as shown in Fig 1.5 C.[73] Laccases are widely distributed in plants, fungi and bacteria and have a broad range of functions that are categorised into three general divisions: monomer cross-linking, polymer degradation and ring cleavage of aromatic compounds.[74,75] In Nature they have been discovered to have many, diverse roles dependent on the host organism. In plants, laccases are responsible for wound healing, iron oxidation and lignifications,[76,77] while in fungi they are involved in delignification, pathogenesis, pigmentation and the formation of fungal fruiting bodies.[78,79,80] Associated pathways in bacteria include biosynthesis of endospore coat proteins and the formation of melanin.[81,82]

Laccases function as either dimeric or tetrameric glycoproteins with each monomer typically containing four copper atoms that may occupy three different copper centres: Type-1 (blue), Type-2 (normal) and Type-3 (binuclear coupled).[83] These copper centres differ in bound ligands and can be differentiated by spectroscopic properties. Copper atoms in Type-1 centres are coordinated to two histidines, a cysteine and methionine, and possess an intense absorbance band centred around 600 nm (deep blue colouration); the ligands in Type-2 are two histidines and water; and Type-3 copper has three histidines and a hydroxyl ligand.[84] Type-2 and -3 copper centres do not absorb strongly in the visible spectrum but can be differentiated by Type-2 being electron paramagnetic resonance (EPR) active and Type-3 being EPR silent.

The monomer structures of plant, fungal and bacterial laccases have been predicted to be composed of three cupredoxin-like domains that are sequentially arranged (domains 1,2 and 3, coloured blue, green and purple respectively in Fig. 1.9). These domains consist of β-sheets and β-strands in a sandwich conformation that forms β-barrel structures.[85] In bacterial laccases, domain 1 within the N-terminal region, differs significantly in conformation to domain 1 found in plants and fungi. Other differences include a coiled section connecting domains 1 and 2, and a large exterior loop region linking domain 2 and

3. In contrast, fungal and plant laccases domains are connected by α-helical segments; the link between domain 2 and 3 is also internal.[82] Domain 1 and 3 contain the catalytic copper centres (brown spheres in Fig. 1.9) while domain 2 acts as a bridging unit.[86] Type-2 and -3 copper sites (tri-nuclear copper cluster) are found at the interface between Domain 1 and 3 with coordinating residues from both domains (shown in the centre of both diagrams in Fig. 1.9). The Type-1 copper site (mononuclear copper) and putative substrate binding site are both located near the surface of Domain 3 (shown as the single copper site positioned at the side of the purple domain in both diagrams in Fig. 1.9).

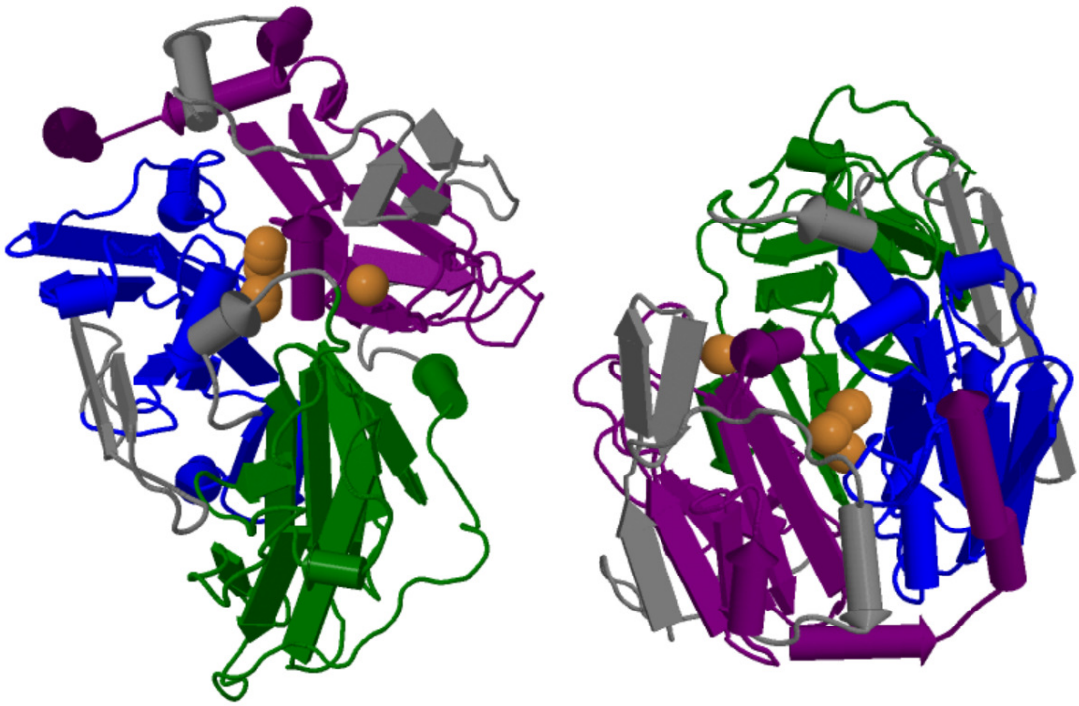

Figure 1.9 Cartoon rocket diagrams of fungal (*Steccherinum murashkinskyi*) laccase from front (left) and top (right). Cupredoxin-like domains are coloured, blue: domain 1, green: domain 2 and purple: domain 3 while coppers are coloured brown. Diagrams created using JSmol and PDB entry (accession code 5E9N)

Similar to peroxidases described earlier, laccases catalyse the oxidation of a range of substrates, however, laccases utilise oxygen as the final electron donor instead of peroxide. In the overall reaction, laccase performs four single electron oxidations of substrates and donates these electrons to molecular oxygen (eq. 11). [87]

$$4RH + O_2 \rightarrow 4R\bullet + 2H_2O \qquad (11)$$

The process is generally described as proceeding through three major steps (Fig. 1.10). The initial step is reduction of Type-1 copper by substrate. This is followed by internal electron transfer from the reduced Type-1 copper to the Type-2-Type-3 trinuclear cluster. Molecular oxygen is then reduced to water at the Type-2-Type-3 site.[79,88]

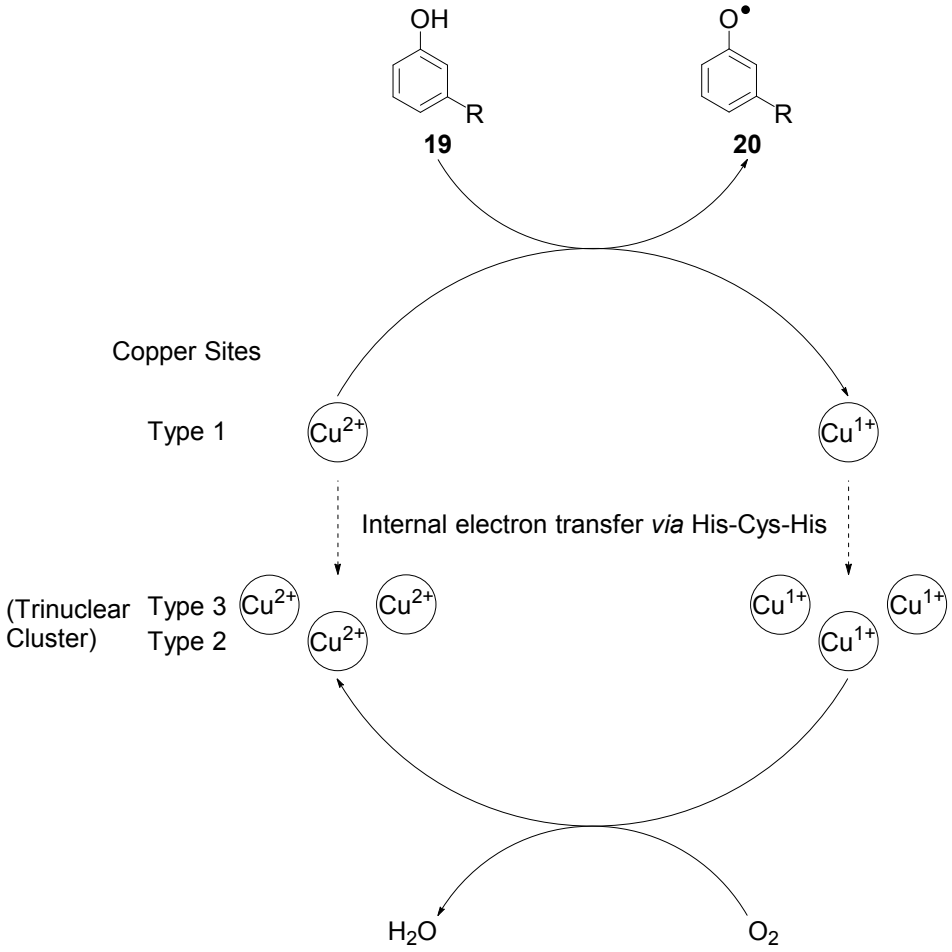

Figure 1.10 Laccase catalytic cycle. Monomeric radical species **20** may polymerise as observed in lignin forming reactions catalysed by laccase.

The ability of laccase to catalyse several reactions such as oxidation, polymerisation and cleavages, and act upon a wide variety of substrates (in particular, phenolic compounds, **19**) has led to studies of their potential application in many industries. [89] Laccase oxidation is capable of degrading natural and synthetic lignin polymer[90] and has found use in the delignification of lignocellulosic material for production of higher quality ruminant feed,[91] the generation of fuels through fermentation[92] and the production of paper (biopulping and biobleaching).[93] Notably, the conventional methods in these industries involve mechanical and/or chemical processing which requires greater energy expenditure and produces toxic effluent. Similarly, in the textile dye bleaching industry, laccases have been found to be a

potentially greener alternative to those employing chemical oxidants such as hypochlorite.[94]

Several medicinal applications have also been discovered for laccases including catalysis of the formation of aromatic aldehydes, flavonoids and heterocyclic compounds facilitating the production of cosmetics and pesticides,[95] while laccase-based products such as hair dyes and skin lightening cream have been developed.[96,97]

The bleaching ability of laccases has been documented in fabric studies of the oxidation of flavonoids in cotton.[98,99] Although laccases may have the potential to bleach carotenoids on fabrics a major issue is that bleaching may not be specific to carotenoids. In response to this problem there is ongoing research into the development/isolation of laccases fused with a carotenoid binding peptide to enhance specificity.[100]

1.5.4 Carotenoid Cleavage Dioxygenases

Carotenoid cleavage dioxygenases (CCD) are a family of non-heme iron containing enzymes that oxidatively cleave carotenoids at specific positions to generate many important apocarotenoid products such as the chromophore retinal, the hormone abscisic acid and the volatile compound β-ionone used by plants to attract insects.[101] This enzyme family is also referred to as carotenoid cleavage oxygenases (CCO) as the catalytic mechanism (monooxygenase vs dioxygenase) is still debated.

Through sequence alignment and genomic sequencing, a large number of CCDs have been discovered in plants, mammals and micro-organisms. The biological function of CCDs varies widely within each organism (Fig. 1.11). In plants, the rate determining step for the production of abscisic acid **28** is oxidative 11,12-cleavage of 9'-*cis*-neoxanthin **25** by the CCD enzyme 9'-*cis*-epoxycarotenoid cleavage dioxygenase. The resulting apocarotenoids

are C25 and C15 aldehydes. The C15 aldehyde, xanthoxin **26**, undergoes further reactions to abscisic acid aldehyde **27** which is subsequently transformed into abscisic acid **28**, a plant hormone involved in drought tolerance and seed dormancy.[102,103] In mammals, β-carotene-15,15'-dioxygenase catalyses the symmetrical oxidative cleavage of β-carotene **1** to two molecules of retinal **29**, a form of vitamin A that is essential for vision.[104,105]

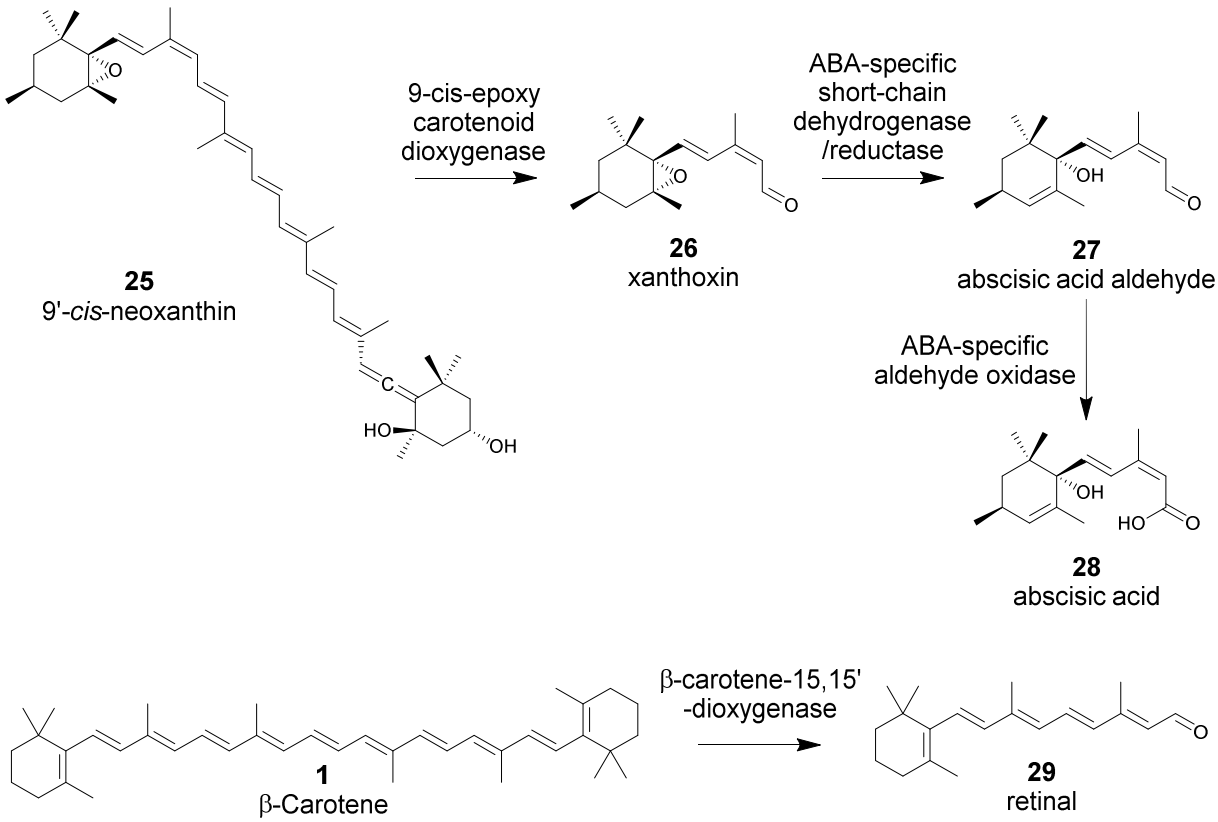

Figure 1.11 Biosynthesis of abscisic acid in plants and retinal in mammals.[102,104]

Debate over the mechanism of CCDs is due to conflicting reports from several studies. An early labelling study of the abscisic acid pathway employing $^{18}O_2$ reported almost complete incorporation at the carboxylic acid position in the turgid leaves of several investigated plants. In stressed leaves and plant tissue, however, singly labelled abscisic acid was far more abundant.[106] *In vitro* studies of CCD1 from *A. thaliana*, also utilising

$^{18}O_2$, reported complete label incorporation in products,[107] while a similar study with mammalian β-carotenoid 15,15'-oxygenase found approximately 50% incorporation of the $^{17}O_2$ label.[108] Observations of less than complete label incorporation have been suggested to be a result of aldehyde products exchanging with unlabelled water.

At present, there is no direct experimental evidence for specific CCD substrate intermediates formed during catalysis. Despite the lack of mechanistic data, the oxidative cleavage mechanism of CCDs has been suggested to be similar to other non-heme iron containing dioxygenases/monooxygenases (Fig. 1.12).[109] Based on the mechanism of extradiol catechol dioxygenases and 2-oxoglutarate-dependent dioxygenases a potential mechanism has been proposed, beginning with activation of coordinated molecular O_2 by single electron transfer from the non-heme Fe^{2+}.[110,111] This is followed by radical reaction with carotenoid substrate at the polyene backbone and single electron transfer to the Fe^{3+} forming a resonance stabilised substrate cation. The products are formed after nucleophilic attack of the cationic substrate by water, a Criegee rearrangement, quenching of the cationic substrate by Fe^{2+} hydroxide and breakdown of the intermediate. Another proposed mechanism from the cationic substrate to aldehyde products is via a 1,2-dioxetane intermediate.

A potential monooxygenase mechanism involves the formation of an epoxide after CCD oxidation utilising only one atom of molecular oxygen. Nucleophilic attack by water forms an α,β-diol. This intermediate, however would then require a further oxidation step for conversion to the aldehyde products.[109]

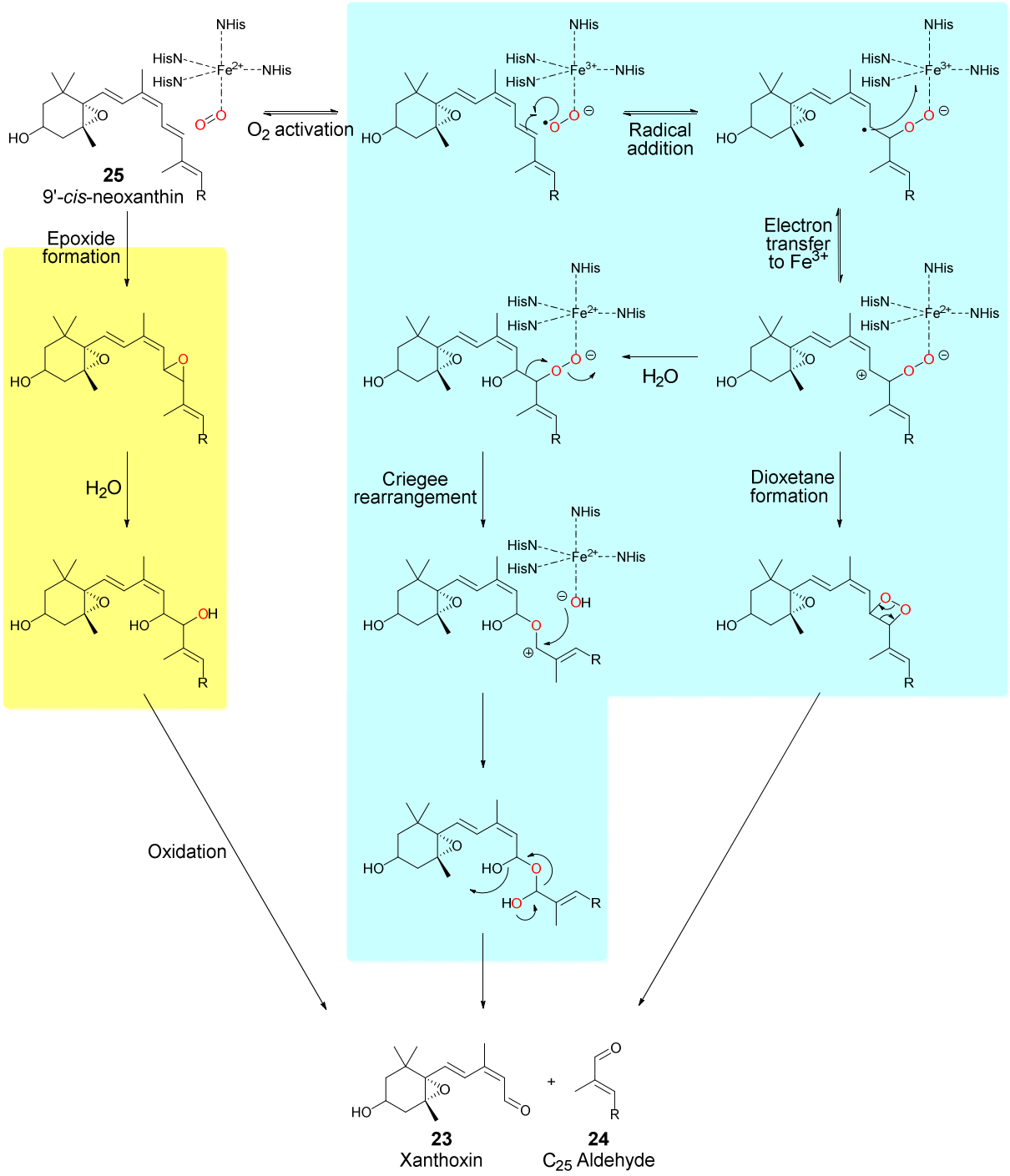

Figure 1.12 Proposed mono-oxygenase and dioxygenase pathways for CCDs.[109]

Analysis of the structures of characterised CCDs, as well as sequence alignments of known CCDs, reveal that overall amino acid sequence identity within the family is variable, though there are highly conserved regions. For example, the catalytic iron is coordinated to four histidine residues (shown as ball and stick models in bottom diagram of Fig. 1.13) and the second shell of the active site contains three glutamate residues.[112,113,114] Both the chelating histidines and second shell glutamates are completely conserved. The available crystal structures of CCDs include RPE65 from *Bos Taurus*, VP14 from *Zea mays*, and apocarotenoid oxygenase (ACO) from *Synechocystis*.[115,116,114] Remarkably, the CCDs from animals, plants and bacteria possess a similar overall structure: a rigid seven bladed propeller where blades I, II, IV and V consist of four antiparallel β-strands and blades VI and VII of five antiparallel β-strands. The bottom diagram of Fig. 1.13 shows blade I at the top of the propeller with blades numbered anti-clockwise. Blade III of RPE65 has a two strand extension relative to VP14 and apocarotenoid oxygenase. Additionally the secondary structures connecting blades together (α-helices, pairs of short β-sheets and loops) are identical.

Figure 1.13 Cartoon rocket diagrams of *Synechocystis* ACO from side (top) and below (bottom). Helix structures are coloured pink/purple, β-sheets yellow and iron orange. Histidines coordinated to the catalytic iron centre are represented as ball and stick models in the bottom diagram. Diagrams created using JSmol and PDB entry (accession code 2BIW)

The majority of α-helical, strands and loops that are not within the blade structures are arranged tightly together at the centre of the top face forming a dome region above the propeller region (see top diagram of Fig. 1.13). In contrast to the propeller component, the dome is more variable in both tertiary structure and sequence homology. This dome structure encloses the catalytic non-heme iron that is bound at the top of the propeller structure. The four conserved, coordinating histidine residues (shown as ball and stick models in bottom diagram of Fig. 1.13) are contributed from the strand and loop region at the base of blades II, III, IV and VII while the conserved glutamate residues are found in the same region from blades I, V and VI. Due to the highly variable nature of the dome component relative to the conserved propeller structure, the dome region is thought to determine substrate specificity.[117]

Analysis of the surface residues of solved crystal structures has revealed large patches of hydrophobic residues.[117] As most carotenoid substrates are extremely hydrophobic and typically localise in thylakoid membranes, in plants and bacteria, or liposomes, in animals, these hydrophobic patches are thought to facilitate CCD interaction with membranes and extraction of carotenoid substrate. Adjacent to these hydrophobic areas is a cavity that extends to the active site and runs perpendicular to the propeller axis. The internal surface area of this cavity is lined with hydrophobic residues and is therefore believed to function as a conduit for substrates and products. Crystal structures also reveal three phenylalanine residues surrounding the non-heme iron which may have roles in substrate and cleavage specificity. Notably, mutagenesis of hydrophobic residues within the cavity of RPE65 resulted in either the abolishment of activity or an alteration in products.[118,119]

At present CCDs do not seem to be utilised widely in industry, although potential applications would perhaps focus on their ability to cleave specific bonds. Many CCDs are highly specific, however from a detergency perspective, this could limit application as these enzymes may have only a single substrate with the requirement of multiple enzymes for different cleavage products of a specific carotenoid: β-carotene 15,15' dioxygenase and

β-carotene 9,10 dioxygenase in animal retinoid biosynthesis for example.[120,121] Although there are enzymes within this family that display substrate promiscuity, each enzyme is specific to the double bond that they cleave.[122] In comparison with the previously described carotenoid bleaching enzymes, CCDs are highly specific and interact directly with the carotenoid to catalyse degradation rather forming a general bleaching agent. However, the products of carotenoid cleavage dioxygenase reactions are not further degraded leading to incomplete bleaching.

1.6 Summary

Carotenoids are highly coloured pigments traditionally found in foodstuffs containing tomato or red pepper. Structurally, they contain a large, conjugated hydrocarbon system which confers strong colouration, a highly hydrophobic nature and various antioxidant properties. Many health benefits in humans are attributed to the antioxidant ability of dietary carotenoids and as a result, food industries seek to incorporate more carotenoids into foods and increase their stability. Consequently, carotenoids are more prevalent in foods stains and there is growing interest in new cleaning strategies.

Carotenoid stains are particularly problematic as their hydrophobic nature causes strong adsorption to fabrics and plastic food containers. Additionally, carotenoids possess extremely large extinction coefficients meaning relatively small amounts of stain material will remain visible. Due to the difficulty of complete removal of stain material, cleaning strategies have instead become focussed on methods of specific bleaching of carotenoids. Carotenoid foodstuffs usually contain appreciable concentrations of polyunsaturated fatty acids which localise in the same areas as carotenoids due to also being hydrophobic. A common carotenoid bleaching mechanism known as autoxidation involves conversion of polyunsaturated fatty acids to hydroperoxide species which subsequently react and oxidatively cleave carotenoids to colourless products. This process is relatively slow and there has been interest in enzymatic approaches.

Several enzyme families could potentially be exploited for accelerated carotenoid bleaching though the current literature suggests lipoxygenases may offer the simplest solution in terms of bleaching specificity and extent of carotenoid degradation. Lipoxygenases catalyse the conversion of polyunsaturated fatty acids to hydroperoxides and so share many similarities with autoxidative carotenoid bleaching. Although these enzymes are relatively sluggish, there has been a reported bleaching synergy in the literature between two isozymes of soybean lipoxygenase which could be exploited.

As most of the studies of carotenoid degradation have been performed in relation to stability in food, there is little data on bleaching in laundry wash conditions. Our aim is to perform a comprehensive study of the degradation of carotenoids under a range of surfactant and pH conditions. Surfactants will include those utilised in formulations in the detergency industry as well as those commonly used in the laboratory. In particular, our focus is to quantify several aspects of the fatty acid dependent autoxidative and the lipoxygenase catalysed bleaching of carotenoids – the exploration of the reported bleaching synergy between soybean lipoxygenases is of key interest. Our initial aim will be to study carotenoid bleaching kinetics in oil-in-water solutions. Carotenoid bleaching will then be studied in the presence of fabrics allowing for comparison between the two systems.

1.7 References

[1] G. Britton, S. Liaaen-Jensen, and H. P. Pfander, *Carotenoids: handbook*, Birkhauser, 2004.
[2] S. Lu, and L. Li, *J. Integr. Plant Biol.*, 2008, **7**, 778-785.
[3] M. H. Walter, and D. Strack, *Nat. Prod.*, 2011, **4**, 663–92.
[4] J. T. Landrum, *Carotenoids*, Taylor and Francis Group, LLC, 2010.
[5] L. H. Tonucci, J. M. Holden, G. R. Beecher, F. Khachik, C. S. Davis and G. Mulokozi, *J. Agric. Food Chem.*, 1995, **43**, 579–586.
[6] C. Fisher, and J. Kocis, *J. Agric. Food Chem.,* 1987, **35**, 55-57.
[7] A. Mortensen, *Pure Appl. Chem.*, 2006, **8**, 1477–1491.
[8] W. K. Subczynski, E. Markowska, W. I. Gruszecki, and J. Sielewiesiuk, *Biochim. Biophys. Acta.*, 1992, **1**, 97.
[9] A. Vershinin, *Comp. Biochem. Physiol. - B Biochem. Mol. Biol.,* 1996, **113,** 63–71.
[10] N. Mishra, G. Y. Liu, M. R. Yeaman, C.C. Nast, Proctor RA, J. McKinnell, and A.S. Bayer, *Antimicrob. Agents Chemother,* 2011, **55**, 526–531.
[11] N. P. Kutuzov, A. R. Brazhe, A. I. Yusipovich, G. V. Maksimov, O. E. Dracheva, V. L. Lyaskovskiy, F. V. Bulygin and A. B. Rubin, *Laser Phys. Lett.*, 2013, **10**, 75606.
[12] N. P. Kutuzov, A. R. Brazhe, G. V. Maksimov, O. E. Dracheva, V. L. Lyaskovskiy, F. V. Bulygin and A. B. Rubin, *Biophys. J.*, 2014, **107**, 891–900.
[13] R. J. Cogdell and H. A. Frank, *BBA Rev. Bioenerg.*, 1987, **895**, 63–79.
[14] Demmig-Adams, B., and Adams, W. W., *Trends Plant Sci.*, 1996, **1**, 21-26.
[15] C. S. Foote and R. W. Denny, *J. Am. Chem. Soc.*, 1968, **90**,6233-6235
[16] S. P. Stratton, W. H. Schaefer and D. C. Liebler, *Chem. Res. Toxicol.*, 1993, **6**, 542–7
[17] R. Farhoosh, V. Chynwat, R. Gebhard, J. Lugtenburg, and H. A. Frank, *Photochem. Photobiol.*, 1997, **1**, 97-104.
[18] P. Faller, A. Pascal, and A. W. Rutherford, *Biochemistry.*, 2001, **21**, 6431-6440.
[19] L. D. Kispert, and N. E. Polyakov, *Chem. Lett.*, 2010, **3**, 148–155.
[20] A. El-Agamey, G. M. Lowe, D. J. McGarvey, A. Mortensen, D. M. Phillip, T. G. Truscott, and A. J. Young, *Arch. Biochem. Biophys.*, 2004, **1**, 37–48.
[21] G. A. Armstrong, *J. Bacteriol.*, 1994, **16**, 4795-4802.
[22] N. I. Krinsky, and E. J. Johnson, *Mol. Aspects Med.*, 2005, **6**, 459-516.
[23] J. L. Schwartz, R. P. Singh, B. Teicher, J. E. Wright, D. H. Trites and G. Shklar, *Biochem. Biophys. Res. Commun.*, 1990, **169**, 941–946.
[24] N. Nishino, M. Murakoshi, H. Kitana, R. Iwasaki, Y. Tanaka, M. Tsushima, T. Matsuno, H. Okabe, J. Okuzumi, T. Hasegawa, J. Takayasu, Y. Satomi, H. Tokuda, A. Nishino and A. Iwashima, *Lipid-Soluble Antioxidants: Biochemistry and Clinical Applications*, 1992, Birkhauser, 228-242
[25] M. Karas, H. Amir, D. Fishman, M. Danilenko, S. Segal, A. Nahum, A. Koifmann, Y. Giat, J. Levy and Y. Sharoni, *Nutr. Cancer*, 2000, **36**, 101-111
[26] V. N. Sumantran, R. Zhang, D. S. Lee and M. S. Wicha, *Cancer Epidemiol. Biomarkers Prev.*, 2000, **9**, 257–263.
[27] M. M. Ciccone, F. Cortese, M. Gesualdo, S. Carbonara, A. Zito, G. Ricci, F. De Pascalis, P. Scicchitano and G. Riccioni, *Mediators Inflamm.*, 2013.
[28] S. P. Juraschek, E. Guallar, L. J. Appel, and E. R. Miller III, *Am. J. Clin. Nutr.*, 2012, **95**, 1079-1088.
[29] R. M. Salonen, K. Nyyssönen, J. Kaikkonen, E. Porkkala-Sarataho, S. Voutilainen, T. H. Rissanen, T. P. Tuomainen, V. P. Valkonen, U. Ristonmaa, H. M. Lakka, M. Vanharanta, J. T. Salonen and H. E. Poulsen, *Circulation*, 2003, **107**, 947–953.
[30] B, Frei, *Crit. Rev. Food Sci. Nutr.*, 1995, **35**, 83-98
[31] B. A. Clevidence and J. G. Bieri, *Methods Enzymol.*, 1993, **214**, 33-46
[32] A. Shaish, A. Harari, L. Hananshvili, H. Cohen, R. Bitzur, T. Luvish, E. Ulman, M. Golan, A. Ben-Amotz, D. Gavish, Z. Rotstein and D. Harats, *Atherosclerosis*, 2006, **189**, 215–221.
[33] A. Harari, D. Harats, D. Marko, H. Cohen, I. Barshack, Y. Kamari, A. Gonen, Y. Gerber, A. Ben-amotz and A. Shaish, *J. Nutr.*, 2008, **138**, 1923–1930.
[34] P. S. Bernstein, F. Khachik, L. S. Carvalho, G. J. Muir, D. Y. Zhao and N. B. Katz, *Exp. Eye Res.*, 2001, **72**, 215–23.

[35] K. J. Yeum, A. Taylor, G. Tang and R. M. Russell, *Investig. Ophthalmol. Vis. Sci.*, 1995, **36**, 2756–2761.
[36] C. S. Boon, D. J. McClements, J. Weiss and E. A. Decker, *Crit. Rev. Food Sci. Nutr.*, 2010, **50**, 515–32.
[37] A. A. Woodall, S. W. Lee, R. J. Weesie, M. J. Jackson and G. Britton, *Biochim. Biophys. Acta*, 1997, **1336**, 33–42.
[38] N. I. Krinsky and K. J. Yeum, *Biochem. Biophys. Res. Commun.*, 2003, **305**, 754–760.
[39] Burton, G. W., and Ingold, K. U., *Science*, 1984, **4649**, 569-573.
[40] R. C. Mordi, J. C. Walton, G. W. Burton, L. Hughes, I. U. Keith, L. A. David, and M. J. Douglas, *Tetrahedron*, 1993, **4**, 911-928.
[41] T. A. Kennedy, and D. C. Liebler, *Chem. Res. Toxicol.*, 1991, **3**, 290-295.
[42] D. C. Liebler, and T. D. McClure, *Chem. Res. Toxicol.*, 1996, **1**, 8-11.
[43] D. L. Baker, E. S. Krol, N. Jacobsen, and D. C. Liebler, *Chem. Res. Toxicol.*, 1999, **6**, 535-543.
[44] A. A. Woodall, S. W. M. Lee, R. J. Weesie, M. J. Jackson, and G. Britton, *Biochimica et Biophysica Acta (BBA)-General Subjects*, 1997, **1**, 33-42.
[45] H. D. Martin, C. Ruck, M. Schmidt, S. Sell, S. Beutner, B. Mayer, and R. Walsh, *Pure Appl. Chem.*, 1999, **12**, 2253-2262.
[46] J. E. Packer, J. S. Mahood, V. O. Mora-Arellano, T. F. Slater, R. L. Willson, and B. S. Wolfenden, *Biochem. Biophys. Res. Commun.*, 1981, **4**, 901-906.
[47] T. J. Hill, E. J. Land, D. J. McGarvey, W. Schalch, J. H. Tinkler, and T. G. Truscott, *J. Am. Chem. Soc.*, 1995, **32**, 8322-8326.
[48] T. A. Kennedy, and D. C. Liebler, *Chem. Res. Toxicol.*, 1991, **4**, 290-295.
[49] H. D. Martin, C. Ruck, M. Schmidt, S. Sell, S. Beutner, B. Mayer and R. Walsh, *Pure Appl. Chem.*, 1999, **71**, 2253-2262.
[50] C. C. Berton-Carabin, M. H. Ropers and C. Genot, *Compr. Rev. Food Sci. Food Saf.*, 2014, **13**, 945–977.
[51] Z. Wu, D. S. Robinson, R. K. Hughes, R. Casey, D. Hardy and S. I. West, *J. Agric. Food Chem.*, 1999, **47**, 4899–906.
[52] J. L. Guil-Guerrero, and M. M. Rebolloso-Fuentes, *J. Food Comp. Anal.,* 2009, **2**, 123-129.
[53] A. Pérez-Gálvez, J. Garrido-Fernándes, M. I. Mínguez-Mosquera, M. Lozano-Ruiz, and V. Montero-de-Espinosa, *J. Am. Oil Chem. Soc.,* 1999*,* **2**, 205-208.
[54] A. Andreou and I. Feussner, *Phytochemistry*, 2009, **70**, 1504–10.
[55] C. O. Ikediobi and H. E. Snyder, *J. Agric. Food Chem.*, 1977, **25**, 124–7.
[56] V. F. J. Agric, D. F. Hildebrand and T. Hymowitz, *J. Agric. Food Chem.*, 1982, **30**, 705–708.
[57] S. Aziz, Z. Wu and D. S. Robinson, *FOOD Chem.*, 1999, **64**, 227–230.
[58] C. S. Ramadoss, E. K. Pistorius and B. Axelrod, *Arch. Biochem. Biophys.*, 1978, **190**, 549–552.
[59] N. C. Veitch and A. T. Smith, *Adv. Inorg. Chem.*, 2001, **51**, 107–162.
[60] Y. P. Chau and K. S. Lu, *Acta Anat.*, 1995, **153**, 135-144.
[61] N. C. Veitch, *Phytochemistry*, 2004, **65**, 249–259.
[62] G. I. Berglund, G. H. Carlsson, A. T. Smith, H. Szöke, A. Henriksen and J. Hajdu, *Nature*, 2002, **417**, 463–468.
[63] M. Gajhede, D. J. Schuller, a Henriksen, a T. Smith and T. L. Poulos, *Nat. Struct. Biol.*, 1997, **4**, 1032–1038.
[64] D. J. Schuller, N. Ban, R. B. van Huystee, A. McPherson and T. L. Poulos, *Structure*, 1996, **4**, 311–321.
[65] J. H. Dawson, *Science*, 1988, **240**, 433–439.
[66] A. Henriksen, A. T. Smith and M. Gajhede, *J. Biol. Chem.*, 1999, **274**, 35005–35011.
[67] S. Nakamoto and N. Machida, *Water Res.*, 1992, **26**, 49–54.
[68] S. V. Mohan, K. K. Prasad, N. C. Rao and P. N. Sarma, *Chemosphere*, 2005, **58**, 1097–1105.
[69] I. M. Banat, P. Nigam, D. Singh and R. Marchant, *Bioresour. Technol.*, 1996, **58**, 217–227.
[70] P. Matile and E. Martinoia, *Plant Cell Rep.*, 1982, **1**, 244–246.
[71] K. Zelena, B. Hardebusch, B. Hülsdau, R. G. Berger and H. Zorn, *J. Agric. Food Chem.*, 2009, **57**, 9951–9955.
[72] H. Zorn, S. Langhoff, M. Scheibner, M. Nimtz and R. G. Berger, *Biol. Chem.*, 2003, **384**, 1049-1056.
[73] B. G. Malmström, a F. Agrò and E. Antonini, *Eur. J. Biochem.*, 1969, **9**, 383–391.
[74] S. Kawai, T. Umezawa, M. Shimada, T. Higushi, *FEBS Lett.*, 1988, **236**, 309–311.
[75] P. Baldrian, *FEMS Microbiol. Rev.*, 2006, **30**, 215–242.
[76] J. T. Hoopes and J. F. D. Dean, *Plant Physiol. Biochem.*, 2004, **42**, 27–33.
[77] B. M. McCaig, R. B. Meagher and J. F. D. Dean, *Planta*, 2005, **221**, 619–636.

[78] G. F. Leatham and M. a. Stahmann, *Microbiology*, 1981, **125**, 147–157.
[79] C. F. Thurston, *Microbiology*, 1994, **140**, 19–26.
[80] M. Nagai, M. Kawata, H. Watanabe, M. Ogawa, K. Saito, T. Takesawa, K. Kanda and T. Sato, *Microbiology*, 2003, **149**, 2455–2462.
[81] P. Sharma, R. Goel and N. Capalash, *World J. Microbiol. Biotechnol.*, 2007, **23**, 823–832.
[82] F. J. Enguita, L. O. Martins, A. O. Henriques and M. A. Carrondo, *J. Biol. Chem.*, 2003, **278**, 19416–19425.
[83] E. I. Solomon, M. J. Baldwin and M. D. Lowery, *Chem. Rev.*, 1992, **92**, 521-542
[84] F. J. Enguita, L. O. Martins, A. O. Henriques and M. A. Carrondo, *J. Biol. Chem.*, 2003, **278**, 19416–19425.
[85] P. F. Lindley, I. Bertini, A. Sigel and H. Sigel (Eds.), Multi-copper oxidases. In Handbook on Metalloproteins, Marcel Dekker, Inc., New York, 2001, pp. 763–811.
[86] F. Xu, W. Shin, S. H. Brown, J. A. Wahleithner, U. M. Sundaram and E. I. Solomon, *Biochim. Biophys. Acta - Protein Struct. Mol. Enzymol.*, 1996, **1292**, 303–311.
[87] U. N. Dwivedi, P. Singh, V. P. Pandey and A. Kumar, *J. Mol. Catal. B Enzym.*, 2011, **68**, 117–128.
[88] A. I. Yaropolov, O. V. Skorobogat'ko, S. S. Vartanov and S. D. Varfolomeyev, *Appl. Biochem. Biotechnol.*, 1994, **49**, 257–280.
[89] D. S. Arora and R. K. Sharma, *Appl. Biochem. Biotechnol.*, 2010, **160**, 1760–1788.
[90] C. Eggert, U. Temp, K. E. Eriksson, C. Eggert and U. Temp, 1996, **62**, 1151–1158.
[91] D. S. Arora and R. K. Sharma, *J. Anim. Feed Sci.*, 2009, **18**, 151–161.
[92] J. B. Kristensen, L. G. Thygesen, C. Felby, H. Jørgensen and T. Elder, *Biotechnol. Biofuels*, 2008, **1**, 5.
[93] P. Widsten and A. Kandelbauer, *Enzyme Microb. Technol.*, 2008, **42**, 293–307.
[94] I. Ciullini, S. Tilli, A. Scozzafava and F. Briganti, *Bioresour. Technol.*, 2008, **99**, 7003–7010.
[95] A. Mikolasch, E. Hammer, U. Jonas, K. Popowski, A. Stielow and F. Schauer, *Tetrahedron*, 2002, **58**, 7589–7593.
[96] G. Lang and J. Cotteret, (L'Oreal, Fr.), International Patent Application, WO9936036, 1999.
[97] K. Golz-Berner, B. Walzel, L. Zastrow and O. Doucet, International Patent Application, WO2004017931, 2004.
[98] L. Pereira, C. Bastos, T. Tzanov, A. Cavaco-Paulo and G. M. Guebitz, *Environ. Chem. Lett.*, 2005, **3**, 66–69.
[99] H. Hadzhiyska, M. Calafell, J. M. Gibert, J. M. Dagà and T. Tzanov, *Biotechnol. Lett.*, 2006, **28**, 755–759.
[100] G. G. Janssen, T. M. Baldwin, D. S. Winetzky, L. M. Tierney, H. Wang and C. J. Murray, *J. Pept. Res.*, 2004, **64**, 10-24.
[101] G. Giuliano, S. Al-Babili and J. von Lintig, *Trends Plant Sci.*, 2003, **8**, 145–149.
[102] I. B. Taylor, T. Sonneveld, T. D. H. Bugg and A. J. Thompson, *J. Plant Growth Regul.*, 2005, **24**, 253–273.
[103] E. Nambara and A. Marion-Poll, *Annu. Rev. Plant Biol.*, 2005, **56**, 165–185.
[104] W. Yan, G. F. Jang, F. Haeseleer, N. Esumi, J. Chang, M. Kerrigan, M. Campochiaro, P. Campochiaro, K. Palczewski and D. J. Zack, *Genomics*, 2001, **72**, 193–202.
[105] T. M. Redmond, S. Gentleman, T. Duncan, S. Yu, B. Wiggert, E. Gantt and F. X. Cunningham, *J. Biol. Chem.*, 2001, **276**, 6560–6565.
[106] J. A. Zeevaart, T. G. Heath and D. A. Gage, *Plant Physiol.*, 1989, **91**, 1594–601.
[107] H. Schmidt, R. Kurtzer, W. Eisenreich and W. Schwab, *J. Biol. Chem.*, 2006, **281**, 9845–9851.
[108] M. G. Leuenberger, C. Engeloch-Jarret and W.-D. Woggon, *Angew. Chemie Int. Ed.*, 2001, **40**, 2613–2617.
[109] P. J. Harrison and T. D. H. Bugg, *Arch. Biochem. Biophys.*, 2014, **544**, 105–111.
[110] T. D. H. Bugg, *Tetrahedron*, 2003, **59**, 7075–7101.
[111] T. D. Bugg and S. Ramaswamy, *Curr. Opin. Chem. Biol.*, 2008, **12**, 134–140.
[112] P. D. Kiser, M. Golczak, D. T. Lodowski, M. R. Chance and K. Palczewski, *Proc. Natl. Acad. Sci. U. S. A.*, 2009, **106**, 17325–17330.
[113] S. A. J. Messing, S. B. Gabelli, I. Echeverria, J. T. Vogel, J. C. Guan, B. C. Tan, H. J. Klee, D. R. McCarty and L. M. Amzel, *Plant Cell*, 2010, **22**, 2970–2980.
[114] D. P. Kloer, S. Ruch, S. Al-Babili, P. Beyer and G. E. Schulz, *Science (80-.).*, 2005, **308**, 267–269.
[115] P. D. Kiser, M. Golczak, D. T. Lodowski, M. R. Chance and K. Palczewski, *Proc. Natl. Acad. Sci. U. S. A.*, 2009, **106**, 17325–17330.

[116] S. A. J. Messing, S. B. Gabelli, I. Echeverria, J. T. Vogel, J. C. Guan, B. C. Tan, H. J. Klee, D. R. McCarty and L. M. Amzel, *Plant Cell*, 2010, **22**, 2970–2980.
[117] X. Sui, P. D. Kiser, J. Von Lintig and K. Palczewski, *Arch. Biochem. Biophys.*, 2013, **539**, 203–213.
[118] T. M. Redmond, E. Poliakov, S. Kuo, P. Chander and S. Gentleman, *J. Biol. Chem.*, 2010, **285**, 1919–1927.
[119] P. Chander, S. Gentleman, E. Poliakov and T. M. Redmond, *J. Biol. Chem.*, 2012, **287**, 30552–30559.
[120] J. von Lintig and K. Vogt, *J. Biol. Chem.*, 2000, **275**, 11915-11920.
[121] C. Kiefer, S. Hessel, J. M. Lampert, K. Vogt, M. O. Lederer, D. E. Breithaupt and J. von Lintig, *J. Biol. Chem.*, 2001, **276**, 14110-14116.
[122] M. E. Auldridge, D. R. McCarty and H. J. Klee, *Curr. Opin. Plant Biol.*, 2006, **9**, 315–321.

CHAPTER 2

Non-enzymatic bleaching of β-carotene

2.0 Foreword

As mentioned in the previous chapter, one of the major pathways of carotenoid degradation is oxidative cleavage by reaction with radical species. Within carotenoid foodstuffs and stains, radical species formed by fatty acid hydroperoxides are among the most important due to the high concentration of free fatty acids and their susceptibility to oxidation. This chapter will present studies of fatty acid autoxidation and the subsequent bleaching of carotenoids. Section 2.1 overviews the mechanisms of fatty acid oxidation with a focus on autoxidation and the subsequent bleaching reaction with carotenoids, as well as the effect of surfactant. Section 2.2 details our results from β-carotene bleaching assays in the presence of fatty acids and surfactants, and the results are discussed in section 2.3. A summary of our conclusions is in section 2.4.

2.1 Introduction

2.1.1 Oxidation Pathways of Fatty Acids

There are three main oxidation pathways for the conversion of fatty acids to fatty acid hydroperoxides, as shown for linoleic acid **10** in Scheme 2.1.[1] Both autoxidation and lipoxygenase catalysed oxidation (route A of Scheme 2.1) proceed via a resonance stabilised radical **11** ($R^{\bullet}$) following hydrogen abstraction from the central methylene group of a 1,4-pentadiene moiety found in many polyunsaturated fatty acids. Molecular oxygen then reacts at the terminal end of the radical system to yield a hydroperoxide radical **12** ($ROO^{\bullet}$). In an autoxidation process, the initial hydrogen abstraction is performed by metal ion or radical whereas enzymatic oxidation involves a non-heme iron prosthetic group at the active site of a lipoxygenase enzyme. Additionally, the hydrogen donor in the final step to yield hydroperoxide is usually another polyunsaturated fatty acid molecule in autoxidation while hydrogen is abstracted from the active site in enzymatic oxidation. In contrast to auto- and enzymatic oxidation, the photoinitiation pathway (route B of Scheme 2.1) is a concerted reaction between singlet oxygen and the 1,4-pentadiene moiety of the fatty acid. The singlet oxygen species is generated *in situ* by a photosensitiser upon exposure to light. Radical species **12** and **30** involved in the bleaching of carotenoid

pigments may be formed from linoleic acid hydroperoxide **13** by reaction with metal ions in solution. As described in Sections 1.3 and 1.4 of Chapter 1, hydroperoxy radical species such as **12** and **30** react with carotenoids resulting in oxidative cleavage (Scheme 2.2). The products of this reaction possess less conjugation leading to a loss of colouration. This thesis will focus on autoxidation studies in this chapter and lipoxygenase-catalysed fatty acid oxidation in Chapter 3.

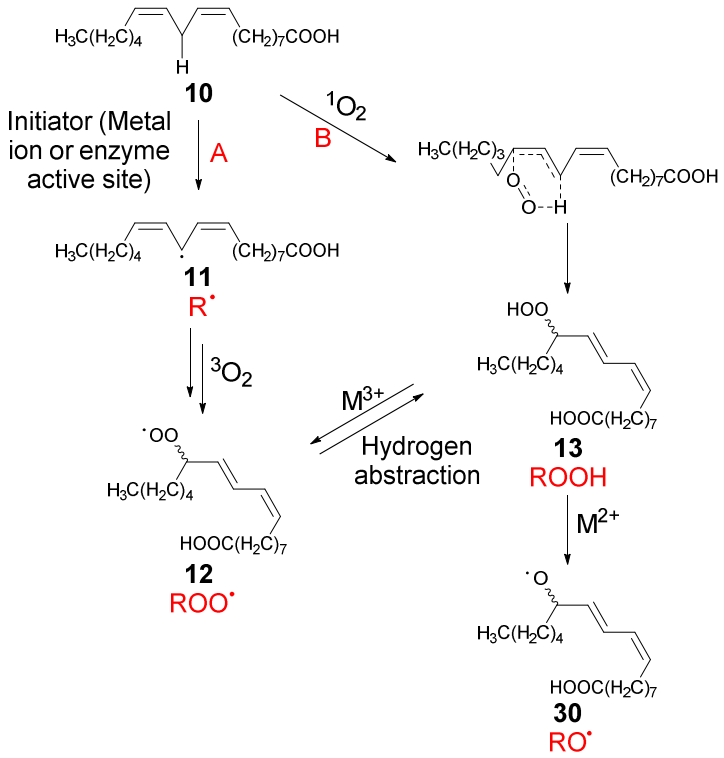

Scheme 2.1 Pathways for the conversion of linoleic acid to oxidised radical species: Auto or enzymatic oxidation (A) and photoinitiation (B).

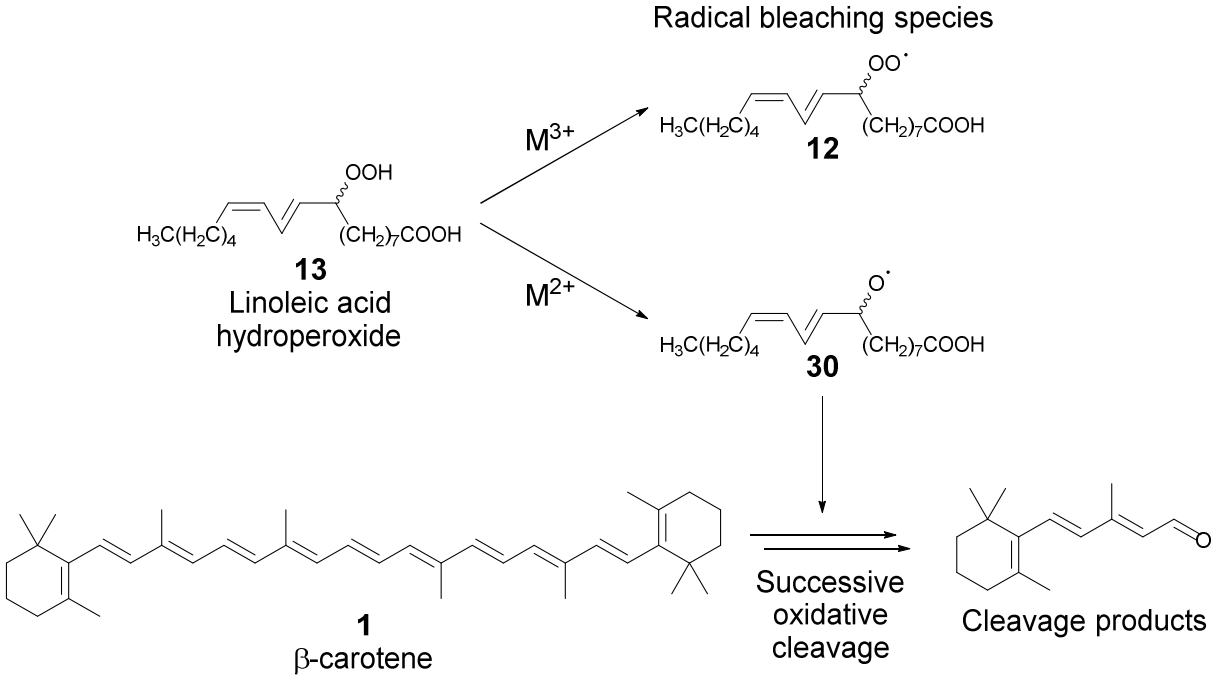

Scheme 2.2 Oxidative degradation of carotenoids by fatty acid hydroperoxide radical species.

2.1.2 History of Lipid Autoxidation

Research into oxidation of lipids has been ongoing for at least two centuries beginning with observations of the rancidification of fats.[2] Early research by Braconnot suggested rancidity was related to the formation of acids (now known to be caused by oxidation of aldehyde products to carboxylic acids) while Thenard and Parmentier proposed reaction with oxygen to be the cause, leading to confusion as to whether triglyceride hydrolysis or oxidation was the most important factor in rancidity.[3] Clarification came much later from a study of light-accelerated oxidation of fats by Lea in 1931.[4] Oxygen was found to be necessary for the production of rancidity, and in early stages, there was no concomitant increase in acidity with the onset of rancidity. This work provided evidence that rancidification of fats was due to oxidation and that the process was autocatalytic, however, the mechanism of lipid oxidation was not discovered until progress was made in the general understanding of the oxidation of alkenes.[5]

The first breakthrough came from oxidation studies of cyclohexene derivatives where oxygen addition was observed to occur alpha to the double bond and the initial products were hydroperoxides.[6,7,8] For polyunsaturated fatty acid systems, oxidation studies were primarily performed by Farmer, Bolland and Bateman of the British Rubber Producers Association. They observed increases in absorption at low wavelengths during oxidation, which they attributed to formation of a conjugated diene and subsequently deduced that this involved abstraction of hydrogen from a methylene group flanked by two double bonds.[9] This group also deduced rate equations for oxidation,[10] bond dissociation energies for α-hydrogen abstraction from 23 unsaturated hydrocarbons [11] and demonstrated hydroquinone could act as an effective inhibitor of fatty acid oxidation by chain breaking antioxidant activity.[12]

2.1.3 Mechanism of Fatty Acid Oxidation

Oxidation of fatty acids by triplet state molecular oxygen is commonly known as autoxidation. The term fatty acid peroxidation is also used (more so in Biology) and is a reference to the initial chemical species formed in the reaction. The process of autoxidation is a free radical mechanism. There are three distinct stages in this mechanism: initiation, propagation and termination. [8]

Initiation is essential in the autoxidation reaction as fatty acid and triplet state oxygen possess opposite spins and the activation energy for direct reaction is too large.[13] In order to overcome the spin barrier, the first stage of autoxidation involves fatty acid hydrogen abstraction (usually from the allylic or bisallylic position) by an initiator forming carbon radical **11** (R•) (eq. 1).

$$RH \rightarrow R^{\cdot} + H^{\cdot} \qquad (1)$$

Many species may act as initiators although the most significant are metal ions, oxygen radicals and radicals derived from fatty acid hydroperoxides. Transition metal ions may directly react with fatty acids to generate fatty acid radicals (eq. 2), or alternatively, metals such as iron may catalyse the formation of oxygen radicals (eq. 3 and 4), which are also capable of performing the hydrogen abstraction step (eq. 5).[14]

$$RH + M^{3+} \rightarrow R^{\cdot} + H^{+} + M^{2+} \quad (2)$$

$$Fe^{2+} + O_2 \rightarrow Fe^{3+} + O_2^{-\cdot} \quad (3)$$

$$H_2O_2 + Fe^{2+} \rightarrow HO^{\cdot} + OH^{-} + Fe^{3+} \quad (4)$$

$$HO^{\cdot} + RH \rightarrow H_2O + R^{\cdot} \quad (5)$$

Systems containing fatty acids will commonly also contain small concentrations of the hydroperoxide product. These species readily decompose to radicals by reduction or oxidation by metal ions (eq. 6 and 7) or by thermal decomposition (eq. 8 and 9).[15,16]

$$LOOH + M^{2+} \rightarrow LO^{\cdot} + OH^{-} + M^{3+} \quad (6)$$

$$LOOH + M^{3+} \rightarrow LOO^{\cdot} + H^{+} + M^{2+} \quad (7)$$

$$LOOH \rightarrow LO^{\cdot} + HO^{\cdot} \quad (8)$$

$$2LOOH \rightarrow LO^{\cdot} + H_2O + LOO^{\cdot} \quad (9)$$

Following the initiation stage, the alkyl radicals react rapidly with triplet oxygen to form peroxyl radicals (eq. 10) which abstract hydrogen from fatty acid molecules (eq. 11), propagating the chain reaction.

$$R^{\cdot} + O_2 \rightarrow ROO^{\cdot} \quad (10)$$

$$ROO^{\cdot} + RH \rightarrow ROOH + R^{\cdot} \quad (11)$$

The final stage of autoxidation is termination and involves reaction between two radical species (eq. 12 and 13). A wide range of radical species may be formed in the previous stages resulting in many termination products.

$$2\,ROO^{\cdot} \rightarrow RO + ROH + O_2 \quad (12)$$

$$ROO^{\cdot} + R^{\cdot} \rightarrow ROOR \quad (13)$$

2.1.3.1 Autoxidation of Unsaturated Fatty Acids

The susceptibility of fatty acids to autoxidation is based on the dissociation energy of the C-H bond as hydrogen abstraction is rate limiting. The bond dissociation energies of saturated, allylic and bisallylic C-H bonds are 100, 74 and 65 kcal/mol, respectively.[17,18] Autoxidation susceptibility therefore increases as fatty acids become more unsaturated with observed relative rates of autoxidation of ethyl linoleate, ethyl linolenate and methyl arachidonate being in the ratio 1:2.4:4.8,[19] or approximately a 2-fold increase in rate per additional double bond in other fatty acids.[20]

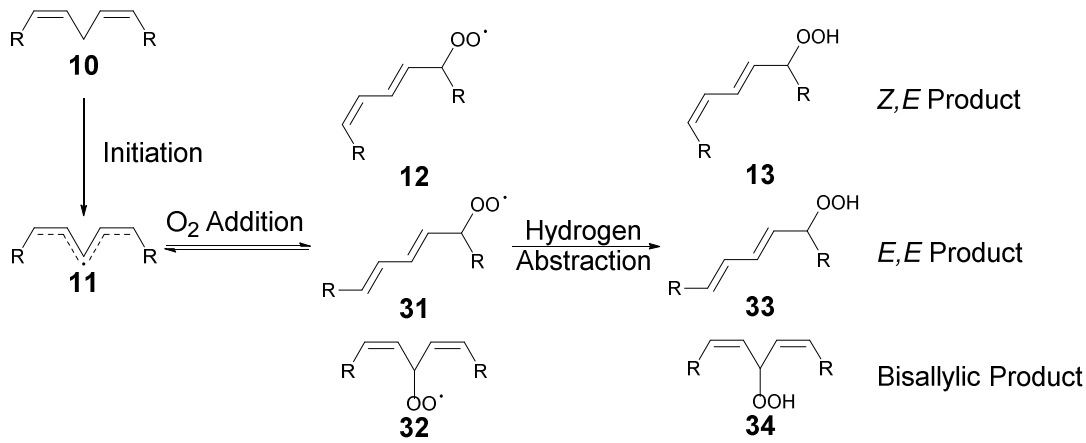

Scheme 2.3 Autoxidation mechanism and potential products for linoleic acid.[21,22]

Early mechanistic studies of autoxidation of linoleic acid **10** observed the conversion of non-conjugated diene in the starting material to conjugated diene in the hydroperoxide product.[9] The proposed mechanism for this transformation was hydrogen abstraction from the bisallylic position (the weakest C-H bond) forming a resonance stabilised radical **11**, followed by attack of molecular oxygen at the termini of the radical intermediate to give either the *Z,E* **13** or *E,E* **33** product. The ratio of these isomers is explained by competitive hydrogen abstraction by peroxyl radical and reversible oxygen addition, which allows for the isomerisation of the radical intermediate.[17,23]

One problem with the proposed mechanism, however, is the absence of the bisallylic product **34** under most experimental conditions. ESR studies and calculations show spin density to be greatest at the central carbon and therefore the most probable site for oxygen addition.[24,25] Numerous attempts were made to acquire the bisallylic product **34**, performing experiments at low temperature and in the presence of hydrogen donors such as 1,4-cyclohexadiene or phenols.[26] Formation of the bisallylic product **34** during autoxidation was first observed to occur in experiments at -20 °C in the presence of high concentrations of α-tocopherol, a highly potent chain breaking antioxidant and hydrogen donor.[25] Further studies revealed that the bisallylic hydroperoxide **34** only formed when α-

tocopherol concentrations were in the range 0.1-1 M and was the major product at the kinetic limit – consistent with measurements observing the greatest spin density at the central carbon.[27] Kinetic studies determined that the rate constant for propagation of linoleate peroxidation (peroxyl radical hydrogen abstraction from another linoleate molecule) was 62 M^{-1} s^{-1} compared to an α-tocopherol inhibition rate constant (peroxyl radical hydrogen abstraction from α-tocopherol) of 3.5 x 10^6 M^{-1} s^{-1}.[28,29] The oxygen partition factor of the peroxyl/pentadiene radical was determined to be 0.45 x 10^6 s^{-1} for oxygen addition and 2.6 x 10^6 s^{-1} for loss of oxygen,[26] thus the bisallylic radical **32** is only trapped at relatively high concentrations of α-tocopherol when hydrogen abstraction is able to compete with the loss of oxygen from peroxyl radical – at lower α-tocopherol concentrations the peroxyl radical is able to undergo rearrangement to form the conjugated thermodynamic products.

2.1.3.2 Autoxidation of Saturated Fatty Acids

Lipid autoxidation is more commonly observed in unsaturated rather than saturated systems. An early experiment monitoring rates of oxygen absorption at 100 °C of methyl esters of linolenic **41**, linoleic **10**, oleic **38** and stearic acid **37** (fatty acid structures shown in Fig. 2.1) gave relative rates of 179:114:11:1, respectively, demonstrating the effect of unsaturation upon autoxidation susceptibility.[30] Although saturated fatty acids constitute a large proportion of total fats within many foods they possess a relatively higher stability towards autoxidation and are therefore a less significant factor in food deterioration. As a result the majority of fatty acid autoxidation research has instead focused on unsaturated fatty acids.

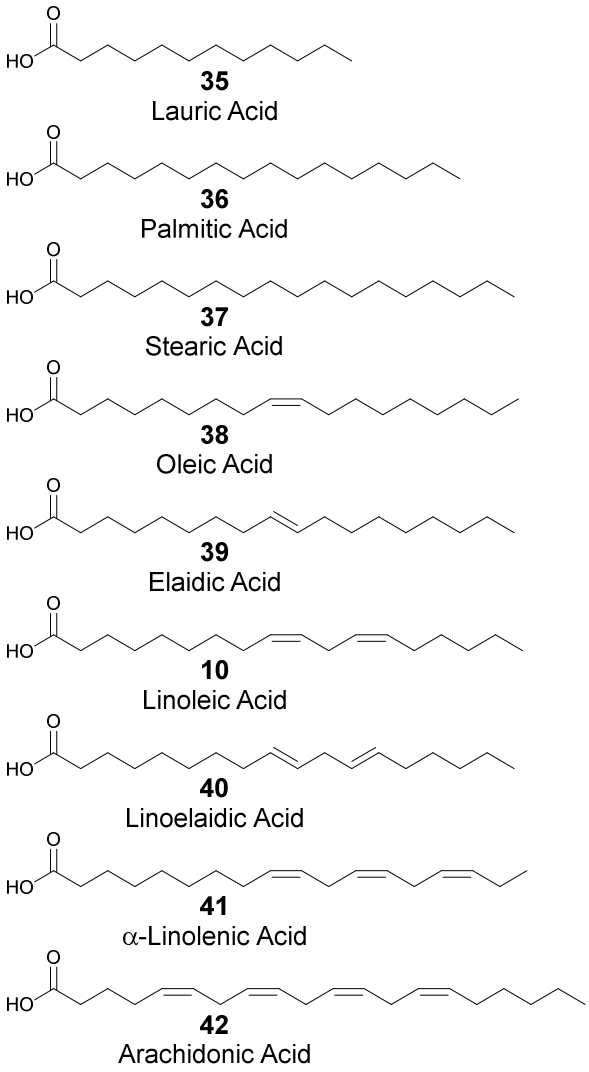

Figure 2.1 Structures of fatty acids referred to in this thesis.

Several structural factors other than unsaturation may affect the rate of autoxidation of fatty acids. A study of the oxidation of 5-methylnonane **43** at 90 °C showed that the relative rates of hydrogen abstraction (autoxidation initiation stage) were 76:4:1 for tertiary, secondary and primary carbons (reduced autoxidation products under various conditions shown in Fig 2.2).[31] Similarly, autoxidation rate constants for isodecane were found to be larger compared to those of *n*-decane.[32] Fatty acid autoxidation stability was also discovered to be dependent on chain length. An oxidation study performed at 150 °C in the presence of 0.1% $KMnO_4$ found that stearic acid **37** (18:0) oxidized to shorter fatty acids,

lactones and hydroxylated compounds while lauric acid (12:0) **35** remained relatively stable.[33] Similar studies also found that the oxidative stability of saturated fatty acids decreased as chain length increased, both in the presence of catalyst [34, 35] and in autocatalytic conditions.[36,37]

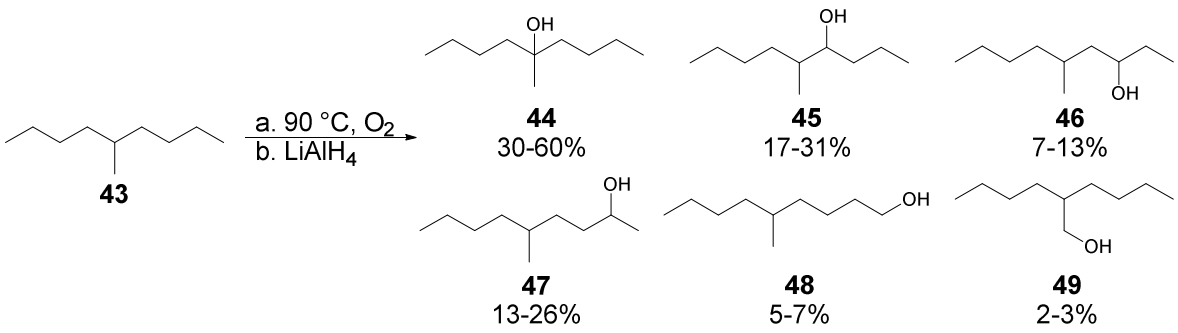

Figure 2.2 Proportions of alcohol products obtained from the reduction of oxidation products of 5-methylnonane **38**.[31]

Early studies of the oxidation products of laurate (12:0), palmitate (16:0) and stearate (18:0) esters (fatty acid structures shown in Fig. 2.1, **35**, **36** and **37**) suggested the mechanism for saturated fatty acid autoxidation followed the established mechanism for unsaturated fatty acid systems after an initial dehydrogenation step.[36,38] Experiments performed by Brodnitz *et al.* however, found that no unsaturation was present in the oxidised products of the methyl ester of palmitic acid **36** (16:0) and proposed that the initial step was formation of radical.[39] Additionally, the study found that similar to unsaturated systems the initial oxidation products were hydroperoxides, however, in contrast to unsaturated systems, attack of oxygen occurred along the entire molecule. The centre of the methyl palmitate hydrocarbon chain was found to be relatively more susceptible to oxidation as a higher proportion of products were oxidised at carbons 5-11.

2.1.4 Pro-oxidant Properties of Fatty Acids

The effect of free fatty acids on the oxidative stability of other components within bulk oil or emulsion systems is an active area of research as the pro-oxidant behaviour of fatty acids can lead to the degradation of nutrients and reduce the shelf life of foodstuffs. As described in Chapter 1, this behaviour can be exploited for the oxidative degradation and bleaching of carotenoid compounds. One of the main pathways for promotion of oxidation by fatty acids is the formation of hydroperoxide radicals, however numerous, recent studies in the literature suggest that other important mechanisms exist.

In bulk oil model systems (representative of cooking oils), free fatty acids have been established to possess a significant pro-oxidant effect. A study monitoring vegetable oil oxidation highlighted the importance of the carboxylate group of free fatty acids.[40] An increase in oleic acid **38** concentration resulted in a decrease in the induction time for lipid oxidation while the presence of methyl oleate did not affect lipid oxidation susceptibility (Table 2.1, an increase in concentration of oleic acid **38** to sunflower and olive oil reduce induction times while addition of the methyl ester has no effect). Similar experiments performed with purified olive oil also found that increases in free fatty acid concentration resulted in lower induction times and a greater extent of triglyceride oxidation (Table 2.1, mixture of free fatty acid has a pro-oxidant effect in purified olive oil).[41] The authors suggested free fatty acid pro-oxidant effects were primarily due to accelerating the decomposition of pre-existing hydroperoxide to oxidising radical species rather than the increased formation of these hydroperoxides. An earlier study by Miyashita and Takagi demonstrated the importance of the free fatty acid carboxylate group in oxidation studies of fatty acids.[42] Observed rates of autoxidation of neat samples of methyl esters of oleic, linoleic and linolenic acids were found to be lower than their acid analogues (fatty acid structures shown in Fig. 2.1, **38**, **10** and **41**). Furthermore, the addition of stearic acid **37** to methyl linoleate accelerated rates of autoxidation and hydroperoxide decomposition. The pro-oxidant ability of free fatty acids was attributed to the carboxylic acid group promoting the homolytic cleavage of either the O-O or O-H bond of the hydroperoxide. Aubourg assessed the effect of free fatty acids on the oxidative stability of marine lipids and

discovered that at 30 °C, shorter chain and more unsaturated fatty acids promoted higher degrees of oxidation.[43] Higher degrees of unsaturation were proposed to be more pro-oxidative through a greater ability to form hydroperoxides, while chain length was suggested to affect the accessibility of the carboxylate group.

Table 2.1 Effect of free fatty acid and methyl ester concentration on the oxidation induction times of bulk oil systems.[40,41]

Bulk Oil Sample	Fatty Acid Additive	Additive Content in Sample (%)	Induction Time (h)
Sunflower Oil	Oleic Acid	1.4	14
		2.0	12
		2.4	11
		3.1	10
		4.0	8
Virgin Olive Oil	Oleic Acid	0.5	7
		1.1	5
		1.6	4
		2.0	4
		2.6	3
		3.3	3
Virgin Olive Oil	Methyl Oleate	0.0	6
		0.7	6
		1.2	6
		1.8	6
		2.4	6
		3.2	6
Purified Olive Oil	Free Fatty Acid Mixture (from purified sample of saponified olive oil)	0.0	10
		0.3	9
		0.5	7
		1.0	6
		3.0	4

In emulsion systems, oxidative mechanisms are more complex due to the different partitioning behaviours of reactants into the oil, water and interface (see Fig. 2.3 for a representation of a micelle in an oil-in-water emulsion). In oil-in-water emulsions

hydrophobic substrates such as lipids or carotenoids will occupy the hydrophobic core of micelles while metal ions and other polar molecules will solubilise in the aqueous phase. Amphiphilic molecules such as fatty acids or oxidised lipids will be present at the interface. Due to the reactants localising in different phases, cooxidation reactions are dependent on the dynamics of substrate interchange between oil and water phases, which is highly influenced by the properties of surfactants comprising the interface (example structures shown in Fig. 2.4).

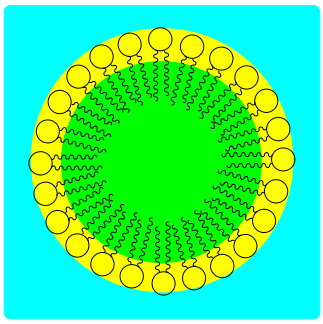

Aqueous Phase
- Initiators, hydrogen abstraction (eq. 2-5)
- Hydroperoxide decomposition catalysts (eq. 6 and 7)
- Metal Ions (M^{2+} and M^{3+}) and $O_2^{-\bullet}$

Micelle Surface/Interface
- Surfactants
- Carboxylate group of free fatty acids
- Polar oxidation products (hydroperoxides, aldehydes)

Micelle Interior
- Carotenoids
- Acyl chain of free fatty acids

Figure 2.3 Micelle in an oil-in-water emulsion system and localisation of species involved in autoxidation and carotenoid bleaching processes.

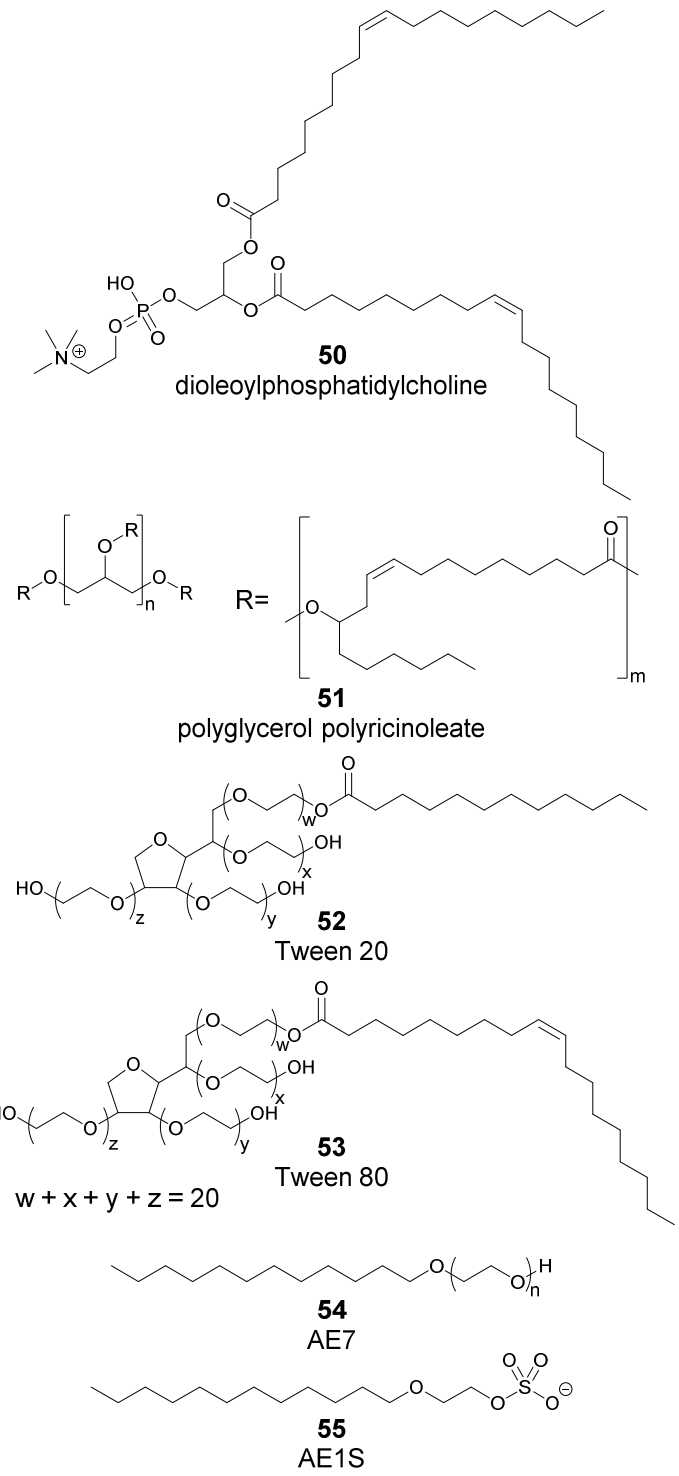

Figure 2.4 Structures of surfactants referred to in this thesis

Kittipongpittaya *et al.* compared the pro-oxidative activity of polar lipid oxidation products (aldehydes and ketones, see eq. 12), including free fatty acids and hydroperoxides,

in bulk oil and oil-in-water emulsions.[44] Polar lipid oxidation products in combination were able to promote oxidation in bulk oil but not in emulsions. When individual components of the polar fraction (free fatty acids and hydroperoxides separated by liquid chromatography) were tested no pro-oxidant activity was observed. The authors suggested that the lack of pro-oxidant activity was due to low accumulation of free fatty acid and hydroperoxide at the interface caused by a combination of relatively low concentrations of these components in the isolated polar products and out competition for interfacial space by the surfactants employed in the study, surfactant **52** (Tween 20) and **50** (dioleoylphosphatidylcholine).

The effect of fatty acid structure was investigated by Waraho *et al.* by oxidation measurements of oil-in-water emulsions in the presence of several C18 fatty acids of differing unsaturation and *cis-trans* stereochemistry (Table 2.2).[45] More oxidised samples contained a greater concentration of hydroperoxide and hexanal. Prior to this study, several reports found that more unsaturated fatty acids oxidised more rapidly in bulk oil[46] or bulk free fatty acid systems[47], however, the opposite was observed in oil-in-water emulsions.[48] Waraho *et al.* observed pro-oxidant activity in all fatty acids, however the effect decreased as unsaturation increased (see first section of Table 2.2). Additionally, linoelaidic acid **40** (*trans,trans*) possessed higher pro-oxidant activity compared to linoleic acid **10** (*cis,cis*), and was comparable to oleic **38** (*cis*) and elaidic **39** (*trans*) acid (see second section of Table 2.2).

Measurements of micelle surface charge also found that the presence of less unsaturated fatty acids resulted in more negative surface charge. Pro-oxidant activity was suggested to be related to fatty acid geometry – more linear fatty acids could have greater access to the micelle interface and consequently increase the negative charge at the surface. This would be expected to attract a greater concentration of metal ions to lipids within the micelle and promote initiation reactions.

Table 2.2 Extent of oxidation of 1.0% stripped soybean oil-in-water emulsions containing 0.50% (wt% of oil) of fatty acid additive at pH 7.0 during storage at 15 °C in two separate experiments.[45] Fatty acid structures shown in Fig. 2.1.

Additive	Hydroperoxide concentration after 5 days storage (mmol/kg oil)	Hexanal concentration after 5 days storage (mmol/kg oil)
None (Control)	310	6
Oleic Acid **38**	1000	37
Linoleic Acid **10**	820	20
Linolenic Acid **41**	510	10
None (Control)	50	3
Oleic Acid **38**	500	16
Linoleic Acid **10**	200	8
Elaidic Acid **39**	550	20
Linoelaidic **40**	500	15

Another study of fatty acid promoted oxidation in water-in-oil emulsions was performed by Yi *et al.* with a greater range of free fatty acids, including saturated examples, and employed polyglycerol polyricinoleate **51** as surfactant instead of the more hydrophilic Tween 20 **52**.[49] Induction times for oxidation were substantially decreased in the presence of oleic acid at concentrations as low as 0.05% w/w demonstrating the high pro-oxidant potential of free fatty acids. Experiments performed with a series of saturated acids found the order of pro-oxidant activity was lauric **35** > palmitic **36** > stearic **37** (see first section of Table 2.3). This order was also conserved for surface activity and negative charge of micelles containing these fatty acids in aqueous solutions at pH 7.0. In the presence of metal chelator, EDTA, the pro-oxidant activity of all fatty acids decreased but was still greater than control samples not containing fatty acid. The greater pro-oxidant activity of shorter chain saturated fatty acids was therefore attributed to higher surface activity allowing greater influence of the micelle surface charge at pH's that result in ionisation of the carboxylate group. The higher negative charge attracts pro-oxidant transition metals to the micelle, however, the authors suggested that other free fatty acid pro-oxidative

mechanisms must exist as samples containing fatty acid and EDTA still oxidised faster than control samples containing only EDTA. Contrary to Waraho *et al.* and others, pro-oxidant activity of unsaturated fatty acids increased with greater unsaturation (see first section of Table 2.3) and was suggested to be based on the greater susceptibility to hydroperoxide formation.

Table 2.3 Extent of oxidation of 2% water –in-stripped walnut oil emusions containing 0.50% w/w of emulsion fatty acid additive during storage at 45 °C in two separate experiments.[49]

Additive	Hydroperoxide concentration after 10 days storage (mmol/kg oil)	Hexanal concentration after 10 days storage (µmol/kg oil)
Control	900	800
Control + EDTA	200	300
Lauric Acid **35**	2500	2100
Lauric Acid **35** + EDTA	500	700
Palmitic Acid **36**	1400	1400
Palmitic Acid **36** + EDTA	400	400
Stearic Acid **37**	1100	1200
Stearic Acid **37** + EDTA	400	400
Control	300	800
Oleic Acid **38**	800	1800
Linoleic Acid **10**	1600	2000
Linolenic Acid **41**	2500	4000

2.2 Results

As described in Chapter 1, carotenoids are strongly coloured pigments that are found in a wide range of foodstuffs. Stains caused by carotenoid containing foods are difficult to completely remove from fabrics and are highly visible leading to an interest in new strategies to decolourise the remaining carotenoid material. One potential strategy is to employ lipoxygenase (LOXs), enzymes that catalyse the conversion of polyunsaturated fatty acids to hydroperoxides and subsequently accelerate the oxidative degradation of carotenoids. While there have been extensive studies of the LOX mechanism there has been no thorough quantitative assessment of the application of LOXs in carotenoid stain bleaching.

Similarly, there have been few quantitative studies of the background degradation of carotenoids in the presence of polyunsaturated acids under conditions that are representative of carotenoid stain bleaching in a wash cycle. Additionally, although there are many studies of fatty acid autoxidation and pro-oxidant behaviour within bulk oil and emulsion systems, no standard conditions for experiments have been established to allow for direct comparison, particularly with results from enzymatic systems. Notably, studies have mainly focused on bulk oil or water-in-oil emulsions as these systems are most analogous to carotenoid containing foodstuffs. Studies of lipoxygenase catalysed oxidation of fatty acids and bleaching of carotenoids, however, are performed in oil-in-water emulsions.

This chapter will report our studies of the effect of pH and surfactant conditions on initial rates of fatty acid autoxidation (as shown in Scheme 2.1 and 2.3 on p43 and 48, respectively) in oil-in-water emulsions. The structures of surfactants **52** (Tween 20), **53** (Tween 80), **54** (AE7) and **55** (AE1S), employed in these experiments, are shown in Fig. 2.4 (p56) and some of their physical properties are shown in Table 2.4.

Relative to the alcohol ethoxy (AE) class the Tween surfactants are larger molecules with molecular weights (MWs) approximately 3- to 4-fold greater. The structures of these two types of surfactants also differ significantly. While both contain a single hydrocarbon chain as a hydrophobic component, the AE surfactants possess a single linear chain structure with a small polar head group compared to the much larger, sorbitan ring and branched polyethoxylate chains comprising the polar region of the Tween surfactants. The larger polar region featured in the Tween surfactants results in higher hydrophilicity relative to AE surfactants which is reflected by the larger hydrophilicity-lipophilicity balance (HLB) and hydrophilicity index (HI) values. The polar head groups for Tween 20, 80 and AE7 are uncharged while the sulfate group of AE1S is negatively charged. The critical micelle concentration (CMC) of the studied surfactants range from 11 to 121 μg mL^{-1} and are in the order AE1S > Tween 20 > Tween 80 > AE7.

Table 2.4 Physical properties of surfactants studied

Surfactant	CMC[a]		Type	MW (g/mol)	HLB[b]	HI[c]
	(μg mL^{-1})	(μM)				
Tween 20 **52**	60-68[50]	49-55	Non-ionic	1227.54	16.7	15.9
Tween 80 **53**	13-15[50]	9.9-11.5	Non-ionic	1309.61	15.0	14.9
AE7 **54**	11[51]	22	Non-ionic	508.40	12-13	11.09
AE1S **55**	121[52]	390	Anionic	310.45	15.43	6.25

[a] Critical micelle concentration: concentration of surfactant at which micelles form. [b] Hydrophilicity-lipophilicity balance: quantitative comparison of hydrophilic and hydrophobic groups on a molecule.[53] [c] Hydrophilic index: MW of hydrophilic components as a proportion of total MW.[54]

The influence of fatty acid, pH and surfactant will also be quantified for the subsequent carotenoid oxidative degradation reaction (shown in Scheme 2.2) under the same experimental conditions. These conditions are maintained in experiments described in Chapter 3 which utilise LOXs to promote the carotenoid bleaching reaction. The present

results will be used in Chapter 3 to enable correction for background non-enzymatic oxidation of linoleic acid **10** and β-carotene bleaching from observed initial rates in the presence of enzyme.

Each experiment described in Section 2.2 is accompanied by a representative plot of the raw data (absorbance versus time) and table of calculated initial rates for one set of conditions. Tables of calculated initial rates for all conditions tested may be found in Appendix A.

2.2.1 Solubilisation of fatty acids and β-carotene in aqueous media

UV-Vis spectrophotometry was used to monitor the progress of reaction and thus required samples to be homogenous. Fatty acids were easily solubilised in the presence of surfactants **52** (Tween 20), **53** (Tween 80), **54** (AE7) and **55 (**AE1S) as detailed in Section 2.5, however, solubilisation of β-carotene **1** was more difficult. Acetone and ethanol were initially employed as cosolvents to solubilise β-carotene **1** as described by Ramadoss *et al.*,[55] however turbidity was observed in stock solutions of β-carotene **1** in acetone of >0.05 mg mL^{-1}. Furthermore, the presence of acetone in analogous fatty acid experiments interfered with absorbance measurements.

A procedure was attempted utilising chlorinated solvents and surfactants including **52** (Tween 20), **53** (Tween 80), **54** (AE7) and **55 (**AE1S) to initially form a residue[56] of β-carotene **1**. Homogenous, aqueous stock solutions containing 0.1 mg mL^{-1} β-carotene **1** were produced with surfactants **53** (Tween 80) and **54** (AE7) at concentrations ≥ 10 mg mL^{-1}. At lower surfactant concentrations or when utilising surfactants **52** (Tween 20) or **55 (**AE1S), insoluble red particles were observed.

2.2.2 Autoxidation reactions of linoleic acid followed by UV-Vis spectrophotometry

Autoxidation of linoleic acid **10** was studied initially in the absence of β-carotene **1** to measure the effect of pH on the background formation of hydroperoxide **13**. A concentration of 500 μM linoleic acid **10** was chosen in order to maintain identical conditions with enzymatic assays which require this concentration of substrate for LOXs to operate at maximal enzymatic activity, V_{max}. Data was not acquired at pH ≤ 4.00 with surfactant **54** (AE7) as solutions were turbid preventing UV-vis spectrophotometric measurements.

Autoxidation experiments were performed in buffered solutions of either 50 mM acetate (pH 4.00), phosphate (pH 6.50 – 8.00) or borate (pH 8.50 – 9.00) at 30 °C in the presence of surfactants **52** (Tween 20), **53** (Tween 80), **54** (AE7) and **55** (AE1S) (Fig. 2.4) at concentrations above the CMC. Reactions were initiated by addition of linoleic acid **10** stock solution stored at 0 °C, to cuvettes containing buffer at 30 °C.

A representative absorbance versus time plot obtained at pH 8.50 in the presence of surfactant **53** (Tween 80) is shown in Fig. 2.5. A representative set of initial rates observed in the presence of **53** (Tween 80) is shown in Table 2.4. Autoxidation of linoleic acid **10** was monitored by the increase in absorbance at 234 nm. The initial rate of change in absorbance at 234 nm was obtained from a linear fit in the steepest region of the absorbance versus time graph from the raw data. This value was used to calculate the initial rates of autoxidation using the extinction coefficient for linoleic acid hydroperoxide **13** (ε = 22,500 M^{-1} cm^{-1}).[57] From the data in the inset of Fig 2.5, the slope of the steepest linear region (0-12 min) was obtained as 2.0 x 10^{-3} ΔA_{234} min^{-1}, which corresponds to an initial rate of 0.089 μM min^{-1}. The observed initial rates for linoleic acid **10** autoxidation in the presence of the surfactants **52** (Tween 20), **53** (Tween 80), **54** (AE7) and **55** (AE1S) are shown in Tables A1 – A4 of Appendix A and the pH profile for each of the surfactants will be discussed in Section 2.3.

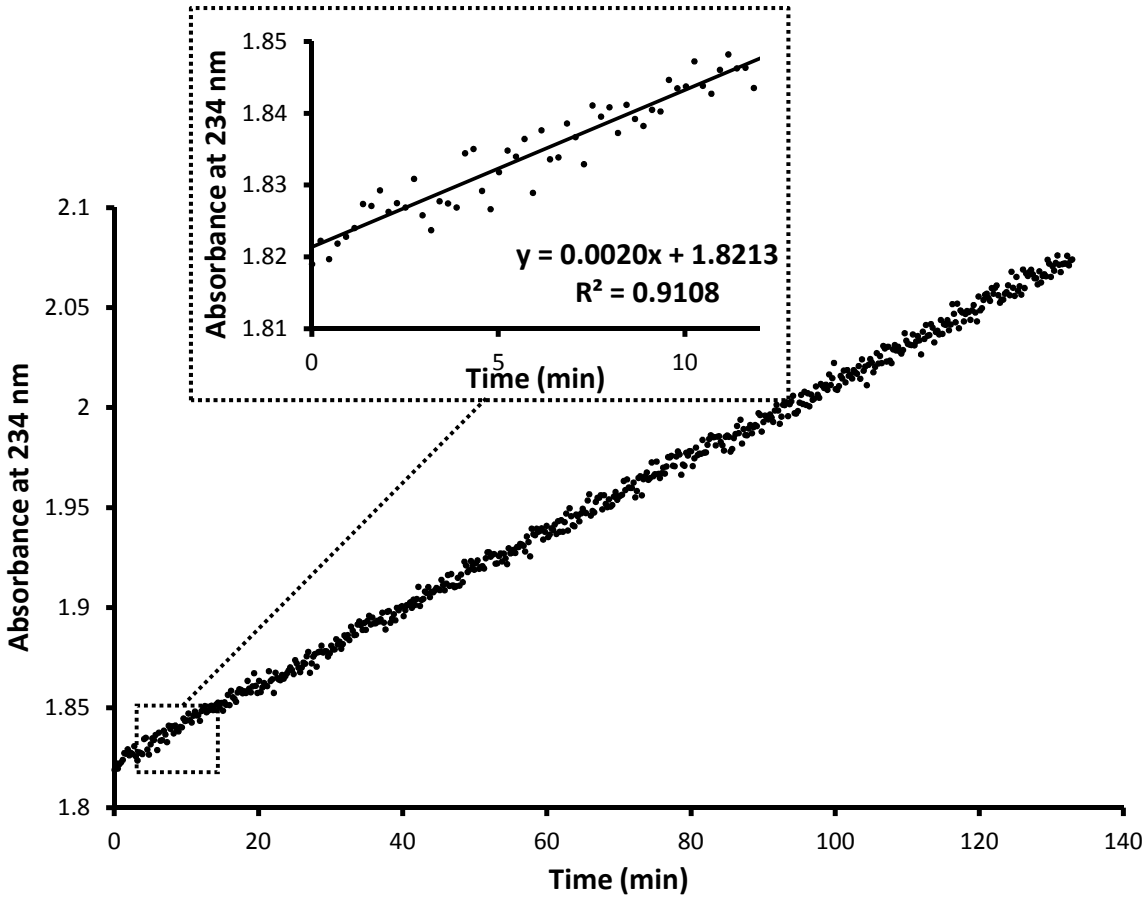

Figure 2.5 Representative plot of the oxidation of linoleic acid **10** (500 μM) over time (~2% conversion of substrate) in borate buffer (50 mM) with surfactant **53** (Tween 80) (200 μg ml^{-1}), at pH 8.50 and 30 °C. Inset shows linear region from 0-12 min of reaction.

Table 2.4 Initial rates of oxidation of linoleic acid in the presence of surfactant **53** (Tween 80).

pH[b]	Initial Rates (υ, μM min^{-1})[a]			
	υ1	υ2	υ3	υ_{av} ± SD[c]
4.00	7.11 x 10^{-2}	8.00 x 10^{-2}	8.44 x 10^{-2}	(7.85 ± 0.68) x 10^{-2}
6.50	1.87 x 10^{-1}	1.78 x 10^{-1}	1.87 x 10^{-1}	(1.84 ± 0.051) x 10^{-1}
7.00	1.47 x 10^{-1}	1.47 x 10^{-1}	2.18 x 10^{-1}	(1.70 ± 0.41) x 10^{-1}
7.50	1.24 x 10^{-1}	1.11 x 10^{-1}	1.11 x 10^{-1}	(1.16 ± 0.077) x 10^{-1}
8.00	1.38 x 10^{-1}	1.33 x 10^{-1}	1.38 x 10^{-1}	(1.36 ± 0.026) x 10^{-1}
8.50	8.89 x 10^{-2}	1.02 x 10^{-1}	7.11 x 10^{-2}	(8.74 ± 1.6) x 10^{-2}
9.00	1.60 x 10^{-1}	1.24 x 10^{-1}	1.11 x 10^{-1}	(1.32 ± 0.25) x 10^{-1}

[a] Reaction mixtures were maintained at 30 °C and contained linoleic acid **10** (500 μM) and surfactant **53** (Tween 80) (200 μg ml^{-1}). [b] Acetate, phosphate or borate buffer (50 mM) were used to maintain pH 4.00, 6.50-8.00 and 8.50-9.00, respectively. [c] Standard deviation (SD) was calculated using the following formula: $SD = \sqrt{\frac{\sum(x-\mu)^2}{(n-1)}}$ where μ is the mean and n is the number of samples.

2.2.3 Oxidative degradation of β-carotene followed by UV-Vis spectrophotometry

Oxidative degradation of β-carotene **1** was initially studied in the absence of fatty acids to assess the intrinsic oxidative stability of β-carotene **1** under our conditions. Oxidative degradation was then studied in the presence of linoleic acid **10** over the same pH range tested in section 2.2.1 (pH 4.00 – 9.00) and then in the presence of fatty acids of different degrees of unsaturation over a range of fatty acid concentrations.

Bleaching experiments were performed in buffered solutions of either 50 mM acetate (pH 4.00), phosphate (pH 6.50 – 8.00) or borate (pH 8.50 – 9.00) at 30 °C in the presence of surfactants **53** (Tween 80) and **54** (AE7) (Fig. 2.4). For bleaching experiments in the absence of fatty acids, reactions were initiated by addition of β-carotene **1** stock solution at 0 °C, to cuvettes containing buffer at 30 °C.

A representative absorbance versus time plot obtained at pH 9.00 in the presence of surfactant **54** (AE7) is shown in Fig. 2.6. A representative set of initial rates observed in the presence of surfactant **54** (AE7) is shown in Table 2.5. Initial rates of bleaching of β-carotene **1** were determined from fitting the steepest linear region of plots of absorbance at 456 nm versus time. Absorbance units were converted to concentration using the extinction coefficient for β-carotene **1** (ε = 130000 M^{-1} cm^{-1}).[58] From the data in the inset of Fig 2.4, the slope of the steepest linear region (0-12 min) was obtained as 1.0 x 10^{-4} ΔA_{456} min^{-1}, which corresponds to an initial rate of 0.77 nM min^{-1}. The observed initial rates for β-carotene **1** bleaching in the absence of fatty acid and the presence of the surfactants **53** (Tween 80) and **54** (AE7) are shown in Tables A5 and A6 of Appendix and graphs of initial rates at pH 4.0, 6.5 and 9.0 will be discussed in Section 2.3.

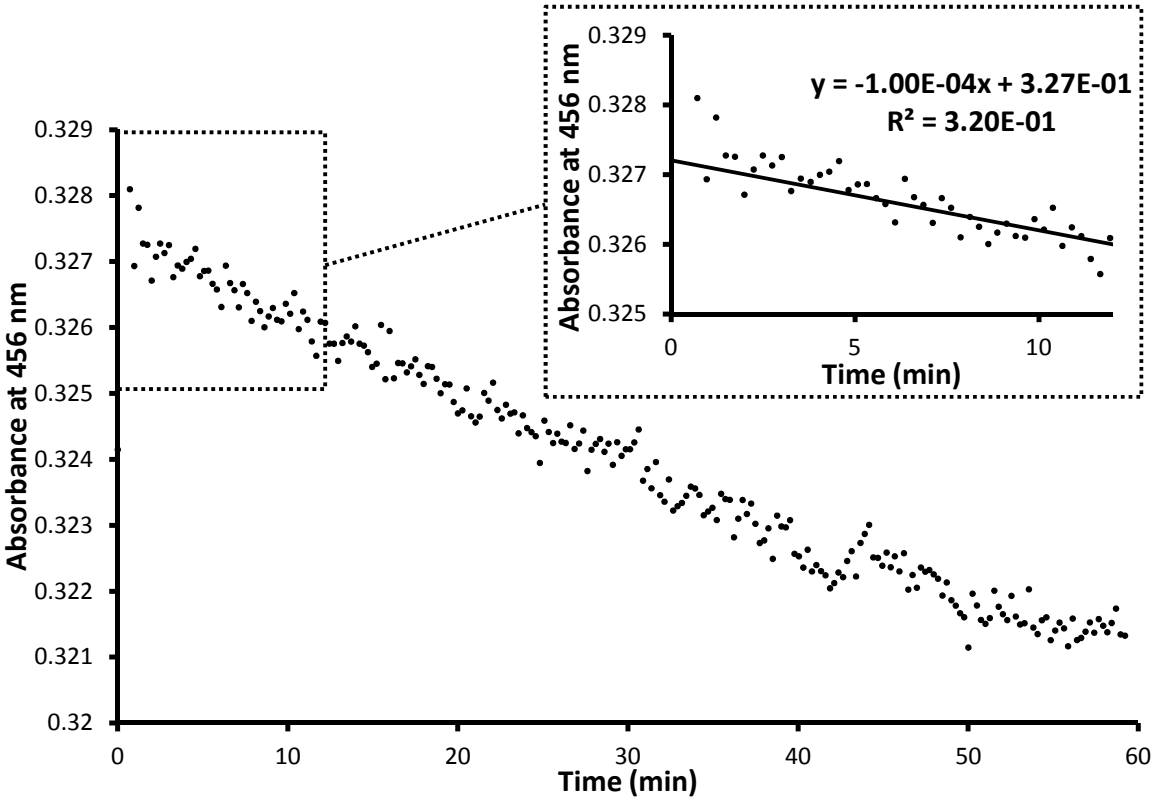

Figure 2.6 Representative plot of the bleaching of β-carotene **1** (3.1 μM) against time (~2% conversion of substrate) in 50 mM borate buffer with surfactant **54** (AE7) (167 μg ml^{-1}) in the absence of fatty acid at pH 9.0 and 30 °C. Inset shows linear region from 0-12 min of reaction.

Table 2.5 Initial rates of oxidative of β-carotene **1** degradation (bleaching) with **49** (AE7) as surfactant.

pH[b]	Initial Rates (υ, μM min^{-1})[a]			
	υ1	υ2	υ3	υ_{av} ± SD[c]
4.00	1.54 x 10^{-3}	2.31 x 10^{-3}	1.54 x 10^{-3}	(1.79 ± 0.44) x 10^{-3}
6.50	1.54 x 10^{-3}	6.20 x 10^{-4}	7.70 x 10^{-4}	(0.97 ± 0.49) x 10^{-4}
9.00	2.31 x 10^{-3}	1.54 x 10^{-3}	7.70 x 10^{-4}	(1.54 ± 0.77) x 10^{-3}

[a] Reaction mixtures were maintained at 30 °C and contained β-carotene **1** (3.1 μM) and surfactant **54** (AE7) (167 μg ml^{-1}). [b] Acetate, phosphate or borate buffer (50 mM) were used to maintain pH 4.00, 6.50 and 9.00, respectively. [c] Standard deviation (SD) was calculated using the following formula: $SD = \sqrt{\frac{\sum(x-\mu)^2}{(n-1)}}$ where μ is the mean and n is the number of samples.

Initial bleaching experiments in the presence of linoleic acid **10** were performed in buffered solutions of either 50 mM acetate (pH 4.00), phosphate (pH 6.50 – 8.00) or borate (pH 8.50 – 9.00) at 30 °C. Further experiments in the presence of stearic **37**, oleic **38**, linoleic **10**, linolenic **41** and arachidonic acid **42** were performed in buffered solutions of 50 mM phosphate (pH 7.00). For bleaching experiments in the presence of fatty acid, reactions were initiated by addition of fatty acid stock solution at 0 °C, to cuvettes containing a mixture of buffer and β-carotene **1** stock solution at 30 °C.

A representative absorbance versus time plot obtained at pH 7.00 in the presence of linoleic acid **10** and surfactant **53** (Tween 80) is shown in Fig. 2.7 and a representative set of initial rates observed in the presence of **53** (Tween 80) is shown in Table 2.6. From the data in Fig 2.6, the slope of the steepest linear region (0-5 min) was obtained as 1.34 x 10^{-2} ΔA_{456} min^{-1}, which corresponds to an initial rate of 1.03 x 10^{-1} μM min^{-1}. The observed initial rates for bleaching of β-carotene **1** in the presence of linoleic acid **10** and the

presence of surfactants **53** (Tween 80) and **54** (AE7) are shown in Tables A7 and A8 of Appendix A and a pH profile for each of the surfactants will be discussed in Section 2.3.

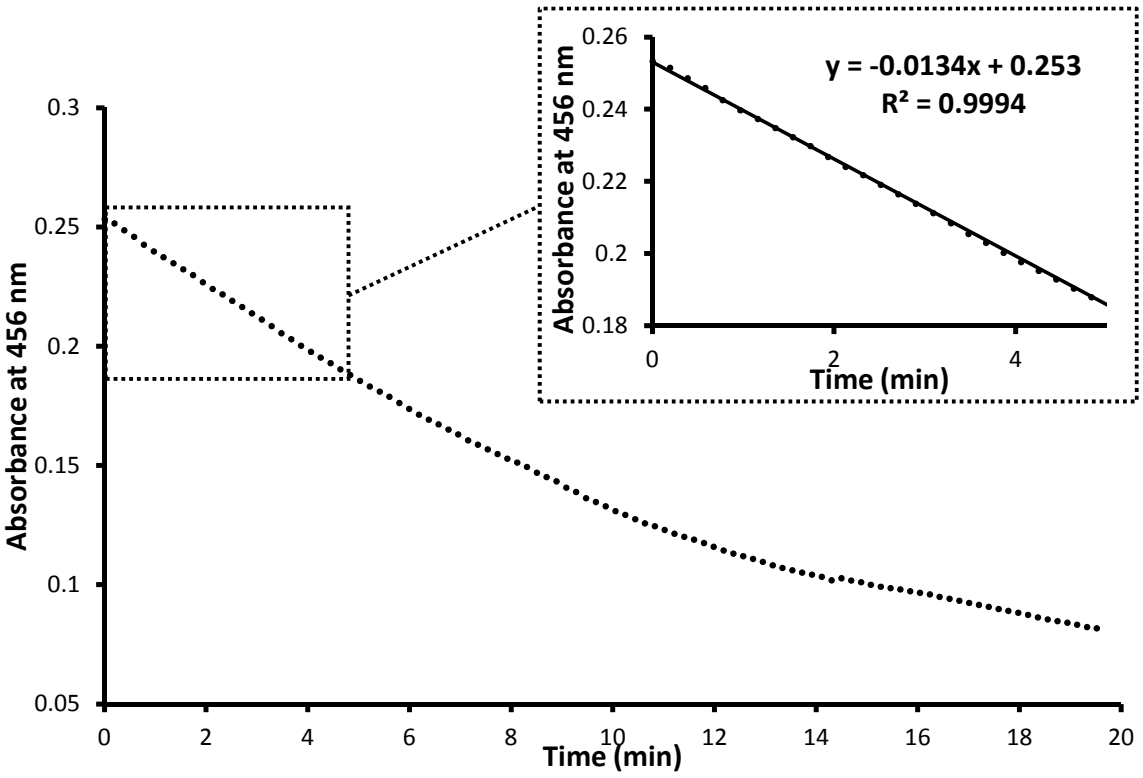

Figure 2.7 Representative plot of bleaching of β-carotene **1** (3.1 μM) against time (~80% conversion of substrate) in the presence of linoleic acid **10** (500 μM) with surfactant **53** (Tween 80) (367 μg ml^{-1}) at pH 7.0 and 30 °C. Inset shows linear region from 0-5 min of reaction.

Table 2.6 Initial rates of oxidative degradation (bleaching) of β-carotene **1** in the presence of linoleic acid **10** with surfactant **53** (Tween 80).

pH[b]	Rate Constants (μM min^{-1})[a]			
	υ1	υ2	υ3	υ_{av} ± SD[c]
4.00	4.60 x 10^{-3}	3.10 x 10^{-3}	4.60 x 10^{-3}	(4.10 ± 0.90) x 10^{-3}
6.50	5.08 x 10^{-2}	4.77 x 10^{-2}	6.23 x 10^{-2}	(5.36 ± 0.77) x 10^{-2}
7.00	1.03 x 10^{-1}	9.92 x 10^{-2}	1.01 x 10^{-1}	(1.01 ± 0.019) x 10^{-1}
7.50	7.46 x 10^{-2}	8.38 x 10^{-2}	7.62 x 10^{-2}	(7.82 ± 0.49) x 10^{-2}
8.00	3.62 x 10^{-2}	3.15 x 10^{-2}	3.31 x 10^{-2}	(3.36 ± 0.24) x 10^{-2}
8.50	1.77 x 10^{-2}	2.00 x 10^{-2}	2.31 x 10^{-2}	(2.03 ± 0.27) x 10^{-2}
9.00	2.38 x 10^{-2}	1.92 x 10^{-2}	2.77 x 10^{-2}	(2.36 ± 0.42) x 10^{-2}

[a] Reaction mixtures were maintained at 30 °C and contained β-carotene **1** (3.1 μM), linoleic acid **10** (500 μM), **53** (Tween 80) (367 μg ml^{-1}). [b] Acetate, phosphate or borate buffer (50 mM) were used to maintain pH 4.00, 6.50-8.00 and 8.50-9.00, respectively. [c] Standard deviation (SD) was calculated using the following formula: $SD = \sqrt{\frac{\sum(x-\mu)^2}{(n-1)}}$ where μ is the mean and n is the number of samples.

A representative absorbance versus time plot obtained at pH 7.00 in the presence of oleic acid **38** and surfactant **54** (AE7) is shown in Fig. 2.8 and a representative set of initial rates observed in the presence of **54** (AE7) is shown in Table 2.7. From the data in Fig 2.8, the slope of the steepest linear region (0-4 min) was obtained as 2.60 x 10^{-3} ΔA_{456} min^{-1}, which corresponds to an initial rate of 0.0200 μM min^{-1} after conversion using the extinction coefficient for β-carotene. The observed initial rates for β-carotene **1** bleaching in the presence of fatty acids **37**, **38**, **10**, **41** and **42** (structures shown in Fig. 2.1) and the presence of the surfactants **53** (Tween 80) and **54** (AE7) are shown in Tables A9 and A10 of Appendix A and an initial bleaching rate versus fatty acid concentration plot for each of the fatty acids and surfactants will be discussed in Section 2.3.

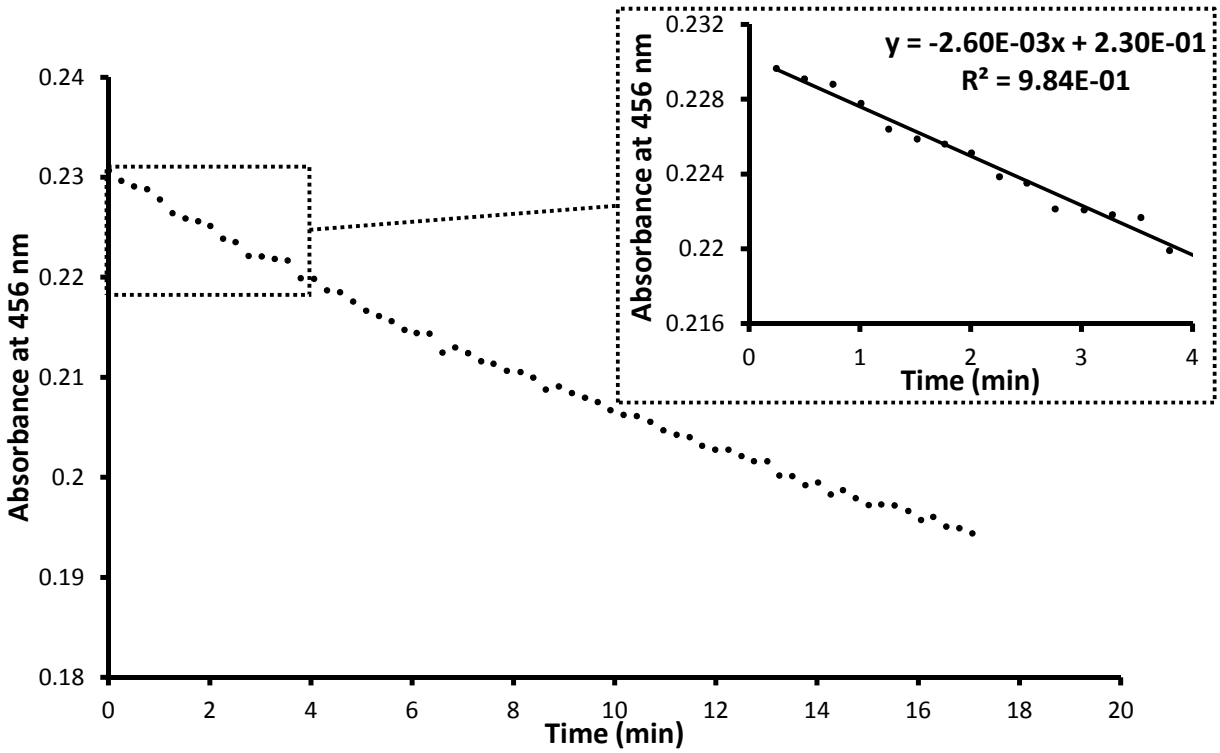

Figure 2.8 Representative plot of β-carotene **1** (3.1 μM) bleaching against time (~50% conversion of substrate) in the presence of oleic acid **38** (100 μM) at 30 °C with **54** (AE7) (367 μg ml^{-1}) as surfactant at pH 7.0. Inset shows linear region from 0-4 min of reaction.

Table 2.7 Initial rates of oxidative degradation (bleaching) of β-carotene **1** in the presence of fatty acid with surfactant **54** (AE7).

Fatty Acid	Concentration (μM)	Rate Constants (μM min^{-1})[a] υ1	υ2	υ_{av} ± SD[b]	Fatty Acid	Concentration (μM)	Rate Constants (μM min^{-1})[a] υ1	υ2	υ_{av} ± SD[b]
Stearic	10	3.80×10^{-3}	4.60×10^{-3}	$(4.20 \pm 0.50) \times 10^{-3}$	Linolenic	10	4.60×10^{-3}	3.80×10^{-3}	$(4.20 \pm 0.50) \times 10^{-3}$
37	50	1.08×10^{-2}	1.00×10^{-2}	$(1.04 \pm 0.050) \times 10^{-2}$	**41**	50	1.15×10^{-2}	1.54×10^{-2}	$(1.35 \pm 0.27) \times 10^{-2}$
	100	1.38×10^{-2}	1.38×10^{-2}	$(1.38 \pm 0.00) \times 10^{-2}$		100	1.23×10^{-2}	1.38×10^{-2}	$(1.31 \pm 0.11) \times 10^{-2}$
	500	6.20×10^{-3}	5.40×10^{-3}	$(5.80 \pm 0.50) \times 10^{-3}$		500	1.38×10^{-2}	1.62×10^{-2}	$(1.50 \pm 0.16) \times 10^{-2}$
Oleic	10	3.10×10^{-3}	3.10×10^{-3}	$(3.10 \pm 0.00) \times 10^{-3}$	Arachidonic	10	3.80×10^{-3}	3.80×10^{-3}	$(3.80 \pm 0.00) \times 10^{-3}$
38	50	1.15×10^{-2}	1.23×10^{-2}	$(1.19 \pm 0.050) \times 10^{-2}$	**42**	50	7.70×10^{-3}	6.90×10^{-3}	$(7.30 \pm 0.50) \times 10^{-3}$
	100	1.92×10^{-2}	2.00×10^{-2}	$(1.96 \pm 0.050) \times 10^{-2}$		100	1.08×10^{-2}	1.00×10^{-2}	$(1.04 \pm 0.050) \times 10^{-2}$
	500	3.31×10^{-2}	3.62×10^{-2}	$(3.46 \pm 0.22) \times 10^{-2}$		500	1.92×10^{-2}	1.62×10^{-2}	$(1.77 \pm 0.22) \times 10^{-2}$
Linoleic	10	4.60×10^{-3}	3.10×10^{-3}	$(3.80 \pm 1.1) \times 10^{-3}$					
10	50	1.23×10^{-2}	1.31×10^{-2}	$(1.27 \pm 0.050) \times 10^{-2}$					
	100	2.92×10^{-2}	2.92×10^{-2}	$(2.92 \pm 0.00) \times 10^{-2}$					
	500	5.54×10^{-2}	6.08×10^{-2}	$(5.81 \pm 0.38) \times 10^{-2}$					

[a]Reaction mixtures were maintained at 30 °C and contained fatty acid, β-carotene **1** (3.1 μM), surfactant **54** (AE7) (367 μg ml^{-1}) and phosphate buffer (50 mM) to maintain pH 7.00. [b]Standard deviation(SD) was calculated using the following formula: $SD = \sqrt{\frac{\sum(x-\mu)^2}{(n-1)}}$ where μ is the mean and n is the number of samples.

2.2.4 Micelle dynamics analysis by stopped-flow spectrophotometry

The dynamics of micelle structures within surfactant containing systems has been proposed to affect several physical processes in industry,[59] and may also influence the autoxidation of fatty acids and the oxidative degradation of carotenoids within our experiments. Micelle dynamics involves two relaxation processes: the rapid exchange of monomers in bulk solution and monomers within micelles (τ_1, μs timescale), and the formation and disassembly of micelles (τ_2, ms to min timescale). Measurements of τ_2 employing stopped-flow apparatus were attempted using buffered solutions containing dye material Eosin Y (2 mM) and either surfactant **53** (Tween 80) or **54** (AE7). Initially, λ_{max} changes of Eosin Y were studied in surfactants **53** (Tween 80) and **54** (AE7). Data from these measurements were then used to select appropriate surfactant concentrations for the determination of micelle kinetics.

Measurements of the UV-visible absorbance spectra of Eosin Y in the presence of surfactants **53** (Tween 80) and **54** (AE7) were performed in buffered solutions (1% phosphate or carbonate) with either linoleic acid **10**, oleic acid **38**, stearic acid **37**, β-carotene **1** or no substrate. Representative absorbance versus wavelength plots of Eosin Y obtained in buffered solutions (1% phosphate) containing surfactant **53** (Tween 80) are shown in Fig. 2.9A and a representative plot of λ_{max} versus surfactant concentration is shown in Fig. 2.9B. A representative set of λ_{max} measurements for Eosin Y with surfactant **53** (Tween 80) in the presence of different substrates and buffer systems is shown in Table 2.8. Complete sets of measurements are shown in Tables A11 and A12 of Appendix A.

A

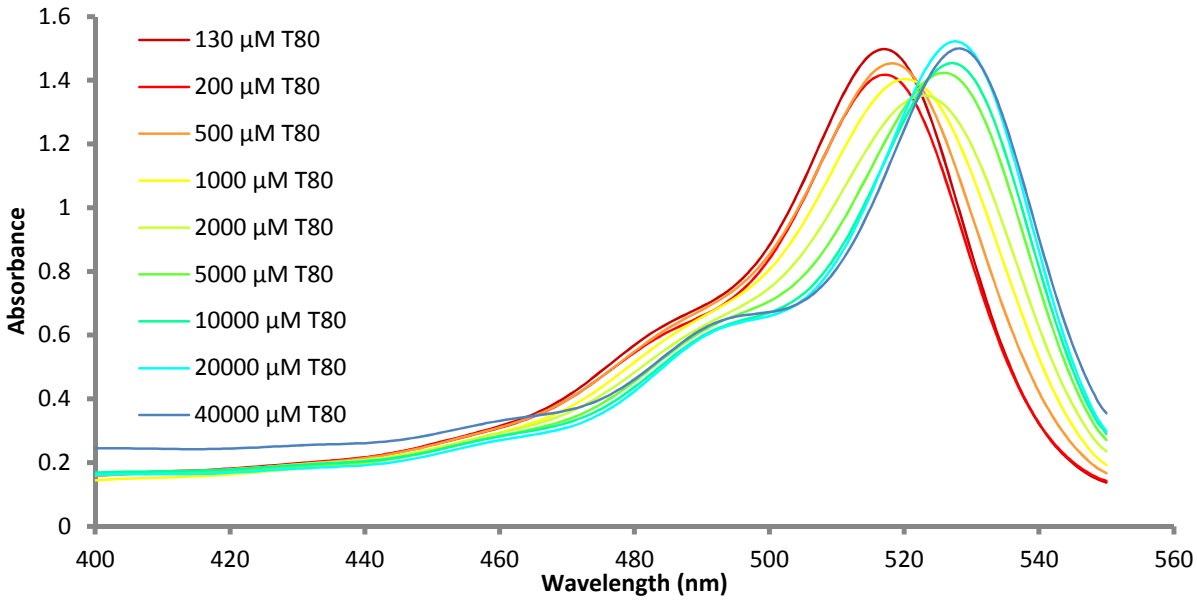

B

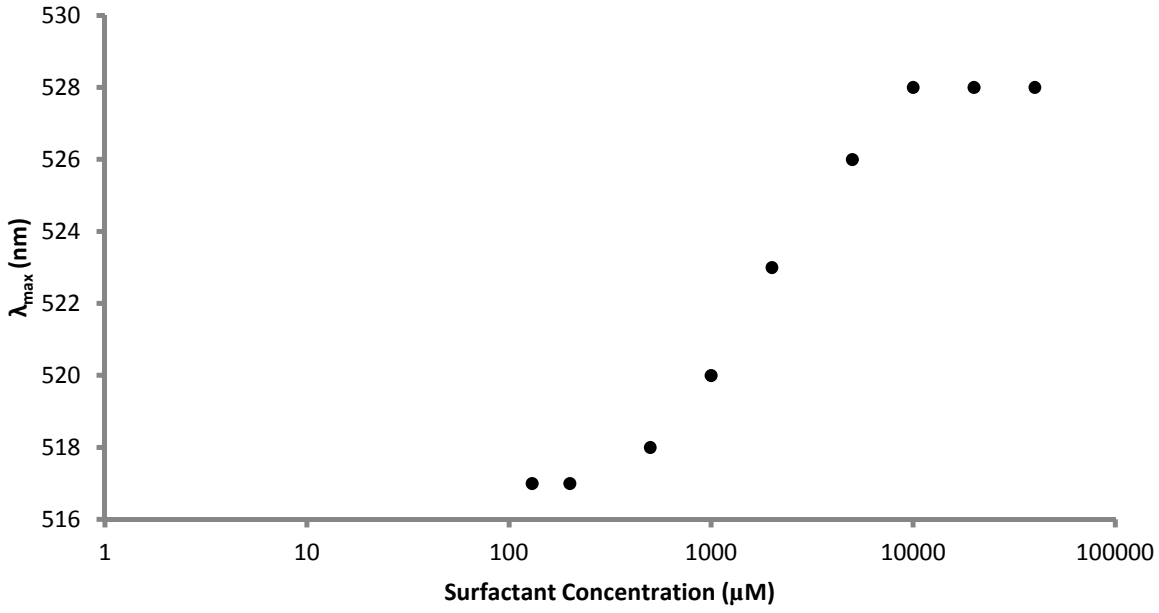

Figure 2.9 Representative plots of (A) absorbance spectra of Eosin Y in phosphate buffer with surfactant **53** (Tween 80) and (B) changes in λ_{max} of Eosin Y as a function of surfactant **53** (Tween 80) concentration at 30 °C.

Table 2.8 Range of concentrations of surfactant **53** (Tween 80) showing changes in Eosin Y λ_{max} (517–528 nm).

Buffer System[a]	Substrate Additives	Surfactant concentration range (mM)
KH_2PO_4	none	0.20-10.00
K_2CO_3	none	0.20-10.00
KH_2PO_4	500 μM linoleic acid **10**	1.00-20.00
K_2CO_3	500 μM linoleic acid **10**	1.00-10.00
KH_2PO_4	3.2 μM β-carotene **1**	0.20-10.00
K_2CO_3	3.2 μM β-carotene **1**	0.50-10.00
KH_2PO_4	500 μM linoleic acid **10**, 3.2 μM β-carotene **1**	1.00-20.00
K_2CO_3	500 μM linoleic acid **10**, 3.2 μM β-carotene **1**	1.00-20.00
KH_2PO_4	500 μM oleic acid **38**	1.00-20.00
K_2CO_3	500 μM oleic acid **38**	1.00-20.00

[a]1% buffer concentration at 30 °C.

Measurements of τ_2 were attempted utilising a stopped flow apparatus to rapidly dilute the concentration of surfactant and monitor the change in absorbance spectra of Eosin Y. Representative spectra of Eosin Y in the presence of surfactant **53** (Tween 80) and linoleic acid **10** are shown in Fig. 2.10.

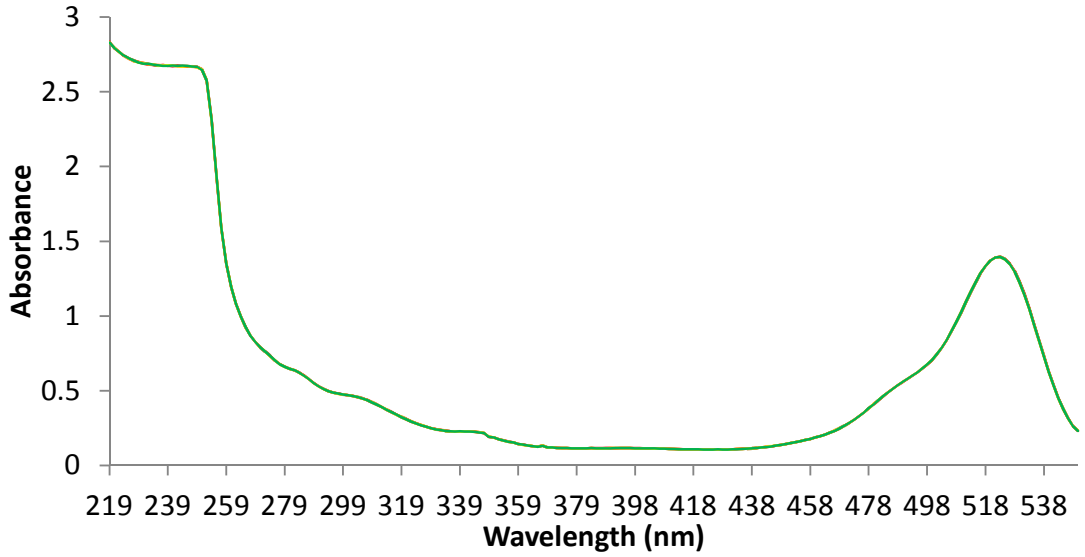

Figure 2.10 Representative absorbance spectrum of Eosin Y over time in phosphate buffer in the presence of linoleic acid **10** upon dilution of surfactant **53** (Tween 80) concentration from 5000 to 2500 μM monitored utilizing stopped flow apparatus. No changes in absorbance over the monitored wavelengths was observed over time (30 – 510 s).

2.3 Discussion

2.3.1 Autoxidation of linoleic acid

The pH-dependence of the initial rates of oxidation of linoleic acid 11 is shown in Fig 2.11 for four surfactants. Over the pH range tested, initial rates of linoleic acid **10** autoxidation were greatest in samples employing **55** (AE1S) as surfactant. Initial autoxidation rates in the presence of **52** (Tween 20) were approximately 10% lower, while those in presence of **53** (Tween 80) and **54** (AE7) were 2- to 3-fold lower and showed altered pH dependencies. Initial rates for autoxidation in the presence of **55** (AE1S) and **52** (Tween 20) decrease as pH increases, with a 90% decrease in initial rates at pH 9.0 relative to pH 4.0. In comparison, the effect of pH in the presence of **53** (Tween 80) and **54** (AE7) is smaller with differences between initial rates of < 20% in the pH range 6.50-8.0.

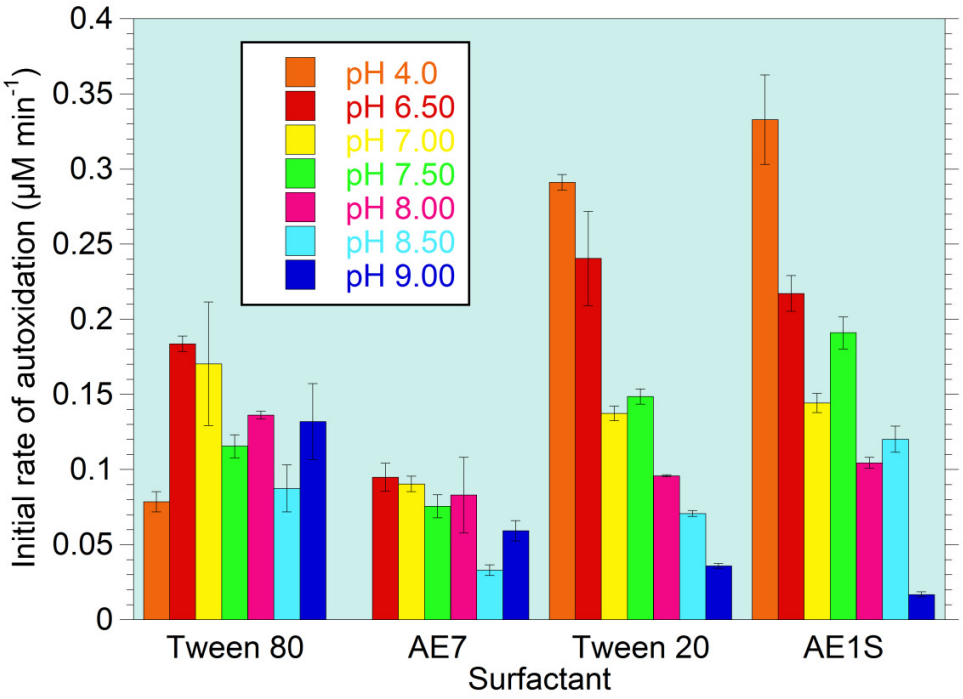

Figure 2.11 pH-Initial rate profile of the oxidation of linoleic acid **10** (500 μM) in buffered aqueous media in the presence of surfactant (200 μg ml^{-1}).

There are numerous reports on studies of the effect of pH on the oxidative stability of fatty acids with many authors highlighting the role of metal ions and the fatty acid carboxylate group as key factors. Studies of fatty acid autoxidation in oil-in-water emulsions of fish and flaxseed oil stabilised by either **53** (Tween 80) or sodium dodecyl sulphate (SDS) reported greater rates of oxidation at pH 3.0 compared to pH 7.0. [60,61,62] The authors of these reports attributed these results to greater solubility of transition metal ions at low pH. Additionally, in experiments containing reducing agents (ascorbate), low pH was predicted to facilitate the reduction of Fe^{3+} to Fe^{2+}. In contrast, other fatty acid oxidation studies in oil-in-water emulsions of salmon, canola and rapeseed oil employing **52** (Tween 20) and SDS as surfactant reported greater oxidation rates at higher pH. [63,64,65] The authors speculated that the pro-oxidant ability of the fatty acid carboxylate group could be dependent on the protonation state (pK_a ~5.2). At higher pH, with a greater proportion of deprotonated carboxylate groups, anionic fatty acids localising at the interface could attract cationic metal ions in bulk solution to the micelle surface.

Results for experiments with **52** (Tween 20) and **55** (AE1S) are in agreement with the former studies with greater initial oxidation rates observed at lower pH. Assays containing **53** (Tween 80) and 5**4** (AE7) also seem to follow a similar trend though initial rates over the observed pH range vary by a smaller extent. Surfactant properties in Table 2.4 show that the CMC and HLB values of **53** (Tween 80) and **54** (AE7) are lower relative to those of **52** (Tween 20) and **55** (AE1S). A lower CMC corresponds to a greater concentration of micelles at a given concentration of surfactant while a lower HLB represents greater affinity to hydrophobic molecules. A possible explanation for the reduced autoxidation pH dependency in **53** (Tween 80) and **54** (AE7) systems is that in the presence of these surfactants, linoleic acid **10** may be more sequestered away from the interface in the more hydrophobic interior with less influence over the micelle surface charge.

2.3.2 Oxidative degradation of β-carotene

To assess the intrinsic oxidative stability of β-carotene **1** under our experimental conditions, the oxidative cleavage of β-carotene **1** in the absence of fatty acid was initially monitored. Fig. 2.12 shows that all mixtures were found to be stable towards bleaching with initial rates of < 0.002 μM min^{-1} when measured overnight. The effect of surfactant or pH on bleaching under these conditions was not evaluated more broadly as absolute changes in absorbance were extremely small.

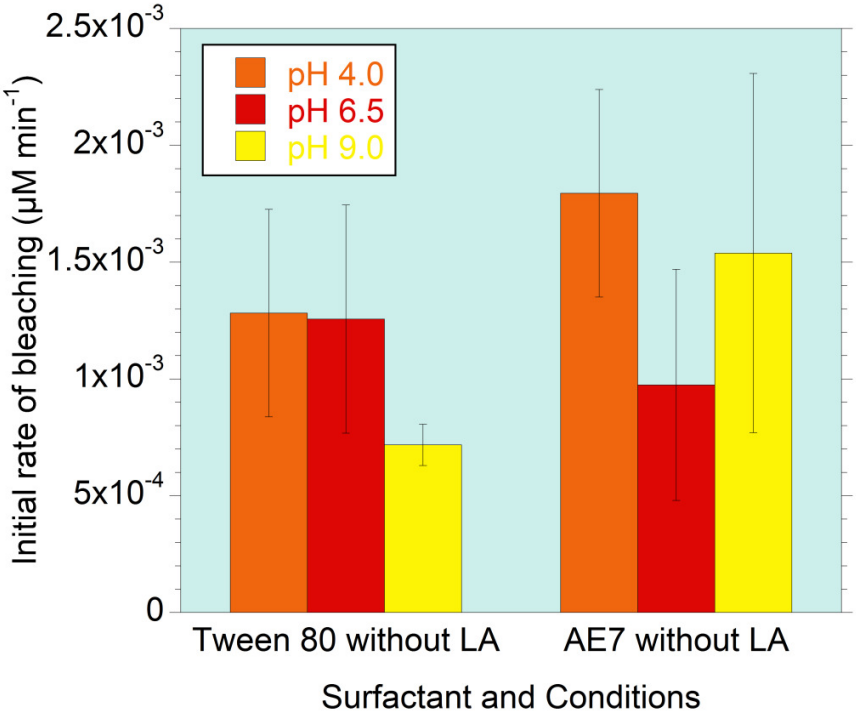

Figure 2.12 Initial rates of bleaching of β-carotene **1** (3.1 μM) in aqueous surfactant solutions (200 μg ml^{-1}) in the absence of fatty acid.

The process of linoleic acid dependent β-carotene oxidative degradation is shown in Scheme 2.2. Fig. 2.13 shows that the addition of 500 μM linoleic acid **10** to the reaction mixture increased the initial rate of bleaching of β-carotene **1** by up to two orders of magnitude depending on pH. The optimum pH for bleaching reactions in surfactants **53** (Tween 80) and **54** (AE7) was found to be pH 7.0 with a decrease in magnitude upon

moving to pH 4.0. Rates of oxidation of β-carotene **1** were ~2-fold faster in **53** (Tween 80) relative to **54** (AE7) as observed for the oxidation of linoleic acid **10**. Notable properties of **53** (Tween 80) are the relatively large mass compared to other low molecular weight surfactants, high hydrophilicity, and a critical micelle concentration (CMC) 26-fold lower than the surfactant concentration used in our studies (367 μg ml^{-1}). By comparison AE7 has an unbranched polyethoxylate structure, a smaller mass and volume occupied, more balanced hydrophilicity-hydrophobicity but similar CMC to Tween 80.

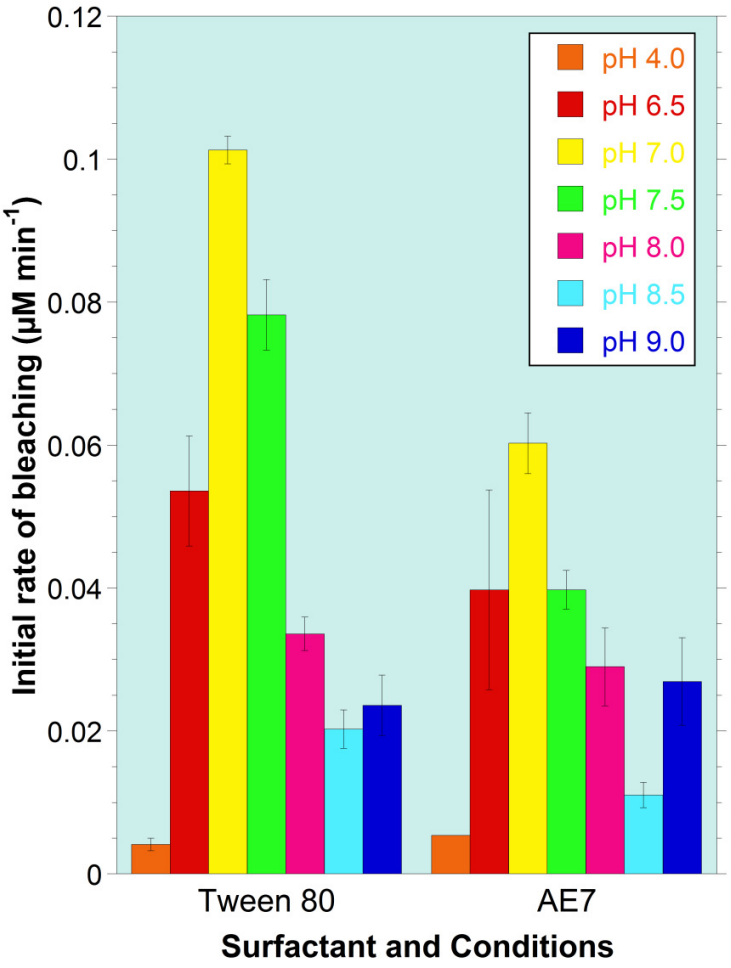

Figure 2.13 pH-Initial rate profile of bleaching of β-carotene **1** (3.1 μg ml^{-1}) in the presence of linoleic acid **10** (500 μM) and surfactant (367 μg ml^{-1}).

Both surfactants form a microemulsion in the reaction mixture due to the surfactant concentration being above the CMC. Carotenoids and fatty acids should preferentially locate within the hydrophobic core of micelles, while initial formation of radicals usually takes place in the aqueous phase. The reaction of molecules occupying different phases must therefore occur at the interface, which is heavily influenced by the concentration and type of surfactants present. The micelle structure of **54** (AE7) would be expected to be denser and thus the hydrophobic core of β-carotene could be less accessible to the aqueous phase. Additionally, the higher hydrophilicity of Tween 80, as indicated by higher HLB and HI values, may allow greater solubilisation of the more polar hydroperoxy fatty acid, facilitating greater interaction with β-carotene **1**.

The changes in initial rates for oxidation of linoleic acid **10** in the absence of β-carotene **1** over the same pH range were significantly smaller in the same surfactant solutions. Thus, observed changes in initial rates for oxidative bleaching of β-carotene **1** may not be simply ascribed to the generation of different concentrations of linoleic acid-derived radicals and other factors must also contribute including accessibility of these radicals to β-carotene **1**. Further investigation of the effect of fatty acid concentration and degree of unsaturation was performed at pH 7.0, the observed optimal pH for β-carotene **1** bleaching in the presence of linoleic acid.

2.3.3 Effect of degree of unsaturation of fatty acid

Overall, initial rates of bleaching of β-carotene **1** were comparable to background bleaching at fatty acid concentrations of 10 μM. Initial rates increased by 8 to 50-fold relative to background at 500 μM fatty acid. It was not possible to produce a homogenous stock solution of stearic acid with surfactant **53** (Tween 80) using our method, thus data was not obtained under these conditions. Under our conditions, maximal bleaching was observed in the presence of linoleic acid **10**. Fig. 2.14 shows that the observed order of β-carotene **1** bleaching in the presence of surfactant **53** (Tween 80) was as follows: linoleic **10** > oleic **38** > linolenic **41** > arachidonic acid **42**. A similar trend was observed in the

presence of surfactant **54** (AE7), with the initial rates of bleaching of stearic acid **37** comparable to linolenic acid **36**. Lower initial rates were observed in the presence of the more unsaturated acids, linolenic **41** and arachidonic acid **42**. This is likely a result of the increased susceptibility to self-oxidative cleavage, which depletes the active concentration of fatty acid (unavoidable oxidation was evident from immediate yellow colouration during stock preparation). In general, with the exception of stearic acid **37**, β-carotene **1** bleaching increased with the concentration of fatty acid. Although bleaching rates increased with fatty acid concentration, there is a levelling effect at higher concentrations. One possible explanation for this levelling effect is the saturation of fatty acids at the interface thereby limiting the extent of hydroperoxidation activity.

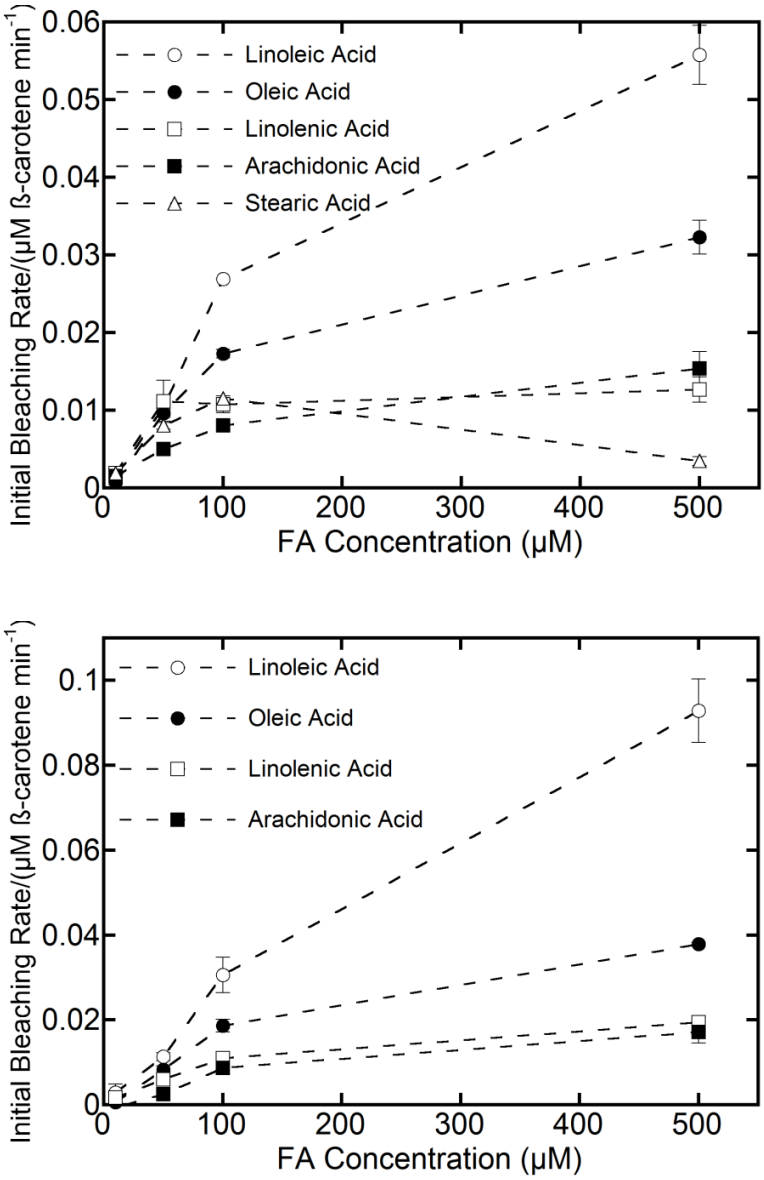

Figure 2.14 Initial rates of bleaching of β-carotene **1** (3.1 μM) in the presence of different concentrations of fatty acids utilising surfactant **54** (AE7) (top) or **53** (Tween 80) (bottom) (367 μg ml^{-1}). Dotted lines are for clarity and no specific fitting was attempted.

Surprisingly, stearic acid **37**, which lacks unsaturation, could promote bleaching of β-carotene in surfactant 5**4** (AE7) with a relatively high initial rate that was only ~1 to 14-fold lower than for linoleic acid **10** over the concentration range studied. This would not

be predicted if carotenoid bleaching was based exclusively on the rates of formation of radicals from fatty acid autoxidation. Rates of formation of these species are influenced by the strength of the C-H bond with saturated, allylic and bisallylic possessing ~105, 88 and 76 kcal mol-1, respectively, and on this basis, radical formation would be predicted to be significantly slower for stearic acid under our experimental conditions. In our observations, at 100 μM fatty acid, utilising AE7 as surfactant, the relative initial bleaching rates for stearic : oleic : linoleic acid were 1.0 : 1.5 : 2.3, respectively. An additional factor that could influence initial bleaching rates is accessibility of β-carotene **1** to fatty acid radicals, which will be influenced by rates for interchange of β-carotene **1** and fatty acids between micelles.

In order to probe micellar dynamics, measurements of τ_2 for systems containing **53** (Tween 80) or **54** (AE7) were attempted. The slow relaxation time, τ_2, corresponds to the formation of micelles from monomers of surfactant in bulk solution as well as the disassembly of micelles.[59] Measurements of τ_2 employed Eosin Y, a water soluble dye that integrates into micelles and has UV-Vis absorbance properties that are strongly influenced by the surrounding hydrophilic/hydrophilic environment. Measurements of λ_{max} were observed to change from 517 nm at low concentrations of surfactant to 528 nm at high concentrations. In the absence of fatty acid and β-carotene, these changes in λ_{max} occurred from 500–20000 μm of surfactant **54** (AE7) and 200–10000 μm of surfactant **53** (Tween 80). The addition of β-carotene did not significantly alter the surfactant concentration range over which these spectral changes were observed. However, the addition of fatty acids caused these changes in λ_{max} to be observed at higher concentrations of surfactant: 2000–40000 μm for surfactant **54** (AE7) and 1000–20000 μm for surfactant **53** (Tween 80).

Changes in λ_{max} for Eosin Y are likely to be dependent on the integration of dye molecules within the interior of micelle structures which may be sensitive to experimental conditions and not reflect the onset of formation of micelles. The integration of Eosin Y molecules may require the formation of micelle structures that are large enough to accommodate the

dye within the hydrophobic interior. Additionally, the integration of other hydrophobic molecules such as fatty acids may compete with dye. These measurements were therefore only used as an indicator for the surfactant concentration ranges over which changes in λ_{max} for Eosin Y may be observed.

Measurements of measurements of τ_2 were attempted utilising a stopped flow apparatus to dilute the concentration of surfactant within systems containing Eosin Y. Surfactant concentrations were selected using the data obtained for λ_{max} of Eosin Y versus surfactant concentration. These measurements showed no changes in absorbance spectra over time despite reports of τ_2 values for non-ionic systems having a second to minute timescale.[59] These measurements could indicate a rapid disassembly of micelles or possibly a fast dissociation of dye molecules from micelle structures.

Observed initial rates for bleaching are again consistently higher in surfactant **53** (Tween 80) relative to **54** (AE7) for equivalent fatty acid and β-carotene **1** concentrations. Initial bleaching rates were found to be consistently larger by up to 50% when identical concentrations of surfactant **53** (Tween 80) were used to solubilise substrates rather than **54** (AE7). As mentioned earlier, the differences in initial rates in these surfactant systems may be caused by a combination of the larger, more branched Tween 80 molecular structure forming a less densely packed micelle as well as possessing greater hydrophilicity allowing greater solubilisation of hydroperoxy fatty acids.

2.4 Summary

Although fatty acid autoxidation and fatty acid dependent oxidative cleavage of carotenoids is well-documented the majority of studies have been performed under conditions representative of carotenoid containing food stuffs (bulk oil or water-in-oil emulsions). Our experiments have quantified both fatty acid autoxidation and β-carotene **1** bleaching using UV-Vis spectrophotometry in buffered oil-in-water emulsions at 30 °C as a function of pH and surfactant. Additionally these conditions are analogous to those employed for LOX promoted linoleic acid **10** hydroperoxidation and β-carotene **1** bleaching, which will be presented in the following chapter, allowing for direct comparison between non-enzymatic and enzymatic systems.

Our results (Fig. 2.11) show that linoleic acid **10** autoxidation in an oil-in-water emulsion is highly influenced by surfactant but is relatively pH independent. The order of initial rates of autoxidation was observed to be surfactant **55** (AE1S) > **52** (Tween 20) > **53** (Tween 80) > **54** (AE7). Initial rates of autoxidation decreased as pH increased in all experiments, however, the effect of pH was observed to be less in the presence of surfactant **53** (Tween 80) and **54** (AE7) with only a ~20% difference in observed initial rates over the tested pH range. In contrast a ~90% decrease was observed between pH 4.0 to pH 9.0 in the presence of **55** (AE1S) and **52** (Tween 20). However, these differences were observed over the pH range of 4.0 to 9.0. Studies of the effect of pH have attributed these trends to the increased solubility of metal ions (key initiators in fatty acid autoxidation) at lower pH values. Differences in results in surfactant solutions may be dependent on some of the properties shown in Table 2.4 – surfactant **53** (Tween 80) and **54** (AE7) possess lower CMC and HLB values relative to **55** (AE1S) and **53** (Tween 20) which could affect micelle morphology and the accessibility of linoleic acid to the interface.

Under our experimental conditions, β-carotene **1** was observed to be relatively stable to degradation in the absence of fatty acid (Fig. 2.12). Addition of linoleic acid **10** (500 μM)

resulted in an increase in the initial rate of degradation of β-carotene **1** of 2 orders of magnitude (Fig. 2.13). Initial rates of degradation were found to be consistently 2-fold higher in the presence of surfactant **53** (Tween 80) compared to **54** (AE7) and the optimum pH was found to be pH 7.0 for both surfactant systems. The observed pH optimum may be the result of a combination of metal ion solubility at lower pH and the deprotonated state of fatty acid attracting trace metal ions in solution to the interface at higher pH. Due to the highly branched structure of **53** (Tween 80) relative to the linear structure of **54** (AE7), **53** (Tween 80) is expected to form less densely packed micelles allowing for greater accessibility to the hydrophobic interior and therefore greater degradation of β-carotene **1**. Additionally, the greater hydrophilicity of **53** (Tween 80) may facilitate the solubilisation of polar fatty acid hydroperoxides allowing greater interaction between β-carotene **1** and the bleaching species.

Further studies of β-carotene **1** degradation at pH 7.0 in the presence of fatty acids of varying unsaturation (Fig. 2.14) showed that all fatty acids, including saturated stearic acid **37**, promoted the degradation of β-carotene **1**. Linoleic acid **10** was found to accelerate β-carotene **1** degradation the most followed by oleic **38**, linolenic **41**, arachidonic **42** and stearic acid **37**. Although greater fatty acid unsaturation was predicted to increase the rate of hydroperoxide formation, arachidonic **42** and linolenic acid **41** were found to be highly susceptible to oxidation leading to autoxidation during stock preparation. Stearic acid **37** was not expected to promote bleaching at comparable initial rates as the other fatty acids due to the lack of unsaturation and therefore relatively slow formation of hydroperoxide species. Similar work in the literature attribute stearic acid **37** (saturated fatty acid) dependent β-carotene **1** degradation to the carboxylate group attracting metal ion initiators to the surface of the micelle.[49]

From the perspective of the detergent industry our results present several interesting observations. Although initial rates of bleaching were largest for linoleic acid **10** the presence of any free fatty acid significantly increased rates of β-carotene **1** bleaching. As

well as studying strategies to increase rates of fatty acid oxidation (by LOXs for example, which is discussed in Chapter 3) another potential method to promote β-carotene **1** bleaching could be to increase the concentration of free fatty acids in stain material. This may be achievable with lipases. These enzymes catalyse the hydrolysis of triglycerides to free fatty acids and glycerol, and are currently utilised in biological detergents. Another aspect of our results is that autoxidation of fatty acids and bleaching of β-carotene **1** were sensitive to the surfactant present in reaction mixtures. This could suggest that selection of certain surfactant properties in detergent formulations could be optimised for bleaching of carotenoid stains.

2.5 Experimental

2.5.1 Materials

Linoleic acid **10** (L1376), arachidonic acid **42** (A9673), stearic acid **37** (S4751), oleic acid **38** (O1008), linolenic acid **41** (L2376), β-carotene **1** (220c40), Tween 80 **53** (P1754) and Tween 20 **52** (P1379) surfactants were purchased from Sigma-Aldrich. AE7 **54** and AE1S **55** surfactants were kindly donated by Procter & Gamble.

2.5.2 Methods

2.5.2.1 Solubilisation of materials

A solution of β-carotene **1** in dichloromethane (1 mg/ml) was added to neat surfactant (100 mg ml^{-1} β-carotene **1** solution). The solvent was then evaporated under reduced pressure to afford a viscous, red residue. Deionised water (10 ml per 1 mg β-carotene **1**) was added to the residue and mixed until a homogenous orange solution was obtained.

Fatty acid was solubilised by addition of NaOH (800 µl, 0.5 M) to fatty acid (0.2 mmole) followed by addition of surfactant diluted in deionised water (4 ml, 4 mg/ml). The solution was gently mixed until homogenous then diluted by addition of deionised water (16.2 ml). Preparations of solutions containing stearic acid **37** necessitated heating to 70 °C while mixing. All other fatty acid solutions were prepared at room temperature.

2.5.2.2 Reaction mixture preparation

Stock solutions of β-carotene **1** and fatty acid were prepared immediately before use and stored at 0 °C. The pH of reaction mixtures were maintained using 50 mM buffer (acetate pH 4.5-6.0, phosphate pH 6.5-8.0, borate pH 8.5-10.0). Stock solutions of β-carotene **1** (50 µL) and buffer (2800 µL) were initially mixed in the cuvette, followed by addition of linoleic acid (150 µL) to initiate the bleaching reaction.

2.5.2.3 Absorbance measurements

Absorbance measurements were obtained using Varian Cary 50 and Cary 100 UV-visible spectrophotometers. The Kinetics Program was used to measure absorbance at 234 nm and 456 nm to monitor fatty acid hydroperoxidation and carotenoid cooxidation, respectively. Triplicate runs of each assay at each condition were performed. A PCB-150 Peltier water bath and Peltier heating/refrigeration unit were employed to maintain a constant temperature of 30 °C. Measurements were made in 3 ml quartz cuvettes with 1 cm path length. Changes in absorbance units per minute were converted to concentration per minute using extinction coefficients of 140,000 and 22,500 M^{-1} cm^{-1} for β-carotene **1** and fatty acid hydroperoxide respectively.[57,58]

2.6 References

[1] C. C. Berton-Carabin, M.-H. Ropers and C. Genot, *Compr. Rev. Food Sci. Food Saf.*, 2014, **13**, 945–977.
[2] E. G. Hammond and P. J. White, *J. Am. Oil Chem. Soc.*, 2011, **88**, 891–897.
[3] H. Braconnot, *Ann. Chim.*, 1815, **93**, 271-277.
[4] C. H. Lea, *Proc. R. Soc. Lond. Ser. B. Biol. Sci.*, 1931, **108**, 175-189.
[5] L. Bateman, *Quart. Rev.*, 1954, **8**, 147-167.
[6] H. N. Stephens, *J. Am. Chem. Soc.*, 1928, **50**, 568-571.
[7] R. Criegee, H. Pilz and H. Flygare, *Ber. Deuts. Chem. Gesel.*, 1933, **72B**, 1799-1804.
[8] E. H. Farmer and A. Sundralingam, *J. Chem. Soc.*, 1942, **1942**, 121-139.
[9] E. H. Farmer and D. A. Sutton, *J. Chem. Soc.*, 1946, **1946**, 10-13.
[10] J. L. Bolland and G. Gee, *Trans. Faraday Soc.*, 1946, **42**, 236-243.
[11] J. L. Bolland, *Trans. Faraday Soc.*, 1950, **46**, 358-368.
[12] J. L. Bolland and P. ten Have, *Proc. Int. Cong. Pure Appl. Chem.*, 1947, **11**, 325-332.
[13] H. D. Belitz, W. Grosch and P. Schieberle, *Food Chem. 3rd Rev. Ed.*, 2004, Springer-Verlag Berlin Heidelberg.
[14] K. M. Schaich, *Bailey's Industrial Oil and Fat Products*, 2005, John Wiley & Sons.
[15] E. N. Frankel, *J. Sci. Food Agric.*, 1991, **54**, 495–511.
[16] E. N. Frankel, *Lipid Oxidation*, 2005, Oily Press.
[17] N. A. Porter, *Am. Chem. Soc.*, 1986, **19**, 262–268.
[18] H. W. Gardner, *Free Radic. Biol. Med.*, 1989, **7**, 65–86.
[19] R. Holman and O. Elmer, *J. Am. Oil Chem. Soc.*, 1947, **24**, 127–129.
[20] J. P. Cosgrove, D. F. Church and W. A. Pryor, *Lipids*, 1987, **22**, 299–304.
[21] D. A. Pratt, K. A. Tallman and N. A. Porter, *Acc. Chem. Res.*, 2011, **44**, 458–67.
[22] N. A Porter, *J. Org. Chem.*, 2013, **78**, 3511–24.
[23] N. A. Porter, S. E. Caldwell and K. A. Mills, *Lipids*, 1995, **30**, 277–290
[24] E. Bascetta, F. D. Gunstone and J. C. Walton, *J. Chem. Soc., Perkin Trans.* 2, 1984, 401–409.
[25] A. R. Brash, *Lipids*, 2000, **35**,947–952.
[26] D. A. Pratt, K. A. Tallman and N. A. Porter, *Acc. Chem. Res.*, 2011, **44**, 458–67.
[27] K. A. Tallman, D. A. Pratt and N. Porter, *J. Am. Chem. Soc.*, 2001, **123**, 11827–11828.
[28] G. W. Burton and K. U. Ingold, *Acc. Chem. Res.*, 1986, **19**, 194–201.
[29] L. Ross, C. Barclay, M. R. Vinqvist, F. Antunes and R. E. Pinto, *J. Am. Chem. Soc.*, 1997, **119**, 5764–5765.
[30] A. J. Stirton, J. Turer and R. W. Riemenschneider , *Oil and Soap*, 1945, **4**, 81.
[31] B. R. R. Arndt, J. B. Barbour, E. J. Engles, D. H. S Horn and D. A. Sutton, *J. Chem. Soc.*, 1959, 3258.
[32] Z. K. Maizus, I. P. Skibida, N. M. Emanuel and V. N. Yakovleva, *Kinetica i Kataliz.*, 1960, **1**, 55.
[33] H. Nobori, *J. Soc. Chem. Ind. (Japan)*, 1942, **45**, 453.
[34] N. Nobori and M. Noguchi, *J. Soc. Chem. Ind. (Japan)*, 1942, **46**, 146.
[35] C. Paquot and F. de Goursac, *Bull. Soc. Chim. France*, 1950, 172.
[36] V. Ramanathan, T. Sakuragi and F. A. Kummerow, *J. Am. Oil Chem. Soc.*, 1959, **36**, 244.
[37] J. Nonaka, *Bull. Japan Soc. Sci. Fisheries*, 1954, **19**, 1001.
[38] J. G. Endres, V. R. Bhalerao and F. A. Kummerow, *J. Am. Oil Chem. Soc.*, 1962, **39**, 159–162.
[39] M. H. Brodnitz, W. W. Nawar and I. S. Fagerson, *Lipids*, 1968, **3**, 65–71.
[40] N. Frega, M. Mozzon and G. Lercker, *J. Am. Oil Chem. …*, 1999, **76**, 325–329.
[41] V. M. Paradiso, T. Gomes, R. Nasti, F. Caponio and C. Summo, *Food Res. Int.*, 2010, **43**, 1389–1394.
[42] K. Miyashita and T. Takagi, *J. Am. Oil Chem. Soc.*, 1986, **63**, 1380–1384.
[43] S. Aubourg, *J. Sci. Food Agric.*, 2001, **81**, 385–390.
[44] K. Kittipongpittaya, B. Chen, A. Panya, D. J. McClements and E. a. Decker, *J. Am. Oil Chem. Soc.*, 2012, **89**, 2187–2194.
[45] T. Waraho, D. J. McClements and E. a Decker, *Food Chem.*, 2011, **129**, 854–9.
[46] E. A. Decker and D. J. McClements, 2008, Chapter 4: Lipids in S. Damodaran, K. L. Parkin and O. R. Fennema (Eds.), *Fennema's Food Chemistry, 4th ed.*, (pp. 155–216). Boca Raton, FL: CRC Press
[47] T. Takagi and K. Miyashita, *J. Am. Oil Chem. Soc.*, 1987, **64**, 407–413.

[48] K. Miyashita and E. Nara, *Biosci. Biotechnol. Biochem.*, 1993, **57**, 1638–1640.
[49] J. Yi, Z. Zhu, W. Dong, D. J. McClements and E. A. Decker, *Eur. J. Lipid Sci. Technol.*, 2013, **115**, 1013–1020.
[50] S. K. Hait and S. P. Moulik, *Int. J. Thermophys.*, 2001, **4**, 303–309.
[51] C. Genova, U. Schoenkaes, D. Smith and M. Stolz, *J. Surfactants Deterg.*, 2003, **6**, 365-372
[52] M. F. Cox, *J. Am. Oil Chem.*, 1989, **66**, 1637–1646.
[53] W. C. Griffin, *J. Soc. Cosmet. Chem.*, 1949, **1**, 311-326.
[54] P. K. Reddy, E. S. Sadlowski, R. W. Boswell and J. W. English, *WO Pat.*, WO2000027958 A1, 2000
[55] C. S. Ramadoss, E. K. Pistorius and B. Axelrod, *Arch. Biochem. Biophys.*, 1978, **2**, 549–552.
[56] Z. Wu, D. S. Robinson, R. K. Hughes, R. Casey, D. Hardy and S. I. West, *J. Agric. Food Chem.*, 1999, **47**, 4899–906.
[57] M. J. Gibian and P. Vandenberg, *Anal. Biochem.*, 1987, **163**, 343–349.
[58] G. Britton, S. Liaaen-Jensen, and H. P. Pfander, *Carotenoids: handbook*., 2004, Birkhauser.
[59] A. Patist, J. R. Kanicky, P. K. Shukla and D. O. Shah, *J. Colloid Interface Sci.*, 2002, **245**, 1–15.
[60] A. M. Haahr and C. Jacobsen, *Eur. J. Lipid Sci. Technol.*, 2008, **110**, 949–961.
[61] A. D. M. Sørensen, A. M. Haahr, E. M. Becker, L. H. Skibsted, B. Bergenståhl, L. Nilsson and C. Jacobsen, *J. Agric. Food Chem.*, 2008, **56**, 1740–1750.
[62] G. F. Branco, M. I. Rodrigues, L. A. Gioielli and I. a. Castro, *J. Agric. Food Chem.*, 2011, **59**, 12183–12192.
[63] J. R. Mancuso, D. J. McClements and E. A. Decker, *J. Agric. Food Chem.*, 1999, **47**, 4112–4116.
[64] H. T. Osborn-Barnes and C. C. Akoh, *J. Agric. Food Chem.*, 2003, **51**, 6851–6855.
[65] C. Berton, M. H. Ropers, M. Viau and C. Genot, *J. Agric. Food Chem.*, 2011, **59**, 5052–5061.

CHAPTER 3

Enzymatic bleaching of β-carotene

3.0 Foreword

This chapter of the report will detail the aspects of lipoxygenases (LOXs) that are relevant to the project with the main focus on the structure, function and reaction mechanism. Key studies of plant and animal LOXs will be detailed to give a complete overview of the current knowledge of LOXs but particular emphasis will be placed on studies of LOX1 and LOX3 from soybean (*Glycine max*), the two enzymes investigated in the project. Section 3.1 introduces LOXs including their role in Nature, protein structure, catalytic mechanism and studies of the LOX1-LOX3 carotenoid bleaching synergy. Section 3.2 presents results from experiments monitoring the effect of pH and surfactant on LOX1/3 activity and expands upon the experiments performed in Chapter 2 on non-enzymatic bleaching by monitoring analogous experiments in the presence of enzymes. Section 3.3 discusses these results and a summary of our conclusions is in Section 3.4.

3.1 Introduction

3.1.1 LOX overview

LOXs (EC 1.13.11.-) are non-haem, iron containing enzymes that catalyse the conversion of polyunsaturated fatty acids containing a *Z,Z*-1,4-pentadiene moiety (such as linoleic acid **10**) into hydroperoxides by the insertion of oxygen as shown in Scheme 3.1. The mechanism for LOX catalysed oxidation of fatty acids is comparable to autoxidation (Scheme 2.1), proceeding through the same resonance stabilised radical intermediate, though reaction takes place within an active site with the assistance of a non-haem iron. Hydrogen abstraction is the initial and rate limiting step for the reaction. A C-H bond at the central methylene group of the 1,4-pentadiene moiety **10** is cleaved homolytically with electron transfer to the ferric non-haem iron and proton transfer to a hydroxide ligand. This step affords the resonance stabilised fatty acid radical intermediate **11** common to both autoxidation and LOX catalysed oxidation pathways. Under physiological conditions with LOX in a native conformation, molecular oxygen is directed to a specific face at one of the terminal ends of the 1,4-pentadiene radical system, forming the hydroperoxide radical **12**. Oxygen insertion and hydrogen abstraction have an antarafacial relationship, occurring on

opposite faces of the plane formed by the pentadiene system. Hydrogen transfer to the hydroperoxide radical **12** occurs in two steps: electron transfer from the ferrous non-haem iron, regenerating the ferric iron and reducing the radical **12** to the hydroperoxide anion **56**; followed by proton transfer from the water ligand to yield the fatty acid hydroperoxide **13**.

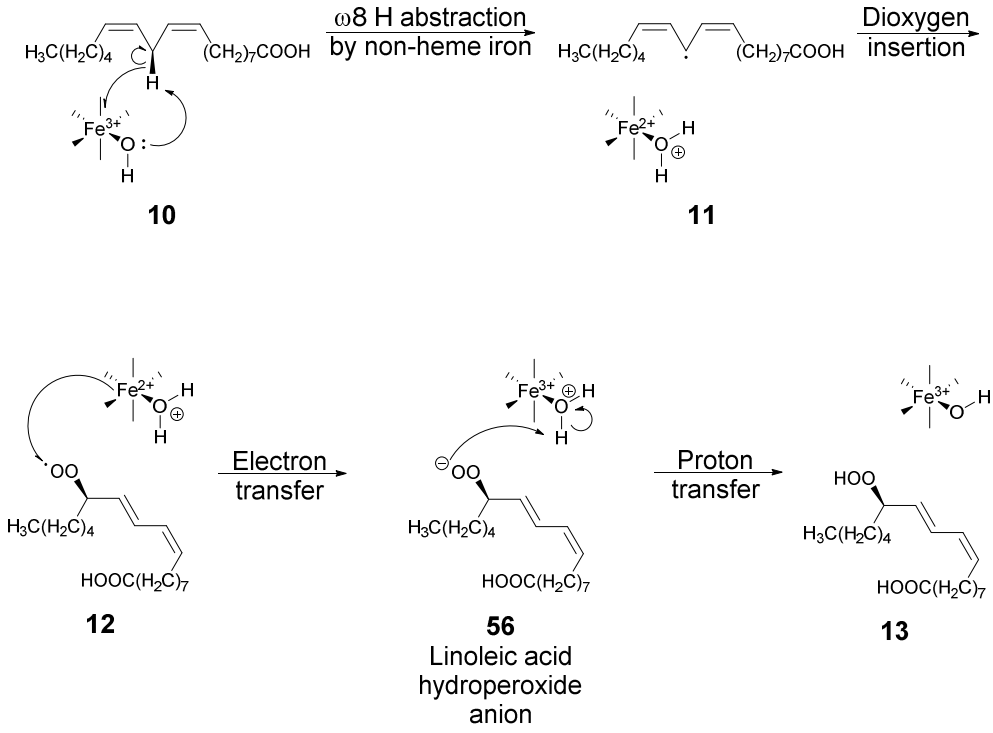

Scheme 3.1 General mechanism for the LOX catalysed conversion of a polyunsaturated fatty acid (linoleic acid) to a hydroperoxide (13S-hydroperoxy-9,11-octadecadienoic acid).

This is the general mechanism for all LOXs however specific regio/stereochemistry is dependent on the particular LOX, fatty acid substrate and reaction conditions. The reaction shown in Scheme 3.1 is for linoleic acid and soybean LOX1 at pH 9.0 and 30 °C where the pro-*S* hydrogen is abstracted and oxygen insertion is directed to the 13 position to give 13S-hydroperoxy-9Z, 11E-octadecadienoic acid. [1] Other polyunsaturated fatty acids may be utilised as substrate, however, for LOX1 from soybean, hydrogen abstraction usually requires a bisallylic methylene group to be positioned in the ω8 position and oxygen

insertion typically occurs at the ω6 position. The structural elements of polyunsaturated fatty acids required for LOX catalysis and the features of the LOX mechanism were first discovered for LOX1 and linoleic acid in 1967.[2] In addition to the antarafacial relationship between hydrogen abstraction and oxygen insertion, another characteristic feature of the LOX reaction is the presence of a lag phase.[3] This is due to active site non-haem iron requiring activation from the ferrous state to the catalytically active ferric state. LOX is converted from the inactive state by reaction with products or other hydroperoxides with a treatment of equimolar amount of hydroperoxides eliminating the lag phase.[4]

3.1.2 Historical LOX studies

The ability of soybean meal to bleach coloured pigments such as carotene, lutein and xanthopyll has been known for at least a century, finding an application in the bleaching of bread dough. As a result, when LOXs from soybean were first discovered by Bohn and Haas in 1928 they were originally known as "carotene oxidase" enzymes.[5] However, after being further studied by Sumner and Dounce, and Sumner and Sumner the family of enzymes were later renamed to lipoxidases as they were found to catalysed the conversion of unsaturated fatty acids to hydroperoxide species which subsequently caused the oxidation and decolourisation of carotenoids.[6, 7] The first isozyme of LOX to be characterised was LOX1 from soybean (sometimes referred to as the "Theorell Enzyme" – a reference to Hugo Theorell who was the first to crystallise the enzyme in 1947).[8] Studies involving soybean LOXs continued intermittently throughout the 20th century with speculation that there were perhaps several enzymes/isoezymes of LOX in soybean meal due to crude soybean extracts having an optimum pH of 6.5[6] and crystalline LOX having an optimum of 9.0.[9] These theories were proved to be correct by the work of Christopher *et al.* who isolated LOX2 in 1970[10] and LOX3 in 1972.[11]

In 1978, Ramadoss *et al.* reported that the presence of individual soybean isozymes were ineffective at promoting carotenoid bleaching and were reliant upon a synergy between LOX3 with either LOX1 or LOX2.[12] The existence of this synergy was challenged by

Grosch and Laskawy the following year.[13] There have been few studies since relating to the synergistic bleaching of carotenoids by soybean LOXs but the most recent work in the literature found that effective bleaching only occurred when there was a combination of LOX1 and LOX3 or LOX2 and LOX3.[14]

3.1.3 LOX in Nature

LOXs are common in plants,[15] animals[16] and fungi, but have also been discovered in some bacteria.[17] The only kingdom of life found to be lacking LOXs is archaea. Possible reasons are that many of these organisms thrive in extreme physiological conditions and some can be sensitive to molecular oxygen, a key reagent in the LOX reaction. LOXs are commonly classified by both their regioselectivity and stereoselectivity for reaction with particular polyunsaturated fatty acids. The hydroperoxide product will form at the carbon denoted by the number prefix while *S* and *R* will describe the stereochemistry at the carbon at which oxygen is inserted. For mammalian LOXs the following families exist: 5-LOX, 8-LOX, 11-LOX, 12-LOX and 15-LOX.[18] For plants the LOX families are 9-LOX and 13-LOX.[19] Mammalian LOX are classified by their reaction with arachidonic acid (Fig. 3.1) while reaction with linoleic acid is observed for plant LOX. The regioisomers result from a combination of stereoselective hydrogen abstraction and oxygen insertion. For plant LOXs, hydrogen abstraction of C-18 polyunsaturated fatty acids occurs almost exclusively at C-11.[20]

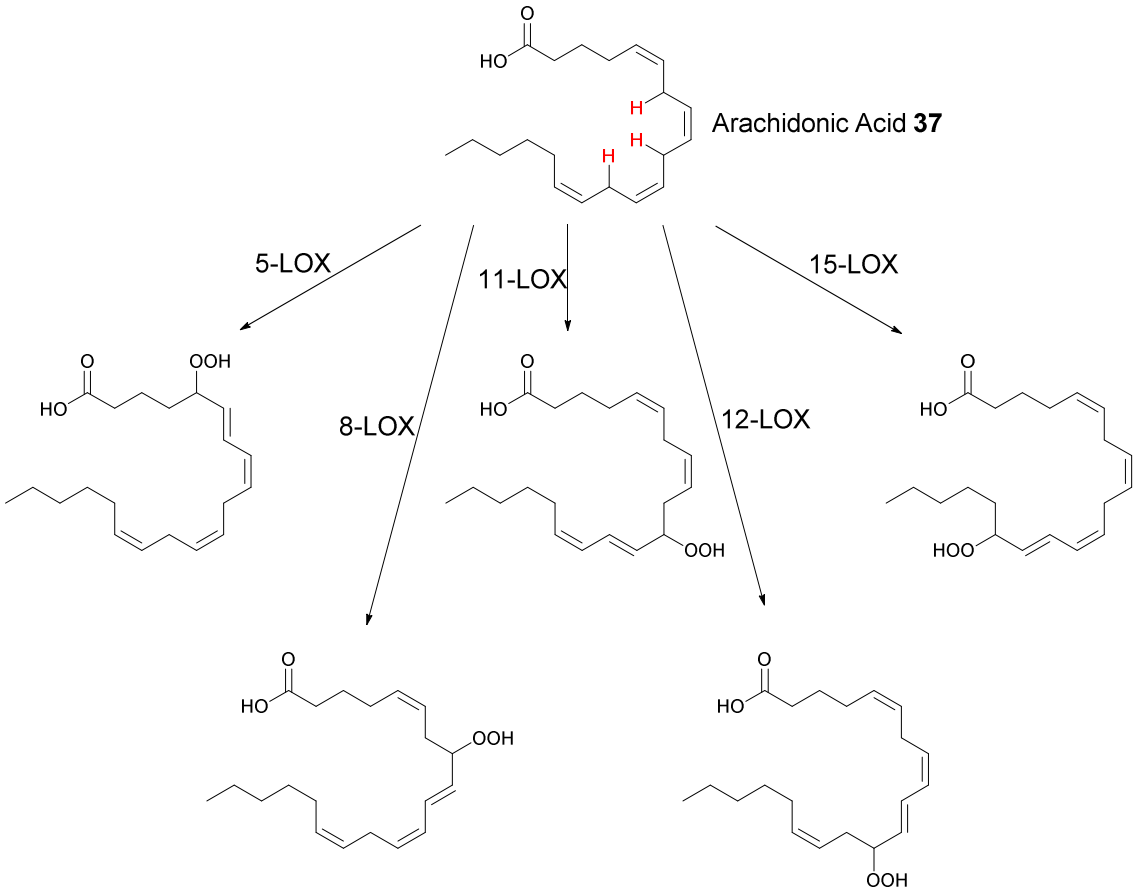

Figure 3.1. The conversion of arachidonic acid **37** to hydroperoxide by different isozymes of mammalian LOX. Hydrogens (highlighted in red) are abstracted based on position relative to the catalytic non-haem iron in the active site of LOXs.

This system of classification can be misleading as LOXs may have variable catalytic activity, regioselectivity and stereoselectivity depending on the fatty acid substrate. Regio- and stereoselective hydrogen abstraction and oxygen insertion are a complex processes that are controlled by substrate binding in relation to the active site with important factors such as the depth the substrate penetrates into the enzyme and the orientation of the substrate.[19,20] Studies have demonstrated that while some LOXs maintain similar product specificity for a range of fatty acid substrates others have been found to lose or show a different specificity.[21,22]

Another method of classification of LOXs is based on optimum pH for maximal enzymatic activity. Type 1-LOXs have an optimum pH in the alkaline region around pH 9 whereas Type 2-LOXs have an optimum pH of 6-7.[23] This system was developed in the 1970s when different isozymes of LOX from soybean were isolated and recognised by differences in optimum pH values. More recently, however, the terms have come to represent very different categories of LOX in a new classification system.[24] In plants, Type 1 and Type 2 describe the subcellular location of the LOX. Type 1-LOXs do not have a transit peptide and are extraplastidial enzymes with >75% sequence similarity with respect to other members of this family. Type 2-LOX have a chloroplast transit peptide sequence and are thus plastidial LOXs. This category of LOXs shows lower sequence similarity between members (>35%) and to date are all 13-LOXs.

The role of LOXs varies between organisms. In plants, products of the LOX reaction with polyunsaturated fatty acids are further metabolised to jasmonates and volatile aldehydes; signalling molecules involved in the plant defence mechanism and wound healing.[25] In mammals the LOX pathway is a major source for eicosanoids, which are involved in wound healing by haemostasis but are also involved in inflammation.[26] Fungi regulate mycotoxin production through the metabolism products from hydroperoxides (diols and lactones).[27]

The significance of LOX research for human health has been recognized since the mid 1970s with the discovery that LOXs contribute to the production of leukotrienes and other eicosanoids. Leukotrienes are formed by the metabolism of arachidonic acid via two major pathways – the cyclooxygenase and LOX pathways. These biological mediators are important for haemostasis and the maintenance of blood pressure, renal function and the immune and reproduction systems, as well as being involved in inflammation, hypersensitivity and many acute and chronic diseases when formed in excess.[28,29] The role

of LOXs in the production of leukotrienes and the relation to human diseases is an active area of research.[26]

3.1.4 LOX Structure

The X-ray crystal structures of animal (rabbit 12/15-LOX,[30] coral 8R-LOX)[31] and plant (soybean LOX1[32] and LOX3[33]) LOXs reveal that the majority of these enzymes form a two domain structure from a single polypeptide chain. The larger domain is the C-terminal domain which consists of mostly helical structures (upper section shown in Fig. 3.2). The smaller of these domains is the N-terminal β-barrel domain (lower section shown in Fig. 3.2). Plant LOXs are typically 95-100 kDa in size with the C-terminal domain around 55-65 kDa and the N-terminal domain around 25-30 kDa. LOXs from lower organisms can be fusion proteins.[34] Frequently the fused protein will be an independent catalytic domain that metabolises the hydroperoxy fatty acids produced by the linked LOX domain. The LOX domain is always linked to the C-terminus of the other catalytic domain in these fusion proteins allowing the C-terminus of the LOX domain to remain coordinated to the non-haem iron and maintain activity.

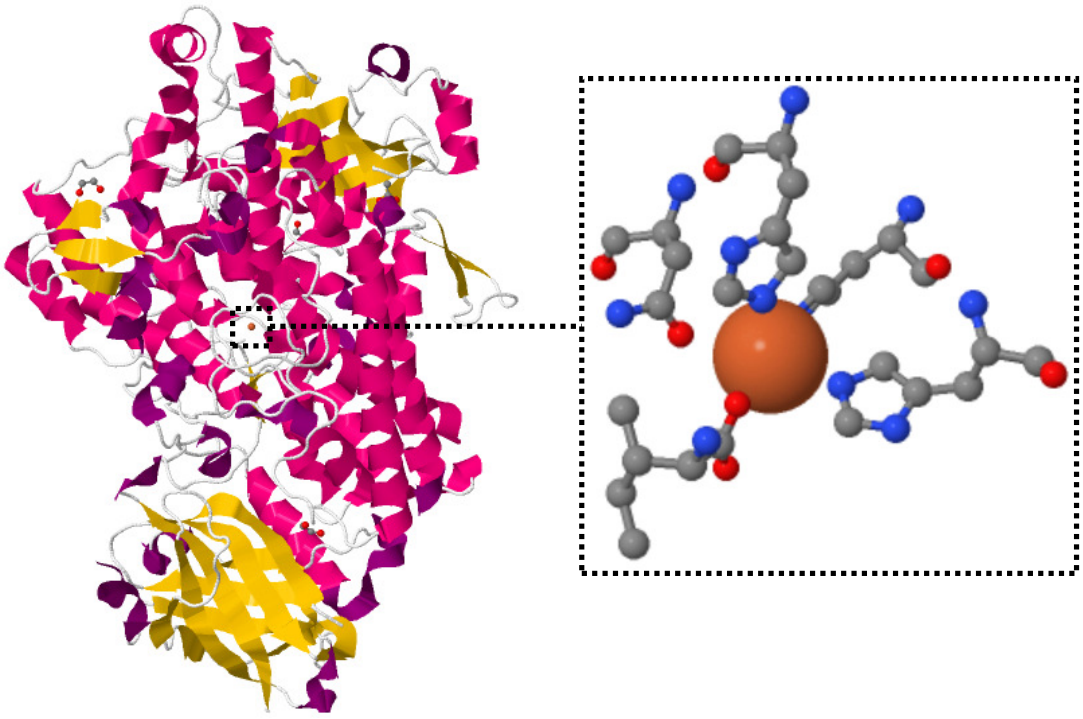

Figure 3.2. Ribbon diagram (left) and non-haem active site residues (right) of soybean LOX1 crystal structure from JSmol, PDB.[32] The α-helices are shown in pink and β-sheets in yellow. The structure clearly shows the smaller N-terminal β-barrel domain at the bottom of the diagram consisting predominantly of β-sheets, while the rest of the enzyme is the mostly helical C-terminal domain which contains the non-haem iron active site. The non-haem iron ligands include the side chains of His-499, His-504, His-690 and Asn-694, the terminal carboxylate of Ile-839 and a water molecule (not shown) in an octahedral conformation.

3.1.4.1 The N-terminal domain

Currently available LOX crystal structures show that the N-terminal β-barrel domain is mostly comprised of anti-parallel β-strands and is similar to the C2-domain of pancreatic lipase in overall structure.[35,36] The C2-domain has been discovered to have a role in membrane binding.[37] The β-barrel domain varies in size significantly for different LOXs from different sources, with soybean isoforms larger than animal enzymes. Despite this variation the domains are similar in overall structure. The β-barrel domain is linked covalently via a randomly coiled oligopeptide to the C-terminal domain and the two domains meet each other at an inter-domain contact plane. The area of this contact plane is 1600 $Å^2$ in rabbit 12/15-LOX and 2600 $Å^2$ in soybean LOX1. The larger area in soybean LOX1 implies that there are more extensive interactions between the domains possibly leading to less flexibility/mobility.

The N-terminal β-barrel domain and catalytic domain structure is highly conserved in LOXs implying that the N-terminal possesses some important function. Research into this domain has led to the production and study of "mini-LOX" – a truncated LOX obtained when soy LOX1 is subjected to limited proteolysis.[38] As a result mini-LOX lacks the N-terminal domain. The effects of this truncation are that mini-LOX shows lower affinity towards linoleic acid (K_M = 24.2 μM for mini-LOX versus 11.2 μM for native LOX1), an increased V_{max} (363 s^{-1} for mini-LOX versus 55 s^{-1} for native LOX1), and the possibility for the non-haem iron contained in the active site to be reversibly removed, unlike native LOX1. [39] The implications are that the N-terminal truncation leads to structural modifications in the active site that allow the iron to dissociate more freely however, crystal structures for mini-LOX have yet to be obtained preventing detailed insight into the structural modifications of the active site. A decrease in catalytic efficiency k_{cat}/K_M (0.14 μM^{-1} s^{-1} for the truncated mutant versus 1.43 μM^{-1} s^{-1} for the native enzyme) was observed for rabbit 12/15-LOX subjected to gene technical truncation of the N-terminal β-barrel domain.[40] Another interesting feature of this truncated mutant was that during oxygenation of arachidonic acid, suicidal inactivation was accelerated compared to the native enzyme.

These studies indicate that the N-terminal domain has a role in substrate binding and regulation of turnover.

As mentioned above, the N-terminal domain resembles the structure of the membrane binding C2-domain of pancreatic lipase[35] suggesting a similar role in the LOX enzyme.[41,42] The N-terminal truncated mutant of rabbit 12/15-LOX displays a reduction in membrane binding while the LOX1 truncated mutant shows enhanced membrane binding.[38,43] For human 5-LOX, and coral 8R-LOX, tryptophan and phenylalanine residues in the N-terminal domain were found to be surface exposed. Site-directed mutagenesis of these particular hydrophobic residues resulted in reduced membrane binding.[44,45] A possible explanation of these results is that there are surface-exposed hydrophobic residues in the N-terminal and C-terminal domains that have a role in membrane binding.

These hydrophobic residues in the N-terminal domain are found on loops that are stabilised by proximal Ca^{2+} binding sites in some LOXs. Human 5-LOX,[46] rabbit 12/15-LOX[47] and coral 8R-LOX show increased membrane binding and turnover upon Ca^{2+} binding, although only 8R-LOX has been found to have specific Ca^{2+} binding sites.[45] Notably, the putative Ca^{2+} binding sites in human 5-LOX, the surface exposed tryptophan residues and the cavity leading to the substrate pocket are all located on the same side of the enzyme suggesting that Ca^{2+} binding induces membrane binding that positions the enzyme to obtain substrates from lipid bilayers.

3.1.4.2 The C-terminal domain

The C-terminal domain contains the non-haem iron active site (arrow points to non-haem iron in Fig. 3.2) and is predominantly α-helices with two anti-parallel β-sheets. In soybean LOX1 the central structural element is helix 9 (residues 473-518, length 65 Å).[48] Most of the other helical structures of the C-terminal domain align with helix 9 so to be parallel or anti-parallel creating a helix bundle at the core of the domain. The C-terminal domain is similar in other LOXs from other organisms. In rabbit 12/15-LOX, the C-terminal domain contains 21 helices arranged in the same manner.[35] Similarly a small β-sheet domain is also present. In coral 8R-LOX there are 23 helices.[31]

The active site is found in the C-terminal domain comprising of a non-haem iron octahedrally coordinated (with rhombic distortion) to five amino acids and a water/hydroxide ligand. The amino acids in soybean LOX1 and coral 8R-LOX are the side chains of three histidines and one asparagine and the carboxylate group of the C-terminal isoleucine. The asparagine side chain is thought to be weakly coordinated to the iron relative to the other ligands due to crystal structures showing it to be approximately 3 Å from the iron centre. Interestingly, the asparagine side chain is connected to His499, another iron ligand in the equatorial position, through a hydrogen bond network formed with Gln495 and Gln697; residues residing in the second coordination sphere.[49,50] The non-haem iron is coordinated similarly in animals: four histidines and the carboxylate group of isoleucine. In rabbit 12/15-LOX, His545 aligns with the Asn residue found in plants and is similarly further from the iron centre relative to the other ligands. Gln495 and Gln697 in soybean LOX1 align with Glu357 and Gln548 respectively in rabbit 12/15-LOX, and are involved in a hydrogen bonding network that stabilises His545.[35]

3.1.4.3 Structural flexibility

Motional flexibility in solution is observed in both rabbit 12/15-LOX and soybean LOX1 to varying degrees possibly due to the large difference in the area of the inter-domain contact planes – 1600 and 2600 $Å^2$ respectively.[35,48] Small angle X-ray scattering (SAXS), fluorescence resonance energy transfer and dynamic fluorescence measurements were used to assess LOX structure in aqueous solution and compare it to the crystal structures. The rabbit 12/15 LOX structure was found to be sensitive to temperature and possess a greater global conformational flexibility.[51] When the X-ray coordinates and the SAXS data were compared, catalytic domain structures were almost identical.[52] However the N-terminal β-barrel domain appeared to be elongated in solution relative to the crystal structure. One interpretation of this data was that the β-barrel domain possesses enough flexibility to move away from the catalytic domain. In contrast the soybean LOX1 was discovered to have a far more rigid structure in solution. In particular, the data suggests that the β-barrel domain may only move slightly from the catalytic domain with extensive non-covalent interactions of the two domains across the relatively large inter-domain plane holding them together rigidly.[53]

3.1.4.4 Substrate binding pocket

Comparisons have also been made between rabbit 12/15-LOX and plant LOXs with respect to structural alterations that occur upon ligand binding. The substrate-binding pocket of rabbit 12/15-LOX adopts an open conformation when ligand is not bound. The non-haem iron of the active site is visible from the surface when looking down the substrate-binding pocket cavity which tapers out towards the surface.[30] The structure closes and condenses significantly upon ligand binding. Helix 2, located at the surface opening of the substrate-binding cavity translocates across by ~12 Å closing off the entrance. Simultaneously helix 18 within the catalytic domain withdraws causing an expansion of the substrate binding pocket. Conformation changes of this magnitude are not observed when comparing the free and ligand bound structures of soybean LOX3. The greatest translocation observed upon ligand binding occurs for residues between Leu331

and Gln341, which neighbour helix 4.[54,55] However this translocation was only 3 Å. The secondary structure elements are ordered more compactly in plant LOXs, which may limit the magnitude of conformational changes.

The substrate-binding pocket of LOXs shows significant differences in shape but generally seems to feature a cavity that allows penetration of the substrate into the enzyme adjacent to the active site; amino acid residues that bind and orientate the substrate relative to the active site; and another cavity leading to the active site that directs oxygen to the reaction centre. Fig. 3.3 shows representations of these cavities along with important residues. As mentioned previously, the substrate binding pocket of rabbit 12/15-LOX changes dramatically upon ligand binding. The open conformation that is adopted when ligand is not bound is characterised by a shallow substrate-binding pocket that tapers out towards the surface. Transformation into the closed conformation occurs upon ligand binding and features a closed off entrance and a deeper, arched cavity that is curved inwards by the side chain of Leu408. The interior of the cavity is formed from residues from helices H2, H7, H9, H10, H16, H18 and the loop linking H9 to H10.[30] A total of 23 mostly hydrophobic amino acids are contributed by these secondary structural elements to form the cavity which may interact favourably with fatty acid substrates. Additionally, H18 seems to control the depth that the substrate penetrates into the cavity. When ligand is not bound, Leu597 on the C-terminus end of H18 protrudes into the cavity restricting access to deeper areas. H18 withdraws 6 Å upon ligand binding, allowing substrates to move deeper into the cavity so that the methyl end is in contact with Ile418, Phe353 and I593, collectively known as the triad constituents. Arg403 found at the opening of the cavity binds the carboxylate group of the substrate and is suspected of initiating the transformation from the open to the closed conformation. Three potential oxygen channels were identified in rabbit 15-LOX, however, only one (shown in Fig. 3.3) was found to remain open upon ligand binding. This channel intersects the substrate binding cavity from the opposite side to the non-haem iron active site possibly contributing to the antarafacial relationship observed in hydrogen abstraction and oxygen insertion. Leu367 is found near the opening of the putative oxygen channel and is thought to play a role in oxygen transport. This

channel joins to the substrate binding pocket from the opposite side of the non-haem iron active site.

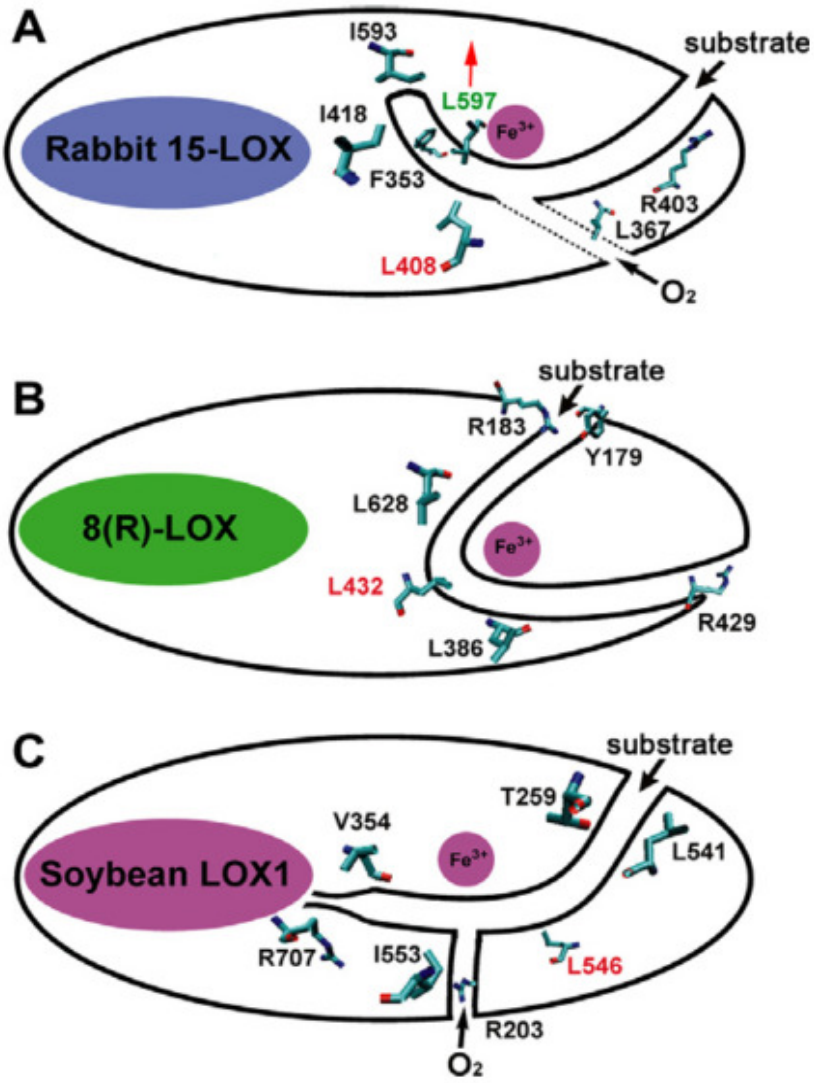

Figure 3.3 Diagrams representing the significant cavities (substrate binding pocket and oxygen channel) within LOXs and the relative locations of amino acids which may influence substrate binding orientation/conformation.[81] (A) shows rabbit 15-LOX in the open conformation;(B) 8(R)-LOX; and (C) Soybean LOX1.

The substrate binding-pocket of coral 8R-LOX (Fig. 3.3 B) is within an arched tunnel that reaches the surface at both ends.[45] It is possible that substrate could access the non-haem iron at the active site by penetration from either end of the tunnel. Indeed, there is a positively charged Arg residue at the opening of both ends (Arg183 and Arg 429), reminiscent of Arg403 in the rabbit 12/15 LOX, which are suspected to play a similar role of binding the carboxylate group of the fatty acid substrate. The entrance with Arg183 is suspected of being the functional substrate binding pocket as a carboxylate binding at this location is consistent with the positional specificity of the enzyme. The Arg429 residue at the other entrance is found to play a structural role by forming a salt bridge with Glu394. This interaction secures the helix bundle that forms the active site to the arched helix that forms the interior of the tunnel. The tunnel is formed from two cavities that are separated by Leu628, which protrudes into the tunnel. Open access across the two cavities can occur when Leu628 withdraws from the tunnel – a conformational change that requires the simultaneous translocation of Tyr179 and Leu386. The crystal structure of coral 8R-LOX reveals that both entrances to the tunnel are closed but the flexibility of LOXs such as rabbit 12/15-LOX imply that the binding pocket may be accessible to fatty acids in solution.

LOX1 possesses two internal cavities that form a junction near to the non-haem iron active site.[56] They are named Cavity I and II. Cavity II is divided by the side chains of Arg707 and Val354 into the subcavities IIa (the substrate binding site) and IIb. Both are formed by two walls of helices – one side comprising H9 and H11 the other made from H2, H6, H18 and H21. The putative oxygen channel is thought to intersect cavity IIa between Ile553 and Trp500. Originally Ile553 was believed to play a role in controlling oxygen access to the reaction centre after site-directed mutagenesis studies found that the I553F mutant showed a 20 fold decrease in $k_{cat}/K_M(O_2)$,[57,58] but further studies have suggested it may have a role in positioning the substrate correctly.[59] Fatty acid substrates are believed to be navigated to cavity IIa by conformational changes in the side chains of Thr259 and Leu541 located near the surface.[48] Similar to other LOXs, an amino acid residue would be expected to bind with the carboxylate group of the fatty acid substrate, however positively charged amino

acid residues seem to be absent from the proximity of this opening. An important feature of the soybean LOX isozymes (LOX1, LOX3, VLX-B and VLX-D) is that cavity IIa, the substrate binding pocket, varies significantly in dimensions and shape.[60] For example, cavity IIa in LOX1 is a single, open channel but the substrate-binding site in other isozymes is more restrictive to substrate penetration due to the presence of bottlenecks and protrusions. In addition to this, the residues at the opening of the cavity vary in polarity and steric bulk between the isozymes.

3.1.4.5 Oxygen directing in LOXs

Data regarding distribution of molecular oxygen in proteins reveals that oxygen does not diffuse freely into proteins and is not distributed homogeneously.[61] Reinforcing this are reports that several proteins have been found to possess preformed oxygen diffusion channels.[62,63] These results are particularly significant for LOXs and other dioxygenase enzymes as molecular oxygen from the atmosphere is a substrate in their reactions. The putative oxygen diffusion channel in LOX1 that merges with cavity IIa is lined with Ile553. Mutation of this residue to Phe, which possesses a bulkier side chain, results in catalytic efficiency decreasing by 20-fold, a possible consequence of oxygen diffusion being restricted.[57]

Comparisons of rabbit 12/15-LOX and soybean LOX1 structural data illustrates that there is not an analogous putative oxygen diffusion channel found in 12/15-LOX. The structure of the enzyme was modelled in 3D and the Gibbs free energy for oxygen diffusion was mapped.[64] To calculate this, molecular oxygen was situated in any 1 $Å^3$ space in the enzyme. Low energy pathways were then searched to place oxygen in this location from a vacuum. Areas with minimum energy distribution corresponded to oxygen rich areas. The global minimum was found to be within 4 Å of the C15 of arachidonic acid with a significant preference over C11 when compared with a 3D model of the enzyme-substrate complex (12/15-LOX with arachidonic acid). This is in agreement with the regiochemistry of 12/15-LOX. The ligand free form showed that the global energy minimum was

connected to the surface by three major channels. Of these three, only one channel remains open upon ligand binding. This channel travels from the active site to the opposite side of the enzyme. Subsequently, site directed mutagenesis of Leu367, a residue lining this channel, to the more bulky Phe resulted in a 10-fold increase in K_M for oxygen, verifying the importance of this channel for oxygen diffusion to the active site.

3.1.5 Substrate binding conformation

The diagrams shown in Fig. 3.4 illustrate some of the concepts discussed in this section. Early models and mechanisms of LOX substrate complexes have typically been in the tail-first form, wherein the fatty acid substrate penetrates the enzyme, methyl end first into the hydrophobic substrate-binding pocket, as opposed to the head-first model that involves fatty acid entering the substrate-binding pocket with the carboxylate group in front. The head-first model has been debated thoroughly as it necessitates the stabilisation of the positively charged carboxylate group within a predominantly hydrophobic environment.[65] A tail-first model for the binding of arachidonic acid in rabbit 12/15-LOX was developed from the data gathered for soybean LOXs and suggested the major interactions securing the substrate in a particular conformation in the substrate-binding pocket are: hydrophobic interactions between the fatty acid chain and the lining of the cavity which is made predominantly from hydrophobic residues; π-π interactions between the double bonds of the polyunsaturated fatty acid with the side chains of aromatic residues; and ionic interactions between the carboxylate group at the end of the fatty acid with Arg403 at the opening of the cavity.[66] In this conformation the active site non-haem iron is situated between C13 and C10 of the fatty acid. These are both central carbons in a 1,4-pentadiene system meaning that hydrogen abstraction by the non-haem iron is possible at both positions. Also of particular importance in substrate binding is the distance between the methyl end and the carbon (central carbon of the 1,4-pentadiene system) reacting with the non-haem iron. This was demonstrated in experiments that reacted soybean LOX12 and rabbit 12/15-LOX[67] with synthetic fatty acid isomers that varied the position of the bisallylic methylene carbon relative to the methyl end.

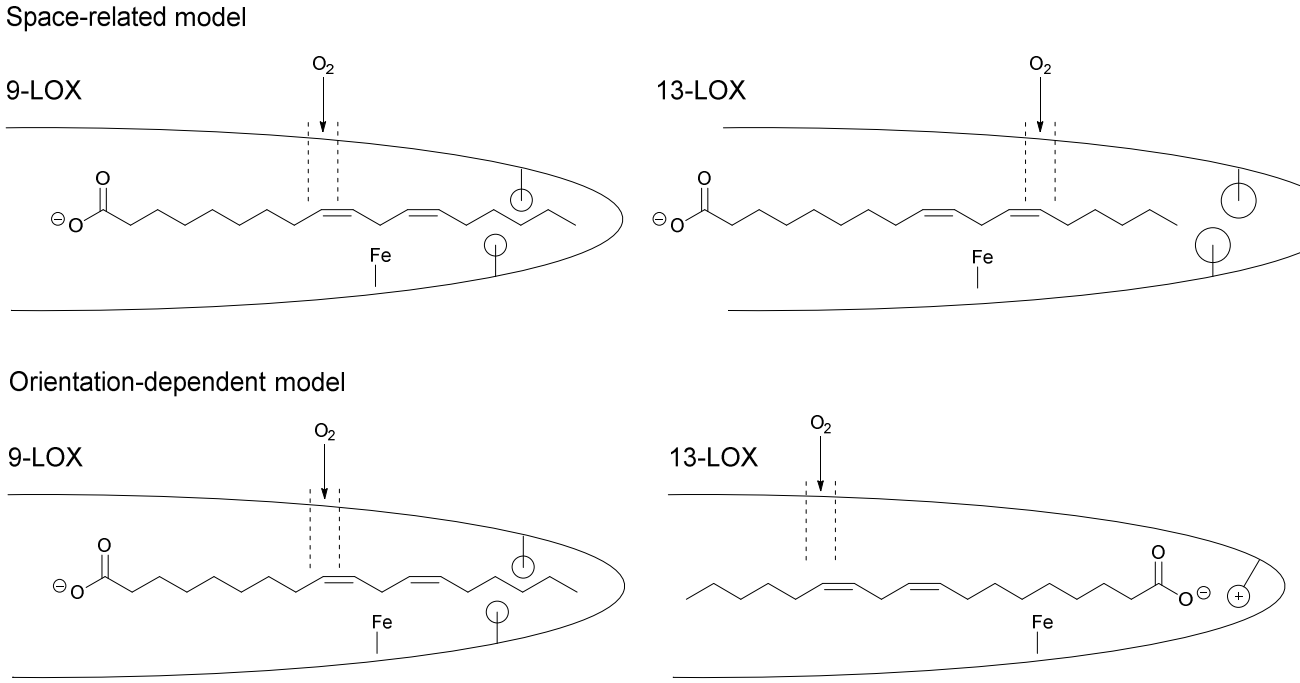

Figure 3.4 These diagrams illustrate how different conformations/alignments of substrate binding could affect the product specificity for linoleic acid, although the models could be applied to different substrates.[68]

All models in Fig. 3.4 show the non-haem iron centre aligning with the central carbon of the 1,4-pentadiene system. With regard to the space-related model (top half) this would mean that the depth of the substrate pocket and the location of the non-haem iron is positioned to react with a specific bisallylic methylene in the substrate (more relevant to arachidonic **42** and linolenic **41** rather than linoleic acid **10**). The depth of the pocket relative to the location to which oxygen is directed is also important as this could contribute to favouring oxygen insertion at one of the particular terminal ends of the 1,4-pentadiene radical. The bottom half of the diagram shows the tail-first or methyl end first model (left) and the head-first or carboxylate end first model (right). Again, if oxygen is directed to the same location relative to the non-haem iron, different products will result from tail-first and head-first binding. The substrate-binding pocket is lined predominantly with hydrophobic residues suggesting the substrate should adopt the tail-first conformation as the methyl end could be bound with hydrophobic interactions, while a head-first

unfavourably forces a charged group into the hydrophobic space. However, the existence of Arg707 and Arg726 found at the end of the substrate-binding pocket of LOX1 and LOX3 respectively suggest that binding in the head-first conformation is possible when a positively charged residue is available to stabilise the carboxylate group. Due to this reliance on ionic interactions of charged residues it is important to note that the head-first conformation of binding is predicted to be influenced heavily by conditions such as pH.

Although wild type animal LOXs show little alterations in product selectivity when pH is varied over a range slightly greater than physiological conditions,[69] targeted mutagenesis and adjustment of substrate concentration however result in highly pH sensitive enzymes. The human 15-LOX2 mutant (V603H) produces the 8 isomer as the major product at low pH but this switches to the 15 isomer at higher pH. Additionally, there have been several studies that have documented the alterations in positional specificity in plant LOXs as a result of pH.[74,70]

Consideration for a head-first type of binding was renewed when the crystal structure of soybean LOX3-13S-HpODE [71] complex, determined in 2001 at 2 Å, showed the carboxylate group coordinated to Arg726. This Arg residue is conserved in many plants but not in mammals. In fact, the corresponding location is covered by uncharged amino acids making this data difficult to relate to mammal LOXs. The significance of this conserved Arg in plant LOXs was elaborated by site-directed mutagenesis in cucumber 13S-LOX.[72] This enzyme was believed to bind linoleic acid in a tail first configuration as this alignment conforms to the observed stereochemistry of the product. The Arg758 residue in 13S-LOX was found to be shielded from interactions with the carboxylate group of the substrate by His608. Mutation of His608 to uncharged Val produced a mutant that catalyzed linoleic acid hydroperoxidation primarily at the 9S position. The interpretation of this observation was that the Arg758 was no longer shielded in the R758V mutant allowing the Arg758 to interact with the carboxylate group and favour a head-first configuration at the substrate binding-site. A recent study, applying the orientation model

to soybean LOX1 and linoleic acid has shown that at high pH LOX1 is a 13-LOX and interestingly the substrate adopts the head-first conformation with the carboxylate group interacting with the positively charged Arg707.[73] The current data suggests that fatty acids may bind in both the head-first and tail-first conformation. Furthermore it is likely that the preferred orientation of binding may be affected by experimental conditions.[74,75]

A notable feature linked to stereochemistry of the product of LOX reactions is that the majority of S-LOXs possess an Ala residue in a critical location within the substrate binding pocket. In R-LOXs this residue is a Gly residue instead.[19,76,77] Mutations of this Gly residue to an Ala residue in coral 8R-LOX and human 12R-LOX resulted in the S products (12S and 8S respectively) becoming the major products. A significant change in products was observed for the mouse 12R-LOX mutant, but the proportion of S products was limited to only 40%.[78] The inverse experiments were also conducted. The A416G mutant of human 15S-LOX2 produced the 11R product (70% of the share of products). Modifications in stereoselectivity were also observed in soybean LOX1,[79] mouse 8S-LOX, Aribidopsis thaliana and tomato LOX[80] but to a lesser extent. An initial mechanism to explain this phenomenon was that the enzyme restricts oxygen insertion to the side of the pentadiene radical system that is opposite to hydrogen abstraction.[76] If the hydrogen from C13 is abstracted this would limit the oxygen insertion positions to 15S and 11R. The side chain of the Ala residue found in S LOXs would then prohibit oxygen insertion at the 11R position to give the 15S as the major product. Mutation of this Ala to a less bulky Gly would therefore allow oxygen insertion at the 11R position. Unfortunately this mechanism does not fully explain the data, particularly for the opposite cases in R LOXs. Additional information obtained from the study of coral 8R-LOX implicating the role of a Leu side chain has aided in refinement of this mechanism.[31] Mutation of this residue (Leu432) to Ala or to Phe resulted in reduced and increased stereospecificity respectively, although with reduced catalytic activity. The interpretation for this data is that the side chain of Leu432 blocks oxygen access to the 12S position in the native enzyme while in the Gly428Ala mutant the Leu side chain is displaced by the bulkier side chain so that it blocks access to the 8R position instead.

Mutation of Ala542 to Gly in soybean LOX1 modifies the enzyme so that instead of producing the 13S product almost exclusively from linoleic acid, 40% of the product obtained is 9R.[79] The antarafacial relationship is still maintained between hydrogen abstraction and oxygen insertion but radical rearrangement occurs in inverse directions (9Z, 11E in the wild type and 10E, 12Z in the A542G mutant).

Several hypotheses have been summarised relating to why positions on the pentadienyl radical are favoured, giving the stereoselective, regiospecific product.[81] The delocalising hypothesis suggests interactions of the radical intermediate with electron attracting amino acids in the substrate binding pocket may cause increased electron density on certain carbons of the radical. The distortion hypothesis instead proposes that the relative electron densities on the carbons of the pentadienyl radical are the result of the planar radical being distorted. In the oxygen targeting hypothesis the electron densities are disregarded and the main factor considered is which locations on the radical are more accessible to oxygen. The final hypothesis is that the oxygen insertion reaction is random, but reversible and the stereoselective step is the reduction of the radical (reduction hypothesis). At present it is unknown which of these factors contribute to the overall product selectivity observed in the LOX reaction. Data of the probability of oxygen occupancy in areas of the rabbit 12/15-LOX are available and illustrate that for arachidonic acid, at C15 the probability is 7-fold higher than at C11 and gradual changes in probability over ~6 Å are observed. While this conforms to the observed regiospecificity, if oxygen targeting was the only factor involved in the mechanism, 15% of the product would be the 11 isomer and furthermore it would be expected that oxygen occupancy probability would change sharply to give small, discrete regions of higher probability. This data therefore, illustrates that oxygen targeting contributes to the selectivity of the mechanism but is not the only factor involved.

3.1.6 LOX mechanism

The mechanism of LOXs (Scheme 3.1) has garnered wide interest. LOXs react with a variety of different substrates – polyunsaturated fatty acids that contain a *Z,Z*-1,4-pentadiene structure. They are regiospecific in that they react with the central carbon, C3, of the 1,4-pentadiene structure and show high selectivity to a single site when multiple carbons are flanked by carbon-carbon double bonds. LOX1 for example reacts with the methylene group at ω8 and inserts oxygen at ω6 for substrates such as arachidonic acid and linolenic acid.2 The reaction is also highly stereospecific. The first step involves abstraction of a specific hydrogen from the central carbon of the 1,4-pentadiene system to produce a radical that conjugates over the whole pentadiene system. Following radical rearrangement, this system then reacts stereospecifically with molecular oxygen at a specific terminal of the pentadiene system and from the opposite face to which the hydrogen was abstracted in relation to the plane of the pentadiene system. The stereospecificity of the dioxygenation stage of reaction can be influenced by conditions such as temperature, substrate concentration, oxygen concentration and pH. As an example, at 30 °C, pH 9.0 with excess substrate and oxygen concentration LOX1 will abstract the pro-*S* hydrogen from the carbon flanked by the carbon-carbon double bonds and convert linoleic acid into 13S-hydroperoxy-9Z, 11E-octadecadienoic acid (Scheme 3.1). In addition to this the mechanism for soybean LOX1 exhibits the highest kinetic isotope effect recorded for a biological system making it a primary example for studying the evolution and application of hydrogen tunnelling in enzymes. [82,83,84]

3.1.6.1 Hydrogen Abstraction

The first stage of the reaction is the abstraction of hydrogen from the central carbon of the 1,4-pentadiene system in the absence of oxygen. This step was verified in kinetic studies in 1996 by steady state[85] and in 1997 by pre-steady state kinetic analyses.[86] The hydrogen abstraction causes a reduction of the Fe^{3+} to Fe^{2+} and converts the hydroxide ligand to water. The driving force behind this reaction is the high redox potential of Fe^{3+} ($\varepsilon°$=+600 mV)[87] and the pK_a difference for water bound to Fe^{3+} compared to Fe^{2+}.[88] Evidence implicating hydrogen tunnelling was discovered in 1996.[89] A tunnelling KIE (k_H/k_D = 48 at 25 °C) was observed, along with a small enthalphy of activation (1.2 kcal mol^{-1}) for the reaction. This aspect of the mechanism of the LOX reaction has been studied extensively by the Klinman group and has led to the proposal that hydrogen tunnelling is utilised in a wide range of enzymatic systems.[82]

3.1.6.2 Oxygen Insertion

The next major half of the reaction is the insertion of dioxygen into the pentadienyl radical system and formation of the hydroperoxy product. Considered as step wise reactions, the steps are firstly dioxygen insertion to form the hydroperoxy radical; reduction of the radical to the anion and oxidation of the Fe^{2+} to regenerate the active Fe^{3+}; proton transfer from the water ligand to the anion (electron and proton transfer may be concerted); and the final step is dissociation of the product from the enzyme. With the exception of the final step, all the reaction steps were demonstrated to be reversible in a study in which hydroperoxide products of polyunsaturated acids were added to LOX in the active Fe^{3+} state.[90] Data from Klinman *et al.* suggests that the rate determining step of this half of the reaction is the conversion of the hydroperoxy radical to the hydroperoxy anion.[91] Oxygen insertion into the radical system and the release of the product from the enzyme were found to be non rate limiting after the rate showed no change when solvent viscosity was altered. Similarly the rate remained unchanged when D_2O was used suggesting proton transfer was not the slow step. KIEs were observed however with ^{18}O implying that the rate determining step occurs after the formation of the hydroperoxy radical. In addition, the

binding and release of linoleic acid to LOX1 has been observed to be rapid.[92] This evidence suggests that product dissociation is also fast and non-rate limiting.

Speculation by Klinman on the evolution of dioxygenases is that the non-haem iron in the active site of LOXs is modulated to have a redox potential of +600 mV as well as a barrier shape optimised for hydrogen tunnelling to allow for efficient hydrogen abstraction from the 1,4-pentadiene system.[93] The redox potential is suggested to be a compromise as a high redox potential makes the regeneration of the ferric-hydroxide from the ferrous-water unfavourable. A possible consequence of this is a build up of the peroxyl radical-enzyme complex during catalytic turnover. Klinman cites the discovery of mammalian LOXs undergoing suicidal inactivation as possible evidence[94] – the radical species could be reacting with residues in the substrate binding pocket. Although only speculation it is an interesting facet of the LOX reaction in relation to the project as it is these radical species that are responsible for the bleaching of carotenoids.

3.1.7 LOX-1/3 synergy

The synergy between LOX1/LOX2 and LOX3 from soybean for cooxidation of β-carotene was first documented by Ramadoss *et al.* in 1978 (Fig. 3.5).[12] The motive behind the study was the discovery that LOX1 was not effective at bleaching β-carotene despite being able to promote hydroperoxidation of polyunsaturated fatty acids. Originally hydroperoxidation and cooxidation were believed to be two functions attributed to one enzyme. Surprisingly, when LOX1, LOX2 and LOX3 were tested individually for cooxidation activity, they all performed poorly. However when assays combined either LOX1 and LOX3 or LOX2 and LOX3, a notable synergy effect was observed. A combination of LOX1 and LOX2 was not as effective at bleaching β-carotene. These results were based on cooxidation assays performed at pH 6.5 in phosphate buffer, using methyl linoleate as substrate with 0.1 units of enzyme (combination assays used 0.05 units of each enzyme).

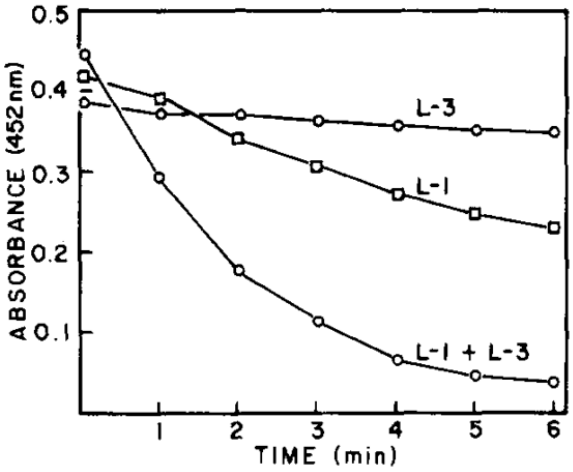

Figure 3.5 Observed carotenoid bleaching synergy for LOX1 and LOX3 by Ramadoss *et al.*.[12]

Further experiments were used to probe the observed synergy. Staggered assays were performed in which LOX1 or LOX2 was added to the reaction mixture followed by LOX3, 5 minutes later. A sharp increase in β-carotene bleaching was observed. LOX1 and LOX3 individually caused a reduction in absorbance at 456 nm of 40% and 10% respectively, during the 6 minute assay. In comparison the LOX1 and LOX3 combination caused 100% bleaching at the end of the 6 minutes.[12] When the order of addition was reversed this increase in β-carotene bleaching was not as dramatic. The staggered reactions used linoleic acid as substrate. Linoleic acid was used again for experiments analysing the hydroperoxides formed by each of the isozymes and addition of these products to cooxidation assays containing individual isozymes. The presence of the 13-hydroperoxy isomer **13** increased β-carotene bleaching by 4-fold more than the analogous 9 isomer **57** (structures shown in Fig 3.6). Products of LOX1 and LOX2 were found to be effective in enhancing β-carotene bleaching when added to LOX3 but products from LOX1, LOX2 and LOX3 were not found to improve bleaching when added to LOX1 or LOX2.

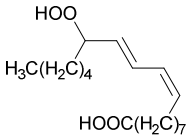

13
13-hydroperoxyoctadecadienoic acid

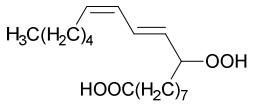

57
9-hydroperoxyoctadecadienoic acid

Figure 3.6 Isomers of linoleic acid hydroperoxide products of the LOX1 and LOX3 reaction.

The Axelrod group suggested that the bleaching synergy was related to availability of the 13-hydroperoxy isomer for LOX3. Analysis of products from hydroperoxidation assays using LOX3 individually revealed that LOX3 was ineffective at producing the 13-hydroperoxy isomer.[10] However LOX3 was discovered to possess a greater peroxidase activity than LOX1 and LOX2. The conclusion was that LOX3 can utilise the 13-hydroperoxide for effective carotenoid bleaching but is unable to produce the 13-hydroperoxide in high yield. Inversely, LOX1 and LOX2 possess high activity in converting linoleic acid to the 13-hydroperoxy isomer but low activity when utilising the 13-hydroperoxy isomer for carotenoid bleaching. Therefore, a system containing LOX1 and LOX3 together will have the capability to produce the 13-hydroperoxy isomer in high yield and utilise this product for carotenoid bleaching.

These results were disputed a year later by Grosch & Laskawy[13] who repeated the cooxidation experiments and isozyme purification. The results obtained for enzyme purification agreed with those of Ramadoss *et al.* but cooxidation assay comparisons showed some contrasting results. Ramadoss *et al.* had reported that individual enzyme activities were similar when using linoleic acid or methyl linoleate as substrate for the cooxidation assays,[12] however Grosch & Laskawy observed greater activities of cooxidation using linoleic acid as substrate. Individually, LOX2 showed cooxidation activities similar to those determined by Ramadoss *et al.* when linoleic acid was used as substrate, while LOX3 was observed to have greater activity. Addition of the products of LOX2 with linoleic acid to LOX3 showed enhancement of cooxidation of activity but only

the 13 isomer was found to be effective. In contrast to Ramadoss *et al.*, the 9 isomer was found to have no effect. Notably, no synergy was observed when LOX2 and LOX3 were combined. The enzymes showed the same activities as when they were assayed individually.

This topic remains unresolved in the literature as there have been few papers to elaborate on the observed synergy. The most recent paper found to address the cooxidation synergy effect was in 2010.[14] In this paper, the cooxidation synergy was investigated using a range of conditions: isozymes were prepared with different isolation methods; temperature was varied over a wide range (4 to 80 °C); and the effect of pH was examined from pH 5.8 to 9.2. Interestingly, LOX1 was found to be relatively thermally stable and showed a high temperature optimum around 80 °C. The other isozymes decrease in activity and perhaps denature at temperatures above 50 °C. The most relevant finding however was that the results support the existence of the cooxidation synergy with mixtures of LOX1 and LOX3; LOX2 and LOX3; and mixtures of all three isozymes showing greater bleaching than those observed for the individual enzymes. To date, all the papers that have investigated the cooxidation synergy have yet to derive kinetic data from the results as cooxidation is reported in time required to fully bleach a solution of β-carotene. Also, there does not seem to be any progress in finding the mechanistic origin behind the bleaching synergy.

3.2 Results

Carotenoid stains may be caused by a wide range of foods that contain derivatives of tomato or red pepper. These stains usually contain a mixture of carotenoid pigments and greasy components, including free fatty acids. Chapter 1 discussed several of the properties of carotenoid stains, including their strong colouration due to the large extinction coefficients of carotenoids and difficulty of removal caused by the hydrophobic nature of the components. Utilisation of radical species as bleaching agents was presented as a solution and Chapter 2 detailed work on carotenoid bleaching in the presence of fatty acid and absence of enzyme (non-enzymatic bleaching). Experiments quantified the effect of pH and surfactant on the autoxidation of linoleic acid and the effect of fatty acid, pH and surfactant on bleaching of β-carotene **1**.

This chapter will focus on enzymatic bleaching. The effect of pH and surfactant on the linoleic acid hydroperoxidation activity of LOX1 and LOX3 (mechanism shown in Scheme 3.1) will be presented first, followed by β-carotene **1** bleaching assays analogous to those in Chapter 2 (Scheme 2.2) utilising the same surfactants **52** (Tween 20), **53** (Tween 80), **54** (AE7) and **55** (AE1S) (structures shown in Fig. 2.4, properties in Table 2.4). Bleaching assays are in the presence of single LOX isozymes and in mixtures in order to fully assess the bleaching activity of the individual enzymes and a potential bleaching synergy.

Each experiment described herein is accompanied by a representative plot of the raw data (absorbance versus time) and representative table of calculated initial rates for one set of conditions. Tables of calculated initial rates for all conditions tested may be found in Appendix B. The effect of surfactant conditions and pH-rate profiles of these results are shown in Section 3.3.

3.2.1 Linoleic acid oxidation in the presence of LOX followed by UV-Vis spectrophotometry

LOX catalysed oxidation of linoleic acid **10** was studied initially in the absence of β-carotene **1** to measure the effect of pH and surfactant on LOX hydroperoxidation activity (enzymatic formation of linoleic acid hydroperoxide **13**). A concentration of 500 μM linoleic acid was chosen in order to maintain identical conditions with non-enzymatic assays and to ensure the LOX enzymes were operating at maximal enzymatic activity, V_{max}.

Initial experiments in the presence of LOX were performed in buffered solutions of either 50 mM phosphate (pH 6.50 – 8.00) or borate (pH 8.50 – 10.00) at 30 °C in the presence of surfactant **52** (Tween 20) (Fig. 2.4). Reactions were initiated by addition of linoleic acid stock solution at 0 °C, to cuvettes containing a mixture of buffer and LOX stock solution at 30 °C.

Representative absorbance versus time plots obtained at pH 9.00 and 6.50 (the reported optima of LOX1 and LOX3) in the presence of surfactant **52** (Tween 20) are shown in Fig. 3.7. A representative set of observed initial rates in the presence of LOX1 and surfactant **52 (**Tween 20) is shown in Table 3.1. LOX catalysed oxidation of linoleic acid **10** was monitored by the increase in absorbance at 234 nm. The initial rate of change in absorbance at 234 nm was obtained from a linear fit in the steepest region of the absorbance versus time data (Fig. 3.7 inset). This value was used to calculate the initial rates of autoxidation using the extinction coefficient for linoleic acid hydroperoxide **13** (22,500 M^{-1} cm^{-1}).[95] From the data in Fig 3.7, the slope of the steepest linear region (0-2 min shown in inset) was obtained as 0.842 ΔA_{234} min^{-1}, which corresponds to an initial rate of 37.4 μM min^{-1}. The observed initial rates for LOX catalysed linoleic acid **10** oxidation in the presence of the surfactants are shown in Tables B1 – 7 of Appendix B and the pH profile for each of the surfactants will be discussed in Section 3.3.

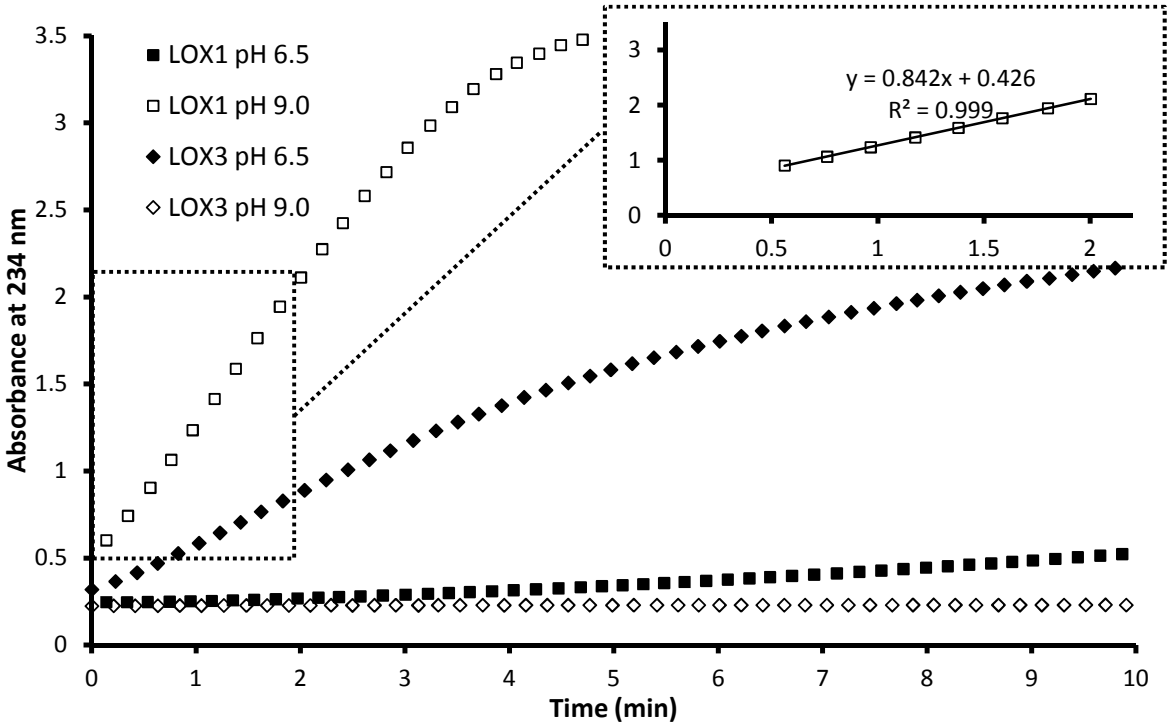

Figure 3.7. Representative plots of LOX catalysed oxidation of linoleic acid **10** (500 μM) at pH 6.5 and 9.0 for LOX1 and LOX3 enzymes from Novozymes (0.33 μg ml^{-1}) in the presence of surfactant **52** (Tween 20) (200 μg ml^{-1}). Inset shows linear region from 0-2 min for reaction at pH 9.0 with LOX1.

Table 3.1 Initial rates of oxidation of linoleic acid **10** in the presence of LOX1 from Novozymes and surfactant **52** (Tween 20).

pH[b]	Rate Constants (μM min^{-1})[a]			
	υ1	υ2	υ3	υ_{av} ± SD[c]
6.50	1.94	1.64	1.64	1.75 ± 0.17
7.00	1.12 x 10^1	1.16 x 10^1	1.16 x 10^1	(1.15 ± 0.026) x 10^1
7.50	2.31 x 10^1	2.40 x 10^1	2.49 x 10^1	(2.41 ± 0.090) x 10^1
8.00	3.46 x 10^1	3.48 x 10^1	3.64 x 10^1	(3.53 ± 0.10) x 10^1
8.50	3.87 x 10^1	3.63 x 10^1	3.60 x 10^1	(3.70 ± 0.15) x 10^1
9.00	3.74 x 10^1	3.76 x 10^1	3.77 x 10^1	(3.76 ± 0.017) x 10^1
9.50	3.72 x 10^1	3.70 x 10^1	3.80 x 10^1	(3.75 ± 0.051) x 10^1
10.00	3.78 x 10^1	3.43 x 10^1	3.56 x 10^1	(3.59 ± 0.18) x 10^1

[a] Reaction mixtures were maintained at 30 °C and contained LOX1 enzyme from Novozymes (0.33 μg ml^{-1}), linoleic acid **10** (500 μM) and surfactant **52** (Tween 20) (200 μg ml^{-1}). [b] Phosphate or borate buffer (50 mM) were used to maintain pH 6.50-8.00 and 8.50-9.00, respectively. [c] Standard deviation (SD) was calculated using the following formula: $SD = \sqrt{\frac{\sum(x-\mu)^2}{(n-1)}}$ where μ is the mean and n is the number of samples.

3.2.1.1 Surfactant effects on initial rates of LOX catalysed linoleic acid oxidation

The effect of surfactants **52** (Tween 20), **53** (Tween 80), **54** (AE7) and **55** (AE1S) was determined for LOX1 and LOX3 enzymes from Novozymes at pH 6.50 and 9.00. A representative absorbance versus time plot obtained at pH 6.5 in the presence of LOX1 and surfactant **55** (AE1S) is shown in Fig. 3.8 and a representative set of initial rates observed for LOX1 at pH 6.5 is shown in Table 3.2. From the data in Fig 3.8, the slope of the steepest linear region (0-2 min) was obtained as 0.697 ΔA_{234} min^{-1}, which corresponds to an initial rate of 30.97 μM min^{-1}. The observed initial rates for LOX catalysed oxidation of linoleic acid **10** in the presence of surfactants are shown in Tables B8 – B11 of Appendix B and a pH profile for each of the surfactants is shown in Section 3.3.

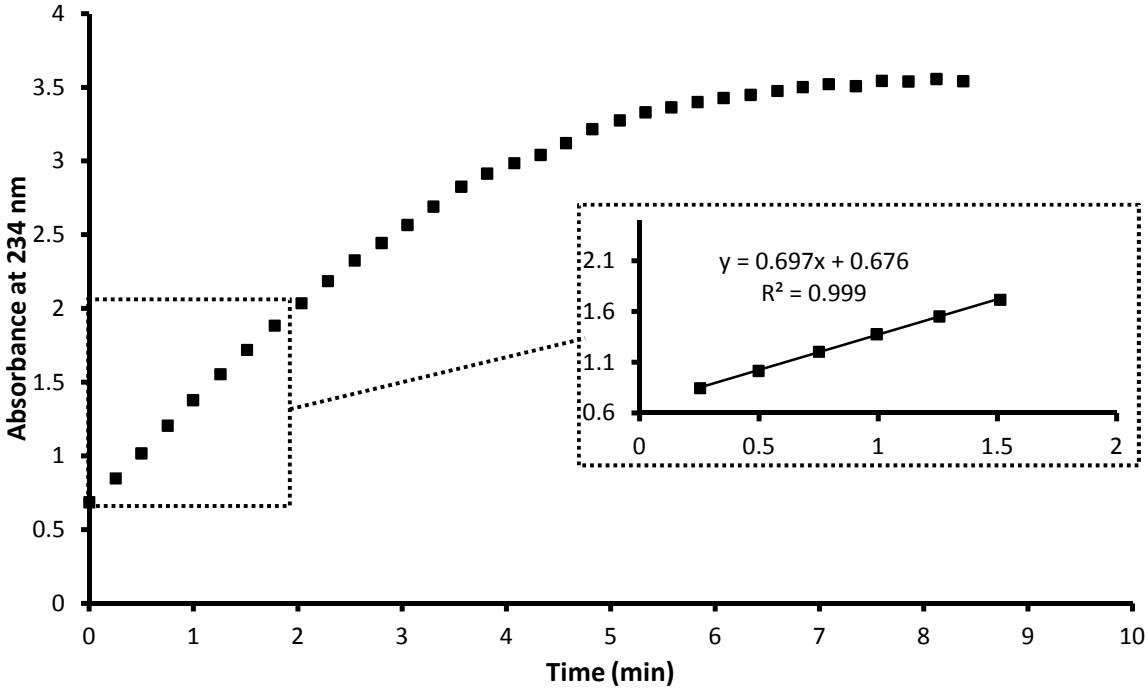

Figure 3.8 Representative plot of LOX1 (0.33 μg ml^{-1}) catalysed oxidation of linoleic acid **10** (500 μM) with surfactant **55** (AE1S) (200 μg ml^{-1}) at pH 6.5 and 30 °C. Inset shows linear region from 0-2 min of reaction (~13% conversion of substrate over this period of time).

Table 3.2 Initial rates of oxidation of linoleic acid **10** in the presence of LOX1 from Novozymes and surfactants **52** (Tween 20), **53** (Tween 80), **54** (AE7) and **55** (AE1S) at pH 9.0.

Surfactant	Concentration ($\mu g\ ml^{-1}$)	Rate Constants ($\mu M\ min^{-1}$)[a]			
		$\upsilon 1$	$\upsilon 2$	$\upsilon 3$	$\upsilon_{av} \pm SD$[b]
Tween 20 **52**	200	3.23×10^1	3.73×10^1	4.41×10^1	$(3.79 \pm 0.60) \times 10^1$
	400	2.63×10^1	2.65×10^1	2.84×10^1	$(2.71 \pm 0.12) \times 10^1$
Tween 80 **53**	200	3.12×10^1	3.46×10^1	3.13×10^1	$(3.24 \pm 0.19) \times 10^1$
	400	2.42×10^1	2.80×10^1	2.59×10^1	$(2.61 \pm 0.19) \times 10^1$
AE7 **54**	200	3.15×10^1	3.09×10^1	2.92×10^1	$(3.06 \pm 0.12) \times 10^1$
	400	2.69×10^1	2.63×10^1	2.71×10^1	$(2.68 \pm 0.040) \times 10^1$
AE1S **55**	200	3.19×10^1	3.09×10^1	2.98×10^1	$(3.09 \pm 0.10) \times 10^1$
	400	2.85×10^1	2.51×10^1	2.60×10^1	$(2.66 \pm 0.17) \times 10^1$

[a] Reaction mixtures were maintained at 30 °C and contained LOX1 enzyme from Novozymes (0.33 $\mu g\ ml^{-1}$), linoleic acid **10** (500 μM) and borate buffer (50 mM) to maintain pH 9.00. [b] Standard deviation (SD) was calculated using the following formula: $SD = \sqrt{\frac{\sum(x-\mu)^2}{(n-1)}}$ where μ is the mean and n is the number of samples.

Unusually large initial rates of oxidation of linoleic acid **10** were observed for LOX1 in the presence of surfactant **55** (AE1S) at pH 6.5 (LOX1 is usually inactive at this pH). The effect of surfactant **55** (AE1S) concentration on LOX1 hydroperoxidation activity was determined at pH 6.50. A representative absorbance versus time plot obtained at pH 6.5 in the presence of LOX1 and 300 $\mu g\ mL^{-1}$ surfactant **55** (AE1S) is shown in Fig. 3.9 and a representative set of initial rates observed in the presence of surfactant **55** (AE1S) at pH 6.5 is shown in Table 3.3. From the data in Fig 3.9, the slope of the steepest linear region (0-1 min) was obtained as 0.348 $\Delta A_{234}\ min^{-1}$, which corresponds to an initial rate of 15.5 $\mu M\ min^{-1}$. A plot of LOX1 activity at pH 6.5 versus surfactant **55** (AE1S) concentration is discussed in Section 3.3.

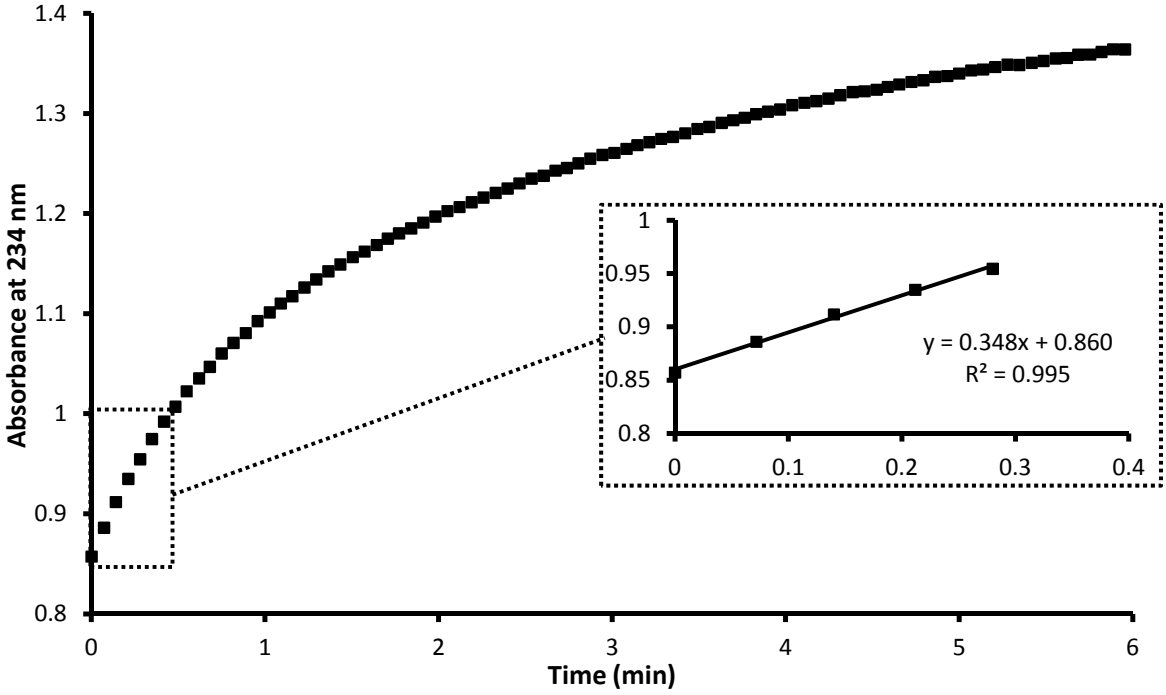

Figure 3.9 Representative plot of LOX1 (0.33 μg ml^{-1}) oxidation of linoleic acid **10** (500 μM) with surfactant **55** (AE1S) (300 μg ml^{-1}) at pH 6.5 and 30 °C. Inset shows linear region from 0-0.3 min of reaction (~1% conversion of substrate over this period of time).

Table 3.3 Initial rates of oxidation of linoleic acid **10** in the presence of LOX1 from Novozymes and surfactant **55** (AE1S) at pH 6.5.

AE1S Concentration (μg mL^{-1})	Initial Rates (υ, μM min^{-1})[a]			
	υ1	υ2	υ3	υ_{av} ± SD[b]
200	1.76 x 10^1	2.19 x 10^1	1.71 x 10^1	(1.89 ± 0.26) x 10^1
300	1.32 x 10^1	8.13	1.59 x 10^1	(1.24 ± 0.40) x 10^1
400	1.03 x 10^1	1.09 x 10^1	5.95	9.08 ± 2.7
500	4.04	1.15 x 10^1	8.44	8.02 ± 3.8
600	3.15	4.04	6.57	4.59 ± 1.8

[a] Reaction mixtures were maintained at 30 °C and contained LOX1 enzyme from Novozymes (0.33 μg ml^{-1}), linoleic acid **10** (500 μM) and phosphate buffer (50 mM) to maintain pH 6.50. [b] Standard deviation (SD) was calculated using the following formula: $SD = \sqrt{\frac{\sum(x-\mu)^2}{(n-1)}}$ where μ is the mean and n is the number of samples.

3.2.2 Oxidative degradation of β-carotene followed by UV-Vis spectrophotometry

LOX promoted oxidative degradation (bleaching) of β-carotene **1** was monitored over the same pH range as experiments detailed in section 3.2.1 (pH 6.50 – 9.00) in aqueous media at 30 °C in the presence of either surfactant **53** (Tween 80) or surfactant **54** (AE7) (structures shown in Fig. 2.4). To probe the potential carotenoid bleaching synergy of LOX1 and LOX3, isozymes were assayed individually and in combination. Bleaching experiments were performed in buffered solutions of either 50 mM phosphate (pH 6.50 – 8.00) or borate (pH 8.50 – 9.00) at 30 °C. Experiments were initiated by addition of linoleic acid stock solution at 0 °C, to cuvettes containing a mixture of buffer, β-carotene stock solution and LOX at 30 °C.

A representative absorbance versus time plot obtained at pH 8.50 in the presence of LOX3 and AE7 **54** surfactant is shown in Fig. 3.10 and a representative set of initial rates observed in the presence of AE7 **54** is shown in Table 3.4. LOX catalysed bleaching of β-carotene **1** was monitored by the decrease in absorbance at 456 nm and converted to initial rates of bleaching using the extinction coefficient for β-carotene **1** ($\varepsilon = 1.3 \times 10^5$ M^{-1} cm^{-1}).[96] From the data in Fig 3.10, the slope of the steepest linear region (1-4 min) was obtained as 0.019 ΔA_{456} min^{-1}, which corresponds to an initial rate of 0.14 nM min^{-1}. Initial rates of bleaching of β-carotene **1** in the presence of different ratios of LOX1 and LOX3 in the presence of surfactant **53** (Tween 80) or **54** (AE7) are shown in Tables B14 and B15 of Appendix B and pH rate profiles are discussed in Section 3.3.

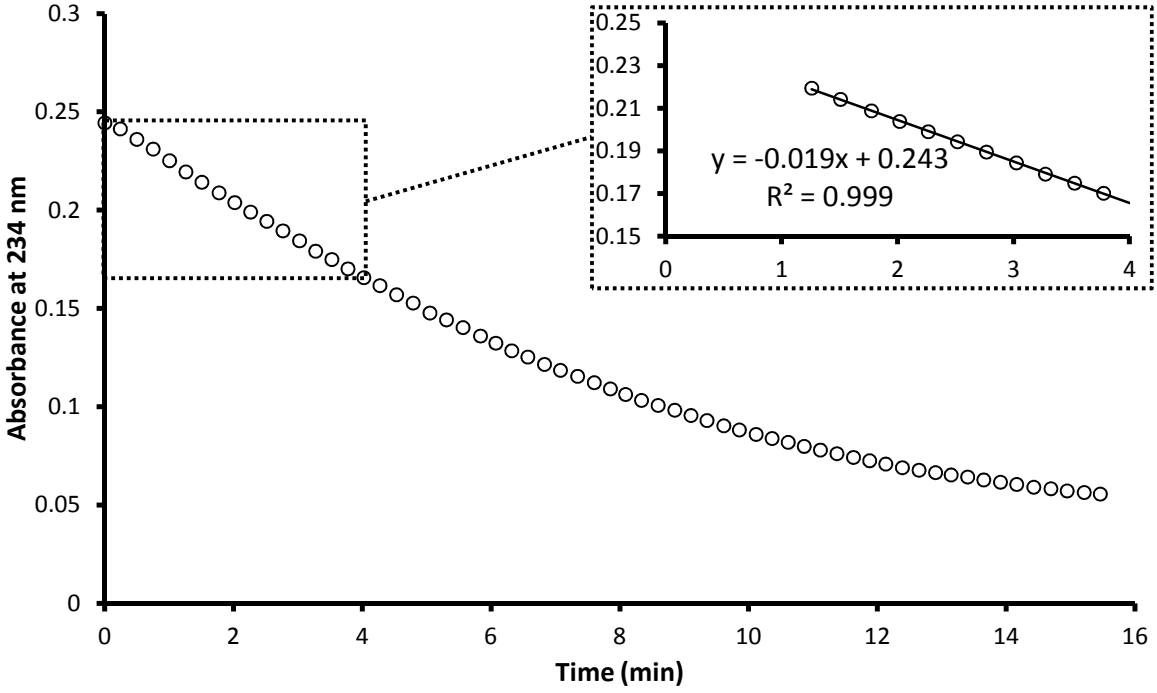

Figure 3.10 Representative plot of LOX promoted bleaching of β-carotene **1** (3.1 μM) (~87% conversion of substrate) in the presence of linoleic acid **10** (500 μM), surfactant **54** (AE7) (367 μg ml^{-1}) and both LOX1 and LOX3 in a 1:1 ratio (0.33 μg ml^{-1} total enzyme concentration) at pH 8.0 and 30 °C. Inset shows linear region from 0-4 min of reaction.

Table 3.4 β-Carotene **1** bleaching rate constants for combinations of LOX1 and LOX3 from Novozymes with linoleic acid and surfactant **54** (AE7).

Isozyme ratio (LOX1:LOX3)	pH[b]	Rate Constants (μM min^{-1})[a]			
		υ1	υ2	υ3	υ_{av} ± SD[c]
100:0	6.50	2.26×10^{-2}	2.56×10^{-2}	2.64×10^{-2}	$(2.49 \pm 1.6) \times 10^{-2}$
	7.00	6.70×10^{-3}	5.90×10^{-3}	1.28×10^{-2}	$(8.50 \pm 8.0) \times 10^{-3}$
	7.50	9.64×10^{-2}	9.03×10^{-2}	1.00×10^{-1}	$(9.56 \pm 0.77) \times 10^{-2}$
	8.00	1.67×10^{-1}	1.77×10^{-1}	1.87×10^{-1}	$(1.78 \pm 0.16) \times 10^{-1}$
	8.50	1.07×10^{-1}	9.82×10^{-2}	1.58×10^{-1}	$(1.21 \pm 0.34) \times 10^{-1}$
	9.00	8.85×10^{-2}	7.00×10^{-2}	8.38×10^{-2}	$(8.08 \pm 1.6) \times 10^{-2}$
70:30	6.50	2.41×10^{-2}	2.49×10^{-2}	2.56×10^{-2}	$(2.49 \pm 1.5) \times 10^{-2}$
	7.00	1.51×10^{-2}	1.44×10^{-2}	1.36×10^{-2}	$(1.44 \pm 0.50) \times 10^{-2}$
	7.50	7.18×10^{-2}	6.79×10^{-2}	6.26×10^{-2}	$(6.74 \pm 0.73) \times 10^{-2}$
	8.00	1.39×10^{-1}	1.50×10^{-1}	1.54×10^{-1}	$(1.48 \pm 0.13) \times 10^{-1}$
	8.50	7.90×10^{-2}	9.90×10^{-2}	1.08×10^{-1}	$(9.54 \pm 1.7) \times 10^{-2}$
	9.00	7.77×10^{-2}	8.23×10^{-2}	8.62×10^{-2}	$(8.21 \pm 1.0) \times 10^{-2}$
50:50	6.50	2.79×10^{-2}	3.56×10^{-2}	3.10×10^{-2}	$(3.15 \pm 1.8) \times 10^{-2}$
	7.00	1.28×10^{-2}	1.05×10^{-2}	1.82×10^{-2}	$(1.38 \pm 0.82) \times 10^{-2}$
	7.50	6.64×10^{-2}	6.18×10^{-2}	6.79×10^{-2}	$(6.54 \pm 0.59) \times 10^{-2}$
	8.00	1.27×10^{-1}	1.34×10^{-1}	1.42×10^{-1}	$(1.35 \pm 0.13) \times 10^{-1}$
	8.50	4.21×10^{-2}	3.90×10^{-2}	3.82×10^{-2}	$(3.97 \pm 0.38) \times 10^{-1}$
	9.00	1.77×10^{-2}	2.46×10^{-2}	3.00×10^{-2}	$(2.41 \pm 1.2) \times 10^{-2}$
30:70	6.50	3.18×10^{-2}	3.49×10^{-2}	3.64×10^{-2}	$(3.44 \pm 1.6) \times 10^{-2}$
	7.00	1.74×10^{-2}	9.70×10^{-3}	1.82×10^{-2}	$(1.51 \pm 0.89) \times 10^{-2}$
	7.50	5.79×10^{-2}	5.41×10^{-2}	5.18×10^{-2}	$(5.46 \pm 0.58) \times 10^{-2}$
	8.00	9.79×10^{-2}	9.87×10^{-2}	1.07×10^{-1}	$(1.01 \pm 0.11) \times 10^{-1}$
	8.50	2.51×10^{-2}	2.74×10^{-2}	2.74×10^{-2}	$(2.67 \pm 0.31) \times 10^{-2}$

	9.00	9.20×10^{-3}	8.50×10^{-3}	1.85×10^{-2}	$(1.21 \pm 1.2) \times 10^{-2}$
0:100	6.50	7.10×10^{-2}	3.41×10^{-2}	2.95×10^{-2}	$(4.49 \pm 3.7) \times 10^{-2}$
	7.00	1.21×10^{-2}	1.44×10^{-2}	1.36×10^{-2}	$(1.33 \pm 0.54) \times 10^{-2}$
	7.50	1.79×10^{-2}	1.87×10^{-2}	2.03×10^{-2}	$(1.90 \pm 0.39) \times 10^{-2}$
	8.00	3.72×10^{-2}	3.79×10^{-2}	2.95×10^{-2}	$(3.49 \pm 1.0) \times 10^{-2}$
	8.50	-2.56×10^{-4}	1.28×10^{-3}	-2.56×10^{-4}	$(2.56 \pm 27) \times 10^{-4}$
	9.00	-2.08×10^{-2}	-1.54×10^{-2}	-2.08×10^{-2}	$(-1.90 \pm 0.92) \times 10^{-2}$

[a] Reaction mixtures were maintained at 30 °C and contained LOX1 and/or LOX3 enzyme from Novozymes (0.33 μg ml^{-1} total concentration), β-carotene **1** (3.1 μM), linoleic acid **10** (500 μM) and surfactant **54** (AE7) (367 μg ml^{-1}). [b] Phosphate or borate buffer (50 mM) were used to maintain pH 6.50-8.00 and 8.50-9.00, respectively. [c] Standard deviation (SD) was calculated using the following formula: $SD = \sqrt{\frac{\sum(x-\mu)^2}{(n-1)}}$ where μ is the mean and n is the number of samples.

3.3 Discussion

3.3.1 LOX catalysed oxidation of linoleic acid

The LOX catalysed oxidation of linoleic acid was followed by UV-Vis spectrophotometry in aqueous buffered solutions containing surfactants at 30 °C as described in Section 3.2.1.1. The LOX mechanism for linoleic acid oxidation is shown in Scheme 3.1.

Enzymatic oxidation of linoleic acid and subsequent bleaching of β-carotene was studied utilising two Glycine max isozymes of LOX, an enzyme that catalyses the formation of hydroperoxides from linoleic acid. Hydrogen is abstracted from the central methylene by the non-haem iron forming the same radical intermediate generated during the initiation stage of autoxidation. The enzyme then directs molecular oxygen to a specific face at one terminus of the radical system. Reduction and proton transfer afford the hydroperoxide and regenerate the non-haem iron. Although not their primary function, LOXs are also known to promote the bleaching of carotenoids.

Initially, the linoleic acid oxidation activity of LOXs from Novozymes and Sigma were assessed in the presence of surfactant **52** (Tween 20). In the presence of 500 μM linoleic acid **10** substrate, LOX1 and LOX3 from Novozymes were found to possess pH optima at pH 9.0 and 6.5 while LOX1 samples from Sigma had a broad activity range (Fig. 3.11A). At lower substrate concentrations (80 μM), activity of LOX3 from Novozymes was not observed while LOX1 from Novozymes remained active (Fig. 3.11B). Notably, the activity-pH profile of LOX1 from Sigma at 80 μM substrate became similar to that of LOX1 from Novozymes. LOX1 from Sigma was thought to be a mixture of LOX1 and LOX3, and was not used in future assays.

A

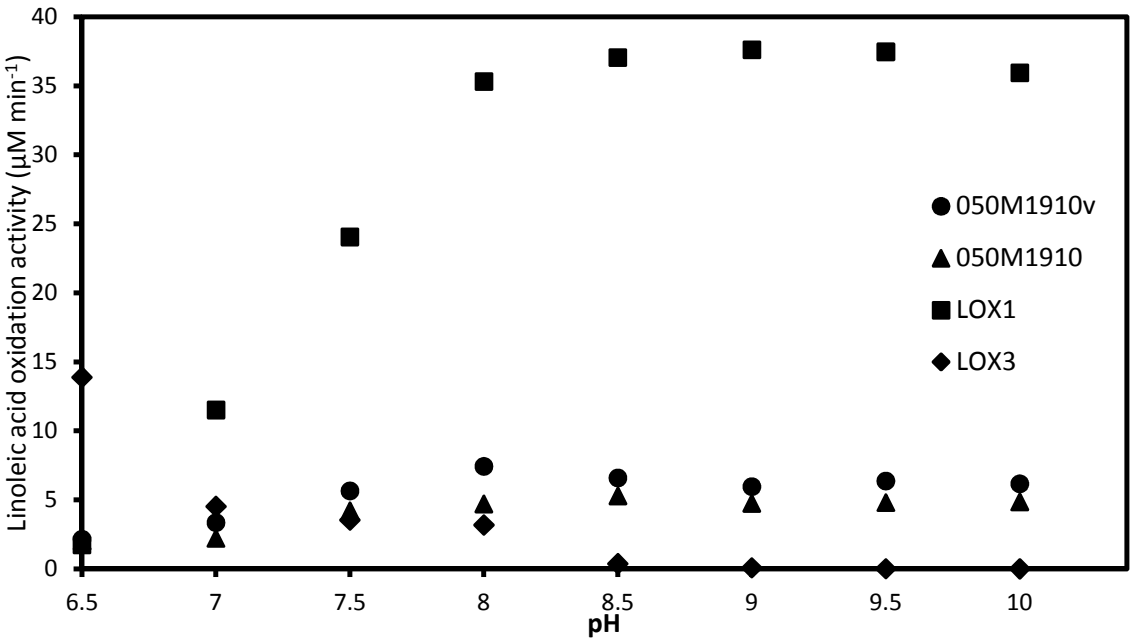

B

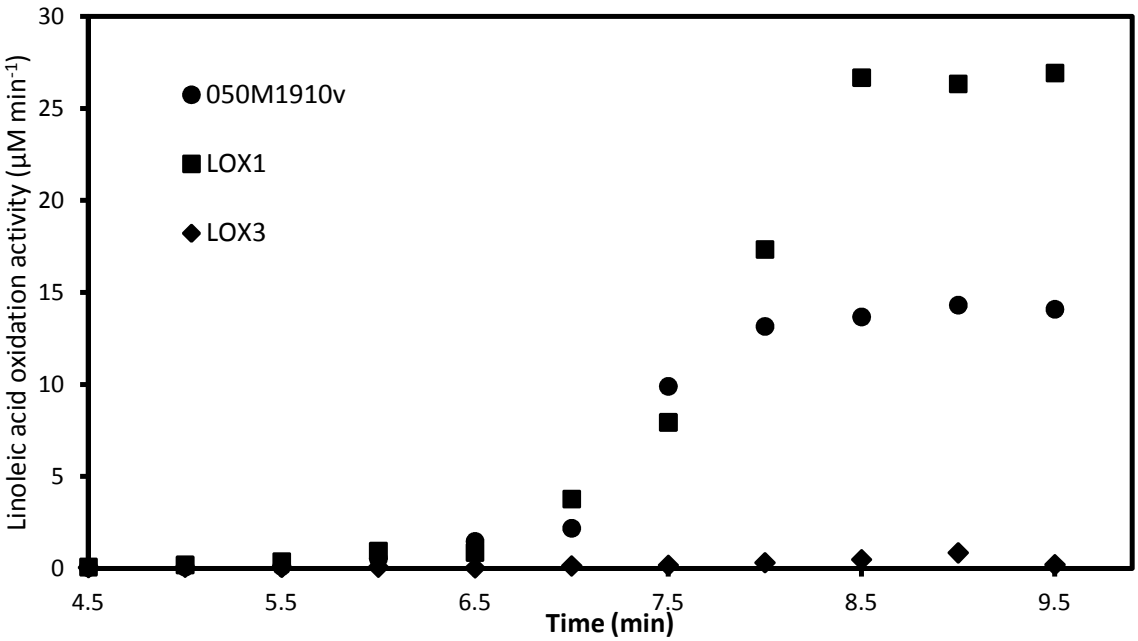

Figure 3.11 pH-Rate profiles for 050M1910v from Sigma and LOX1/3 from Novozymes in the presence of (A) 500 and (B) 80 µM linoleic acid **10**.

Linoleic acid **10** concentration was maintained at 500 μM for enzymatic experiments, both to enable direct comparison with non-enzymatic results and also to ensure maximal V_{max} activity as this concentration is 37 to 45-fold larger than the reported K_m values for LOX 1 (11[92] and 13.25 μM[97]). K_m values for LOX3 have not been published and may be the result of LOX3 having greater sensitivity to experimental conditions. LOX1 is reported to possess optimal activity ~ pH 9.0 with relatively low activity at neutral pH. This is based on studies in aqueous buffer with sodium linoleate and Tween 20.[98] In contrast, LOX3 was reported to have a lower pH optimum of 6.5 for reaction in similar conditions.[98] The effect of surfactant on enzymatic oxidation of linoleic acid **10** could be assessed using several additional surfactants that did not solubilise β-carotene **1**. Hydroperoxide formation was monitored with surfactant concentrations of 200 μg ml^{-1} (as in the non-enzymatic experiments) and 400 μg ml^{-1}. As established in Chapter 2, the minimum surfactant concentration required to solubilise fatty acid was 200 μg ml^{-1}. Higher concentrations of surfactant (400 μg ml^{-1}) were studied to observe the effect on LOX.

LOX1, from our data shown in Fig. 3.12, is the more active and stable of the two isozymes. At optimum pH (9.0) LOX1 (0.33 μg ml^{-1}) was active at all surfactant conditions with initial rates of 30-38 μM min^{-1} at 200 μg ml^{-1} surfactant with a ~20% decrease in activity at 400 μg ml^{-1} surfactant. Changing surfactant did not appear to significantly affect LOX1 at pH 9.0 as differences in activity are ~10%. Activity was observed to be highest in surfactant **52** (Tween 20) at concentrations of 200 μg ml^{-1}, while no significant activity differences were observed at 400 μg ml^{-1}. Interestingly, although LOX1 is not usually active at neutral pH, in the presence of surfactant **50** (AE1S), initial rates at pH 6.5 were found to be within 2-4 fold of those at pH 9.0.

In contrast, LOX3 activity was severely affected by changes in surfactant and concentration. No significant activity was observed when surfactant **54** (AE7) or **55** (AE1S) or were present. LOX3 activity was observed at optimum pH (6.5) using 200 μg ml^{-1} of surfactant **52** (Tween 20) or **53** (Tween 80) (6 and 4 μM min^{-1}, respectively), however, no

significant activity relative to background was observed upon increasing surfactant concentration to 400 μg ml^{-1}. Comparing the two LOX isoforms at their respective pH optima, LOX1 was more stable to changes in surfactant conditions and possessed greater activity.

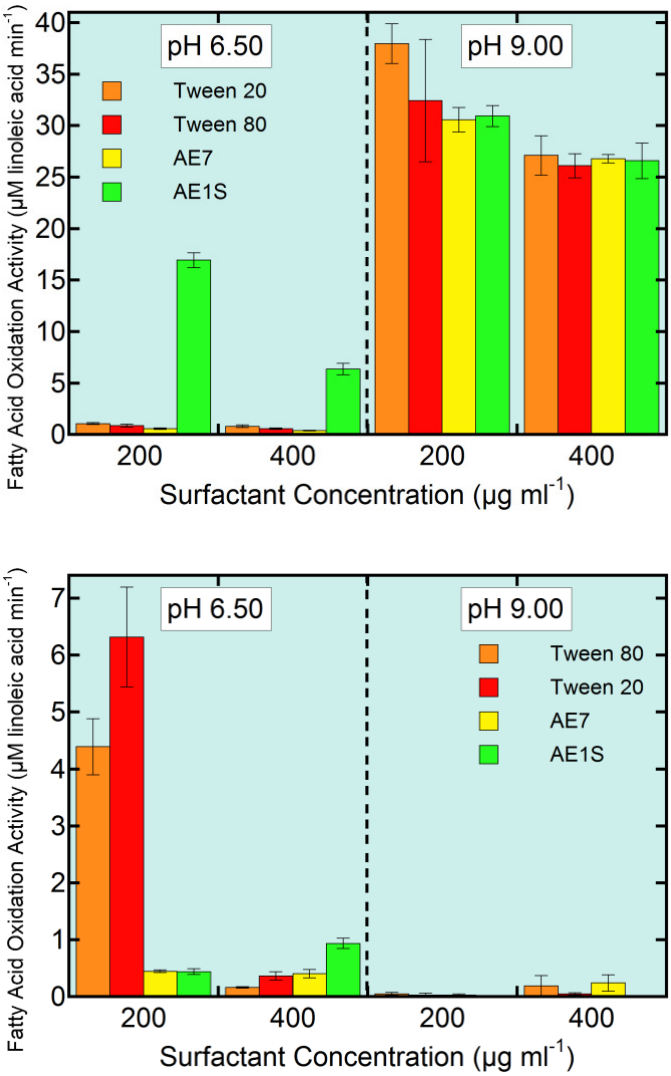

Figure 3.12 Initial rates of oxidation of linoleic acid **10** (500 μM) by LOX1 (0.33 μg ml^{-1}) (above) and LOX3 (0.33 μg ml^{-1}) (below) under different surfactant conditions.

Both binding and formation of surfactant clusters on proteins are typically accompanied by modifications in structure and a concomitant change in activity. Our data show the Tween surfactants to be less disruptive than the alcohol ethoxylate (AE) surfactants towards LOX1/3 activities. The Tween surfactants are more hydrophilic than the AE surfactants based on HLB values, which will affect the micelle structures formed. A study of dodecyl maltoside (DDM) and SDS analogues found that shorter chain analogues (higher HLB/HI) tended to form rod like micelles which are less potent at denaturing proteins than spherical micelles. In agreement with our studies, an early study of LOX1-catalysed hydroperoxidation reported that V_{max} values for linoleic acid oxidation were highest in the presence of Tween 20 relative to other surfactants (Brij 35, CTAB, DOC, SDS). This phenomenon was attributed to stabilising effects at low concentration and less denaturation at higher concentrations of surfactant.

LOX3 activity was affected more dramatically by the type and concentration of surfactant. There are few studies in the literature that address LOX stability or interactions towards surfactants and these reports do not usually offer a comparison between LOX1 and LOX3.[99,100] A recent study of the activities of isozymes isolated from Glycine max by Ma *et al.* over a range of temperatures demonstrated that LOX1 remained active at higher temperatures relative to LOX3 suggesting LOX1 possesses greater intrinsic stability.[101] A structural comparison of LOX1 and LOX3 crystal structures highlights significant differences in the internal cavity sizes for the two isozymes, which may explain the contrasting stabilities in the presence of surfactant. LOX3 features a smaller, restrictive fatty acid binding site, which may be more sensitive to structural changes relative to the more open cavity in LOX1.[54,55] The large inter-domain contact surface, which includes extensive non-covalent interactions, may also contribute to the relative stability of LOX1. The isoelectric points (pIs) of LOX1 and LOX3 are 5.91 and 6.12, respectively, meaning LOX3 will be slightly more cationic than LOX1 at pH values around pH 6.0 and could lead to greater interaction with anionic surfactants such as surfactant **55** (AE1S).

The unusual effect of surfactant **50** (AE1S) observed for LOX1 at pH 6.5 was investigated further by measuring activity over a range of surfactant concentrations (data shown in Fig. 3.13). Background non-enzymatic oxidation decreased as surfactant **55** (AE1S) concentration increased, although differences were small. At pH 6.5 and 200 μg ml^{-1} surfactant **55** (AE1S) the initial background rate was 0.52 μM min^{-1}, ~2.5 fold greater than the initial rates observed for surfactant **53** (Tween 80) under identical conditions. This value decreased to 0.31 μM min^{-1} at 600 μg ml^{-1} surfactant **55** (AE1S). LOX1 catalysed oxidation of linoleic acid **10** also decreased at higher concentrations for surfactant **55** (AE1S) with initial rates of 18.4 μM min^{-1} and 4.3 μM min^{-1} at the lowest and highest surfactant concentrations tested, respectively.

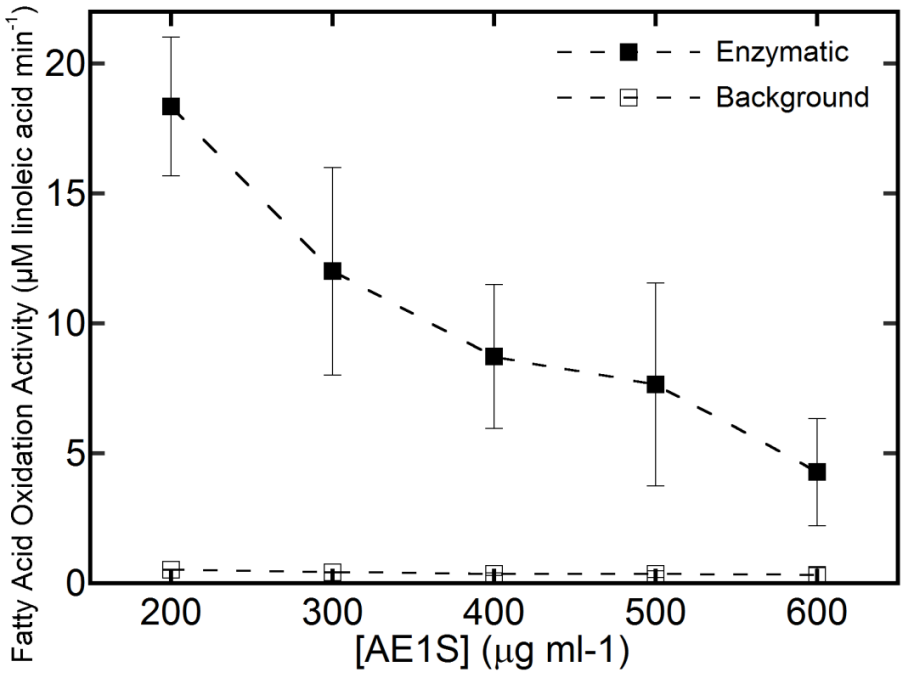

Figure 3.13 Initial rates of oxidation of linoleic acid **10** (500 μM) in the presence (■) and absence (□) of LOX1 over a range of surfactant **55** (AE1S) concentrations at 30°C

In contrast to the other surfactants tested, surfactant **55** (AE1S) is anionic while **52** (Tween 20), **53** (Tween 80) and **54** (AE7) are all non-ionic. Anionic surfactants have a greater affinity to proteins relative to non-ionic, due to the ability to form electrostatic interactions

with positively charged residues. The interactions between surfactants and enzymes may result in significant changes in stability and activity. The unexpectedly large initial oxidation rates for LOX1 at pH 6.5 in the presence of surfactant **55** (AE1S) could be due to a stabilising effect facilitating activity over a greater pH range. Alternatively, anionic surfactant and LOX binding and interaction may be pH dependent with greater influence as LOX1 becomes more cationic.

3.3.2 LOX promoted *in situ* oxidation of β-carotene

LOX-catalysed bleaching of β-carotene **1** was monitored using only surfactants **53** (Tween 80) and **54** (AE7). In our study, we corrected for background non-enzymatic bleaching by linoleic acid **10** such that the initial rates in Fig. 3.14 and 3.15 represent entirely enzymatic bleaching of β-carotene **1**. Reaction mixtures containing only LOX1 (100:0) displayed higher initial bleaching rates around pH 8.0. Activity sharply decreased at pH 7.0 and 6.5. The activity range of LOX1 appears broader when surfactant **53** (Tween 80) was utilised to solubilise substrates compared to surfactant **54** (AE7). The activity of LOX3 individually (0:100) is lower over the pH range tested compared to LOX1 with maximal activity at pH 6.5. LOX3 activity decreased as pH increased, showing no activity at pH 8.5 or higher (initial bleaching rates were actually slightly lower compared to background in the presence of LOX3). As observed in the non-enzymatic studies, the initial rates for β-carotene **1** degradation are larger by approximately 2-fold in assays that utilised surfactant **53** (Tween 80) to solubilise substrates as compared to surfactant **54** (AE7).

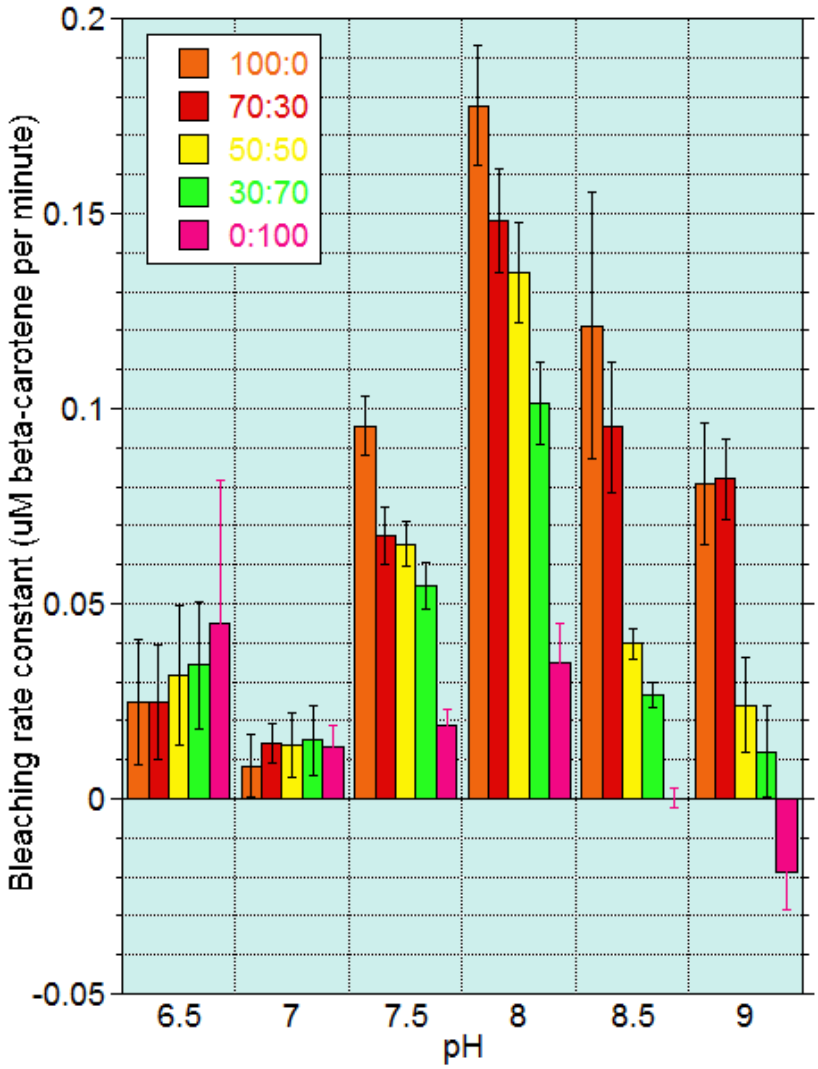

Figure 3.14 pH-Rate profile of the bleaching of β-carotene **1** (3.1 μM) in the presence of different ratios of LOX1/3 (0.33 μg ml^{-1} total concentration), linoleic acid **10** (500 μM) and surfactant **54** (AE7) (367 μg ml^{-1}).

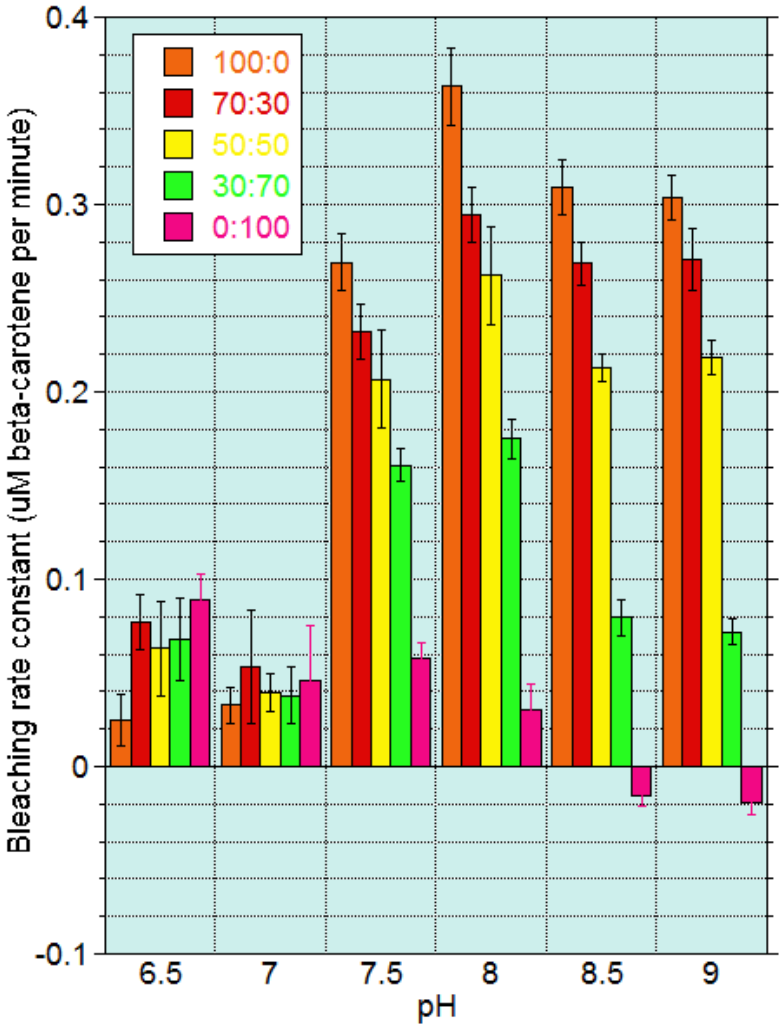

Figure 3.15 pH-Rate profile of the bleaching of β-carotene **1** (3.1 μM) in the presence of different ratios of LOX1/3 (0.33 μg ml^{-1} total concentration), linoleic acid **10** (500 μM) and surfactant **53** (Tween 80) (367 μg ml^{-1}).

A previous study by Ramadoss *et al.* reported a carotenoid bleaching synergy when using a combination of Glycine max isozymes (LOX3 with either LOX1 or LOX2). In contrast to our experiments, these assays contained cosolvents (7.2% acetone and 0.8% ethanol v/v) and were performed at 15 °C. Additionally, reaction mixtures contained substrate concentrations of 6 μM β-carotene **1** and 29 μM methyl linoleate. At pH 6.5, a synergy

effect was observed with complete bleaching occurring 6 times faster than times predicted from assays of individual isozymes.

No cosolvents were utilised in our assays to allow monitoring of the oxidation of linoleic acid **10** spectrophotometrically (λ_{max} 234 nm), to avoid potentially reducing the activity of LOX isozymes and to be more representative of wash conditions. Furthermore, appreciable concentrations of substrates could not be solubilised in cosolvent systems (see Section 2.2.1). Assays containing methyl linoleate were attempted but required the presence of ethanol for solubilisation at all pH values. LOX3 activity was not observed in these experiments either because the K_M for methyl linoleate is large or the presence of ethanol deactivates LOX3.

In our case, the presence of more than one LOX isozyme does not substantially increase the initial bleaching rates above reaction mixtures containing only individual isozymes. In surfactant **53** (Tween 80), a small positive bleaching synergy between LOX1 and LOX3 is observed (≤ 70%) compared to a maximum synergy of 60% in surfactant **54** (AE7). However, under several conditions a small, significant negative synergy (–30%) is also found in the presence of surfactant **54** (AE7). Overall, combinations of LOX isozymes alter the observed initial rates by less than 2-fold relative to those containing single isozymes highlighting the lack of a substantial synergy.

3.4 Summary

LOX promoted linoleic acid oxidation **10** and β-carotene **1** degradation were quantified under analogous conditions to non-enzymatic studies described in the previous chapter to allow for comparison and to assess LOX promoted oxidation activity. Similar to non-enzymatic experiments, initial rates of linoleic acid oxidation and β-carotene degradation were measured by UV-Vis spectrophotometry in buffered oil-in-water emulsions at 30 °C.

Hydroperoxidation assays showed that LOX1 was more stable than LOX3 towards changes in surfactant conditions. At optimum pH, LOX1 remained at similar activity (within 20%) in the presence of the surfactants and concentrations tested. In contrast, LOX3 was only active in the presence of Tween 20 and 80 surfactants at concentrations of 200 μg ml^{-1}. Interestingly, LOX1 was observed to have high activity away from optimum pH when in the presence of surfactant **55** (AE1S). LOX1 activity was assayed over a greater range of surfactant **55** (AE1S) concentrations at pH 6.5 however oxidation activity was found to decrease as surfactant concentration increased.

Bleaching assays of β-carotene **1** showed that initial rates of degradation were greater in the presence of LOX, however the addition of enzyme only accelerated initial rates by one order of magnitude at an enzyme concentration of 0.33 μg mL^{-1}. LOX1 was found to possess greater bleaching activity and had a pH optimum of pH 8.0 in the presence of surfactant **54** (AE7) and a broader optimum around pH 8.5 in the presence of surfactant **53** (Tween 80). LOX3 bleaching activity was highest at pH 6.5 and decreased as pH increased. Combinations of LOX1 and 3 did not substantially increase bleaching activity with a maximum favourable synergy of ~70% in surfactant **53** (Tween 80) and ~60% in **54** (AE7). Similar to non-enzymatic assays, initial rates of bleaching were 2-fold greater in surfactant **53** (Tween 80) as compared to **54** (AE7).

The application of soybean LOX enzymes in the bleaching of carotenoid stains is an attractive solution as linoleic acid **10**, the native substrate of LOX, is present in appreciable concentrations within greasy stains and co-localises with carotenoids. One limitation, however, is that LOX enzymes have been reported to be slow. In order to overcome this limitation P&G has become interested in a reported bleaching synergy between LOX1 and LOX3. Our assessment of the bleaching activity of LOX1 and LOX3, however, show that under our experimental conditions this synergy is small and overall LOX promoted bleaching rates are only 1 to 2 orders of magnitude greater than fatty acid autoxidation promoted bleaching. Furthermore, our assays suggest that LOX3 may be unsuitable for bleaching applications in laundry washing. LOX3 is not active above neutral pH and is highly sensitive to surfactant conditions.

3.5 Experimental

3.5.1 Materials

Linoleic acid **10** (L1376), arachidonic acid **42** (A9673), stearic acid **37** (S4751), oleic acid **38** (O1008), linolenic acid **41** (L2376), β-carotene **1** (22040), lipoxidase from *Glycine max* batch 050M1910v (L7395), Tween 80 **53** (P1754) and Tween 20 **52** (P1379) surfactants were purchased from Sigma-Aldrich. LOXs from *Glycine max* (LOX1 and LOX3) were kindly donated by Dr Keith Gibson (Novozymes) as glycerol stocks of 5.5 and 1.5 mg ml^{-1}, respectively. AE7 **54** and AE1S **55** surfactants were kindly donated by Procter & Gamble.

3.5.2 Methods

3.5.2.1 Solubilisation of materials

A solution of β-carotene **1** in dichloromethane (1 mg/ml) was added to neat surfactant (100 mg per ml β-carotene **1** solution). The solvent was then evaporated under reduced pressure to afford a viscous, red residue. Deionised water (10 ml per 1 mg β-carotene) was added to the residue and mixed until a homogenous orange solution was obtained.

Fatty acid was solubilised by addition of NaOH (800 μl, 0.5 M) to fatty acid (0.2 mmole) followed by addition of surfactant diluted in deionised water (4 ml, 4 mg/ml). The solution was gently mixed until homogenous then diluted by addition of deionised water (16.2 ml). Preparations of solutions containing stearic acid **37** necessitated heating to 70 °C while mixing. All other fatty acid solutions were prepared at room temperature.

3.5.2.2 Reaction mixture preparation

Stock solutions of β-carotene, fatty acid and LOX were prepared immediately before use. The pH of reaction mixtures were maintained using 50 mM buffer (acetate pH 4.5-6.0, phosphate pH 6.5-8.0, borate pH 8.5-10.0). Stock solutions of β-carotene, LOX and buffer

were initially mixed in the cuvette, followed by addition of linoleic acid to initiate the bleaching reaction.

3.5.2.3 Absorbance measurements

Absorbance measurements were obtained using Varian Cary 50 and Cary 100 UV-visible spectrophotometers. The Kinetics Program was used to measure absorbance at 234 nm and 456 nm to monitor fatty acid hydroperoxidation and carotenoid cooxidation, respectively. Triplicate runs of each assay at each condition were performed. A PCB-150 Peltier water bath and Peltier heating/refrigeration unit were employed to maintain a constant temperature of 30 °C. Measurements were made in 3 ml quartz cuvettes with 1 cm path length. Changes in absorbance units per minute were converted to concentration per minute using extinction coefficients of 140,000 and 22,500 M^{-1} cm^{-1} for β-carotene and fatty acid hydroperoxide respectively.[95,96]

3.6 References

[1] J. J. M. C. De Groota, G. A. Veldink, J. F. G. Vliegenthart, J. Boldingh, R. Wever and B. F. Van Gelder, *Biochim. Biophys. Acta*, 1975, **377(1)**, 71–79.
[2] M. Hamberg and B. Samuelsson, *J. Biol. Chem.*, 1967, **22**, 5329–35.
[3] M. Hamberg and G. Hamberg, *Biochem. Biophys. Res. Commun.*, 1980, **3**, 1090–1097.
[4] S. Yamamoto, *Biochim. Biophys. Acta*, 1992, **2-3**, 117–131.
[5] R. M. Bohn and L. W. Haas, *Chem. Meth. Enz.*, ed by Sumner, J. B. & Somers, G. F., 1928, Academic Press, New York.
[6] J. B. Sumner and A. L. Dounce, *Enzymologia*, 1939, **7**, 130.
[7] B. Sumner and J. Sumner, *J. Biol. Chem.*, 1940, **134**, 531–533.
[8] H. Theorell, R. Holman and A. Akeson, *Acta Chem. Scand.*, 1947, **6**, 571–576.
[9] R. T. Holman, *Arch. Biochem.*, 1947, **3**, 403.
[10] J. Christopher, E. Pistorius, and B. Axelrod, *Biochim. Biophys. Acta*, 1970, **1**, 12–19.
[11] J. Christopher, E. Pistorius, and B. Axelrod, *Biochim. Biophys. Acta*, 1972, **1**, 54–62.
[12] C. S. Ramadoss, E. Pistorius, and B. Axelrod, *Arch. Biochem. Biophys.*, 1978, **2**, 549–552.
[13] W. Grosch and G. Laskawy, *Biochim. Biophys. Acta*, 1979, **575**, 439–445.
[14] H. Ma, X. D. Zhang, X. S. Wang and X. L. He, *Soybean Science*, 2010, **4**, 033.
[15] E. H. Oliw, *Prostaglandins & other lipid mediators*, 2002, **68-69**, 313–23.
[16] A. R. Brash, *J. Biol. Chem.*, 1999, **34**, 23679–23682.
[17] T. Koeduka, T. Kajiwara, and K. Matsui, *Curr. Microbiol.*, 2007, **4**, 315-319.
[18] A. Liavonchanka, and I. Feussner, *J. Plant Physiol.*, 2006, **3**, 348–57.
[19] C. Schneider, D. A. Pratt, N. A. Porter, and A. R. Brash, *Chem. Biol.*, 2007, **5** , 473–488.
[20] I. Feussner, and H. Kühn, *Enzymes in Lipid Modification*, 2000, **40**, 309.
[21] I. Feussner, and H. Kühn, *FEBS Lett.*, 1995, **1**, 12-14.
[22] A. Z. Andreou, E. Hornung, S. Kunze, S. Rosahl, and I. Feussner, *Lipids*, 2009, **3**, 207-215.
[23] J. N. Siedow, *Annu. Rev. Plant Physiol. Plant Mol. Biol.*, 1991, **1**, 145–188.
[24] D. Shibata, A. Slusarenko, R. Casey, and E. Bell, *Plant Molecular Biology Reporter*, 1994, **2**, 41–42.
[25] A. Mosblech, I. Feussner, and I. Heilmann, *Plant Physiol. Biochem. : PPB / Société française de physiologie végétale*, 2009, **6**, 511–7.
[26] J. Z. Haeggström, and C. D. Funk, *Chem. Rev.*, 2011, **10**, 5866–98.
[27] D. I. Tsitsigiannis, and N. P. Keller, *Trends Microbiol.*, 2007, **3**, 109–18.
[28] B. Samuelsson, *Science,* 1983, **4597,** 568-575.
[29] A. R. Brash, *J. Biol. Chem.*, 1999, **34**, 23679–23682.
[30] J. Choi, J. K. Chon, S. Kim, and W. Shin, *Proteins*, 2008, **3**, 1023-1032.
[31] D. B. Neau, N. C. Gilbert, S. G. Bartlett, W. Boeglin, A. R. Brash, and M. E. Newcomer, *Biochemistry*, 2009, **33**, 7906-7915.
[32] W. Minor, J. Steczko, J. T. Bolin, Z. Otwinowski, and B. Axelrod, *Biochemistry*, 1993, **25**, 6320–3.
[33] E. Skrzypczak-Jankun, O. Y. Borbulevych, M. I. Zavodszky, M. R. Baranski, K. Padmanabhan, V. Petricek, and J. Jankun, *Acta Crystallogr., Sect D: Biol. Crystallogr.*, 2006, **7**, 766-775.
[34] R. Koljak, O. Boutaud, B. H. Shieh, N. Samel, and A. R. Brash, *Science*, 1997, **5334**, 1994-1996.
[35] S. A. Gillmor, A. Villaseñor, R. Fletterick, E. Sigal, and M. F. Browner, *Nat. Struct. Biol.*, 1997, **12**, 1003-1009.
[36] J. A. Corbin, J. H. Evans, K. E. Landgraf, and J. J. Falke, *Biochemistry*, 2007, **14**, 4322-4336.
[37] H. Chahinian, B. Sias, and F. Carriere, *Curr. Protein Pept. Sci.*, 2000, **1**, 91-103.
[38] M. Maccarrone, M. L. Salucci, G. Van Zadelhoff, F. Malatesta, G. Veldink, J. F. Vliegenthart, and A. Finazzi-Agrò, *Biochemistry*, 2001, **23**, 6819–27.
[39] E. Dainese, C. B. Angelucci, A. Sabatucci, V. De Filippis, G. Mei, and M. Maccarrone, *FASEB J.*, 2010, **6**, 1725-1736.
[40] M. Walther, M. Anton, M. Wiedmann, R. Fletterick, and H. Kuhn, *J. Biol. Chem.*, 2002, **30**, 27360-27366.
[41] C. May, M. Höhne, P. Gnau, K. Schwennesen, and H. Kindl, *Eur. J. Biochem. / FEBS*, 2000, **4**, 1100–9.
[42] S. A. Tatulian, J. Steczko, and W. Minor, *Biochemistry*, 1998, **44**, 15481-15490.
[43] M. Walther, R. Wiesner, and H. Kuhn, *J. Biol. Chem.*, 2004, **5**, 3717–25.
[44] S. Kulkarni, S. Das, C. D. Funk, D. Murray, and W. Cho, *J. Biol. Chem.*, 2002, **15**, 13167–74.

[45] M. L. Oldham, A. R. Brash, and M. E. Newcomer, *J. Biol. Chem.*, 2005, **47**, 39545–52.
[46] X. S. Chen, and C. D. Funk, *J. Biol. Chem..*, 2001, **1**, 811–8.
[47] R. Brinckmann, K. Schnurr, D. Heydeck, T. Rosenbach, G. Kolde, B. R. Brinckmann, *Blood*, 1998, **1**, 64–74.
[48] W. Minor, J. Steczko, B. Stec, Z. Otwinowski, J. T. Bolin, R. Walter, and B. Axelrod, *Biochemistry*, 1996, **33**, 10687–701.
[49] D. R. Tomchick, P. Phan, M. Cymborowski, W. Minor, and T. R. Holman, *Biochemistry*, 2001, **25**, 7509-7517.
[50] G. Schenk, M. L. Neidig, J. Zhou, T. R. Holman, and E. I. Solomon, *Biochemistry*, 2003, **24**, 7294-7302.
[51] G. Mei, A. Di Venere, E. Nicolai, C. B. Angelucci, I. Ivanov, A. Sabatucci, E. Dainese, H. Kuhn, and M. Maccarrone, *Biochemistry*, 2008, **35**, 9234-9242.
[52] M. Hammel, M. Walther, R. Prassl, and H. Kuhn, *J. Mol. Biol.*, 2004, **4**, 917-929.
[53] E. Dainese, A. Sabatucci, G. Van Zadelhoff, C. B. Angelucci, P. Vachette, G. A. Veldink, A. F. Agrò, M. Maccorrone, *J. Mol. Biol.*, 2005, **1**, 143–52.
[54] E. Skrzypczak-Jankun, O. Y. Borbulevych, and J. Jankun, *Acta Crystallogr., Sect D: Biol. Crystallogr.*, 2004, **Pt 3**, 613–5.
[55] O. Y. Borbulevych, J. Jankun, S. H. Selman, and E. Skrzypczak-Jankun, *Proteins*, 2004, **1**, 13–9.
[56] J. C. Boyington, B. J. Gaffney, and L. M. Amzel, *Science*, 1993, **5113**, 1482–1486.
[57] M. J. Knapp, F. P. Seebeck, and J. P. Klinman, *J. Am. Chem. Soc.*, 2001, **12**, 2931–2.
[58] M. J. Knapp, and J. P. Klinman, *Biochemistry*, 2003, **39**, 11466–75.
[59] M. P. Meyer, D. R. Tomchick, and J. P. Klinman, *Proc. Natl. Acad. Sci. U.S.A.*, 2008, **4**, 1146–51.
[60] B. Youn, G. E. Sellhorn, R. J. Mirchel, B. J. Gaffney, H. D. Grimes, and C. Kang, *Proteins*, 2009, **4**, 1008–1020.
[61] M. Karplus, J. A. McCammon, and W. L. Peticolas, *Crit. Rev. Biochem. Mol. Biol.*, 1981, **4**, 293-349.
[62] A. Ostermann, R. Waschipky, F. G. Parak, and G. U. Nienhaus, *Nature*, 2000, **6774**, 205-208.
[63] K. Chu, J. Vojtchovský, B. H. McMahon, R. M. Sweet, J. Berendzen, and I. Schlichting, *Nature*, 2000, **6772**, 921-923.
[64] J. Saam, I. Ivanov, M. Walther, H. G. Holzhütter, and H. Kuhn, *Proc. Natl. Acad. Sci. U.S.A.*, 2007, **33**, 13319-13324.
[65] M. F. Browner, S. A. Gillmor, and R. Fletterick, *Nat. Struct. Biol.*,1998, **3**, 179-179.
[66] T. Schewe, S. M. Rapoport, and H. Kuhn, *Adv. Enzymol. Relat. Areas Mol. Biol.*, 1986, **58**, 191-272.
[67] H. Kühn, H. Sprecher, and A. R. Brash, *J. Biol. Chem.*, 1990, **27**, 16300-16305.
[68] A. Andreou, and I. Feussner, *Phytochemistry*, 2009, **13-14**, 1504–10.
[69] M. Walther, J. Roffeis, C. Jansen, M. Anton, I. Ivanov, and H. Kuhn, *Biochim. Biophys. Acta (BBA)-Molecular and Cell Biology of Lipids*, 2009, **8**, 827-835.
[70] G. A. Veldink, G. J. Garssen, J. F. G. Vliegenthart, and J. Boldingh, *Biochem. Biophys. Res. Commun.*, 1972, **1**, 22–26.
[71] E. Skrzypczak-Jankun, R. A. Bross, R. T. Carroll, W. R. Dunham, and M. O. Funk, *J. Am. Chem. Soc.*, 2001, **44**, 10814–20.
[72] E. Hornung, M. Walther, H. Kühn, and I. Feussner, *Proc. Natl. Acad. Sci. U.S.A.*, 1999, **7**, 4192-4197.
[73] V. C. Ruddat, R. Mogul, I. Chorny, C. Chen, N. Perrin, S. Whitman, V. Kenyon, M. Jacobson, C. Bernasconi, and T. R. Holman, *Biochemistry*, 2004, **41**, 13063-13071.
[74] H. W. Gardner, *Biochim. Biophys. Acta*, 1989, **3**, 274–81.
[75] M. Walther, I. Ivanov, G. Myagkova, and H. Kuhn, *Chem. Biol.*, 2001, **8**, 779-790.
[76] G. Coffa, and A. R. Brash, *Proc. Natl. Acad. Sci. U.S.A.*, 2004, **44**, 15579-15584.
[77] G. Coffa, C. Schneider, and A. R. Brash, *Biochem. Biophys. Res. Commun.*, 2005, **1**, 87-92.
[78] S. Meruvu, M. Walther, I. Ivanov, S. Hammarström, G. Fürstenberger, P. Krieg, P. Reddanna, H. Kuhn, *J. Biol. Chem.*, 2005, **44**, 36633–41.
[79] G. Coffa, A. N. Imber, B. C. Maguire, G. Laxmikanthan, C. Schneider, B. J. Gaffney, and A. R. Brash, *J. Biol. Chem.*, 2005, **46**, 38756–66.
[80] W. E. Boeglin, A. Itoh, Y. Zheng, G. Coffa, G. A. Howe, and A. R. Brash, *Lipids*, 2008, **11**, 979-987.
[81] I. Ivanov, D. Heydeck, K. Hofheinz, J. Roffeis, V. B. O'Donnell, H. Kuhn, and M. Walther, *Arch. Biochem. Biophys.*, 2010, **2**, 161–174.
[82] J. P. Klinman, *Procedia Chemistry*, 2011, **1**, 291–305.
[83] M. H. Glickman, J. S. Wiseman, and J. P. Klinman, *J. Am. Chem. Soc.*, 1994, ***116***, 793–794.

[84] C. C. Hwang, & C. B. Grissom, *J. Am. Chem. Soc.*, 1994, **2**, 795-796.
[85] M. H. Glickman, and J. P. Klinman, *Biochemistry*, 1996, **39**, 12882–92.
[86] M. R. Egmond, P. M. Fasella, G. Veldink, J. Vliegenthart, and J. Boldingh, *Eur. J. Biochem.*, 1977, **2**, 469–479.
[87] M. J. Nelson, *J. Am. Chem. Soc.*, 1988, **9**, 2985-2986.
[88] R. C. Scarrow, M. G. Trimitsis, C. P. Buck, G. N. Grove, R. A. Cowling, and M. J. Nelson, *Biochemistry*, 1994, **50**, 15023-15035.
[89] T. Jonsson, M. H. Glickman, S. Sun, and J. P. Klinman, *J. Am. Chem. Soc.*, 1996, **42**, 10319–10320.
[90] M. J. Nelson, R. A. Cowling, and S. P. Seitz, *Biochemistry*, 1994, **16**, 4966-4973.
[91] M. H. Glickman, S. Cliff, M. Thiemens, and J. P. Klinman, *J. Am. Chem. Soc.*, 1997, **47**, 11357-11361.
[92] M. H. Glickman, and J. P. Klinman, *Biochemistry*, 1995, **43**, 14077–92.
[93] J. P. Klinman, *J. Biol. Inorg. Chem.*, 2001, **1**, 1–13.
[94] S. M. Rapoport, T. Schewe, R. Wiesner, W. Halangk, P. Ludwig, M. Janicke‐Höhne, C. Tannert, C. Hiebsch, and D. Klatt, *Eur. J. Biochem.*, 1979, **3**, 545-561.
[95] M. J. Gibian and P. Vandenberg, *Anal. Biochem.*, 1987, **163**, 343–349.
[96] G. Britton, S. Liaaen-Jensen, and H. P. Pfander, *Carotenoids: handbook*., 2004, Birkhauser.
[97] A. Serpen and V. Gökmen, *Eur. Food Res. Technol.*, 2006, **224**, 743–748.
[98] B. Axelrod, T. M. Cheesbrough and S. Laakso, *Methods Enzymol.*, 1981, **71**, 441–451.
[99] S. Srinivasulu and A. G. A. Rao, *J. Agric. Food Chem.*, 1993, **41**, 366–371.
[100] M. J. Schilstra, G. A. Veldink and J. F. G. Vliegenthart, *Lipids*, 1994, **29**, 225–231.
[101] H. Ma, X. D. Zhang, X. S. Wang and X. L. He, *Soybean Science*, 2010, **4**, 033.

CHAPTER 4

Carotenoid bleaching on fabric

4.0 Foreword

The bleaching of β-carotene in microemulsion solutions in the absence and presence of LOX enzymes were presented in Chapter 2 and 3, respectively. To complement these results, this chapter will present work on the bleaching of carotenoid stains directly on fabrics or in solution in the presence of fabrics. Section 4.1 overviews several of the characteristic, structural features of common clothing textiles and fabric interactions with greasy stain materials in the wash. Section 4.2 details our work on carotenoid bleaching experiments involving fabrics and the results from these experiments are discussed in section 4.3. Our conclusions and a summary are presented in section 4.4.

4.1 Introduction

Removal and degradation of greasy soils on fabrics are dependent on many factors, including: detergent formulation, stain composition, wash temperature and mechanical agitation during the wash. The overall influence of each of these factors in detergency is in turn affected by the type of fabric that has been soiled. For example, while removal of clay and oily soils on textiles such as cotton have been observed to be greatest at the highest wash temperatures evaluated (60–90 °C), removal of nonpolar oily soils from fabrics such as polyester have been found to be greater at low temperatures and not as dependent on the temperature of the wash.[1] Stain distribution on fabrics also differs: synthetic textiles show soil material on the exterior of fibre bundles and within interfibre spaces, while oily soils have also been found to penetrate into the secondary wall and lumen of cotton fibres.[2,3] Processes such as autoxidation of fatty acids, discussed primarily in Chapter 2, may also be affected by the fabric material.[4] This section will introduce some of the structural features of textiles commonly used as clothing material and the interaction of fabrics in stain removal and degradation.

4.1.1 Structure of clothing fabrics

Cotton is a common clothing textile composed predominantly of cellulose fibres (the chemical structure of natural cellulose is shown in Fig. 4.1 where R = H). Cellulose is a linear, polysaccharide chain composed of monomers of β-glucose linked by a 1,4-glycosidic bond. Chains of cellulose possess multiple hydroxyl groups, as shown in Fig. 4.1, which form hydrogen bonds with adjacent cellulose chains conferring high tensile strength. The chemical structure of cellulose may be altered by synthetic chemistry to produce cellulose acetate (diacetate) and carboxymethyl cellulose (R = $COCH_3$ and R = CH_2CO_2H, respectively, in Fig. 4.1). Although neither cellulose acetate or carboxymethylated cellulose are widely used in clothing material at present, studies have characterised fabrics composed of these chemically modified celluloses to observe their effect on soil removal and degradation compared to unmodified cotton. [5,6]

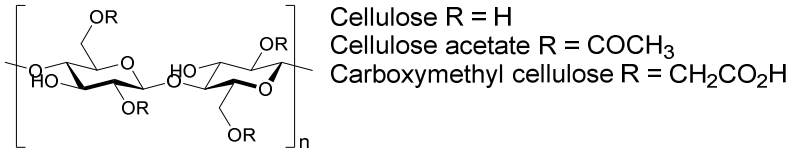

Figure 4.1 Chemical structure of polymerised β-glucose with a 1,4 glycosidic bond (cellulose)

Macromolecules formed from cellulose chains, including cotton, possess a complex structure.[7] The most basic structural units are elementary fibrils, which are composed of cellulose crystallites.[8] Aggregations of elementary fibrils form microfibrils[9] which are arranged together to create the larger cotton fibre structures shown as a representative diagram in Fig. 4.2 A.[10] Cotton fibres are 15 – 25 μm in diameter and 12 – 60 mm long and are composed of concentric cylindrical layers of primarily cellulose microfibrils in different arrangements. The outer surface of the fibre (cuticle in Fig. 4.2 A) is a waxy covering < 0.25 μm thick that contains some of the trace non-cellulosic material in cotton, including proteins and pectins. Below the cuticle is the primary wall which is < 0.5 μm

thick and also has waxes, proteins and pectins similar to the fibre surface, but contains randomly arranged cellulose microfibrils. The outer secondary wall has an alternating open and closed packing of microfibrils that results in a banded structure while the microfibrils in the inner secondary wall are arranged into tightly packed sheets that are angled at 20–30 ° to the axis of the fibre. The inner secondary wall is 5–10 μm thick and is the major (>95% by weight) structural component of the fibre. At the centre of the cotton fibre is the lumen which contains residual protoplasm. After processing, most of the non-cellulosic material in cotton is removed resulting in the lumen becoming a hollow space within the cotton fibre.

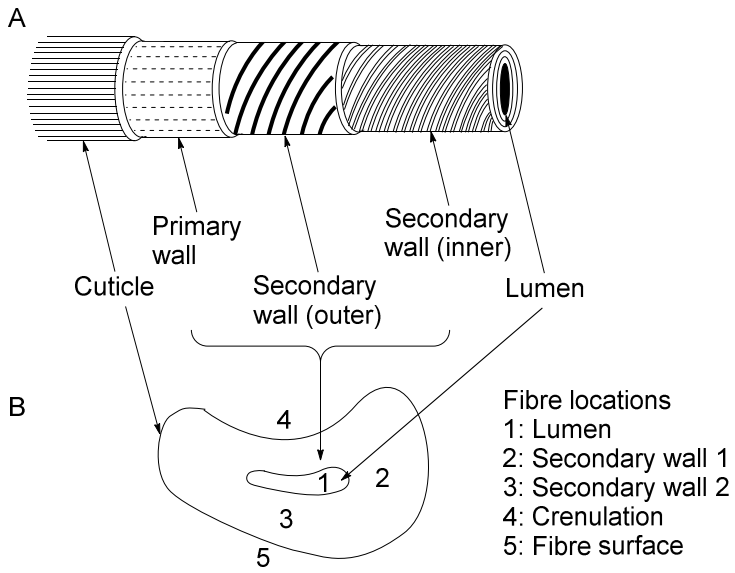

Figure 4.2 Physical macro structure of cotton fibre. (A) Cross section representation of cotton fibre walls. (B) Morphological representation of cotton fibre found in clothes. Diagram recreated from textbook models.[10]

The multilayer, hollow fibre macro structure of cotton is unique when compared with other clothing fabrics that usually contain solid fibre structures. Fig. 4.2 B shows a representative diagram of a fibre in a yarn of processed cotton. Back scattered electron

imaging and energy dispersive X-ray analysis of cotton fibres performed by Obendorf and Borsa found distinct fibre locations that possessed different degrees of accessibility.[6] Interfibre spaces were found to be the most accessible while crenulations (Fig. 4.2 B4), or concave folds in the fibre, were discovered to be slightly less accessible than the other parts of the fibre surface (Fig. 4.2 B4). Similarly, secondary walls on the less compressed edges of the cotton fibre (Fig. 4.2 B2) were found to be less accessible than other sections of the secondary wall (Fig. 4.2 B3). Finally, the lumen (Fig. 4.2 B1) was found to have relatively low accessibility leading to significantly larger amounts of remaining soil material after a wash cycle compared to other locations on the fibre.

Polyester is another widely used material and may be found in clothing fabrics as pure polyester or as a blend, usually containing fibres from another textile such as cotton (polycotton, Fig. 4.3 C). Although the term polyester may denote a family of polymers that contain ester functional groups, in clothing textiles, the name usually refers to the polymer polyethylene terephthalate. Other commonly used synthetic fibres include acrylic and nylon. The chemical structures of the repeating subunit of these polymer based fabrics are shown in Fig. 4.3A.

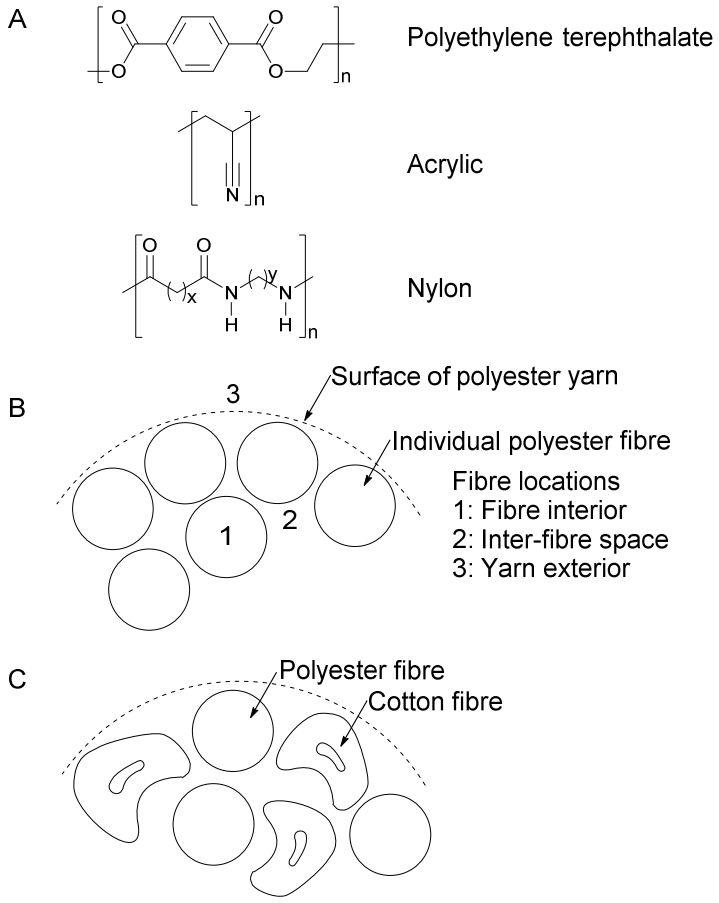

Figure 4.3 (A) Chemical structure of polyethylene terephthalate, acrylic and nylon. (B) Cross section representation of yarn and fibre structure of polyester fabric. (C) Cross section representation of yarn and fibre structure of polycotton fabric.

Similar to other synthetic fabrics shown in Fig. 4.3, polyester yarns are formed from solid fibres that do not contain hollow spaces which contrasts the fibre structures of cotton (Fig. 4.3 B). Another X-ray analysis study by Chi and Obendorf of cotton and polyester fabrics found that inter-fibre spaces retained more soil material relative to the more accessible sides of polyester fibres at the yarn surface.[11] In comparison with cotton fibres which were found to accumulate soil material within the lumen, polyester fibres were found to be mostly inaccessible with no substantial amount of soil material found within the interior. Fig. 4.3C shows a representative cross section of polycotton, which is a mixture of polyester and cotton commonly found in ratios of 65% cotton and 35% polyester or 50%

cotton and 50% polyester in clothing fabrics (swatches used in experiments in Section 4.2 are a 60% cotton and 40% polyester blend).

4.1.2 Fabric interactions in stain removal and bleaching

The decolourisation of coloured stain material is relatively more complex in the presence of fabrics than solution systems. Kissa *et al.* proposed that stain decolourisation on fabrics was mainly dependent on the affinity of stain material to fabric (comparable to the kinetics of fabric dyeing) and occurred in two simultaneous processes: non-oxidative detergency (stain removal) and oxidative degradation of stain.[12] To analyse the kinetics of stain decolourisation, nylon, cotton and polyester were stained by a range of food colouring agents in different media and then monitored throughout washing to measure the degree of stain decolouration. In aqueous media, nylon was found to be stained by both ionic and non-ionic pigments. Ionic stains were found to possess a greater affinity to nylon and the extent of staining was greater at acidic pH. Cotton was stained by cationic and non-ionic colouring agents and also showed a significant increase in staining at lower pH. Polyester was not stained by either ionic or non-ionic food dyes at ambient temperature, however, at higher temperatures, non-ionic dyes were observed to diffuse within polyester fibres and were difficult to remove. Non-ionic colouring agents dissolved in oil medium were able to stain nylon, cotton and polyester, although stain material appeared to remain associated with the oily medium and not the fabrics.

For washing experiments in detergents without bleach, non-oxidative detergency was found to occur faster when stains were water soluble, possessed low affinity to the fabric and were located at the surface of the fabric. In contrast, water insoluble stains that diffused into the interior of fabric fibres were slow to be removed. A similar result was described for decolourisation experiments in the presence of bleach and was proposed to be dependent on the rate of stain material diffusion to the fibre surface and the rate of bleaching agent into the interior of fibres. Stains of β-carotene **1** were not included in these experiments, however, saffron which contains a mixture of carotenoids, including crocin,

zeaxanthin and carotenes, was shown to have relatively high affinity to cotton and nylon, and almost no affinity to polyester.

Investigations of the ageing of oily soil material on fabrics suggest that lipid hydroperoxides formed by autoxidation (as discussed in Chapter 2 for fatty acids) may react with certain fabrics.[4,13] Oily soils of squalene that were oxidised upon ageing were discovered to become yellow and difficult to remove from fabrics. This was attributed to either the formation of high molecular weight oxidation products (polymers) within fabric fibres or the chemical binding of oxidised squalene to fabric. While the product analysis of oxidised squalene showed the formation of high molecular weight oxidation products with yellow colouration these species were easily extracted from polyester, however, not from cotton or nylon. Extraction of squalene from polyester by DMF was independent of ageing while extraction from cotton and nylon became more difficult for squalene stains that were aged. Further experiments showed that glucose monomers could react with oxidized squalene in solution.

A study by Kumarathasan *et al.* on the effect of glucose on the autoxidation of methyl linolenate (methyl ester of linolenic acid **41**) showed that the presence of glucose accelerated the rate of autoxidation.[14] The authors attributed this effect to glucose acting as an efficient hydrogen donor or catalysing the decomposition of the hydroperoxide. Experiments by Franks and Roberts on the oxidation of ethyl linoleate of cotton also showed that cotton fabric may affect autoxidation rates and that reaction with oxidation products may occur through the hydroxyl groups of cellulose.[15] These results suggest that while autoxidation processes may occur at a greater rate on cotton compared to polyester, reaction with cellulose fibres may compete with the degradation of carotenoid species.

4.2 Results

Chapter 2 and 3 detail the bleaching of β-carotene **1** in oil-in-water microemulsions to determine the effect of pH, fatty acid, surfactant and lipoxygenase. This chapter will report on results for experiments on the bleaching of carotenoid stains with fabrics to analyse the effect of fabric type and treatment and also for comparison with the bleaching experiments performed in solution.

The experiments in this section are accompanied by a representative image set of the fabric stains (Fig. 4.5, 4.6 and Table 4.2). Several representative tables of stain removal index (SRI) values that quantify the extent of bleaching are also included while complete sets are shown in Appendix C. SRI values were measured to quantify the extent of stain decolourisation. Clean swatches before application of stain material (100%) and stained swatches left over night (0%) were used as references for the calculation of SRIs. SRI values were calculated from measurements of *L*, *a*, *b* colour space obtained using DigiEye software and hardware. *L* represents the lightness of the fabric while *a* and *b* correspond to red-green and blue-yellow colouration, respectively. These measurements were first converted to ΔE values as shown in eq. 1.

$$\Delta \mathrm{E} = \sqrt{(L_0 - L_{\mathrm{stain}})^2 - (a_0 - a_{\mathrm{stain}})^2 - (b_0 - b_{\mathrm{stain}})^2} \qquad (1)$$

Where L_0, a_0 and b_0 are *L*, *a*, *b* values for clean fabric and L_{stain}, a_{stain} and b_{stain} are *L*, *a*, *b* values for stained fabric. SRI values are calculated from ΔE values of fabric stains at different time points after the wash cycle (ΔE_t) relative to the ΔE value of the fabric stain immediately before the wash cycle (ΔE_{t0}).

$$\mathrm{SRI} = (100 \times (\Delta \mathrm{E}_{t0} - \Delta \mathrm{E}_{t})) / (\Delta \mathrm{E})$$

Plots of SRI values for fabric types, treatments and conditions are shown in the discussion section of this chapter.

4.2.1. Effect of stain composition

Typical stains used in P&G to mimic carotenoid-containing soils are usually composed of capsanthin **3** mixed in lard or sunflower oil (capsanthin **3** is a viscous liquid that is miscible with oil; β-carotene **1** is a solid). Lard and sunflower oil contain variable amounts of triglycerides, free fatty acids and in the case of sunflower oil, small amounts of tocopherols. In order to quantify the effect of linoleic acid **10** and α-tocopherol **52** on the decolourisation of carotenoid stains on fabric, our stains contained capsanthin **3**, linoleic acid **10** and α-tocopherol **58** dissolved in glycerol trioleate **59**.

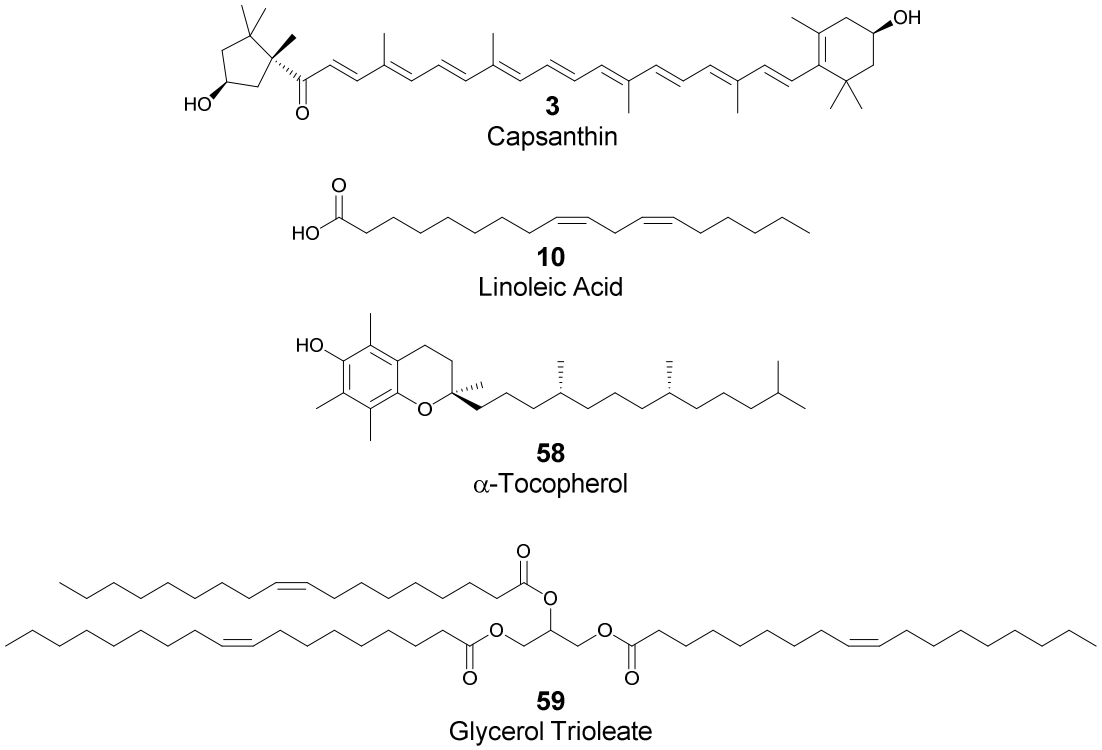

Figure 4.4 Chemical structures of compounds used as stain components.

Bleaching experiments of capsanthin **3** in glycerol trioleate **59** were performed on cotton, polycotton and polyester on separate swatches of each material. Stains were prepared with 0–20% w/w linoleic acid **10** and 0.00–0.10% α-tocopherol **58**, and were left overnight at room temperature in the dark after application on fabric swatches. Reference images of each of the swatches were taken after 16 hours. Stained swatches were then washed by a terg-o-tometer (see Section 4.5 for wash cycle specifications) with Ariel capsule formulation and dried inside a 30 °C oven. Ariel capsule formulation is the standard detergent used in P&G experiments studying carotenoid stain bleaching. Images were taken again after the drying process to monitor the progression of stain bleaching.

Representative images of sets of dried swatches 18 hours after the simulated wash cycle are shown for each fabric tested in Fig 4.5. Representative sets of SRI values for each experiment are shown in Table 4.1.

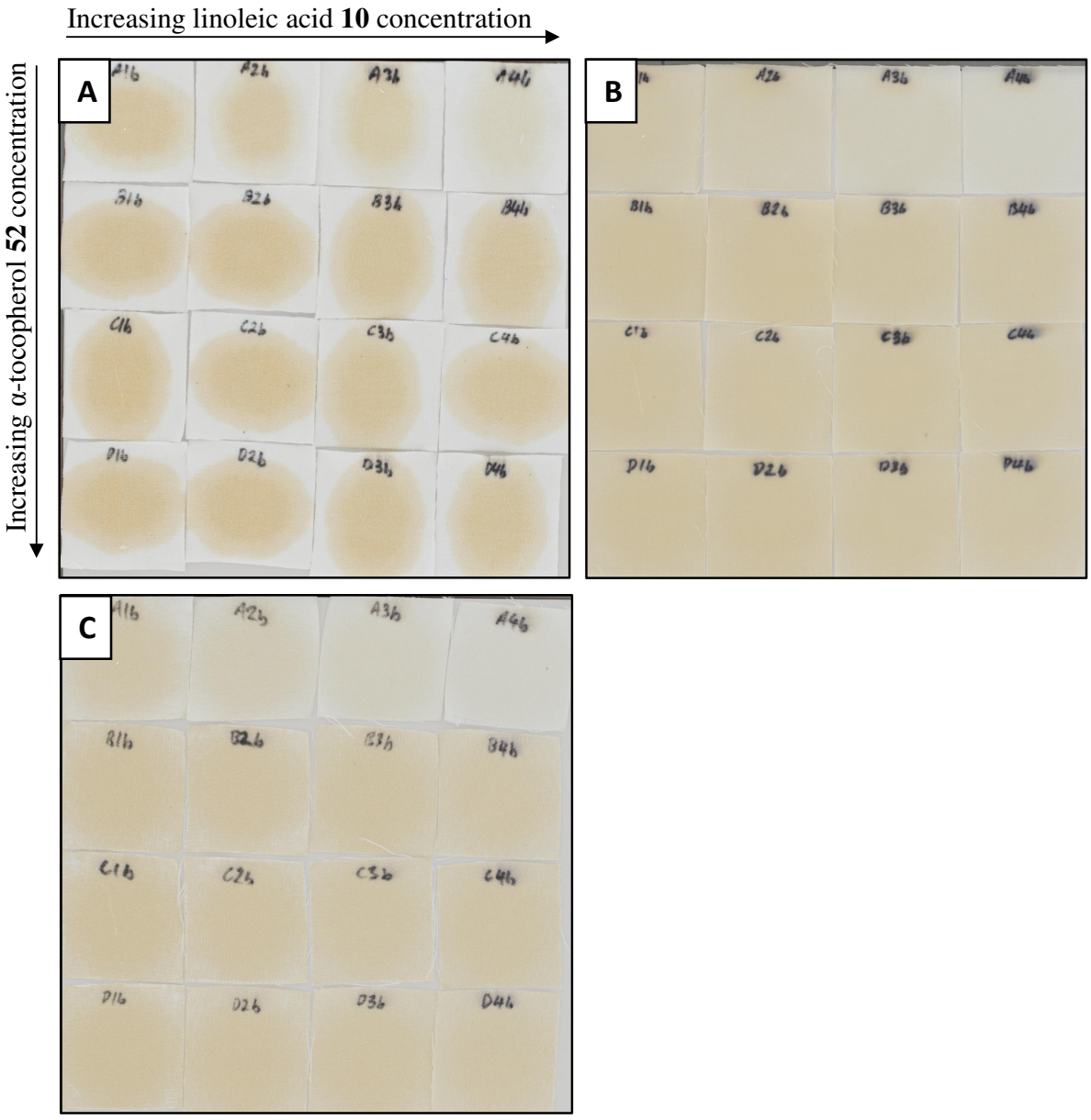

Figure 4.5 Image sets of the bleaching of capsanthin **3** stains on fabric (A: cotton, B: polycotton, C: polyester) in the presence of different concentrations of linoleic acid **10** and α-tocopherol **58** after a wash cycle and 18 hours drying at 30 °C.

Table 4.1 SRI values of capsanthin **3** stains on fabrics in the presence of linoleic acid **10** and α-tocopherol **58**.

Fabric	[α-Tocopherol **51**] (w/w%)	[Linoleic acid **10**] (w/w%)	SRI (%)	Fabric	[α-Tocopherol **51**] (w/w%)	[Linoleic acid **10**] (w/w%)	SRI (%)
Knitted Cotton	0	0	29	Polyester	0	0	34
		5	34			5	48
		10	40			10	60
		20	67			20	74
	0.01	0	20		0.01	0	20
		5	19			5	22
		10	24			10	20
		20	23			20	23
	0.05	0	17		0.05	0	21
		5	17			5	22
		10	21			10	22
		20	24			20	18
	0.10	0	19		0.10	0	19
		5	18			5	22
		10	20			10	21
		20	20			20	21
Poly-cotton	0	0	27				
		5	36				
		10	54				
		20	68				
	0.01	0	11				
		5	11				
		10	10				
		20	12				
	0.05	0	11				
		5	12				
		10	10				
		20	14				
	0.10	0	14				
		5	13				
		10	15				
		20	15				

4.2.2 Effect of fabric type and fabric treatment

Bleaching experiments of capsanthin **3** in sunflower oil stains were performed on multifibre strips. These strips contained diacetate, cotton, polyamide, polyester, acrylic and wool on a single swatch. Treated swatches were washed under treatment conditions within a terg-o-tometer and dried overnight at room temperature before application of stain material. Stain material was applied to each of the different strips of fabric on the swatch and allowed to dry overnight at room temperature in the dark. Reference pictures of each of the swatches were taken 16 hours before the fabrics were washed by a terg-o-tometer with Ariel capsule formulation and dried inside a 20 or 50 °C oven. Pictures were taken at several time points after the wash cycle to monitor the progression of stain bleaching.

Several fabric treatment wash cycles and stained fabric wash cycles contained lipase (from Lipex, a liquid enzyme preparation) and Lenor fabric softener. Lipase is included in many P&G bio detergent formulations. This enzyme hydrolyses triglycerides to glycerol and free fatty acids, facilitating the removal of greasy stains in the wash. In our experiments monitoring the effect on the bleaching of carotenoid stains, the increased concentration of free fatty acids was predicted to promote greater decolourisation of carotenoid. Fabric softeners, such as Lenor, contain deposition agents that coat the exterior of fabric fibres resulting in changes in physical properties of the fabric surface. Lenor was added to pretreatment washes to observe whether these deposition agents would affect the interaction of fabric with stain material and result in differences in stain bleaching.

Table 4.2 shows representative pictures of sets of dried multifibre strips after the simulated wash cycle for each set of pretreatments: no prewash, prewashed, prewashed with lipase and prewashed with lipase and rinsed with Lenor. Representative sets of SRI values for each fabric and treatment conditions are shown in Tables 4.3. Complete image and SRI data sets may be found in Fig. C2 – C5 and Tables C2 – C7 of Appendix C. As before, SRI values were used to quantify stain bleaching, with clean swatches calibrated as 100% and stained swatches before washing as 0%.

Table 4.2 Image sets of the bleaching of capsanthin stains on multifibre at different time points after a wash cycle. Multifibre contained (1) diacetate, (2) cotton, (3) polyamide, (4) polyester, (5) acrylic and (6) wool.

Treatment[a]	Initial stained fabric	Drying condition	1 hour after wash	3 hours after wash	48 hours after wash
No treatment	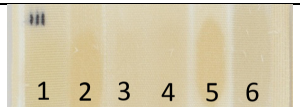	20 °C		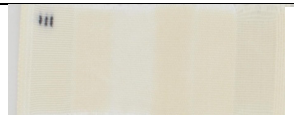	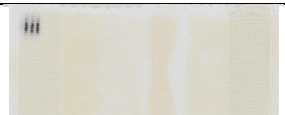
		1 hour at 50 °C followed by drying at 20 °C			
Prewashed		20 °C		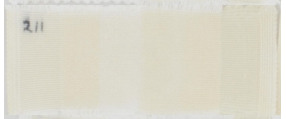	
		1 hour at 50 °C followed by drying at 20 °C			
Prewashed with lipase		20 °C			
		1 hour at 50 °C followed by drying at 20 °C			
Prewashed with lipase and rinsed with Lenor		20 °C			
		1 hour at 50 °C followed by drying at 20 °C		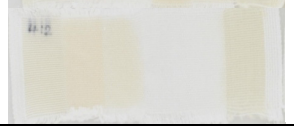	

[a] All prewash cycles contained Ariel capsule detergent formulation.

Table 4.3 Average SRI values of capsanthin **2** stains on treated fabrics 48 hours after a wash cycle.

Pretreatment	Lipase in Wash	Drying Temperature	Diacetate (SRI, %)	Cotton (SRI, %)	Polyamide (SRI, %)	Polyester (SRI, %)	Acrylic (SRI, %)	Wool (SRI, %)
Not pretreated	No	20 °C	68	64	73	62	72	77
		1 hour at 50 °C	65	63	71	58	69	79
	Yes	20 °C	69	66	78	71	79	79
		1 hour at 50 °C	66	66	86	72	83	80
Prewashed	No	20 °C	74	66	72	96	94	81
		1 hour at 50 °C	77	69	78	96	95	88
	Yes	20 °C	76	68	73	96	94	85
		1 hour at 50 °C	81	71	80	95	93	87
Prewashed with lipase	No	20 °C	83	75	83	96	95	90
		1 hour at 50 °C	80	72	84	96	95	92
	Yes	20 °C	84	76	85	96	95	92
		1 hour at 50 °C	87	79	92	96	94	93
Prewashed, rinsed with fabric softener	No	20 °C	78	73	76	97	95	87
		1 hour at 50 °C	79	73	77	97	96	89
	Yes	20 °C	73	71	72	96	95	86
		1 hour at 50 °C	84	76	86	96	95	92

4.2.3 Bleaching of carotenoid microemulsions in the presence of fabric

The effect of fabric on carotenoid bleaching was examined by observing the bleaching of β-carotene microemulsion solutions, employed previously in Chapters 2 and 3, in the presence of fabric. Circular pieces of fabric were cut from swatches to fit the diameter of sample vials (see Fig 4.9). Microemulsion solutions of β-carotene **1** were added to samples containing identical masses of fabric. Similar to experiments in Chapters 2 and 3, a stock solution of fatty acid was added to the sample vial to initiate the bleaching reaction. Reaction mixtures were stored in cell incubators at 30 °C in the dark with a stirring speed of 200 rpm. Aliquots were withdrawn from reaction mixtures for absorbance measurements on a UV-Vis spectrophotometer at several time points to monitor the bleaching of the β-carotene solution. As previously described in Chapters 2 and 3, bleaching was monitored by a decrease in absorbance at 456 nm and absorbance measurements were converted to concentrations of β-carotene **1** using an extinction coefficient of $\varepsilon = 1.3 \times 10^5\ M^{-1}\ cm^{-1}$.[16] The concentration of fatty acid was in large excess over the concentration of β-carotene. Unlike experiments in Chapters 2 and 3, complete bleaching was followed rather than the initial stages of reaction.

Representative pictures of the bleaching of β-carotene **1** solutions in the absence of fabric or in the presence of cotton, polycotton or polyester are shown in Figure 4.6. Rate constants and the extent of bleaching were determined from fitting the concentration of β-carotene **1** versus time data to an exponential decay in Kaleidagraph software. The extent of bleaching was defined as the difference between the initial and final concentrations of β-carotene **1** (concentration at $t = \infty$) as a percentage of the initial concentration of β-carotene **1**. For each experiment a representative plot of raw data fitted to an exponential decay is presented together with a table of rate constants and extent of bleaching. Complete SRI data sets may be found in Tables C8 – C11 of Appendix C. Plots of rate constants and extent of bleaching for each of the fabric conditions will be discussed in Section 4.3.

Time after addition of linoleic acid **10**	No Fabric	Cotton	Polycotton	Polyester
0 hours		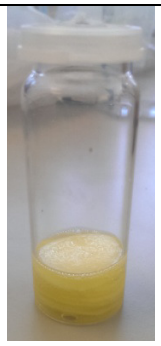		
6 hours				
24 hours				

Figure 4.6 Representative images of the bleaching of carotenoid microemulsions over time in the presence of fabrics.

Initial bleaching experiments in the presence of fabric were performed using surfactant **53** (Tween 80) to solubilise β-carotene **1** and linoleic acid **10**, with sample vials containing 1.00 g of either cotton, polycotton or polyester fabric. Solutions contained 50 mM phosphate buffer to maintain pH 7.0. Representative plots of bleaching versus time are shown in Fig. 4.7. Good fits of the concentration-time data to first-order decay functions were observed as expected due to the large excess of linoleic acid **10** to β-carotene **1**. Pseudo first-order rate constants and extents of bleaching are shown in Table 4.4.

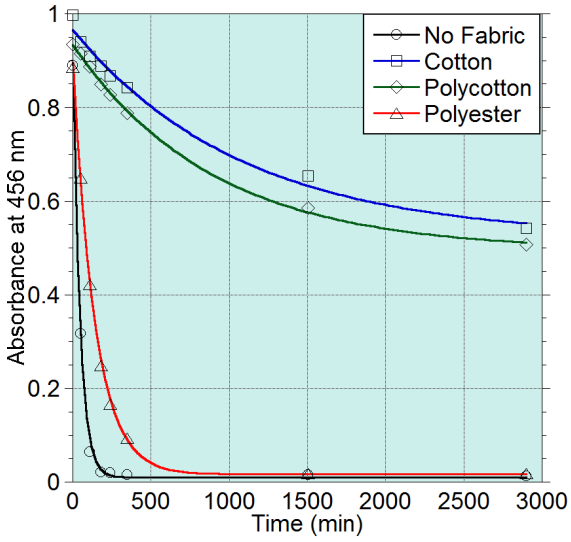

y = m1 + m2*exp(-m3*x)		
	Value	Error
m1	0.010185	0.0060151
m2	0.88266	0.014008
m3	0.022116	0.00091108
Chisq	0.0008386	NA
R	0.99937	NA

y = m1 + m2*exp(-m3*x)		
	Value	Error
m1	0.52204	0.035271
m2	0.44379	0.031739
m3	0.00091915	0.00020568
Chisq	0.0019982	NA
R	0.99393	NA

y = m1 + m2*exp(-m3*x)		
	Value	Error
m1	0.49437	0.0082386
m2	0.43929	0.0075907
m3	0.0011127	6.5621e-5
Chisq	0.00018131	NA
R	0.99947	NA

y = m1 + m2*exp(-m3*x)		
	Value	Error
m1	0.016521	0.0074307
m2	0.87882	0.011903
m3	0.007141	0.00021577
Chisq	0.00064031	NA
R	0.99954	NA

Figure 4.7 Representative plot of bleaching of β-carotene **1** in the presence/absence of fabric in solutions containing linoleic acid **10** (500 μM) and surfactant **53** (Tween 80) at pH 7.0 and 30 °C.

Table 4.4 First order rate constants and extent of bleaching of β-carotene in solutions containing linoleic acid **10**, surfactant **53** (Tween 80) and untreated fabrics.

Fabric	First order bleaching rate constants (min^{-1})				Extent of bleaching (%)			
	$k_{obs}1$[a]	$k_{obs}2$[b]	$k_{obs}3$[b]	k_{obs} ave ± SD	$x1$	$x2$	$x3$	$\bar{x}$
None	2.21×10^{-2}	1.61×10^{-2}	2.05×10^{-2}	$1.96 \pm 0.31 \times 10^{-2}$	100	99	99	99 ± 1
Cotton	9.19×10^{-4}	4.02×10^{-3}	8.53×10^{-4}	$1.93 \pm 1.81 \times 10^{-3}$	39	48	43	43 ± 4
Polycotton	1.11×10^{-3}	8.35×10^{-4}	1.14×10^{-3}	$1.03 \pm 0.17 \times 10^{-3}$	40	47	47	45 ± 4
Polyester	7.14×10^{-3}	6.86×10^{-3}	8.18×10^{-3}	$7.39 \pm 0.69 \times 10^{-3}$	97	98	97	97 ± 1

[a] Obtained from a non-linear least squares fit of reaction data in Figure 4.7 to a first order exponential decay function. [b] Experiments were repeated in triplicate. Data used to determine k_{obs} are in Appendix C.

Analogous to studies in chapter 2 and 3, bleaching experiments were also conducted utilising surfactant **54** (AE7). Representative plots of the concentration of β-carotene **1** versus time and fitting data are shown in Fig. 4.8. First-order rate constants of bleaching and extents of bleaching are shown in Table 4.5.

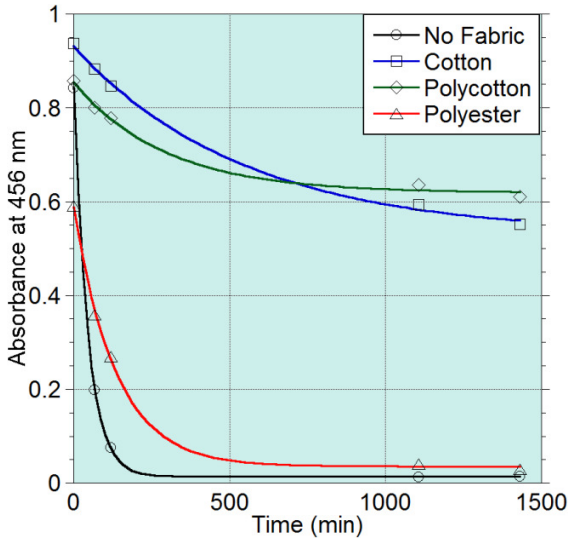

y = m1 + m2*exp(-m3*x)		
	Value	Error
m1	0.014038	0.0014531
m2	0.82843	0.0025744
m3	0.02201	0.00019043
Chisq	9.2235e-6	NA
R	0.99999	NA

y = m1 + m2*exp(-m3*x)		
	Value	Error
m1	0.53011	0.026205
m2	0.40109	0.02196
m3	0.0018198	0.00043461
Chisq	0.00025367	NA
R	0.99898	NA

y = m1 + m2*exp(-m3*x)		
	Value	Error
m1	0.61884	0.009792
m2	0.23579	0.013211
m3	0.0033775	0.00078533
Chisq	0.00028036	NA
R	0.99699	NA

y = m1 + m2*exp(-m3*x)		
	Value	Error
m1	0.035677	0.0073667
m2	0.55215	0.012514
m3	0.007446	0.00038837
Chisq	0.00021678	NA
R	0.99951	NA

Figure 4.8 Representative plot of bleaching of β-carotene **1** in the presence/absence of fabric in solutions containing linoleic acid **10** (500 μM) and surfactant **49** (AE7) at pH 7.0 and 30 °C.

Table 4.5 First order rate constants and extent of bleaching of β-carotene in solutions containing linoleic acid **10**, surfactant **54** (AE7) and untreated fabrics.

Fabric	First order bleaching rate constants (min^{-1})				Extent of bleaching (%)			
	$k_{obs}1$	$k_{obs}2$	$k_{obs}3$	k_{obs} ave ± SD	$x1$	$x2$	$x3$	$\bar{x}$
None	2.20×10^{-2}	2.20×10^{-2}	2.15×10^{-2}	$2.18 \pm 0.03 \times 10^{-2}$	98	99	98	98 ± 0
Cotton	1.82×10^{-3}	1.86×10^{-3}	2.68×10^{-3}	$2.12 \pm 0.49 \times 10^{-3}$	43	44	53	47 ± 5
Polycotton	3.38×10^{-3}	3.80×10^{-3}	4.28×10^{-3}	$3.82 \pm 0.45 \times 10^{-3}$	28	29	29	29 ± 1
Polyester	7.45×10^{-3}	9.46×10^{-3}	9.54×10^{-3}	$8.81 \pm 1.19 \times 10^{-3}$	94	96	94	95 ± 1

[a] Obtained from a non-linear least squares fit of reaction data in Figure 4.7 to a first order exponential decay function. [b] Experiments were repeated in triplicate. Data used to determine k_{obs} are in Appendix C.

Fatty acid dependent bleaching of β-carotene was also studied using oleic acid **38**. Representative plots of the concentration of β-carotene **1** versus time and fitting data are shown in Fig. 4.9. First-order rate constants of bleaching and extents of bleaching are shown in Table 4.6.

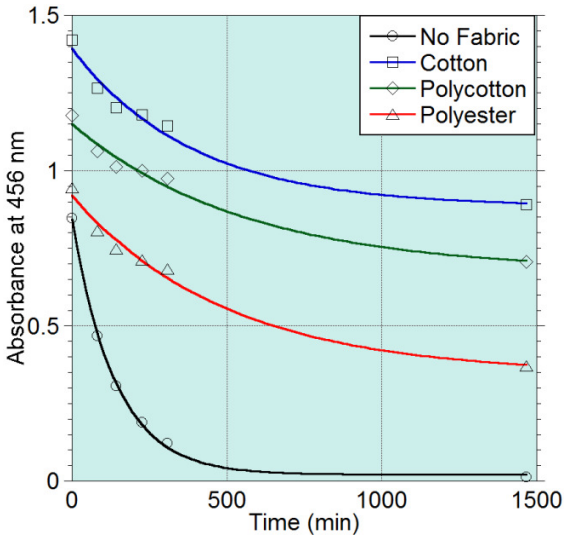

y = m1 + m2*exp(-m3*x)		
	Value	Error
m1	0.020787	0.010232
m2	0.82145	0.014182
m3	0.0072162	0.00027225
Chisq	0.00038529	NA
R	0.99957	NA

y = m1 + m2*exp(-m3*x)		
	Value	Error
m1	0.88366	0.042911
m2	0.50867	0.048643
m3	0.0025681	0.00059344
Chisq	0.0038878	NA
R	0.98703	NA

y = m1 + m2*exp(-m3*x)		
	Value	Error
m1	0.67565	0.052742
m2	0.47467	0.049855
m3	0.0017889	0.00054276
Chisq	0.0029945	NA
R	0.98751	NA

y = m1 + m2*exp(-m3*x)		
	Value	Error
m1	0.34449	0.045651
m2	0.57517	0.045618
m3	0.0019987	0.00043937
Chisq	0.0029201	NA
R	0.99192	NA

Figure 4.9 Representative plot of bleaching of β-carotene **1** in the presence/absence of fabric in solutions containing oleic acid **38** (500 μM) and surfactant **53** (Tween 80) at pH 7.0 and 30 °C.

Table 4.6 First order rate constants and extent of bleaching of β-carotene in solutions containing oleic acid **33**, surfactant **48** (Tween 80) and untreated fabrics.

Fabric	First order bleaching rate constants (s^{-1})				Extent of bleaching (%)			
	$k_{obs}1$	$k_{obs}2$	$k_{obs}3$	k_{obs} ave ± SD	$x1$	$x2$	$x3$	$\bar{x}$
None	7.22×10^{-3}	7.34×10^{-3}	7.15×10^{-3}	$7.23 \pm 0.09 \times 10^{-3}$	98	97	97	97 ± 0
Cotton	2.57×10^{-3}	3.34×10^{-3}	2.83×10^{-3}	$2.91 \pm 0.39 \times 10^{-3}$	38	39	37	38 ± 1
Polycotton	1.79×10^{-3}	1.53×10^{-3}	1.25×10^{-3}	$1.52 \pm 0.27 \times 10^{-3}$	43	45	42	43 ± 1
Polyester	2.00×10^{-3}	1.54×10^{-3}	2.19×10^{-3}	$1.91 \pm 0.33 \times 10^{-3}$	64	88	88	80 ± 14

[a] Obtained from a non-linear least squares fit of reaction data in Figure 4.7 to a first order exponential decay function. [b] Experiments were repeated in triplicate. Data used to determine k_{obs} are in Appendix C.

The influence of fabric on the bleaching of carotenoid microemulsions was also studied in the presence of lower quantities of fabric (0.50 g). Representative plots of the concentration of β-carotene **1** versus time and fitting data are shown in Fig. 4.10. First-order rate constants of bleaching and extents of bleaching are shown in Table 4.7.

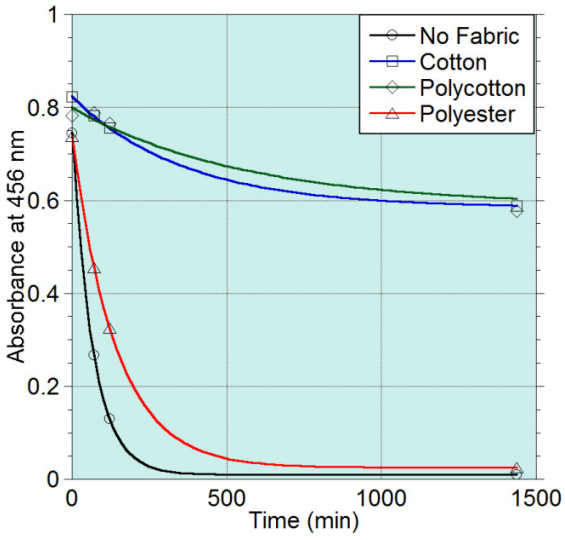

y = m1 + m2*exp(-m3*x)		
	Value	Error
m1	0.010073	0.0020714
m2	0.73464	0.0029335
m3	0.014893	0.00013441
Chisq	4.5328e-6	NA
R	0.99999	NA

y = m1 + m2*exp(-m3*x)		
	Value	Error
m1	0.58429	0.00092944
m2	0.23935	0.0010442
m3	0.0027416	4.9908e-5
Chisq	6.0437e-7	NA
R	0.99999	NA

y = m1 + m2*exp(-m3*x)		
	Value	Error
m1	0.58772	0.084839
m2	0.21232	0.070811
m3	0.0017891	0.0028271
Chisq	0.0012598	NA
R	0.97927	NA

y = m1 + m2*exp(-m3*x)		
	Value	Error
m1	0.025081	0.0013248
m2	0.71277	0.0018463
m3	0.0071178	3.9342e-5
Chisq	1.7605e-6	NA
R	1	NA

Figure 4.10 Representative plot of bleaching of β-carotene **1** in the presence/absence of fabric (0.50 g) in solutions containing linoleic acid **10** (500 μM) and surfactant **53** (Tween 80) at pH 7.0 and 30 °C.

Table 4.7 First order rate constants and extent of bleaching of β-carotene in solutions containing linoleic acid **10**, surfactant **53** (Tween 80) and untreated fabrics (0.50 g).

Fabric	First order bleaching rate constants (s^{-1})				Extent of bleaching (%)			
	$k_{obs}1$	$k_{obs}2$	$k_{obs}3$	k_{obs} ave ± SD	$x1$	$x2$	$x3$	$\bar{x}$
None	1.49×10^{-2}	1.85×10^{-2}	7.69×10^{-3}	$1.37 \pm 0.55 \times 10^{-2}$	99	99	98	98 ± 0
Cotton	2.74×10^{-3}	2.47×10^{-3}	2.37×10^{-3}	$2.53 \pm 0.19 \times 10^{-3}$	29	37	39	35 ± 5
Polycotton	2.64×10^{-3}	1.76×10^{-3}	6.19×10^{-4}	$1.67 \pm 1.02 \times 10^{-3}$	25	33	45	34 ± 10
Polyester	7.12×10^{-3}	4.81×10^{-3}	3.79×10^{-3}	$5.24 \pm 1.70 \times 10^{-3}$	97	96	92	95 ± 3

[a] Obtained from a non-linear least squares fit of reaction data in Figure 4.7 to a first order exponential decay function. [b] Experiments were repeated in triplicate. Data used to determine k_{obs} are in Appendix C.

4.3 Discussion

4.3.1. Effect of stain composition

α-Tocopherol **52** is known to be a highly effective chain-breaking antioxidant, a class of antioxidants that prevent radical chain propagation by acting as strong hydrogen donors and by forming stable radical species. The presence of α-tocopherol **58** would be expected to decrease the rate of formation of the linoleic acid hydroperoxy radical bleaching species and its interaction with capsanthin **2**, however, α-tocopherol **58** was not expected to prevent the bleaching of capsanthin **2** stains at concentrations as low as 0.01% w/w, especially in the presence of a large excess (20% w/w) of linoleic acid **10**. Notably, sunflower oils usually contain total tocopherol concentrations of 0.5 to 0.8% w/w, depending on processing methods,[17] however, experiments performed by P&G did not observed significantly greater stability of capsanthin **2** stains prepared in sunflower oil.

Fig. 4.11 shows that in the absence of α-tocopherol **58**, an increase in linoleic acid concentration within the stain material resulted in an increase in SRI values 18 hours after the wash cycle. SRI values in the absence of α-tocopherol **58** appeared to be slightly larger for polyester fabrics while cotton and polycotton appeared to have comparable SRI values. The addition of ≥0.01% α-tocopherol **58** to stain material resulted in no differences in SRI values for different concentrations of linoleic acid **10**. SRI values appear to be reduced to a base level, as higher concentrations of α-tocopherol **58** do not alter the SRI values. This base level of bleaching appears to be ~20% for cotton and polyester, and ~10% for polycotton.

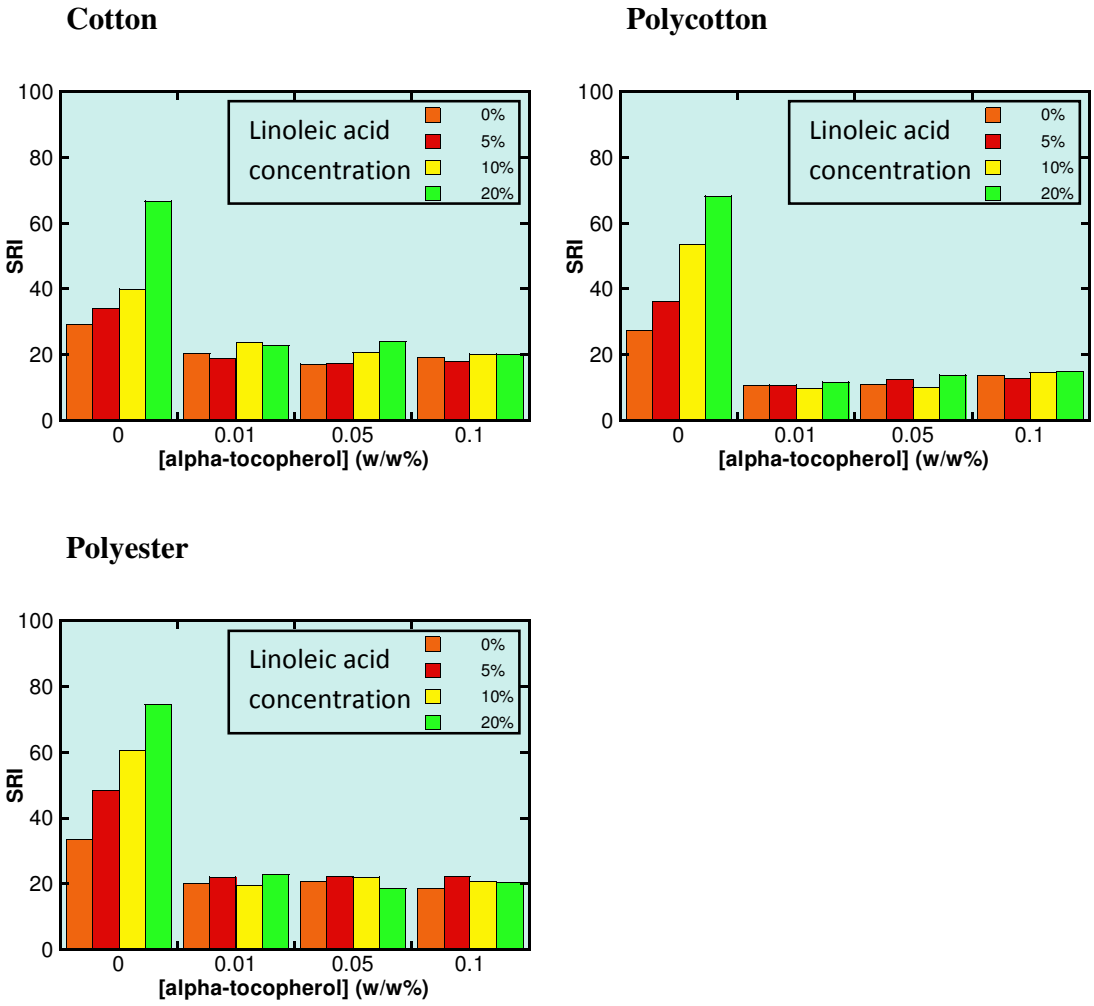

Figure 4.11 Bleaching of capsanthin **2** stains in the presence of varying concentrations of linoleic acid **10** and α-tocopherol **58** on fabrics: cotton, polycotton and polyester. SRI values quantified 18 hours after the wash cycle.

Results for the decolourisation of stains on fabrics, in the absence of α-tocopherol **58**, appear to be consistent with results in Chapter 2 for the bleaching of β-carotene **1** solutions in the presence of different concentrations of linoleic acid **10** (Fig. 2.14). Higher concentrations of linoleic acid **10** result in larger initial rates and higher SRI values. However, results from Chapter 2 showed a levelling effect over the concentration range tested (10–500 μM) with higher concentrations of fatty acids having a reduced influence on the initial rates of β-carotene **1** bleaching. For bleaching on fabric there does not appear

to be a levelling effect for the concentration range tested (5–20% or 160–650 mM), despite the relatively high concentrations of linoleic acid **10**, and bleaching does not appear to be complete even after 18 hours. The disparity between these results could be the influence of the fabric material. Stain material found in inter-fibre spaces or the lumen of cotton fibres are less accessible to the components within the aqueous phase such as trace metals which are essential for the initiation of the autoxidation process.

The base level of decolourisation remaining, which is independent of the action of fatty acid hydroperoxy radicals, may be caused by stain removal in the wash or other bleaching mechanisms. Differences are observed in base levels of decolourisation although these may not be significant as absolute differences are small. Base levels of decolourisation are lower in polycotton relative to cotton and polyester which could suggest that stain removal is more facile on the latter two fabrics. Cotton would, however, be predicted to have the lowest base level because greasy stains tend to more difficult to remove from the secondary walls and lumen of the fibre structure.

4.3.2 Effect of fabric type and fabric treatment

The bleaching of capsanthin stains on fabrics with different pretreatments is shown in Fig. 4.12. As shown in representative image sets in Table 4.2, the different fabrics types were all part of the same swatch. These swatches were washed and dried before the application of stain material to pretreat the fabrics. The pretreatments were: no prewash (control), prewashed, prewashed in the presence of lipase, and prewashed in the presence of lipase then rinsed with fabric softener (all prewash solutions contained Ariel capsule formulation). After stains were prepared on these fabrics, the swatches were washed in the absence or presence of lipase. Washed swatches were then dried at 20 °C or initially at 50 °C for 1 hour followed by 20 °C.

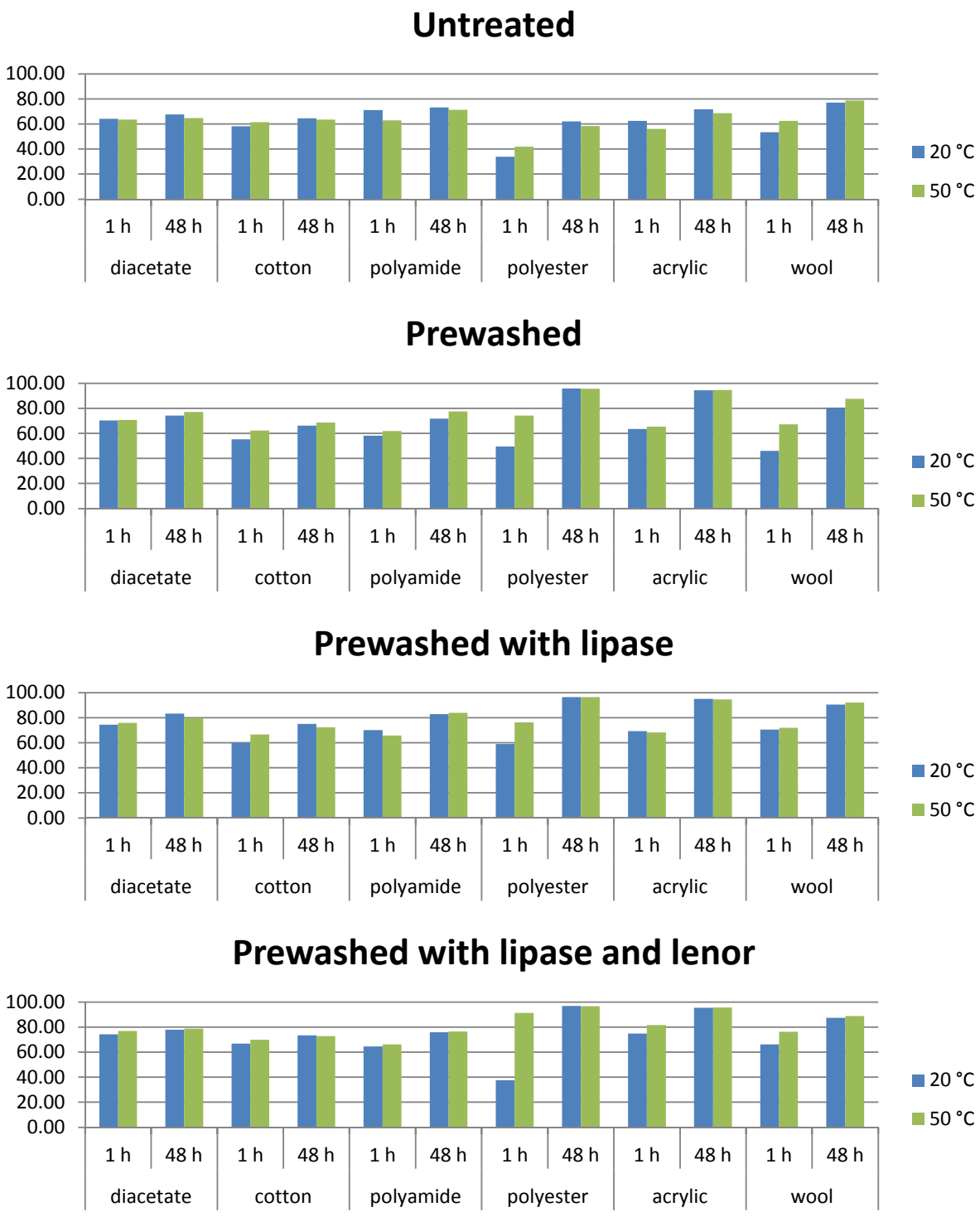

Figure 4.12 SRI values of capsanthin **2** stains on treated fabrics.

Fig. 4.12 shows that for most fabric treatments, initial bleaching (1 hour after wash) was of the order diacetate, cotton > polyamide, acrylic, wool > polyester, however, for bleaching after 48 hours, the order becomes polyester, acrylic > polyamide, wool > diacetate, cotton. Decolourisation at early stages is predominantly based on the removal of the stain material from the fabric during the wash cycle, while decolourisation at later stages is dependent upon the bleaching of stain material remaining on the fabric.

Stain removal during the wash cycle appears to be more facile on fabrics that are more hydrophilic such as polyamide which possesses a backbone of amide bonds, diacetate with numerous carboxylate groups and cotton a polymer containing several hydroxyl moieties. Fabrics with more hydrophobic character such as polyester which contains aromatic rings and wool which is high in alanine and leucine (alkyl side chains) showed lower SRI values at early measurements. This effect may be the result of lower affinity of the oily stain material to hydrophilic fabrics allowing for easier removal in the wash. Another factor could be the interaction of fabric with the aqueous wash medium. More hydrophilic materials may interact more favourably with water and allow for greater access to the stain material.

For decolourisation at later stages, one of the major factors could be the process of autoxidation of fatty acids (described in chapter 2) to form hydroperoxide bleaching species and the subsequent reaction with carotenoid pigments. As mentioned in the introduction, several authors have speculated that fabrics such as cotton and diacetate that possess free hydroxyl groups may react with lipid hydroperoxides.[4,13,14] This could deplete the concentration of bleaching species and reduce bleaching at later stages on these fabrics. The higher hydrophilicity of these fabrics may also result in sequestering of the relatively polar fatty acids and oxidised lipids away from more hydrophobic components within the stain, such as capsanthin. The relatively high SRI values for polyester and acrylic at longer times may be the result of lacking H-bond donor groups that can interact with fatty acids

head groups or oxidised lipids. A lower interaction with fatty acids and bleaching species may result in greater reaction of these species with carotenoid pigment.

Surprisingly, the presence of lipase in prewash treatments and in the wash cycle of stained swatches did not produce any observable differences in SRI values. Lipases are enzymes that hydrolyse triglycerides to free fatty acids and glycerol. As free fatty acids oxidise at a greater rate than triglycerides, the inclusion of lipases would be expected to accelerate the rate of bleaching of carotenoids. However, other factors, such as the interaction of oxidised bleaching species with fabric, may have a greater influence.

Of the different fabric treatments, the most influential appeared to be whether the fabric was prewashed in capsule formulation. Overall, prewashed fabrics of all types showed higher SRI values after 48 hours than those that were not prewashed. Among fabrics that were prewashed, no significant differences in SRI values were observed for the presence of lipase in the prewash or a rinse cycle containing fabric softener. The composition of the capsule detergent was not disclosed by P&G, however, the detergent is likely to contain deposition agents that aid in stain removal or enhance the brightness of material. These deposition agents localise at the surface of fibres and may alter the interactions between stain material and fabric. A reduction in interactions between bleaching species and fabric would perhaps facilitate the bleaching reaction of carotenoids.

Drying conditions of swatches only affected SRI values for prewashed acrylic and polyester at early measurements (1 and 3 hours) with swatches dried at 50 °C for 1 hour showing higher SRI values. This is a surprising result as reactions such as autoxidation of lipids and oxidative degradation of carotenoid would be expected to be faster at higher temperatures. As mentioned previously, the interaction of fabric with bleaching species in the stain may be a more influential factor – an increase in temperature would also increase

the rate of reactions competing with the bleaching of capsanthin, such as reaction of hydroperoxide with fabric.

4.3.3 Bleaching of carotenoid microemulsions in the presence of fabric

Fig. 4.13A and Fig. 4.13B show the pseudo first-order rate constants and extents of bleaching of β-carotene solutions prepared using surfactants **53** (Tween 80) and **54** (AE7) in the absence of fabric and in the presence of cotton, polycotton and polyester (1.0 g). Rate constants were found to be in the order no fabric > polyester > cotton and polycotton for both surfactant systems. Although bleaching rate constants in the absence of fabric were 2 to 3-fold larger than those in the presence of polyester, both samples were fully bleached. The extent of bleaching for both cotton and polycotton was limited to ~40% for samples prepared with surfactants **53** (Tween 80) and **54** (AE7).

Interestingly, pseudo first-order rate constants for the bleaching of β-carotene **1** in the absence of fabric were comparable in samples containing surfactant **53** (Tween 80) to those containing surfactant **54** (AE7). This contrasts the results from Chapters 2 and 3 which show initial rates of bleaching to be consistently 2-fold greater in microemulsions prepared with surfactant **53** (Tween 80) compared with those containing surfactant **54** (AE7). One of the differences between these experiments was that samples in Chapters 2 and 3 were exposed to relatively high intensities of light by remaining in light beam of the spectrophotometer for the uration of the experiment (20–30 minutes). In contrast, experiment samples in this chapter were incubated in the dark with brief exposure to light during absorbance measurements. Photobleaching may be a significant contributing factor in the degradation of β-carotene **1** in samples and may be dependent on the surfactant environment – surfactant **54** (AE7) may stabilise β-carotene **1** more than **53** (Tween 80).

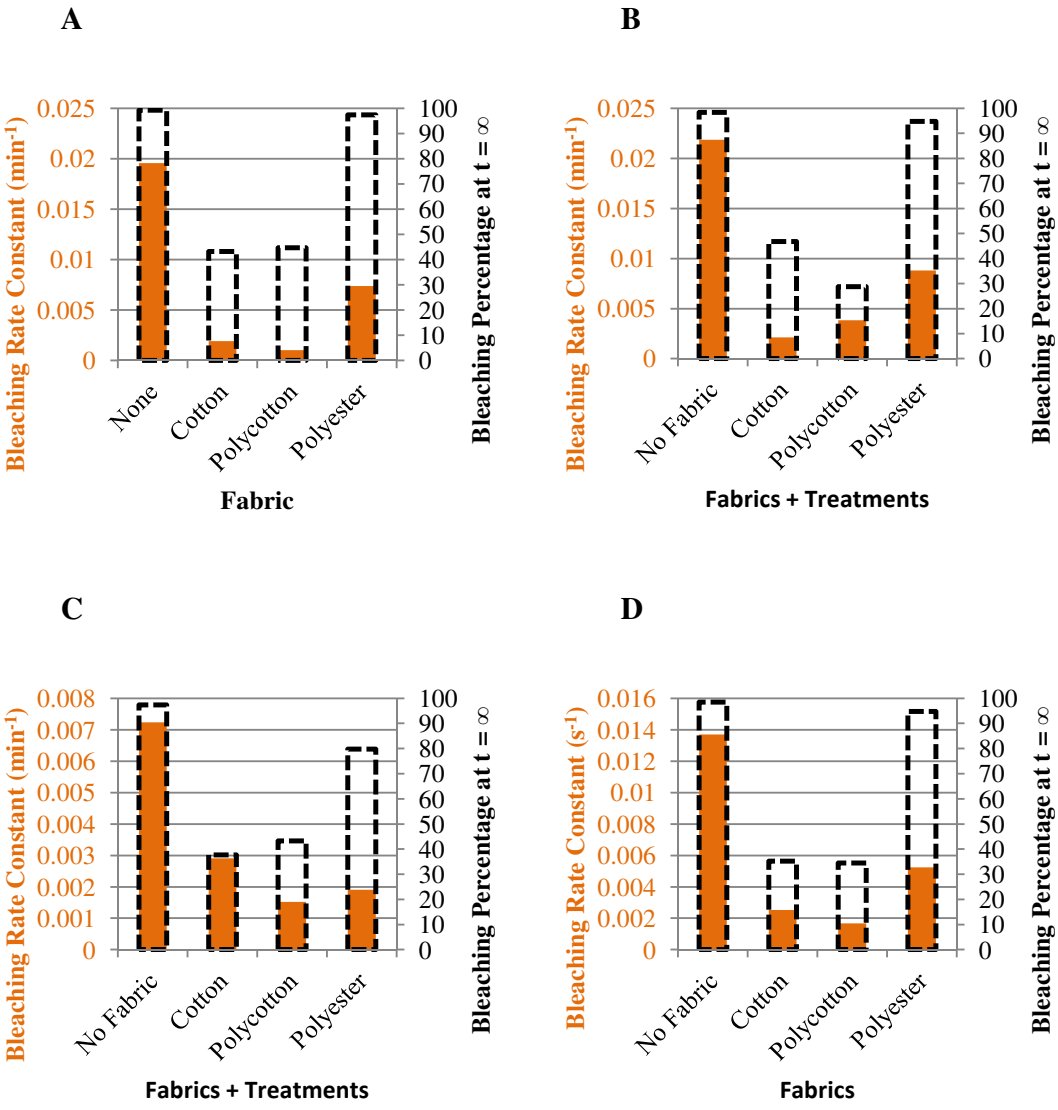

Figure 4.13 First order rate constants (orange columns) and extent of bleaching (black dashed columns) of β-carotene **1** solutions in the presence of fatty acid, surfactant and untreated fabric. (A) Linoleic acid **10**, surfactant **53** (Tween 80) and 1.0 g of fabrics. (B) Linoleic acid **10**, surfactant **54** (AE7) and 1.0 g of fabrics. (C) Oleic acid **38**, surfactant **53** (Tween 80) and 1.0 g of fabrics. (D) 0.5 g of fabrics, linoleic acid **10** and surfactant **53** (Tween 80).

Bleaching of solutions samples in the presence of fabric appear to be consistent with previous results for bleaching of stains on fabric. Rate constants and extent of bleaching substantially lower in samples containing cotton/polycotton compared to those containing polyester. The differences in observed bleaching effects on these fabrics may be explained by interactions with substrates and structural features. The presence of hydroxyl groups in cotton may allow for greater interaction with the carboxylate group of linoleic acid **10** and its oxidation products possibly resulting in cotton fibres sequestering bleaching species away from β-carotene or potentially reacting with radicals, reducing the available concentration of bleaching species. Additionally, cotton fibres possess porous walls and a lumen which could further contribute to the separation of substrates and reactants by the accumulation of hydrophobic compounds in regions that are less accessible to the aqueous phase.

The addition of oleic acid **38** stock solution instead of linoleic acid **10** to initiate the bleaching of β-carotene **1** seemed to reduce rate constants of bleaching overall. Fig. 4.13C shows the rate constants and the extent of bleaching for experiments containing oleic acid **38**. Bleaching rate constants in the absence of fabric and presence of oleic acid **38** decreased by slightly more than 2-fold relative to samples containing linoleic acid **10**, comparable with results obtained in Chapter 2. Bleaching rate constants in the presence of polyester, however, decreased by 4-fold, while rate constants in the presence of cotton and polycotton were similar in both experiments. The extent of bleaching for samples in the absence of fabric and in the presence of cotton and polycotton were comparable for experiments containing oleic acid **38**, however, samples containing polyester showed a decrease in the extent of bleaching (80% with oleic acid **38** versus > 95% linoleic acid **10**).

Lower rate constants of bleaching would be predicted as rates of formation of the hydroperoxide bleaching species are slower for oleic acid **38** compared to linoleic acid **10**. The reduction in saturation may also have an effect on the interactions of oleic acid **38** with fabrics relative to linoleic acid **10**. The saturation of one double bond may suggest

oleic acid **38** is slightly less hydrophobic than linoleic acid **10** and may therefore have less interaction with the hydrophobic polyester surface, however, the shape of the molecule may have a greater influence. Oleic acid **38** possesses a straighter structure which may allow greater penetration and accumulation within the inter-fibre spaces of polyester, sequestering away from solution.

Results from experiments containing lower masses of fabric (0.5 g) showed that bleaching rate constants were relatively faster, however, the extent of bleaching was not affected. Fig. 4.13D shows that samples containing cotton or polycotton were ~6 to 8-fold slower than samples without fabric while samples containing polyester were 2 to 3-fold slower relative to control. Despite increases in the relative rate constants, the extent of bleaching in the presence of fabrics remained at the same (30 to 40% for cotton and polycotton, 95% for polyester). This could suggest that the capacity of the fabric to interact with and sequester fatty acid has not been saturated at this lower mass of fabric.

4.4 Summary

The influence of fabrics on the bleaching of carotenoids was investigated in two series of experiments. The first set monitored the extent of bleaching of simulated carotenoid stains on fabrics of different types and treatments after a wash cycle in a terg-o-tometer (small scale mimic of a washing machine). After drying, the bleaching of stain material was quantified using DigiEye software. The second set of experiments monitored the bleaching of carotenoid microemulsions in the presence of fabric swatches under similar conditions as experiments performed in Chapters 2 and 3. These samples were stored in the dark in cell incubators to maintain a temperature of 30 °C and mixing speed of 200 rpm. Absorbance measurements were taken by UV-Vis spectrophotometry to monitor the bleaching of the carotenoid microemulsions.

Experiments studying the effect of stain composition found that the concentrations of linoleic acid **10** and α-tocopherol **58** were highly influential on the extent of capsanthin **3** bleaching on all the fabrics tested (cotton, polycotton and polyester). In the absence of α-tocopherol **58**, the extent of bleaching increased with higher concentrations of linoleic acid **10**. However, linoleic acid **10** dependent bleaching appeared to be suppressed entirely in the presence of α-tocopherol **58** at all concentrations tested. The effect of stain composition on the extent of bleaching appeared to be similar on all fabrics. These results show similar trends to those in Chapter 2 where higher concentrations of fatty acid resulted in greater initial rates of bleaching. However, solution bleaching experiments progressed faster than fabric stain bleaching and the effect of linoleic acid concentration was found to begin levelling off at higher concentrations. Higher concentrations of linoleic acid **10** are expected to result in greater extents of bleaching in both experiments as rates of autoxidation and the subsequent carotenoid bleaching reaction should increase. Rates of bleaching, however, may be significantly slower on fabric due to interactions between substrates and the fabric material. The effect of α-tocopherol **58** suggested that linoleic acid **10** dependent bleaching of carotenoids was largely dependent on a radical reaction process. α-Tocopherol **58** is known to be a potent chain breaking antioxidant that prevents the propagation of radical chain reactions such as autoxidation.

The effect of fabric type and treatment was examined on swatches of multifibre which contained samples of diacetate, cotton, polyamide, polyester, acrylic and wool. Stain bleaching at early stages after the wash were of the order polyamide > diacetate, cotton, acrylic > wool > polyester, while bleaching after 48 hours were of the order polyester, acrylic > polyamide, wool > diacetate, cotton. Wash treatments such as the inclusion of lipase enzyme in prewash and wash cycles or rinsing in fabric softener did not have substantial effects on the bleaching of carotenoid stains. The only treatment that appeared to significantly improve bleaching was whether the fabric was prewashed. Similarly, increased temperature during drying only promoted the extent of bleaching of stains on prewashed acrylic and polyester. These results were attributed to different interactions between fabric and water during the wash as well as between fabric and stain material. More hydrophilic fabrics were suggested to interact more favourably with water and allow greater access to stain material during the wash. This would result in higher stain bleaching at early stages by removal of stain material. The more hydrophilic materials, particularly those with a H-bond donor, were also suggested to interact with fatty acids and lipid oxidation products more relative to other hydrophobic components of the stain such as capsanthin. This could result in bleaching species being sequestered away from carotenoids and decrease the rate of bleaching at later stages after the wash cycle. Additionally, as reported by authors studying stain ageing, fabrics such as cotton and diacetate, which contain a free hydroxyl group, may react with lipid autoxidation products depleting the concentration of bleaching species. The enhanced stain bleaching observed on fabrics that were prewashed in capsule formulation was proposed to be caused by the accumulation of deposition agents at the fibre surface reducing the interaction between fabric and stain material.

Bleaching of carotenoid solutions upon the addition of fatty acid were found to be significantly affected by the presence of fabric. First-order rate constants of bleaching of samples were in the order: no fabric > polyester > polycotton, cotton for most of the experiments conducted. The same order was observed for the extent of bleaching. Interestingly, only small differences in rate constants of bleaching and extent of bleaching

were observed for solutions containing surfactant **53** (Tween 80) compared to those with surfactant **54** (AE7). This contrasts the results in Chapters 2 and 3 which showed bleaching reactions to be consistently 2-fold faster in the presence of **53** (Tween 80). Samples that were initiated by addition of oleic acid **38** were found to bleach at a lower rate than those with linoleic acid **10** in agreement with results from Chapter 2. For this set of experiments the order of bleaching rate constants was: no fabric > polycotton, cotton > polyester.

Experiments containing lower masses fabric showed larger rate constants of bleaching, however, the extent of bleaching remained similar to experiments containing more fabric. The lower rate constants and extent of bleaching observed for samples containing fabrics was attributed to interaction of fabric with fatty acid resulting in either depletion of bleaching species and/or sequestering away from carotenoid. The similar bleaching rate constants for surfactant **53** (Tween 80) and surfactant **54** (AE7) samples may be the result of different reaction conditions – samples were stored mainly in the dark and were mixed constantly throughout the experiment. The relatively lower bleaching rate constants in samples initiated by oleic acid **38** were attributed to lower rates of autoxidation while the relatively large decrease in bleaching extent observed for polyester may be caused by oleic acid **38** interacting differently with fabric compared to linoleic acid **10**. Overall, results for bleaching of carotenoid stains on fabric show some correlation with results obtained for the bleaching of carotenoid microemulsion solutions.

4.5 Experimental

4.5.1 Materials

Linoleic acid **10** (L1376), oleic acid **38** (O1008), β-carotene **1** (220c40), capsanthin **3** (19081), glycerol trioleate **59** (T7140), α-tocopherol **58** (T3251) and Tween 80 **53** (P1754) were purchased from Sigma-Aldrich. Sunflower oil was purchased from Tesco. AE7 **54** surfactant, lipase enzyme (Lipex), Ariel capsule formulation and fabric swatches (obtained from James Heal) were kindly donated by Procter & Gamble. Polycotton fabrics were a blend of 60% cotton and 40% polyester.

4.5.2 Methods

4.5.2.1 Preparation of fabric stains

Capsanthin **3** (0.1 g) was dissolved in either sunflower oil or glycerol trioleate **59** (50 g). For experiments studying the effect of stain composition, glycerol trioleate **59** stains were used with the addition of linoleic acid **10** and α-tocopherol **58**. Stain material (300 μL) was applied to swatches of individual fabric by pipette and allowed to settle overnight in the dark at room temperature (~20 °C). For experiments studying the effect of fabric type and treatment, sunflower oil stains were used. Stain material (100 μL) was applied to each strip of fabric on the multifibre swatch by pipette and allowed to settle overnight in the dark at room temperature (~20 °C).

4.5.2.2 Wash and dry conditions

Wash cycles were performed on a custom built automated terg-o-tometer at P&G's Newcastle Innovation Centre. The following settings were used:

Product Type: Powder, Water Type: City, Prime Water: 250 ml, 30 °C, Wash Water: 1000 ml, 24 °C, Rinse Water: 1000 ml, Number of Rinses: 1.

Agitator settings

Prime Wash Pot: 2000 RPM speed of rotation, 20 s duration

Prime Agitator: 36000 ° angle of rotation, 1500 ° s^{-1} speed of rotation, 400 ms acceleration, 50 ms deceleration

Dilution: 3600 ° angle of rotation, 2300 ° s^{-1} speed of rotation, 60 s duration

Wash: 3600 ° angle of rotation, 1000 ° s^{-1} speed of rotation, 900 s duration

Rinse: 3600 ° angle of rotation, 1000 ° s^{-1} speed of rotation, 60 s duration

Dry Impeller: 100000 ° angle of rotation, 900 ° s^{-1} speed of rotation, 6500 ms acceleration, 50 ms deceleration

Dry Wash Pot: 750 RPM for 30 s, 1300 RPM for 30 s, 2350 RPM for 30 s, 6000 RPM for 75 s, 500 RPM during filling

Fabrics (4–8 stained swatches and 30 g of ballast) and detergent (1.53 ml per l of wash water) formulation were added manually to wash pots at different stages of the wash cycle.

For drying cycles fabrics were placed on tray grills and left in thermostated dark ovens at either 20 or 50 °C.

4.5.2.3 Measurements of SRI

Photographs and measurements of *L*, *a*, *b* colour space were obtained using DigiEye software and hardware. SRI measurements were calculated by conversion of relative *L*, *a*, *b* colour space of clean and stained fabric to ΔE values:

$$\Delta \mathrm{E} = \sqrt{(L_0 - L_{\mathrm{stain}})^2 - (a_0 - a_{\mathrm{stain}})^2 - (b_0 - b_{\mathrm{stain}})^2}$$

Where L_0, a_0 and b_0 are *L*, *a*, *b* values for clean fabric and L_{stain}, a_{stain} and b_{stain} are *L*, *a*, *b* values for stained fabric.

SRI values are calculated from ΔE values of fabric stains at different time points after the wash cycle relative to the ΔE value of the fabric stain immediately before the wash cycle.

$$SRI = (100 \text{ x } (\Delta E_{t0} - \Delta E_{t})) / (\Delta E)$$

4.6 References

[1] M. A. Morris and H. H. Prato, *Textile Res. J.*, 1982, **52**, 280-286.
[2] S. K. Obendorf, Y. M. N. Namaste and D. J. Durnam, *Text. Res. J.*, 1983, **53**, 375–383.
[3] S. K. Obendorf, A. Varanasi, R. Mejldal and V. S. Nielsen, *J. Surfactants Deterg.*, 2003, **6**, 1–5.
[4] Y.-S. Chi and S. Kay Obendorf, *J. Surfactants Deterg.*, 1998, **1**, 371–380.
[5] S. K. Obendorf, A. Varanasi, R. Mejldal and M. Thellersen, *J. Surfactants Deterg.*, 2001, **4**, 233–245.
[6] S. K. Obendorf and J. Borsa, *J. Surfactants Deterg.*, 2001, **4**, 247–256.
[7] T.P. Nevell and S.H. Zeronian, *Cellulose Chemistry and Its Applications*, edited by T.P. Nevell and S.H. Zeronian, Ellis Horwood Limited, West Sussex, England, 1985, 15.
[8] C. H. Haigler, *Cellulose Chemistry and Its Applications*, edited by T.P. Nevell and S.H. Zeronian, Ellis Horwood Limited, West Sus- sex, England, 1985, 30.
[9] R. A. Young, *Cellulose Structure, Modification and Hydrolysis*, edited by R.A. Young and R.M. Rowell, John Wiley & Sons, New York, 1986, 91.
[10] M.L. Rollins and J.C. Cook, *Handbook of Textile Fibres*, 4th edn., Merrow Publishing Co., Watford, Herts., United Kingdom, 1968, 42
[11] Y.-S. Chi and S. K. Obendorf, *J. Surfactants Deterg.*, 1999, **2**, 1–11.
[12] E. Kissa, J. M. Dohner, W. R. Gibson and D. Strickman, *J. Am. Oil Chem. Soc.*, 1991, **68**, 532–538.
[13] Y.-S. Chi and S. K. Obendorf, *J. Surfactants Deterg.*, 1998, **1**, 407–418.
[14] R. Kumarathasan, A. B. Rajkumar, N. R. Hunter and H. D. Gesser, *J. Am. Oil Chem. Soc.*, 1992, **69**, 338–340.
[15] F. Franks and B. Roberts, *J. Appl. Chem.*, 1963, **13**, 303–309.
[16] G. Britton, S. Liaaen-Jensen, and H. P. Pfander, *Carotenoids: handbook*., 2004, Birkhauser.
[17] M. Tasan and M. Demirci, *Eur. Food Res. Technol.*, 2005, **220**, 251–254.

CHAPTER 5

Conclusions and Future Work

Carotenoids are naturally occurring pigments that may be found in a wide range of foodstuffs that contain tomato or red pepper derivatives. The structural backbone of carotenoids contains a long hydrocarbon chain of up to 11 conjugated carbon-carbon double bonds. This feature confers a hydrophobic character and strong colouration making carotenoid containing stains problematic: hydrophobic compounds may adhere strongly to fabrics, washing in aqueous media can be ineffective at completely removing hydrophobic material and the presence of even small amounts of carotenoid within remaining stain material are highly visible. Due to the difficulty in complete removal of carotenoid stains from fabric, the detergent industry has become interested in strategies to selectively bleach carotenoid compounds within stains.

Processes such as the autoxidation and LOX catalysed oxidation of fatty acids, as well as the subsequent bleaching reactions with carotenoids, are well documented in the literature. However, many reports are from the perspective of the food industry with a focus on stabilising fatty acid and carotenoid compounds within foods, and a thorough, quantitative analysis of carotenoid bleaching processes, in relation to stain bleaching, has yet to be published. We have probed the effect of surfactant, fatty acid and pH on the bleaching of β-carotene containing oil-in-water microemulsion solutions by UV-Vis spectrophotometry. These were performed in the presence and absence of LOX in order to assess the viability of exploiting these enzymes in detergent formulations.

From solution bleaching experiments in the absence of LOX, initial rates of linoleic acid autoxidation ranged from 1.70×10^{-2} to 3.3×10^{-1} μM min^{-1} and were found to be greater in surfactants with higher hydrophilicity-lipophilicity balance. Autoxidation was faster at lower pH but also dependent upon surfactant conditions. These results were attributed to greater accessibility of fatty acid to the aqueous environment and higher solubility of metal ion initiators at low pH. Experiments monitoring the bleaching of β-carotene showed slow background reactions in the absence of fatty acid with initial rates ~ 10^{-3} μM min^{-1} for the pH range and surfactant systems tested. Addition of linoleic acid increased the initial rates

of β-carotene bleaching by up to 2 orders of magnitude depending on pH, with initial rates ranging from 4.10 x 10^{-3} to 1.01 x 10^{-1} μM min^{-1}. Optimal bleaching in the presence of linoleic acid occurred at pH 7.0 which may be the result of the deprotonated carboxylate group of the fatty acid increasing the negative charge at the micelle surface and attracting positively charged metal ion initiators to the interface. Further studies of the effect of fatty acid on the bleaching of β-carotene found that the order of bleaching was linoleic > oleic > linolenic > arachidonic and stearic. Fatty acid dependent bleaching of β-carotene was predicted to be faster for more unsaturated fatty acids as rates of formation of the hydroperoxide bleaching species are greater, however the highly unsaturated fatty acids, arachidonic and linolenic were found to be highly susceptible to oxidation even before addition to the reaction mixture. Surprisingly, stearic acid promoted bleaching was on the same order of magnitude as the unsaturated fatty acids despite being predicted to have a slow formation of hydroperoxide. This effect was attributed to the stearic acid carboxylate group being more accessible at the micelle surface and thus more able to attract metal ions as well as interact with oxidised radical species. The greater presence of stearic acid at the interface compared to the more unsaturated fatty acids may be due to the straighter acyl chain and lower hydrophobicity.

Solution bleaching experiments were performed in the presence of LOX isozymes from soybean under analogous conditions to those employed for analysis of the non-enzymatic background reactions to fully assess the enzymatic contribution towards carotenoid bleaching. LOX1 and LOX3 were found to have optimum pHs of 9.0 and 6.5, respectively, based on linoleic acid oxidation activities. LOX1 appeared to have greater stability towards changes in surfactant conditions, demonstrated by high activities in all surfactants tested at pH 9.0 and by only slight decreases in activity (20%) when increasing surfactant concentrations from 200 μg ml^{-1} to 400 μg ml^{-1}. In comparison, LOX3 only possessed activity in Tween 20 and 80 surfactants at the lower surfactant concentration of 200 μg ml^{-1}. Interestingly, LOX1 possessed a relatively high activity at pH 6.5, away from optimum pH, in the presence of AE1S which may be caused by stabilising interactions with surfactant.

Optimal pHs for LOX1 and LOX3 cayalysed bleaching of β-carotene were pH 8.0 and 6.5, respectively. LOX1 and LOX3 in combination were not observed to substantially increase initial rates of bleaching despite a reported synergy in the literature by Ramadoss *et al.* This study reported that samples containing both LOX1 and LOX3 at pH 6.5 bleached 6 times faster than times predicted from assays of individual isozymes. However, a notable difference compared to our study was the inclusion of cosolvents. The largest initial rate of bleaching of β-carotene observed was 3.63×10^{-7} M min^{-1} at pH 8.0 in the presence of Tween 80 and LOX1. Throughout our studies of solution based carotenoid bleaching, initial rates of bleaching were consistently observed to be 2-fold higher in the presence of Tween 80 surfactant compared to AE7. The origin of this effect was predicted to be possibly based on differences in micelle structure and/or dynamics of exchange. The morphology of micelle structures could affect the accessibility of substrates depending on their position within the micelle. Micelle dynamics can be described as the rates of dissociation of micelles (and association of surfactant monomers) and also may influence the rate of interaction of hydrophobic substrates (carotenoids/fatty acids) with polar molecules (fatty acid hydroperoxides/metal ions). Measurements of micelle dynamics were attempted using a stopped flow spectrophotometer, however, rates of formation/dissociation of micelles appeared to be too rapid to permit quantification.

To understand the effect of surfactant on these oxidative processes it would be beneficial to characterise the micelle structures formed from different surfactants and substrates in solution. Small angle X-ray scattering measurements could potentially determine the dimensions of components of the micelle structure, such as the hydrophobic core, interface and overall diameter of the micelle. This data would perhaps allow comparisons of the accessibility of substrates and the surface area of the interface for different surfactant systems. Although our attempts to determine τ_2 values by a rapid change in surfactant concentration were unsuccessful, other techniques, such as ultrasonic relaxation, pressure- and temperature-jump, could be employed to obtain measurements of τ_2. Relatively large values of τ_2, indicative of higher stability micelles with longer life spans, would be

expected for the AE7 systems as initial rates of oxidation processes were consistently lower in samples containing this surfactant.

Experiments utilising carotenoid stains on fabric were performed at P&G to study carotenoid bleaching under conditions mimicking those in a wash cycle. Stain decolourisation was quantified by SRI values obtained from DigiEye. Results for experiments analysing the effect of stain composition paralleled results in carotenoid microemulsion solutions. Higher concentrations of linoleic acid resulted in greater stain bleaching in the absence of α-tocopherol. Increasing the linoleic acid concentration from 5 to 20% w/w resulted in an increase in SRI from 34 to 67% for stains on cotton observed 18 hours after the wash. The addition of α-tocopherol (even at concentrations as low as 0.01% w/w) to stain material, however, prevented any linoleic acid dependent carotenoid bleaching. As α-tocopherol is a potent chain-breaking antioxidant, these results suggest that linoleic acid dependent carotenoid bleaching is a radical process. Bleaching of carotenoid stains appeared to be affected by the type of stained fabric. Decolourisation of stains immediately after the wash was greater on more hydrophilic fabrics (SRI values for prewashed diacetate and polyester 1 hour after the wash cycle were 70 and 50%, respectively) suggesting greater removal of stain material during the wash cycle. Measurements of decolourisation at later stages, however, were found to be greater on hydrophobic fabrics (SRI values for prewashed diacetate and polyester 48 hours after the wash cycle were 74 and 96%, respectively) and may be the result of bleaching species (oxidised fatty acids) being sequestered by hydrophilic materials or reacting with function groups such as hydroxyls found on cotton. Surprisingly, the only fabric treatment that affected the bleaching of carotenoid stains was whether the fabric was prewashed. The use of lipase or Lenor fabric softener in the prewash had no additional beneficial bleaching effects.

THESIS PART II

CHAPTER 6

Kinetics of triethyloxonium tetrafluoroborate hydrolysis

5.0 Foreword

Trialkyloxonium salts, also known as Meerwein's reagents, are synthetic compounds typically employed in alkylation reactions. These compounds are thought to require dry solvent conditions and the presence of a bulky, non-nucleophilic base as they are highly reactive and generate acid upon reaction. However, one potential use of Meerwein's reagent is the alkylation of biological molecules, which necessitates the use of an aqueous solvent at physiological conditions (the native conformation of biomolecules is not stable in organic solvent and many bioconjugation reactions require an aqueous environment). One of the motivations behind this study has been to assess the application of trialkyloxonium salts in the trapping of carbamates on proteins as shown in Fig. 5.1 (associated with a project analysing carbon sensing in proteins). Due to the relatively hard character of the carbamate oxyanion, trialkyloxonium salts were predicted to be more suitable alkylating reagents compared to methyl iodide.

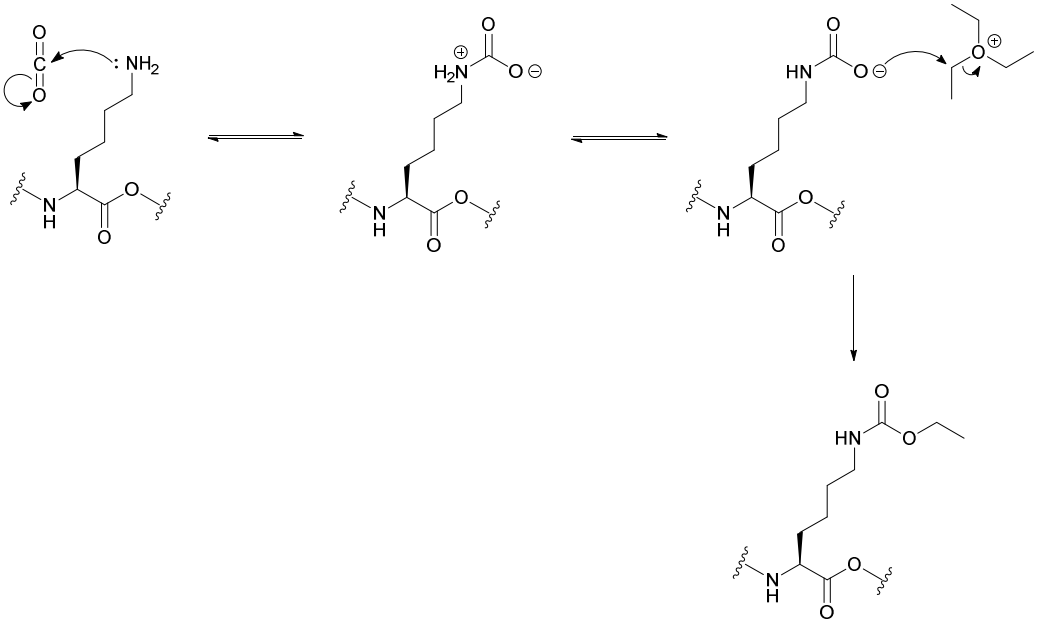

Figure 5.1 Reversible carbamate formation by attack of lysine residue side chain on carbon dioxide followed by trapping by ethylation.

At present there have been few attempts to quantify the rates of hydrolysis of trialkyloxonium salts making it difficult to assess the potentially wider synthetic applications of these compounds under a greater range of aqueous reaction conditions. This chapter will present a preliminary study on the quantification of hydrolysis rate constants of triethyloxonium tetrafluoroborate, which is one of the most frequently used trialkyloxonium salts. Section 5.1 will present the common applications of trialkyloxonium salts and a summary of past hydrolysis studies. Section 5.2 details our results from measurements of hydrolysis rate constants of triethyloxonium tetrafluoroborate. Section 5.3 discusses these preliminary results and Section 5.4 summarises our conclusions and future directions for this project.

5.1 Introduction

5.1.1 Preparation of trialkyloxonium salts

Trialkyloxonium salts are a class of versatile alkylating agents first discovered by Meerwein and coworkers in 1937.[1] While a wide variety of trialkyloxonium salts has since been developed, the triethyl- and trimethyloxonium salts have found the widest use in chemical synthesis, perhaps due to the relative ease of preparation. The most common method of preparation of trialkyloxonium salts involves the reaction of epichlorohydrin with a boron trifluoride-ether complex in excess dry ether (Fig. 5.2). This procedure affords the triethyl- and trimethyloxonium tetrafluoroborate salts in high yields, however trialkyloxonium salts of larger/unsymmetrical alkyl substituents are not obtainable using this method.[2]

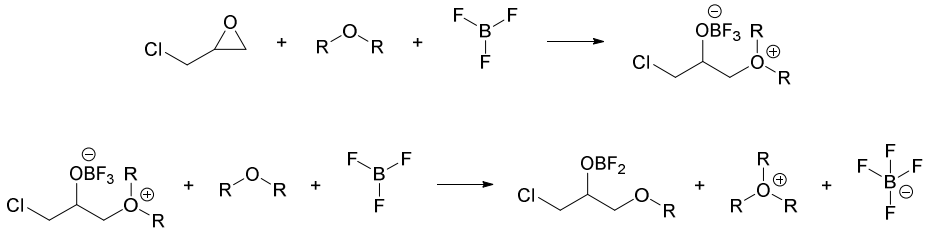

Figure 5.2 Preparation of triethyl- and trimethyloxonium tetrafluoroborate salts

5.1.2 Applications of trialkyloxonium salts

As highly reactive, hard electrophiles, trialkyloxonium salts have found many applications in *O*-alkylation reactions. Alcohols, ethers, epoxides and hydroxylated compounds may be readily alkylated under mild conditions (Fig. 5.3A).[2,3] Carbonyl compounds may also be alkylated (Fig. 5.3B), although these functional groups are less reactive towards trialkyloxonium ions – a study by Meerwein *et al.* found the order of reactivity to be: aldehydes < ketones < esters < lactones < amides < lactams.[4] *N*- or *S*-alkylation reactions are usually performed with milder reagents, however, in cases where the nitrogen or sulfur group are electron deficient, trialkyloxonium salts are often utilised.[5] Triethyloxonium ions also catalyse the homologation of ketones in the presence of diazoacetic esters[6] (Fig. 5.3C) and function as hydride acceptors leading to the formation of carbocations of hydride donors (Fig. 5.3D).[7]

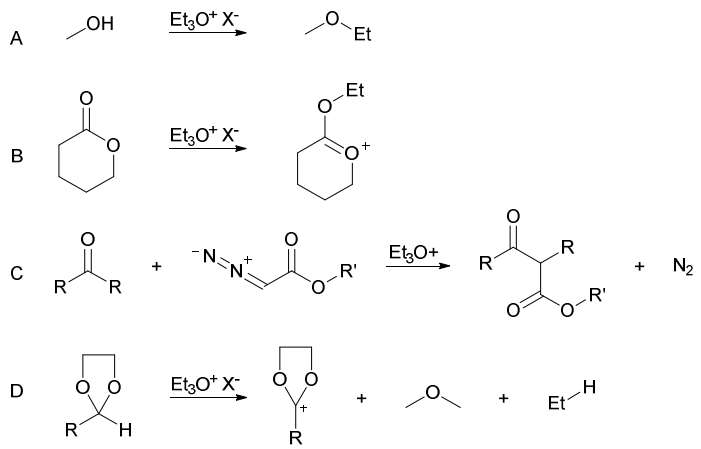

Figure 5.3 Reactions of Trialkyloxonium. **A.** The O-alkylation of an alcohol. **B.** The O-alkylation a lactone. **C.** Homologation reactions of ketones and diazoacetic esters catalysed by triethyloxonium. **D.** The formation of acetal carbocations by hydride transfer to triethyloxonium.

The multitude of reactions in which triethyloxonium salts may be utilised has led to their applications under a diverse range of reaction conditions, although, a reaction medium of dry organic solvent in the presence of a bulky, non-nucleophilic base is generally thought to be optimal.[8,9] These conditions, however, are not always possible, for example, the alkylation of biological molecules requires aqueous solvent near neutral pH to retain stablity and activity.[10] The concern under these conditions is the rate of hydrolysis of trialkyloxonium ions relative to the rate of alkylation of the target molecule. Surprisingly, there are few studies that have measured hydrolysis rate constants for trialklyoxonium salts. The purpose of this investigation is to provide a quantitative study of the pH dependence of triethyloxonium hydrolysis and the effect of acetonitrile cosolvent.

5.1.3 Current understanding of the hydrolysis of trialkyloxonium salts

Early measurements of hydrolysis rates were performed by Meerwein *et al.* by monitoring the reduction in electrical conductivity of an aqueous solution of trialkyloxonium salts[2] – a phenomenon caused by the change in cationic species (oxonium versus hydronium) (eq. 1).

$$R_3O^+ + H_2O \rightarrow ROH + R_2O + H^+ \qquad (1)$$

Several trialkyloxonium tetrafluoroborate salts were studied demonstrating that oxonium salts with larger alkyl substituents are more stable towards hydrolysis (Table 5.1). The paper reports the time taken for complete hydrolysis (point at which conductivity stabilised) allowing for comparisons of the relative rates of hydrolysis for the trialkyloxonium salts, however, absolute rate constants are not reported and cannot be derived from the reported data.

Table 5.1 Comparison of trialkyloxonium hydrolysis rates at 18 °C.[2]

Trialkyloxonium Tetrafluoroborate Salt	Time for complete hydrolysis (min)
Trimethyloxonium	8
Triethyloxonium	80
Tri-*n*-propyloxonium	120
O-ethyl tetrahydropyran	220

An investigation by Kevill and Lin of alkylating agents involved measurements of solvolysis in unbuffered water, methanol and acetonitrile at -23.4 to 0.3 °C.[11] A titration method was employed for monitoring the extents of reaction of alkylating agents (methyl trifluoromethanesulfonate, methyl fluorosulfonate, methyl perchlorate and trimethyloxonium, both the hexafluorophosphate and hexachloroantimonate salts) over time allowing for calculation of first order rate constants. However, accurate measurements for the hydrolysis of trimethyloxonium salts were unobtainable even at low temperatures (0.3 °C) as reactions proceeded too quickly. For other solvents, rate constants for trimethyloxonium salts were the largest of the alkylating agents investigated; 12-fold greater in methanol and 5-fold greater in acetonitrile than methyl trifluoromethanesulfonate, the second fastest reacting alkylating agent.[11] Assuming an approximately 10-fold larger hydrolysis rate constant than methyl trifluoromethanesulfonate would give a rate constant of 4.4×10^{-2} s^{-1} for trimethyloxonium salt at 0.3 °C in water. A similar titration method was utilised for measurements of solvent nucleophilicities by rates of solvolysis with triethyloxonium ion.[12]As before, solvents were unbuffered. Triethyloxonium hexafluorophosphate was reported to have a hydrolysis rate constant of 7.23×10^{-5} s^{-1} in water at 0.0 °C.[12]

The most recent work on triethyloxonium hydrolysis was performed by King *et al.* in 1986.[13] The authors report a pH independent region from pH 4 to 9 with half-lives of 7.4 minutes at 25 °C and 1.95 minutes at 38 °C, although experimental details were not included. These half-lives correspond to first order rate constants of 1.56×10^{-3} and $5.92 \times$

10^{-3} s^{-1}, respectively. King *et al.* speculated the alkylation reaction to be largely S_N1 (see Fig. 5.4) as a result of observing reaction with halide ions to afford alkyl halides. This is in conflict with work by Kevill *et al.* that assumes a S_N2 reaction[12] based on S_N2 mechanisms for solvolysis of ethyl perchlorate[14] and ethyl trifluoromethanesulfonate.[15,16] Both of these compounds are ethylating agents with comparable leaving groups, albeit anionic, to triethyloxonium hexafluorophosphate,. Kevill suggested a S_N2 mechanism of solvolysis of ethyl perchlorate based upon several observations. Rate constants of solvolysis were sensitive to changes in solvent nucleophilicity and ionising power implying the nucleophile is involved in the rate determining step.[17] Entropies of activation for solvolysis of ethyl perchlorate are negative (ranging between -68 and -96 J K^{-1} mol^{-1}) suggesting a bimolecular reaction, in contrast to more positive values determined for 2-admantyl perchlorate (-9 to +55 J K^{-1} mol^{-1}) which would be expected to have an S_N1 mechanism.[18] The rate constant of hydrolysis of ethyl perchlorate is only slightly larger than methyl perchlorate despite differences in stabilities of the carbocation intermediates.[14] Streitwieser *et al.* proposed an S_N2 mechanism for ethyl trifluoromethanesulfonate as solvent effects and secondary deuterium isotope effects indicated a transition state with little positive charge and substantial bonding to a solvent molecule.[15] Additionally, solvolysis experiments of primary alkyl triflates and tosylates did not show evidence for the formation of carbenium ions.[16]

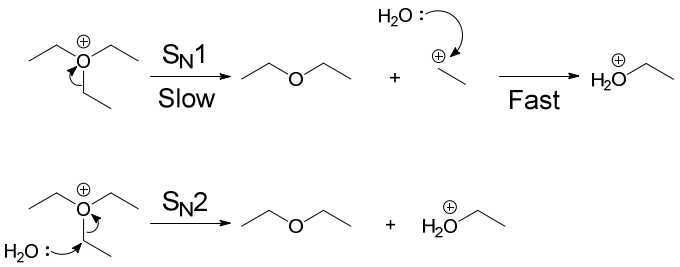

Figure 5.4 S_N1 and S_N2 mechanisms for the hydrolysis of triethyloxonium ion.

5.2 Results

5.2.1 Strategy to determine the rate constants of hydrolysis of triethyloxonium salt by UV-Vis spectrophotometry

As shown in the review of past studies attempting to measure rate constants of hydrolysis of triethyloxonium ion, reaction half-lives were reported to be on the minute timescale. At high pH, reaction with hydroxide ion could potentially result in reaction half-lives on the second timescale. Therefore, UV-Vis spectrophotometry was employed to monitor reactions. The extent of hydrolysis of triethyloxonium ion was measured spectrophotometrically (Fig. 5.5) using a technique adapted from a procedure to monitor hydrolysis of phosphorus chlorides by Delley *et al.*[19,] and carbon dioxide hydration by Khalifah. [20] As triethyloxonium is hydrolysed, acid is generated stoichiometrically (Fig. 5.5A). The formation of acid is measured spectrophotometrically by employing a substituted phenol (Fig. 5.5B) or trinitrobenzene (Fig. 5.5C) indicator possessing a pK_a value within 0.5 pH units of the buffer solution.

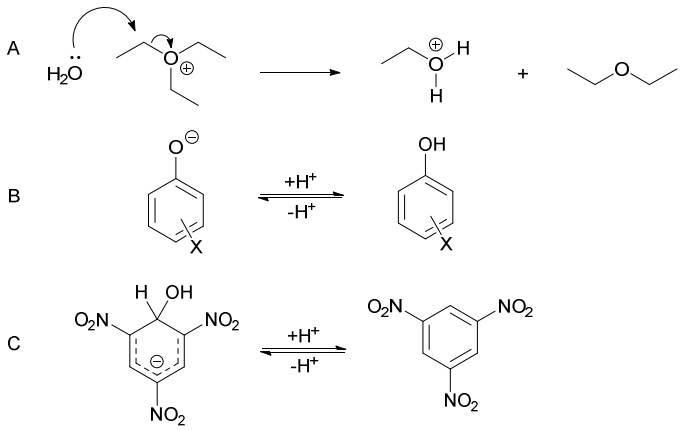

Figure 5.5 Monitoring triethyloxonium ion hydrolysis spectrophotometrically. **A.** Formation of acid upon hydrolysis of triethyloxonium ion. **B.** Proton transfer in phenol indicators. **C.** Formation/consumption of Meisenheimer indicator complex by hydroxide ion.

Proton/hydroxide transfer at indicator compounds results in a change in absorbance. This coupled system could potentially allow monitoring of the hydrolysis of triethyloxonium ion by UV-Vis spectrophotometry, however, a notable limitation of this system is that in order to quantify rate constants of hydrolysis, proton/hydroxide transfer involving indicator must not be rate limiting (requires rate of (de)protonation >> rate of hydrolysis). While proton transfer will certainly be faster than triethyloxonium hydrolysis, the loss of water from trinitrobenzene-hydroxide adduct may become rate limiting. Bersconi determined a second-order rate constant of 37.5 M^{-1} s^{-1} for the addition of hydroxide ion to nitrobenzene and a first order rate constant of 9.8 s^{-1} for the dissociation of the Meisenheimer complex. [21]

5.2.2 Buffer and indicator systems

Employing the strategy outlined in Section 5.2.1, Table 5.2 shows the buffer and indicator systems used to obtain measurements of first order rate constants of hydrolysis of triethyloxonium tetrafluoroborate salt. Aqueous buffer solutions had an ionic strength, I = 1.00 M (KCl or $NaBF_4$).

Table 5.2 Components of reaction mixtures employed for studying pH dependence of triethyloxonium tetrafluoroborate (15 mM) hydrolysis.

Buffer	Initial pH	Indicator	λ_{max} (nm)
0.1-1.0 M HCO_2H/HCO_2K 10% FB	2.57	0.18 mM 2,4 dinitrophenol	401
0.1-1.0 M HCO_2H/HCO_2K 90% FB	4.67	0.18 mM 2,4 dinitrophenol	401
0.05-0.5 M KH_2PO_4/K_2HPO_4 50% FB	6.67	0.27 mM *p*-nitrophenol	398.5
0.035-0.35 M KH_2PO_4/K_2HPO_4 90% FB	7.72	0.27 mM *p*-nitrophenol	398.5
0.025-0.25 M H_3PO_4/NaH_2PO_4 50% FB	1.99	0.5 mM 2-aminobenzoic acid	328
0.025-0.25 M H_3PO_4/NaH_2PO_4 90% FB	3.01	0.5 mM 2-aminobenzoic acid	328
0.025-0.25 M CH_3CO_2H/CH_3CO_2Na 50% FB	4.52	0.18 mM 2,4 dinitrophenol	401
0.025-0.25 M CH_3CO_2H/CH_3CO_2Na 90% FB	5.20	0.18 mM 2,4 dinitrophenol	401
0.05-0.50 M NaH_2PO_4/Na_2HPO_4 50% FB	6.61	0.27 mM *p*-nitrophenol	398.5
0.035-0.35 M NaH_2PO_4/Na_2HPO_4 90% FB	7.40	0.27 mM *p*-nitrophenol	398.5
0.02-0.2 M Tricine/$Tricine^-$ 90% FB	8.64	0.84 mM 3-nitrophenol	410
0.05-0.50 M $NaHCO_3/Na_2CO3$ 50% FB	10.30	0.27 mM phenol	287
0.035-0.35 M $NaHCO_3/Na_2CO_3$ 90% FB	11.30	0.27 mM phenol	287
0.010 M NaOH	11.83[a]	0.3 mM 1,3,5-trinitrobenzene	439
0.050 M NaOH	12.33[a]	0.3 mM 1,3,5-trinitrobenzene	439
0.075 M NaOH	12.42[a]	0.3 mM 1,3,5-trinitrobenzene	439
0.100 M NaOH	12.47[a]	0.3 mM 1,3,5-trinitrobenzene	439

[a] In the absence of a buffer compound with high pH, unbuffered sodium hydroxide solutions were used to access these pHs and were not pH controlled.

5.2.3 UV-Vis spectrophotometric studies of hydrolysis

5.2.3.1 Studies using potassium chloride to control ionic strength

Initial studies to determine pseudo first order rate constants for hydrolysis of triethyloxonium tetrafluoroborate were performed in aqueous formate and phosphate (KH_2PO_4/K_2HPO_4) buffers using KCl to control ionic strength and contained a final concentration of 15 mM triethyloxonium. Representative data for the phosphate experiments are shown in Fig. 5.6. Raw data for this buffer system showed a clear, single exponential decay in absorbance over time. First order rate constants for hydrolysis do not change significantly as a function of buffer concentration at a fixed pH (Fig. 5.7).Thus there is no strong evidence for the participation by buffer. In principle, the buffer species could act as a general base catalyst or, alternatively, directly as a nucleophile in place of water. The latter option would involve consumption of the conjugate base of buffer and would be predicted to have a greater effect at lower total buffer concentration.

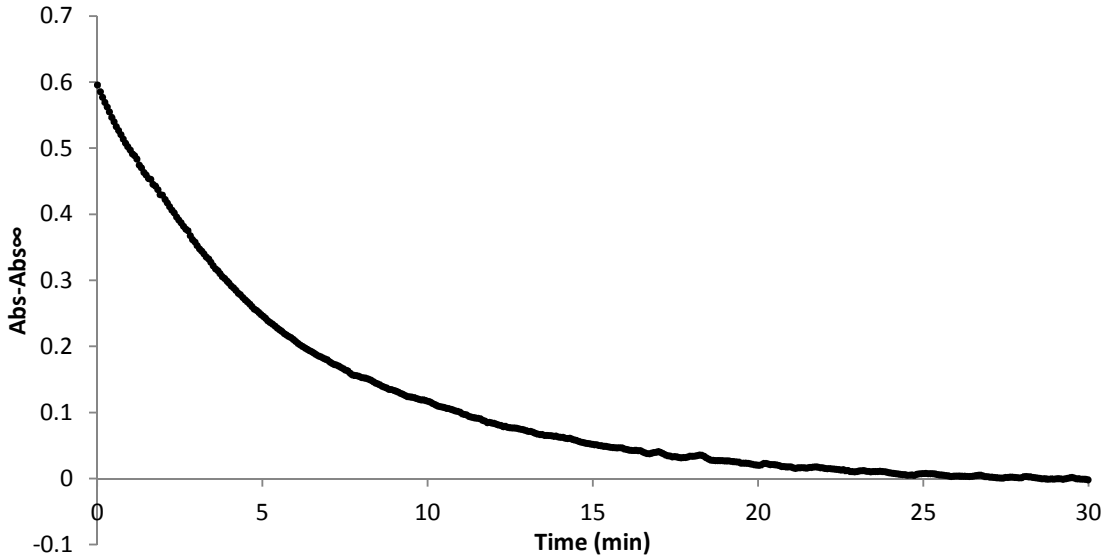

Figure 5.6 Hydrolysis of triethyloxonium tetrafluoroborate (15 mM) in 0.050 M phosphate buffer, KH_2PO_4/K_2HPO_4 50% FB, pH 6.67, I = 1.00 M (KCl) at 25 °C. *p*-Nitrophenol (0.27 mM) was used as indicator and monitored at 398.5 nm.

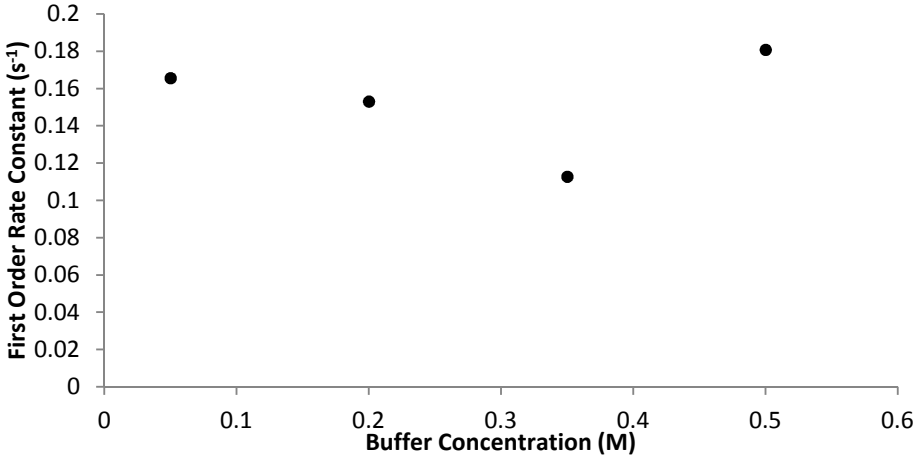

Figure 5.7 Pseudo first order rate constants for hydrolysis of triethyloxonium tetrafluoroborate at a range of phosphate buffer concentrations, KH_2PO_4/K_2HPO_4 50% FB, pH 6.67, I = 1.00 M (KCl) at 25 °C. *p*-Nitrophenol (0.27 mM) was used as indicator and monitored at 398.5 nm.

Hydrolysis data in formate buffers were more complex: representative data for 0.10, 0.40, 0.70 and 1.00 M formate buffer are shown in Fig. 5.8. The absorbance versus time plots show an initial increase followed by a plateau in absorbance before the exponential decay phase. This unusual pre-exponential phase was influenced by buffer concentration – a longer plateau was observed at higher concentrations of buffer. The rate constants for hydrolysis in formate buffer were calculated using only the exponential phase of the data. A buffer plot of these rate constants showed the absence of buffer catalysis (Fig. 5.9).

Regarding the pre-exponential phase, one consideration was the involvement of formate. Reaction of formate (conjugate base) with triethyloxonium ion produces ethyl formate which would then hydrolyse to formic acid and ethanol. Since our spectrophotometric method only monitors the generation of acid/base by decreases/increases in absorbance, the second process would not be detected. The first process which consumes the conjugate base of the buffer should lower pH and result in a decrease in absorbance.

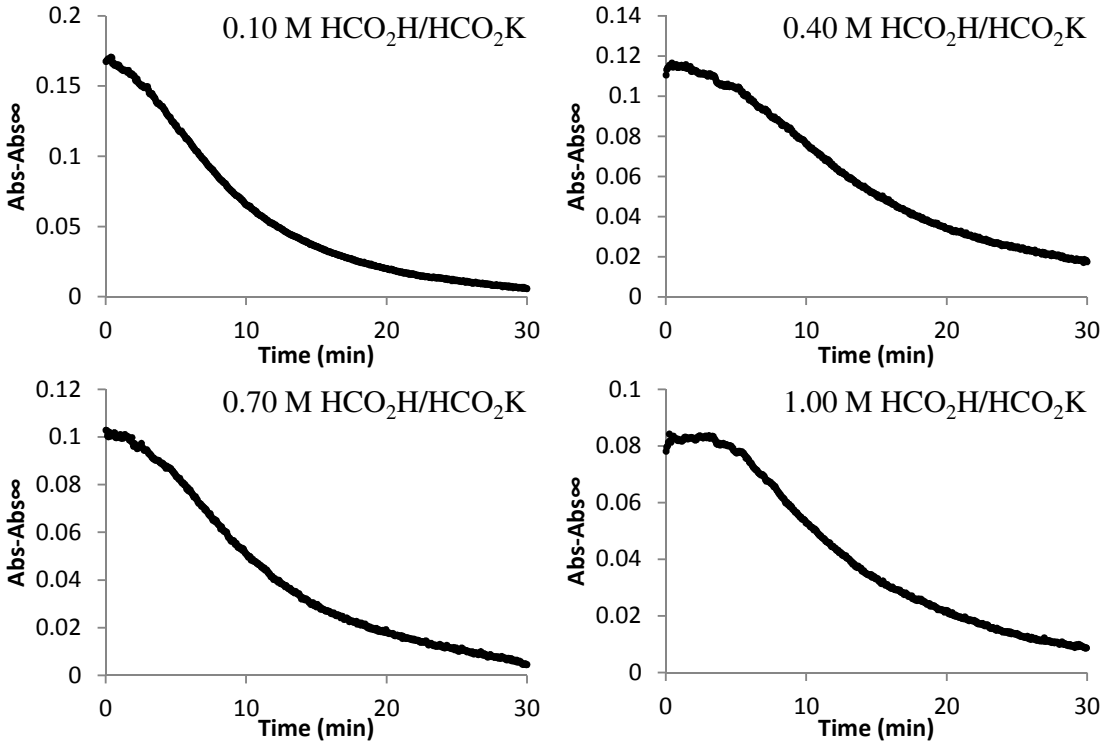

Figure 5.8 Representative raw data for the hydrolysis of triethyloxonium tetrafluoroborate (15 mM) in a range of concentrations of formate buffer 90% FB, pH 4.67, I = 1.00 M (KCl) at 25 °C. 2,4-Dinitrophenol (0.18 mM) was used as indicator and monitored at 401 nm.

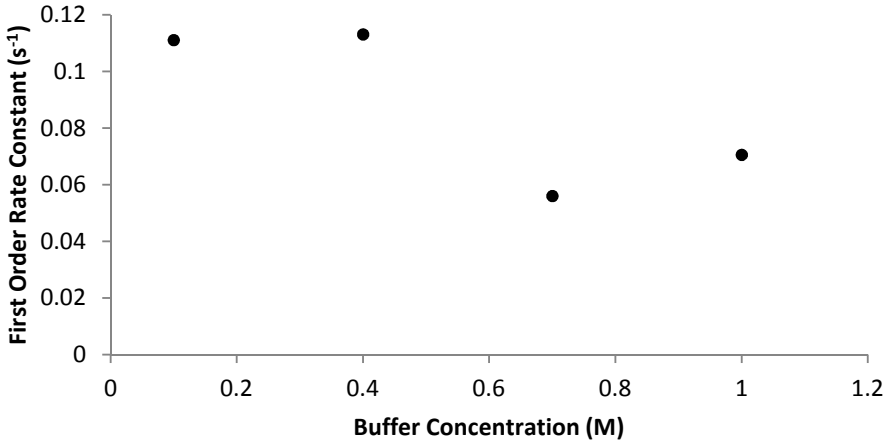

Figure 5.9 Pseudo first order rate constants for hydrolysis of triethyloxonium tetrafluoroborate at a range of formate buffer concentrations, 90% FB, pH 4.67, I = 1.00 M (KCl) at 25 °C. 2,4-Dinitrophenol (0.18 mM) was used as indicator and monitored at 401 nm.

5.2.3.2 Studies using sodium tetrafluoroborate to control ionic strength

The potential reaction of triethyloxonium ion with nucleophilic species, as just mentioned and from reports of reaction with Cl^- ions by King *et al.*[13] prompted us to explore the use of non-nucleophilic $NaBF_4$ instead of KCl to control ionic strength. Pseudo first order rate constants for the hydrolysis of triethyloxonium tetrafluoroborate were determined in aqueous buffer solutions of phosphate, acetate, tricine and carbonate covering the pH range 1.99 to 11.30. These measurements were performed at I = 1.00 M ($NaBF_4$), 25 °C, with final concentrations of 15 mM triethyloxonium tetrafluoroborate and reactions were monitored using a UV-Vis spectrophotometer. Solutions of NaOH without ionic strength control were used to access higher pH values and the faster reactions at these pHs necessitated the use of stopped flow spectrophotometry.

Representative spectra for data acquired using the UV-vis spectrophotometer for several buffer systems are shown in Fig. 5.10. Data for all buffer systems showed exponential decays in absorbance, while absolute changes in absorbance over the time scale of reaction tended to be larger at lower buffer concentrations.

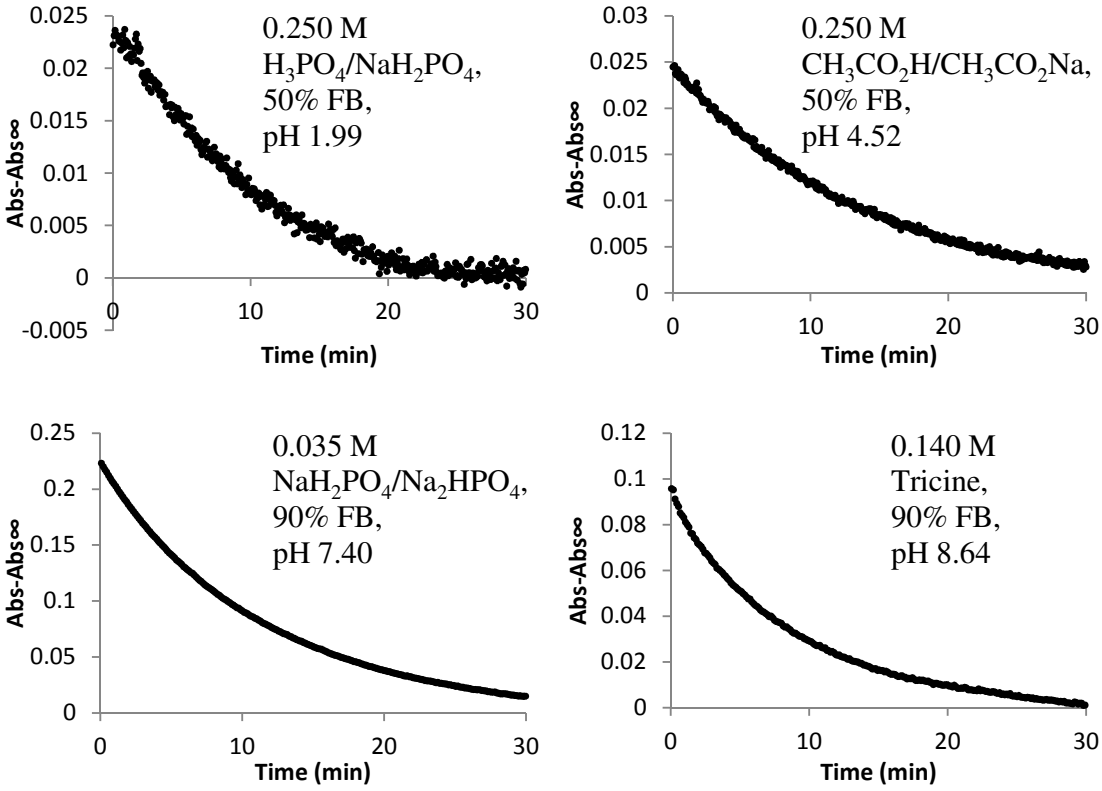

Figure 5.10 Representative raw data for the hydrolysis of triethyloxonium tetrafluoroborate (15 mM) in aqueous buffered solutions, I = 1.00 M ($NaBF_4$) at 25 °C. 2-Aminobenzoic acid (0.5 mM, λ_{max} = 328 nm), 2,4-dinitrophenol (0.18 mM, λ_{max} = 401 nm), *p*-nitrophenol (0.27 mM, λ_{max} = 398.5 nm) and 3-nitrophenol (0.84 mM, λ_{max} = 410 nm) were used as indicators at pH 1.99, 4.52, 7.40 and 8.64, respectively.

5.2.4 Stopped flow spectrophotometric studies of hydrolysis

No significant changes in absorbance were observed by UV-vis spectrophotometry at pH values ≥ 11.8 as triethyloxonium ion hydrolyses were complete before data could be acquired. To quantify hydrolysis rate constants at these pHs the procedure was adapted for

the stopped flow spectrophotometer. Solutions of final concentration 0.010-0.100 NaOH without ionic strength control were employed to access the higher pH range. In these reactions, acetonitrile composed 4% of the total reaction mixture volume based on mixing limitations of the apparatus. Buffer and indicator were loaded into a 2.5 mL drive syringe triethyloxonium tetrafluoroborate in dry acetonitrile was loaded into a 0.1 mL drive syringe. Stopped flow experiments were performed at room temperature (estimated to be ~22 °C).

The rapid mixing of solutions in the stopped flow reaction cell can result in absorbance changes that could interfere with changes due to hydrolysis. Study of mixing phenomena using the stopped flow spectrophotometer revealed significant absorbance changes at early time points upon mixing. Relatively small artifacts were observed for the first 0.2 s upon mixing water and acetonitrile, and seemed to be independent of the ratio of mixing (Fig. 5.11). Mixing 10 mM NaOH solution containing trinitrobenzene indicator (2.5 mL drive syringe) and acetonitrile (0.1 mL drive syringe), as a control in the absence of triethyloxonium ion, resulted in a large increase in absorbance that required ~0.4 s to reach a steady, fixed absorbance (Fig. 5.12). Fitting this increase in absorbance to an exponential gave a first order rate constant of 9.02 s^{-1}.

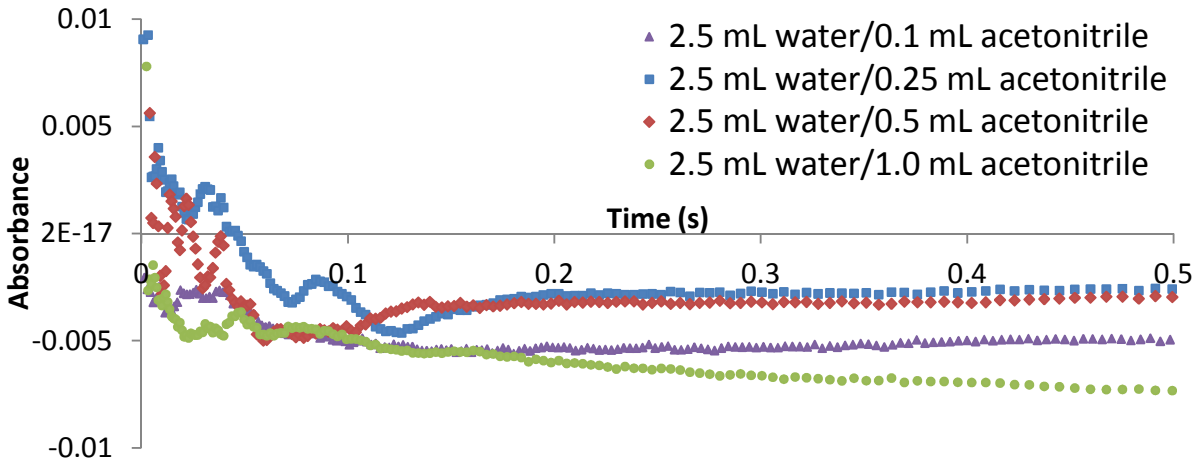

Figure 5.11 Absorbance changes at 439 nm upon mixing unbuffered water and acetonitrile.

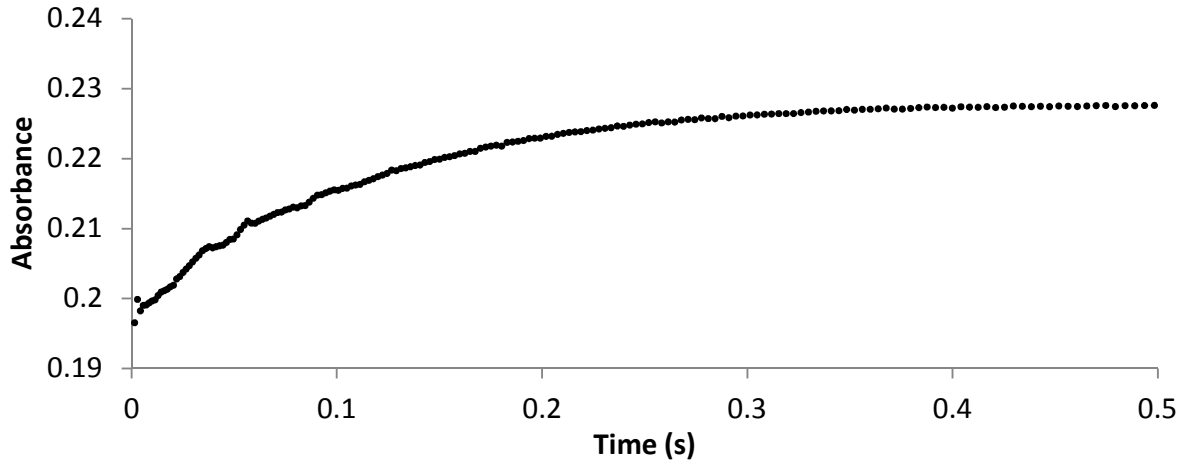

Figure 5.12 Absorbance changes at 439 nm upon mixing NaOH (10 mM) containing trinitrobenzene indicator with acetonitrile in a 25:1 ratio.

This large initial increase in absorbance prevented determination of hydrolysis rate constants as absorbance changes resulting from hydrolysis of triethyloxonium ion overlapped within this time frame. Data for experiments with 15 mM triethyloxonium ion showed only a small exponential decay phase after the initial exponential process (Fig. 5.13). Based upon the observed changes in absorbance, these exponential processes appear to be occurring with half-lives of less than 0.1 seconds. The first order rate constant for the dissociation of the trinitrobenzene-hydroxide adduct (process resulting in a decrease in absorbance, Fig 5.5) was reported to be 9.8 s^{-1}. Since the rate of change of the absorbance of trinitrobenzene indicator was likely to be rate limiting, further experiments at this pH were not attempted.

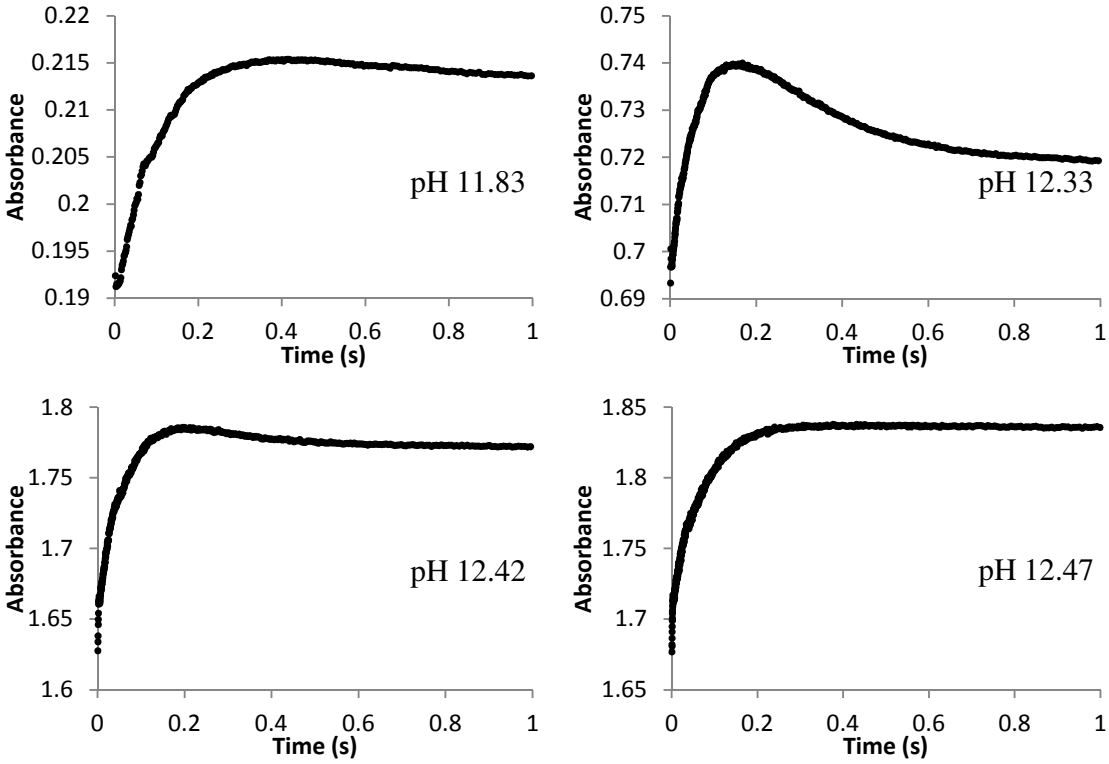

Figure 5.13 Absorbance changes at 439 nm upon addition of triethyloxonium tetrafluoroborate (15 mM) to NaOH solutions monitored using the stopped flow spectrophotometer.

Observed hydrolysis rate constants for triethyloxonium tetrafluoroborate in aqueous buffers are shown in Table 5.3 and a pH-rate profile is discussed in discussion Section 5.3.

Table 5.3 Observed rate constants for the hydrolysis of triethyloxonium tetrafluoroborate.

Buffer	pH	k_{obs} (s^{-1})	log (k_{obs})
0.1-1.0 M HCO_2H/HCO_2K 10% FB	2.57	1.56×10^{-3}	-2.81
0.1-1.0 M HCO_2H/HCO_2K 90% FB	4.67	1.46×10^{-3}	-2.84
0.05-0.5 M KH_2PO_4/K_2HPO_4 50% FB	6.67	2.55×10^{-3}	-2.59
0.035-0.35 M KH_2PO_4/K_2HPO_4 90% FB	7.72	2.71×10^{-3}	-2.57
0.025-0.25 M H_3PO_4/NaH_2PO_4 50% FB	1.99	1.29×10^{-3}	-2.89
0.025-0.25 M H_3PO_4/NaH_2PO_4 90% FB	3.01	1.32×10^{-3}	-2.88
0.025-0.25 M CH_3CO_2H/CH_3CO_2Na 50% FB	4.52	1.32×10^{-3}	-2.88
0.025-0.25 M CH_3CO_2H/CH_3CO_2Na 90% FB	5.20	1.55×10^{-3}	-2.81
0.05-0.50 M NaH_2PO_4/Na_2HPO_4 50% FB	6.61	3.37×10^{-3}	-2.47
0.035-0.35 M NaH_2PO_4/Na_2HPO_4 90% FB	7.40	5.52×10^{-3}	-2.26
0.02-0.2 M Tricine/$Tricine^-$ 90% FB	8.64	1.89×10^{-3}	-2.72
0.05-0.50 M $NaHCO_3/Na_2CO3$ 50% FB	10.30	2.57×10^{-2}	-1.59
0.035-0.35 M $NaHCO_3/Na_2CO_3$ 90% FB	11.30	2.82×10^{-2}	-1.55

5.2.5 Hydrolysis studies in 50% acetonitrile

Conventional nucleophilic substitution reactions involve an anionic nucleophile attacking a neutral electrophile. Moving from a polar protic solvent, such as water, to a less polar aprotic normally results in a rate acceleration, attributed to the desolvation of the anionic nucleophile in aprotic solvent. The effect of acetonitrile cosolvent on the hydrolysis of triethyloxonium ion is of interest as this system features a neutral nucleophile attacking a cationic electrophile. Additionally, biological molecules may be chemically coupled to synthetic compounds that result in greater solubility in cosolvent systems and many bioconjugation reactions take place in the presence of cosolvent.

The effect of co-solvent on the rate constants for hydrolysis of triethyloxonium tetrafluoroborate salt was determined in aqueous buffer solutions with 50% acetonitrile (v/v) from pH 2.60-11.17. Due to the presence of 50% acetonitrile and the potential perturbing effects upon pK_as, pH measurements are denoted as observed pHs (pH_{obs}). The buffer and indicator systems for this pH_{obs} range are shown in Table 5.4. Lower buffer concentrations and an ionic strength of I = 0.5 M ($NaBF_4$) were necessary to obtain a homogenous final reaction mixture (higher ionic strength resulted in biphasic systems). Additionally, large fluctuations in absorbance due to mixing in the stopped flow apparatus did not allow for measurements at higher pH.

Table 5.4 Buffer and indicator systems employed for studying the pH dependence of triethyloxonium tetrafluoroborate hydrolysis in 50% acetonitrile.

Buffer [a]	Initial pH_{obs}	Indicator	λ_{max} (nm)
0.0125-0.0500 M H_3PO_4/NaH_2PO_4 50% FB	2.60	0.5 mM 2-aminobenzoic acid	328
0.0125-0.0500 M H_3PO_4/NaH_2PO_4 90% FB	3.37	0.5 mM 2-aminobenzoic acid	328
0.0125-0.0500M CH_3CO_2H/CH_3CO_2Na 50% FB	5.24	0.18 mM 2,4 dinitrophenol	396
0.0125-0.0500 M CH_3CO_2H/CH_3CO_2Na 90% FB	5.48	0.18 mM 2,4 dinitrophenol	396
0.025 M NaH_2PO_4/Na_2HPO_4 50% FB	7.57	0.27 mM *p*-nitrophenol	401
0.0175 M NaH_2PO_4/Na_2HPO_4 90% FB	7.59	0.27 mM *p*-nitrophenol	401
0.025-0.100 M $NaHCO_3/Na_2CO3$ 50% FB	10.18	0.27 mM phenol	290
0.0175-0.0700 M $NaHCO_3/Na_2CO_3$ 90% FB	11.17	0.27 mM phenol	290

[a] Buffer concentrations are final concentrations after mixing with acetonitrile.

Rate constants for hydrolysis of triethyloxonium tetrafluoroborate were obtained using a UV-Vis spectrophotometer thermostated at 25°C over the pH range 2.60-11.17. Representative UV-Vis data is shown in Fig. 5.14. An exponential decay in absorbance was observed for all data obtained allowing calculation of pseudo first order rate constants by curve fitting to plots of ($Abs - Abs_\infty$) versus time. Observed hydrolysis rate constants are shown in Table 5.5 and a pH-rate profile is discussed in Section 5.3.

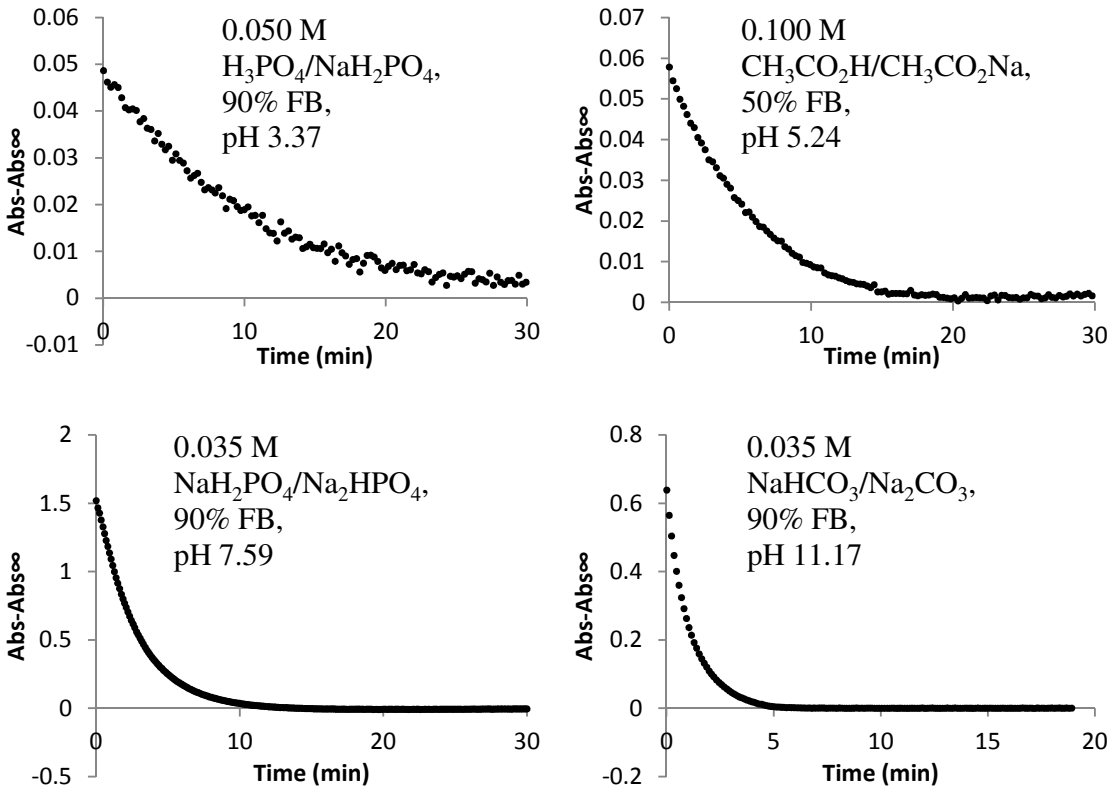

Figure 5.14 Hydrolysis of triethyloxonium tetrafluoroborate in aqueous buffered solutions, I = 0.50 M ($NaBF_4$) containing 50% acetonitrile (v/v) at 25 °C. 2-Aminobenzoic acid (0.5 mM, λ_{max} = 328 nm), 2,4-dinitrophenol (0.18 mM, λ_{max} = 401 nm), *p*-nitrophenol (0.27 mM, λ_{max} = 398.5 nm) and phenol (0.27 mM, λ_{max} = 290 nm) were used as indicators at pH 3.37, 5.24, 7.59 and 11.17, respectively.

Table 5.5 Observed rate constants for the hydrolysis of triethyloxonium tetrafluoroborate in 50% acetonitrile (v/v).

Buffer	pH	k_{obs} (s^{-1})	log (k_{obs})
0.0125-0.0500 M H_3PO_4/NaH_2PO_4 50% FB	2.60	1.02×10^{-3}	-2.99
0.0125-0.0500 M H_3PO_4/NaH_2PO_4 90% FB	3.37	1.66×10^{-3}	-2.78
0.0125-0.0500M CH_3CO_2H/CH_3CO_2Na 50% FB	5.24	3.16×10^{-3}	-2.50
0.0125-0.0500 M CH_3CO_2H/CH_3CO_2Na 90% FB	5.48	4.42×10^{-3}	-2.36
0.025 M NaH_2PO_4/Na_2HPO_4 50% FB	7.57	5.35×10^{-3}	-2.27
0.0175 M NaH_2PO_4/Na_2HPO_4 90% FB	7.59	6.06×10^{-3}	-2.22
0.025-0.100 M $NaHCO_3/Na_2CO3$ 50% FB	10.18	1.75×10^{-2}	-1.76
0.0175-0.0700 M $NaHCO_3/Na_2CO_3$ 90% FB	11.17	2.15×10^{-2}	-1.67

5.3 Discussion

5.3.1 Hydrolysis of triethyloxonium tetrafluoroborate

Raw data of changes in absorbance (due to the processes shown in Fig. 5.5) versus time showed good fits to an exponential decays and could be extrapolated to obtain values for Abs_∞, the final absorbance at complete hydrolysis of triethyloxonium. A non-linear, least squares plot of (Abs – Abs_∞) versus time yielded values of k_{obs} (s^{-1}). The pseudo first order rate constant k_{obs} was assumed to be the sum of the components in eq. 1.

$$k_{obs} = k_{H20} + k_{OH}[HO^-] + k_B[B] \qquad (1)$$

Where k_{H2O} is the first order rate constant for attack by water, k_{OH} is the second-order rate constant for attack by hydroxide ion and k_B is the second-order rate constant for reaction with general base species.

Fig 5.15 shows the pH-rate profile of the hydrolysis of triethyloxonium tetrafluoroborate in buffered aqueous solutions containing 1% acetonitrile at 25 °C. There appears to be a pH independent region from pH 2 to 10 with pseudo first order rate constants ranging from 1.29 to 5.52 × 10^{-3} s^{-1}. Above pH 10 a pH dependent region is observed, however, rate constants were not quantified due to the limitations of the indicator system.

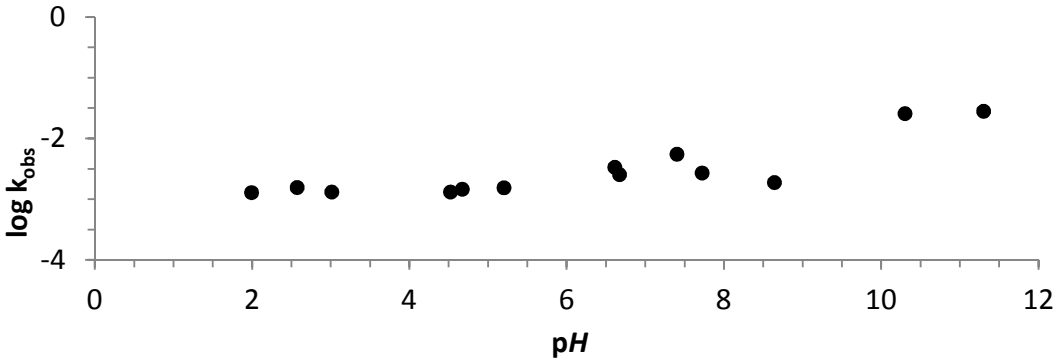

Figure 5.15 pH-rate profile for the hydrolysis of triethyloxonium tetrafluoroborate in buffered aqueous solutions containing 1% acetonitrile at 25 °C.

Table 5.6 lists rate constants of hydrolysis and reaction with hydroxide ion for several electrophiles that may be compared with triethyloxonium ion. Similar to triethyloxonium salts, some of the alkyl halides are employed as electrophilic alkylating agents in reactions such as Friedel-Crafts alkylation. The reported rate constants of hydrolysis for methyl chloride, bromide and iodide are slightly smaller (at a higher temperature) than for triethyloxonium ion. The larger rate constants for triethyloxonium ion may be the result of greater electrostatic contribution to the electrophilicity arising from the positively charged oxygen atom. The pK_a of the triethyloxonium leaving group, diethyl ether, is -3.5[22] and can be compared with other simple alkyl electrophiles with good leaving groups such as mesylate, tosylate and nitrate, although levelling to the pK_a of H_3O^+ (-1.74) will occur in aqueous solution. Rate constants for the hydrolyses of these electrophiles are 1–2 orders of magnitude lower relative to triethyloxonium ion and may also be attributed to the positively charged oxygen of the oxonium species. Rate constants for the reaction of hydroxide ion with triethyloxonium tetrafluoroborate could be predicted to be ~6.8×10^{-1}, assuming a 200-fold increase similar to the relative rate constants for reaction of hydroxide and water for the methyl halides, however, the true value maybe substantially different due to cationic nature of triethyloxonium.

Table 5.6 Rate constants for reaction of a range of electrophiles with water or hydroxide.[23,24]

Electrophile	Nucleophile	Temperature (K)	Rate constant[a]	Leaving group pK_a [b]
Et_3O^+	water	298	1.29 to 5.52 × 10^{-3} [c]	
CH_3Br	water	373.16	1.71 × 10^{-3} [d]	-9.0
	hydroxide	373.16	3.52 × 10^{-1} [d]	
CH_3Cl	water	373.16	1.49 × 10^{-4} [d]	-7.0
	hydroxide	373.16	2.42 × 10^{-2} [d]	
CH_3I	water	373.16	5.44 × 10^{-4} [d]	-10.0
	hydroxide	373.16	1.24 × 10^{-1} [d]	
CH_3F	water	373.16	4.35 × 10^{-6} [d]	3.0
	hydroxide	373.16	8.98 × 10^{-4} [d]	
CH_3NO_3	water	373.16	2.98 × 10^{-5} [d]	-1.6
CH_3OTs	water	298.00	1.39 × 10^{-4} [d]	-2.8
Pr^iOMs	water	298.00	2.0 × 10^{-4} [d]	-1.9

[a] Units of s^{-1} for water, M^{-1} s^{-1} for hydroxide. [b] Taken from [25]. [c] This work. [d] Taken from [23,24].

5.3.2 Hydrolysis of triethyloxonium tetrafluoroborate in 50% acetonitrile

The pH-rate profile for the hydrolysis of triethyloxonium in 50% acetonitrile is shown in Fig. 5.16. Hydrolysis appears to be pH independent between pH 2 to 8 with rate constants ranging from 1.02 to 6.06 × 10^{-3} s^{-1}. The k_{obs} increases to 1.75 × 10^{-2} at pH 10, however, more measurements at higher pH would be required to assess this potentially pH dependent region.

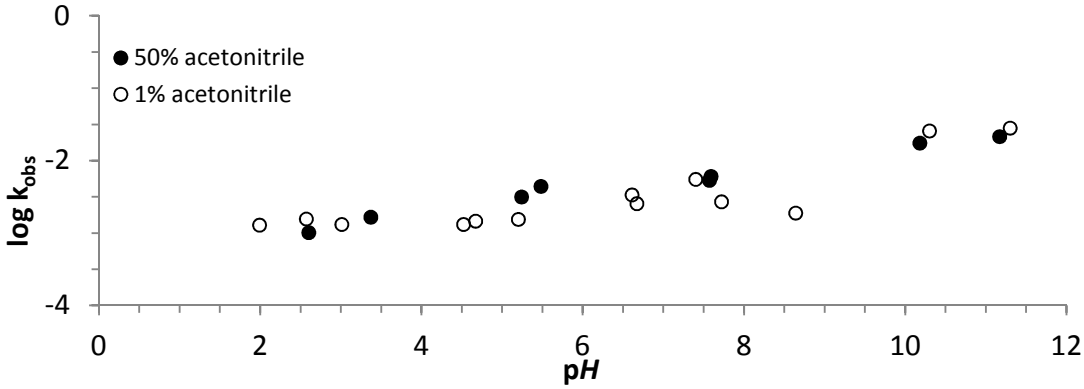

Figure 5.16 (●) pH-rate profile for the hydrolysis of triethyloxonium tetrafluoroborate in buffered aqueous solutions containing 50% acetonitrile (v/v) at 25 °C. (○) Overlay of data from Fig 5.13 for the hydrolysis in buffered aqueous solutions containing 1% acetonitrile (v/v).

Despite the change in solvent system, rate constants of hydrolysis of triethyloxonium in 50% acetonitrile are closely identical to those in aqueous buffer. Several of the physical properties of water and acetonitrile are shown in Table 5.7. Water possesses a larger dielectric constant than acetonitrile suggesting a greater capacity to stabilise charged species. This is reflected in the larger values for both the donor and acceptor number of water, however, notably, the donor number for water is only slightly larger than for acetonitrile while the acceptor number is substantially greater. The implication of these properties is that although water will stabilise ions to a greater extent than acetonitrile the degree of stabilisation will be larger for anions than for cations.

Table 5.7 Solvent properties of water and acetonitrile.[26,27]

Solvent	Dielectric constant ε_r	Polarisation /cm^3	Donor number[a]	Acceptor number[b]
H_2O	78.5	17.3	18	54.8
CH_3CN	37.5	48.4	14.1	18.9

[a] A measurement of electron donation or Lewis basicity, defined as the negative enthalpy of adduct formation between solvent molecule and antimony pentachloride in a solution diluted in dichloromethane (a non-coordinating solvent). [b] A measurement of electrophilicity and derived from the ^{31}P-NMR chemical shift of Et_3PO when dissolved in the solvent. The shift is scaled from 0 (hexane) to 100 (Et_3PO – $SbCl_5$ complex in 1,2-dichloroethane).

Conventional nucleophilic substitution reactions generally feature an anionic nucleophile attacking a neutral or positively charged electrophile. The anionic nucleophile (and anionic transition state, but to a lesser extent) is more solvated in polar protic solvents, such as water, than dipolar aprotic solvents, such as acetonitrile. As a result, the effect of moving from water to acetonitrile is a lower energy of activation and a subsequent rate enhancement.

A similar effect would be expected for the hydrolysis of triethyloxonium ion (Fig. 5.17), however, this system instead features a neutral nucleophile attacking a positively charged electrophile. Triethyloxonium will be more solvated in water, as compared to 50% acetonitrile resulting in a lower ground state. The cationic intermediate will also be more stable in water but as mentioned earlier the degree of stabilisation will be smaller as the charge is dispersed over a greater number of atoms. Changing the solvent from water to 50% acetonitrile should decrease the energy of activation and accelerate the rate of hydrolysis. However, our results do not show a significant difference in the rate constants of hydrolysis of triethyloxonium in water as compared to those in 50% acetonitrile. A

possible explanation is that the differences in the reactant ground state energies between the water and 50% acetonitrile systems in this reaction are not likely to be as large as for those featuring anionic reactants since the donor numbers of water and acetonitrile differ by a lesser degree than the acceptor numbers (difference in cation solvation < difference in anion solvation). Additionally, the concentration of water is 2-fold lower in 50% acetonitrile, which should decrease the rate constant by 2-fold.

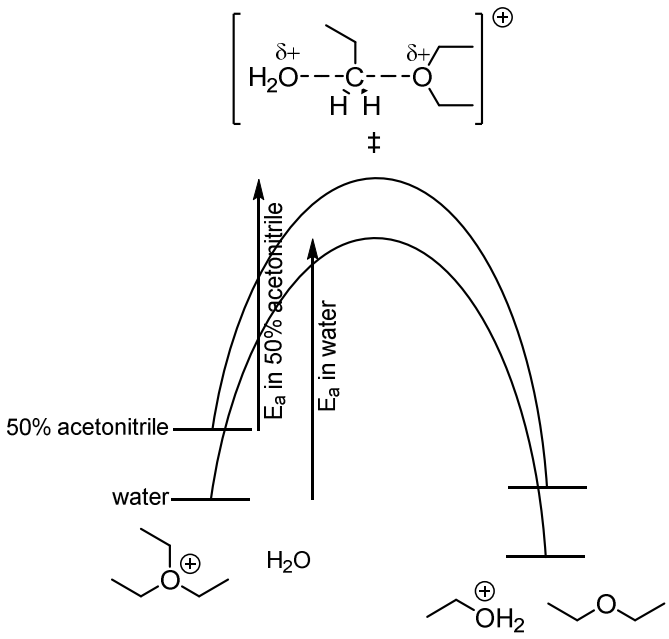

Figure 5.17 Possible reaction coordinates for the hydrolysis of triethyloxonium ion in water and in 50% acetonitrile.

As mentioned briefly in the introduction section of this chapter, one of the potential applications of Meerwein salts is the alkylation of biological molecules, however, this would require reaction in aqueous media under physiological conditions (pH 7.0, 25 °C). One of the motivations behind this work has been to assess the suitability of triethyloxonium tetrafluoroborate as an alkylating agent in a project studying carbon dioxide sensing in proteins. Residues such as lysine have been proposed to react reversibly

with carbon dioxide to form carbamate anions as shown in Fig. 5.18. In order to study this phenomenon, reaction with Meerwein's reagent was proposed as a method to trap residues reacting with carbon dioxide by conversion of the carbamate to an O-ethylated analogue. The main concerns of this reaction protocol were the rate of hydrolysis of triethyloxonium in aqueous buffer and its reactivity towards carbamic acid.

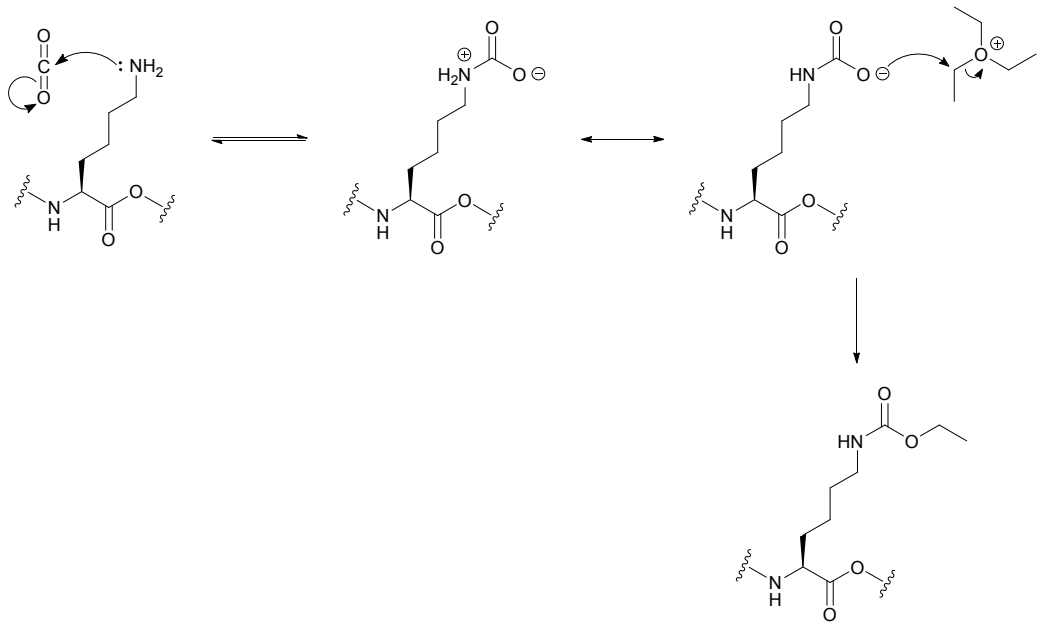

Figure 5.18 Reversible carbamate formation by attack of a lysine residue side chain on carbon dioxide followed by trapping by ethylation.

Our results show that at pH 7.0 and 25 °C, triethyloxonium tetrafluoroborate should have a half life of 133 seconds in aqueous media. For reaction with carbamate versus water, the alkylation of carbamate would be predicted to possess a larger rate constant as the pK_a of carbamic acid is higher than that of hydronium (7.93 for the lysine side chain carbamate[25] vs -1.7). Reaction of triethyloxonium ion with hydroxide ion would be predicted to be faster than carbamate as the hydroxide ion possesses a greater negative charge density, is less sterically hindered than a protein residue and water has a pK_a of 15.5. However, from our data, the hydroxide dependent hydrolysis of triethyloxonium tetrafluoroborate only

occurs at pHs > 10, far above physiological pH. Another consideration is the presence of other nucleophilic residues on the protein. The pK_as of the C-terminal, and the aspartate and glutamate side chains are 2.3, 3.90 and 4.07, respectively, suggesting the carbamate could have a higher nucleophilicity.

5.4 Summary

The rate constants of the hydrolysis of triethyloxonium tetrafluoroborate were determined spectrophotometrically in water and in 50% acetonitrile. Our results show that for reactions in water there is a pH independent region between pH 2 and 10 with a rate constant of hydrolysis. A pH dependent region was observed above pH 10, however, the experimental limitations of the indicator system did not allow for determination of the large second order rate constants for reaction with hydroxide ion. The observed rate constant for pH-independent hydrolysis, kobs = 3×10^{-3} s^{-1}, is higher than for a range of neutral alkyl substrates. The greater electrophilicity of triethyloxonium relative to the methyl halides has been attributed to the positively charged oxygen which may have a larger electrostatic, attractive effect toward hard nucleophiles such as hydroxide and carbamate ions.

Surprisingly, hydrolysis experiments performed in 50% acetonitrile were found to possess similar rate constants to those in water. Although nucleophilic substitution reactions are typically found to have larger rate constants in dipolar aprotic solvents compared to polar protic, this reaction features a neutral nucleophile and a positively charged electrophile as opposed to the normally anionic species. Notably, while anionic species are solvated far more in water than in acetonitrile the ability of these solvents to stabilise cations is relatively similar.

For the application of Meerwein's reagents in the alkylation of proteins, triethyloxonium tetrafluoroborate could potentially be used in the study of carbon dioxide sensing through the trapping of transient carbamate species. Our results show that triethyloxonium tetrafluoroborate possesses an appreciable life time in aqueous solution at pH 7.0. Furthermore rate constants of alkylation of carbamic acid will likely be larger than the rate constant of hydrolysis. Thus there is significant potential for alkylation to out compete hydrolysis. Additionally the pH dependent region for the hydrolysis of triethyloxonium tetrafluoroborate was only observed above pH 10, far removed from physiological pH.

5.5 Experimental

5.5.1 Materials

Triethyloxonium tetrafluoroborate (90520), 2,4-dinitrophenol (34334), *p*-nitrophenol (35836), 2-aminobenzoic acid (10680), 3-nitrophenol (1.06794), phenol (P5566) and 1,3,5-trinitrobenzene (442237) were purchased from Sigma-Aldrich.

5.5.2 Methods

5.5.2.1 Reaction mixture preparation

Stock solutions of triethyloxonium tetrafluoroborate were prepared immediately before use in dry acetonitrile solution and stored at 0 °C. For UV-Vis spectrophotometer experiments buffer solutions were prepared in cuvettes by mixing stock solutions of buffer and indicator and allowed to equilibrate to 25 °C in the cell holder. Hydrolysis of triethyloxonium was initiated by addition of stock solutions of triethyloxonium tetrafluoroborate to equilibrated buffer-indicator solutions. The volume of this stock solution was equivalent to 1 % of the final total reaction mixture volume. Reactions were followed for at least six half-lives and performed in triplicate at four different buffer concentrations to assess for buffer catalysis. Hydrolysis rate constants were calculated from the changes in absorbance. For experiments using the stopped flow spectrophotometer, reaction was initiated by injection of NaOH solution containing trinitrobenzene indicator (2.5 mL reservoir syringe) and triethyloxonium-acetonitrile solution (0.2 mL reservoir syringe) into the stopped flow reaction cell giving a final reaction mixture containing 4% acetonitrile.

5.5.2.2 Absorbance measurements

Absorbance measurements were obtained using a Cary 100 UV-visible spectrophotometer and Applied Photophysics SX-17MV stopped flow apparatus. For measurements on the Cary 100, a Peltier heating/refrigeration unit were employed to maintain a constant

temperature of 25 °C and measurements were taken in 1 ml quartz cuvettes with a 1 cm path length. The λ_{max} of each indicator and buffer system was determined in the absence of triethyloxonium from spectra acquired from the Scan program. The Kinetics program was used to monitor changes at this λ_{max} after addition of triethyloxonium tetrafluoroborate solution. KaleidaGraph software was used to fit processed data (Abs-Abs_{∞}) and acquire rate constants.

5.5.2.3 pH measurements

Measurements of pH of aqueous buffers and pH_{obs} of buffers in 50% acetonitrile were determined at 25 °C using a MeterLab^{TM} PHM 290 pH-Stat Controller equipped with a radiometer combination electrode filled with saturated KCl solution. Calibration was performed with calibration buffers pH 4, pH 7 and pH 10.0, and saturated calcium hydroxide solution (pH 12.45).

5.6 References

[1] H. Meerwein, G. Hinz, P. Hofmann, E. Kroning and E. Pfeil, *J. Prakt.* Chem., 1937, **147**, 257-285
[2] H. Meerwein, E. Battendurg, H. Gold, E. Pfeil and G. Willfang, *J. Prakt.* Chem., 1939, **154**, 83-156
[3] O. Reutov, L. Makarova and T. Tolstaya, *Zh. Org. Khim.*, 1969, **5**, 1521
[4] H. Meerwein, K. Bodembrenner, P. Borner, F. Kunert and K. Winderlich, *Ann. Chem.*, 1960, **632**, 38
[5] V. Granik, B. Pyatin and R. Glushkov, *Russ. C*H*em. Rev.*, 1971, **40**, 747
[6] W. Mock and M. Hartman, *J. Org. Chem.*, 1977, **42**, 459
[7] Z. Parnes, N. Baranetskaya and D. Kursanov, *Russ. Chem. Bull.*, 1962, 11, 2138
[8] D. Raber, P. Gariano, A. Brod and A Gariano, *J. Org. Chem.*, 1979, **44**, 1149
[9] G. Lamoureux and C. Agüero, *Arkivoc*, 2009, **I**, 251
[10] T. Hamada and O. Yonemitsu, *Chem. Pharm. Bull.*, 1971, **19**, 1444
[11] D. Kevill and G. Lin, *Tet. Lett.*, 1978, **11**, 949
[12] D. Kevill and G. Lin, *J. Am. Chem. Soc.*, 1979, **101**, 3916
[13] G. King, C. Gazzola, R. Blakeley and B. Zerner, *Inorg. Chem.*, 1986, **25**, 1078
[14] D. Kevill and B. Shen, *Chem. Ind. (London)*, 1971, 1466
[15] A. Streitwieser, C. Wilkins and E. Kiehlmann, *J. Am. Chem. Soc.*, 1968, **90**, 1598
[16] G. Dafforn and A. Streitwieser, *Tet. Lett.*, 1970, 3159
[17] D. N. Kevill, H. R. Adolf, A. Wang, D. C. Hawkinson and M. J. D. Souza, *J. Chem. Soc. Perkin Trans. II*, 1990, 2023–2028.
[18] D. N. Kevill, M. S. Bahari and S. W. Anderson, *J. Am. Chem. Soc.*, 1984, **106**, 2895-2901
[19] R. J. Delley, A. C. O'Donoghue and D. R. W. Hodgson, *J. Org. Chem.*, 2012, **77**, 5829
[20] R. Khalifah, *J. Bio. Chem.*, 1971, **8**, 2561-2573.
[21] C. Bernasconi, *J. Am. Chem. Soc.*, 1970, **92**, 4682
[22] E. P. Serjeant and B. Dempsey (eds.), 1979, *Ionization Constants of Organic Acids in Solution*, IUPAC Chemical Data Series No. 23, Pergamon Press, Oxford, UK,.
[23] I. Fells and E. A. Moelwyn-Hughes, *J. Chem. Soc.*, 1959, 398–409.
[24] W. Bentley, S. Jurczyk, K. Roberts and D. J. Williams, *J. Chem. Soc. Perkin Trans. II*, 1987, 293–299.
[25] W. P Jencks and Regenstein, Physical and Chemical Data, in Handbook of Biochemistry and Molecular Biology, Vol. 1, 3rd Edition (ed. G. Fassman), Chemical Rubber Company Cleveland, 1976
[26] C. Reichardt, Solvents and Solvent Effects in Organic Chemistry, 3rd Edn., Wiley-VCH, 2004
[27] Y. Marcus, *Chem. Soc. Rev.*, 1993, **22**, 409

Acknowledgements

I would first like to thank my academic supervisor, AnnMarie O'Donoghue, for her guidance throughout my PhD studies. She has been a patient supervisor, contributing invaluable knowledge and enthusiasm towards the project. I would also like to thank Neil Lant and Nazar Momin for their ideas and supervision.

Thank you to all the academic and technical staff who have facilitated the use of the analytic services and biological suite.

Special thanks to the members of the O'Donoghue group, particularly fellow PhD students Richard Massey, Casey Lam, Oliver Maguire, David Tucker, Peter Quinn, Kevin Maduka and Jiayun Zhu who have been great to work with and have provided helpful conversation.

I would like to thank my family for their constant support during my time at university and finally I would like to thank my partner, Anais Ghazali, for her love and encouragement.

Appendices

Appendix A

Table A1 Initial rates of oxidation of linoleic acid in the presence of surfactant **53** (Tween 80).

pH[b]	Initial Rates (υ, μM min^{-1})[a]			
	υ1	υ2	υ3	υ_{av} ± SD[c]
4.00	7.11 x 10^{-2}	8.00 x 10^{-2}	8.44 x 10^{-2}	(7.85 ± 0.68) x 10^{-2}
6.50	1.87 x 10^{-1}	1.78 x 10^{-1}	1.87 x 10^{-1}	(1.84 ± 0.051) x 10^{-1}
7.00	1.47 x 10^{-1}	1.47 x 10^{-1}	2.18 x 10^{-1}	(1.70 ± 0.41) x 10^{-1}
7.50	1.24 x 10^{-1}	1.11 x 10^{-1}	1.11 x 10^{-1}	(1.16 ± 0.077) x 10^{-1}
8.00	1.38 x 10^{-1}	1.33 x 10^{-1}	1.38 x 10^{-1}	(1.36 ± 0.026) x 10^{-1}
8.50	8.89 x 10^{-2}	1.02 x 10^{-1}	7.11 x 10^{-2}	(8.74 ± 1.6) x 10^{-2}
9.00	1.60 x 10^{-1}	1.24 x 10^{-1}	1.11 x 10^{-1}	(1.32 ± 0.25) x 10^{-1}

[a] Reaction mixtures were maintained at 30 °C and contained linoleic acid **10** (500 μM) and surfactant **53** (Tween 80) (200 μg ml^{-1}). [b] Acetate, phosphate or borate buffer (50 mM) were used to maintain pH 4.00, 6.50-8.00 and 8.50-9.00, respectively. [c] Standard deviation (SD) was calculated using the following formula: $SD = \sqrt{\frac{\sum(x-\mu)^2}{(n-1)}}$ where μ is the mean and n is the number of samples.

Table A2 Initial rates of oxidation of linoleic acid in the presence of surfactant **54** (AE7).

pH[b]	Initial Rates (υ, μM min^{-1})[a]			
	υ1	υ2	υ3	υ_{av} ± SD[c]
6.50	8.44 x 10^{-2}	9.78 x 10^{-2}	1.02 x 10^{-1}	(9.48 ± 0.93) x 10^{-2}
7.00	8.44 x 10^{-2}	9.33 x 10^{-2}	9.33 x 10^{-2}	(9.04 ± 0.51) x 10^{-2}
7.50	7.11 x 10^{-2}	7.11 x 10^{-2}	8.44 x 10^{-2}	(7.56 ± 0.77) x 10^{-2}
8.00	7.56 x 10^{-2}	1.11 x 10^{-1}	6.22 x 10^{-2}	(8.30 ± 2.5) x 10^{-2}
8.50	3.69 x 10^{-2}	3.24 x 10^{-2}	2.98 x 10^{-2}	(3.30 ± 0.36) x 10^{-2}
9.00	5.33 x 10^{-2}	6.67 x 10^{-2}	5.78 x 10^{-2}	(5.93 ± 0.68) x 10^{-2}

[a] Reaction mixtures were maintained at 30 °C and contained linoleic acid **10** (500 μM) and surfactant **54** (AE7) (200 μg ml^{-1}). [b] Acetate, phosphate or borate buffer (50 mM) were used to maintain pH 4.00, 6.50-8.00 and 8.50-9.00, respectively. [c] Standard deviation (SD) was calculated using the following formula: $SD = \sqrt{\frac{\sum(x-\mu)^2}{(n-1)}}$ where μ is the mean and n is the number of samples.

Table A3 Initial rates of oxidation of linoleic acid in the presence of surfactant **52** (Tween 20).

pH[b]	Initial Rates (υ, μM min^{-1})[a]			
	υ1	υ2	υ3	υ_{av} ± SD[c]
4.00	2.96 x 10^{-1}	2.90 x 10^{-1}	2.86 x 10^{-1}	(2.91 ± 0.051) x 10^{-1}
6.50	2.76 x 10^{-1}	2.20 x 10^{-1}	2.24 x 10^{-1}	(2.40 ± 0.31) x 10^{-1}
7.00	1.41 x 10^{-1}	1.32 x 10^{-1}	1.38 x 10^{-1}	(1.37 ± 0.049) x 10^{-1}
7.50	1.49 x 10^{-1}	1.53 x 10^{-1}	1.43 x 10^{-1}	(1.49 ± 0.052) x 10^{-1}
8.00	9.64 x 10^{-2}	9.51 x 10^{-2}	9.60 x 10^{-2}	(9.59 ± 0.070) x 10^{-2}
8.50	7.16 x 10^{-2}	7.20 x 10^{-2}	6.84 x 10^{-2}	(7.07 ± 0.19) x 10^{-2}
9.00	3.52 x 10^{-2}	3.47 x 10^{-2}	3.78 x 10^{-2}	(3.59 ± 0.17) x 10^{-2}

[a] Reaction mixtures were maintained at 30 °C and contained linoleic acid **10** (500 μM) and surfactant **52** (Tween 20) (200 μg ml^{-1}). [b] Acetate, phosphate or borate buffer (50 mM) were used to maintain pH 4.00, 6.50-8.00 and 8.50-9.00, respectively. [c] Standard deviation (SD) was calculated using the following formula: $SD = \sqrt{\frac{\sum(x-\mu)^2}{(n-1)}}$ where μ is the mean and n is the number of samples.

Table A4 Initial rates of oxidation of linoleic acid in the presence of surfactant **55** (AE1S).

pH[b]	Initial Rates (υ, μM min^{-1})[a]			
	υ1	υ2	υ3	υ_{av} ± SD[c]
4.00	3.18 x 10^{-1}	3.12 x 10^{-1}	3.67 x 10^{-1}	(3.33 ± 0.30) x 10^{-1}
6.50	2.08 x 10^{-1}	2.30 x 10^{-1}	2.12 x 10^{-1}	(2.17 ± 0.12) x 10^{-1}
7.00	1.36 x 10^{-1}	1.48 x 10^{-1}	1.48 x 10^{-1}	(1.44 ± 0.064) x 10^{-1}
7.50	1.98 x 10^{-1}	1.96 x 10^{-1}	1.78 x 10^{-1}	(1.91 ± 0.11) x 10^{-1}
8.00	1.01 x 10^{-1}	1.08 x 10^{-1}	1.03 x 10^{-1}	(1.04 ± 0.036) x 10^{-1}
8.50	1.29 x 10^{-1}	1.19 x 10^{-1}	1.12 x 10^{-1}	(1.20 ± 0.087) x 10^{-1}
9.00	1.50 x 10^{-2}	1.83 x 10^{-2}	1.73 x 10^{-2}	(1.70 ± 0.17) x 10^{-2}

[a] Reaction mixtures were maintained at 30 °C and contained linoleic acid **10** (500 μM) and surfactant **55** (AE1S) (200 μg ml^{-1}). [b] Acetate, phosphate or borate buffer (50 mM) were used to maintain pH 4.00, 6.50-8.00 and 8.50-9.00, respectively. [c] Standard deviation (SD) was calculated using the following formula: $SD = \sqrt{\frac{\sum(x-\mu)^2}{(n-1)}}$ where μ is the mean and n is the number of samples.

Table A5 Initial rates of oxidative of β-carotene **1** degradation (bleaching) with **53** (Tween 80) as surfactant.

pH[b]	Initial Rates (υ, μM min^{-1})[a]			
	υ1	υ2	υ3	υ_{av} ± SD[c]
4.00	7.70 x 10^{-4}	1.54 x 10^{-3}	1.54 x 10^{-3}	(1.28) ± 0.44) x 10^{-3}
6.50	1.54 x 10^{-3}	1.54 x 10^{-3}	6.90 x 10^{-4}	(1.26 ± 0.49) x 10^{-3}
9.00	7.70 x 10^{-4}	6.20 x 10^{-4}	7.70 x 10^{-4}	(7.20 ± 0.90) x 10^{-4}

[a] Reaction mixtures were maintained at 30 °C and contained β-carotene **1** (3.1 μM) and surfactant **53** (Tween 80) (167 μg ml^{-1}). [b] Acetate, phosphate or borate buffer (50 mM) were used to maintain pH 4.00, 6.50 and 9.00, respectively. [c] Standard deviation (SD) was calculated using the following formula: $SD = \sqrt{\frac{\sum(x-\mu)^2}{(n-1)}}$ where μ is the mean and n is the number of samples.

Table 2.6 Initial rates of oxidative of β-carotene **1** degradation (bleaching) with **54** (AE7) as surfactant.

pH[b]	Initial Rates (υ, μM min^{-1})[a]			
	υ1	υ2	υ3	υ_{av} ± SD[c]
4.00	1.54 x 10^{-3}	2.31 x 10^{-3}	1.54 x 10^{-3}	(1.79 ± 0.44) x 10^{-3}
6.50	1.54 x 10^{-3}	6.20 x 10^{-4}	7.70 x 10^{-4}	(0.97 ± 0.49) x 10^{-4}
9.00	2.31 x 10^{-3}	1.54 x 10^{-3}	7.70 x 10^{-4}	(1.54 ± 0.77) x 10^{-3}

[a] Reaction mixtures were maintained at 30 °C and contained β-carotene **1** (3.1 μM) and surfactant **54** (AE7) (167 μg ml^{-1}). [b] Acetate, phosphate or borate buffer (50 mM) were used to maintain pH 4.00, 6.50 and 9.00, respectively. [c] Standard deviation (SD) was calculated using the following formula: $SD = \sqrt{\frac{\sum(x-\mu)^2}{(n-1)}}$ where μ is the mean and n is the number of samples.

Table A7 Initial rates of oxidative degradation (bleaching) of β-carotene **1** in the presence of linoleic acid **10** with surfactant **53** (Tween 80).

pH[b]	Initial Rates (υ, μM min^{-1})[a]			
	υ1	υ2	υ3	υ_{av} ± SD[c]
4.00	4.60 x 10^{-3}	3.10 x 10^{-3}	4.60 x 10^{-3}	(4.10 ± 0.90) x 10^{-3}
6.50	5.08 x 10^{-2}	4.77 x 10^{-2}	6.23 x 10^{-2}	(5.36 ± 0.77) x 10^{-2}
7.00	1.03 x 10^{-1}	9.92 x 10^{-2}	1.01 x 10^{-1}	(1.01 ± 0.019) x 10^{-1}
7.50	7.46 x 10^{-2}	8.38 x 10^{-2}	7.62 x 10^{-2}	(7.82 ± 0.49) x 10^{-2}
8.00	3.62 x 10^{-2}	3.15 x 10^{-2}	3.31 x 10^{-2}	(3.36 ± 0.24) x 10^{-2}
8.50	1.77 x 10^{-2}	2.00 x 10^{-2}	2.31 x 10^{-2}	(2.03 ± 0.27) x 10^{-2}
9.00	2.38 x 10^{-2}	1.92 x 10^{-2}	2.77 x 10^{-2}	(2.36 ± 0.42) x 10^{-2}

[a] Reaction mixtures were maintained at 30 °C and contained β-carotene **1** (3.1 μM), linoleic acid **10** (500 μM), **53** (Tween 80) (367 μg ml^{-1}). [b] Acetate, phosphate or borate buffer (50 mM) were used to maintain pH 4.00, 6.50-8.00 and 8.50-9.00, respectively. [c] Standard deviation (SD) was calculated using the following formula: $SD = \sqrt{\frac{\sum(x-\mu)^2}{(n-1)}}$ where μ is the mean and n is the number of samples.

Table A8 Initial rates of oxidative degradation (bleaching) of β-carotene **1** in the presence of linoleic acid **10** with surfactant **54** (AE7).

pH[b]	Initial Rates (υ, μM min^{-1})[a]			
	υ1	υ2	υ3	υ_{av} ± SD[c]
4.00	5.40 x 10^{-3}	5.40 x 10^{-3}	5.40 x 10^{-3}	(5.40 ± 0.00) x 10^{-3}
6.50	5.54 x 10^{-2}	3.54 x 10^{-2}	2.85 x 10^{-2}	(3.97 ± 1.4) x 10^{-2}
7.00	6.00 x 10^{-2}	6.46 x 10^{-2}	5.62 x 10^{-2}	(6.03 ± 0.42) x 10^{-2}
7.50	4.00 x 10^{-2}	3.69 x 10^{-2}	4.23 x 10^{-2}	(3.97 ± 0.27) x 10^{-2}
8.00	2.31 x 10^{-2}	3.00 x 10^{-2}	3.38 x 10^{-2}	(2.90 ± 0.55) x 10^{-2}
8.50	1.31 x 10^{-2}	1.00 x 10^{-2}	1.00 x 10^{-2}	(1.10 ± 0.18) x 10^{-2}
9.00	3.38 x 10^{-2}	2.23 x 10^{-2}	2.46 x 10^{-2}	(2.69 ± 0.61) x 10^{-2}

[a] Reaction mixtures were maintained at 30 °C and contained β-carotene **1** (3.1 μM), linoleic acid **10** (500 μM), **54** (AE7) (367 μg ml^{-1}). [b] Acetate, phosphate or borate buffer (50 mM) were used to maintain pH 4.00, 6.50-8.00 and 8.50-9.00, respectively. [c] Standard deviation (SD) was calculated using the following formula: $SD = \sqrt{\frac{\sum(x-\mu)^2}{(n-1)}}$ where μ is the mean and n is the number of samples.

Table A9 Initial rates of oxidative degradation (bleaching) of β-carotene **1** in the presence of fatty acid with surfactant **54** (AE7).

Fatty Acid	Concentration (μM)	Initial Rates (υ, μM min^{-1})[a]		
		υ1	υ2	υ_{av} ± SD[b]
Stearic	10	3.80×10^{-3}	4.60×10^{-3}	$(4.20 \pm 0.50) \times 10^{-3}$
	50	1.08×10^{-2}	1.00×10^{-2}	$(1.04 \pm 0.050) \times 10^{-2}$
	100	1.38×10^{-2}	1.38×10^{-2}	$(1.38 \pm 0.00) \times 10^{-2}$
	500	6.20×10^{-3}	5.40×10^{-3}	$(5.80 \pm 0.50) \times 10^{-3}$
Oleic	10	3.10×10^{-3}	3.10×10^{-3}	$(3.10 \pm 0.00) \times 10^{-3}$
	50	1.15×10^{-2}	1.23×10^{-2}	$(1.19 \pm 0.050) \times 10^{-2}$
	100	1.92×10^{-2}	2.00×10^{-2}	$(1.96 \pm 0.050) \times 10^{-2}$
	500	3.31×10^{-2}	3.62×10^{-2}	$(3.46 \pm 0.22) \times 10^{-2}$
Linoleic	10	4.60×10^{-3}	3.10×10^{-3}	$(3.80 \pm 1.1) \times 10^{-3}$
	50	1.23×10^{-2}	1.31×10^{-2}	$(1.27 \pm 0.050) \times 10^{-2}$
	100	2.92×10^{-2}	2.92×10^{-2}	$(2.92 \pm 0.00) \times 10^{-2}$
	500	5.54×10^{-2}	6.08×10^{-2}	$(5.81 \pm 0.38) \times 10^{-2}$
Linolenic	10	4.60×10^{-3}	3.80×10^{-3}	$(4.20 \pm 0.50) \times 10^{-3}$
	50	1.15×10^{-2}	1.54×10^{-2}	$(1.35 \pm 0.27) \times 10^{-2}$
	100	1.23×10^{-2}	1.38×10^{-2}	$(1.31 \pm 0.11) \times 10^{-2}$
	500	1.38×10^{-2}	1.62×10^{-2}	$(1.50 \pm 0.16) \times 10^{-2}$
Arachidonic	10	3.80×10^{-3}	3.80×10^{-3}	$(3.80 \pm 0.00) \times 10^{-3}$
	50	7.70×10^{-3}	6.90×10^{-3}	$(7.30 \pm 0.50) \times 10^{-3}$
	100	1.08×10^{-2}	1.00×10^{-2}	$(1.04 \pm 0.050) \times 10^{-2}$
	500	1.92×10^{-2}	1.62×10^{-2}	$(1.77 \pm 0.22) \times 10^{-2}$

[a]Reaction mixtures were maintained at 30 °C and contained fatty acid, β-carotene **1** (3.1 μM), surfactant **54** (AE7) (367 μg ml^{-1}) and phosphate buffer (50 mM) to maintain pH 7.00. [b]Standard deviation(SD) was calculated using the following formula: $SD = \sqrt{\frac{\sum(x-\mu)^2}{(n-1)}}$ where μ is the mean and n is the number of samples.

Table A10 Initial rates of oxidative degradation (bleaching) of β-carotene **1** in the presence of fatty acid with surfactant **53** (Tween 80).

Fatty Acid	Concentration (μM)	Initial Rates (υ, μM min^{-1})[a]		
		υ1	υ2	υ_{av} ± SD[b]
Oleic	10	2.30×10^{-3}	3.10×10^{-3}	$(2.70 \pm 0.50) \times 10^{-3}$
	50	1.00×10^{-2}	1.08×10^{-2}	$(1.04 \pm 0.050) \times 10^{-2}$
	100	2.00×10^{-2}	2.15×10^{-2}	$(2.08 \pm 0.11) \times 10^{-2}$
	500	4.00×10^{-2}	4.00×10^{-2}	$(4.00 \pm 0.00) \times 10^{-2}$
Linoleic	10	6.20×10^{-3}	3.80×10^{-3}	$(5.00 \pm 1.6) \times 10^{-3}$
	50	1.31×10^{-2}	1.38×10^{-2}	$(1.35 \pm 0.05) \times 10^{-2}$
	100	3.00×10^{-2}	3.54×10^{-2}	$(3.27 \pm 0.38) \times 10^{-2}$
	500	1.00×10^{-1}	9.00×10^{-2}	$(9.50 \pm 0.71) \times 10^{-2}$
Linolenic	10	4.60×10^{-3}	3.10×10^{-3}	$(3.80 \pm 1.1) \times 10^{-3}$
	50	7.70×10^{-3}	8.50×10^{-3}	$(8.10 \pm 0.50) \times 10^{-3}$
	100	1.38×10^{-2}	1.23×10^{-2}	$(1.31 \pm 0.11) \times 10^{-2}$
	500	2.08×10^{-2}	2.23×10^{-2}	$(2.15 \pm 0.11) \times 10^{-2}$
Arachidonic	10	1.50×10^{-3}	1.50×10^{-3}	$(1.50 \pm 0.00) \times 10^{-3}$
	50	4.60×10^{-3}	4.60×10^{-3}	$(4.60 \pm 0.00) \times 10^{-3}$
	100	1.00×10^{-2}	1.15×10^{-2}	$(1.08 \pm 0.11) \times 10^{-2}$
	500	1.77×10^{-2}	2.08×10^{-2}	$(1.92 \pm 0.22) \times 10^{-2}$

[a]Reaction mixtures were maintained at 30 °C and contained fatty acid, β-carotene **1** (3.1 μM), surfactant **53** (Tween 80) (367 μg ml^{-1}) and phosphate buffer (50 mM) to maintain pH 7.00. [b]Standard deviation(SD) was calculated using the following formula: $SD = \sqrt{\frac{\sum(x-\mu)^2}{(n-1)}}$ where μ is the mean and n is the number of samples.

Table A11 Range of concentrations of surfactant **53** (Tween 80) showing changes in Eosin Y λ_{max} (517–528 nm).

Buffer System[a]	Substrate Additives	Surfactant concentration range (mM)
KH_2PO_4	none	0.20-10.00
K_2CO_3	none	0.20-10.00
KH_2PO_4	500 μM linoleic acid **10**	1.00-20.00
K_2CO_3	500 μM linoleic acid **10**	1.00-10.00
KH_2PO_4	3.2 μM β-carotene **1**	0.20-10.00
K_2CO_3	3.2 μM β-carotene **1**	0.50-10.00
KH_2PO_4	500 μM linoleic acid **10**, 3.2 μM β-carotene **1**	1.00-20.00
K_2CO_3	500 μM linoleic acid **10**, 3.2 μM β-carotene **1**	1.00-20.00
KH_2PO_4	500 μM oleic acid **38**	1.00-20.00
K_2CO_3	500 μM oleic acid **38**	1.00-20.00

[a]1% buffer concentration at 30 °C.

Table A12 Range of concentrations of surfactant **54** (AE7) showing changes in Eosin Y λ_{max} (517–528 nm).

Buffer System[a]	Substrate Additives	Surfactant concentration range (mM)
KH_2PO_4	none	0.50-20.00
K_2CO_3	none	0.50-20.00
KH_2PO_4	500 µM linoleic acid **10**	2.00-40.00
K_2CO_3	500 µM linoleic acid **10**	2.00-40.00
KH_2PO_4	3.2 µM β-carotene **1**	1.00-20.00
K_2CO_3	3.2 µM β-carotene **1**	1.00-20.00
KH_2PO_4	500 µM linoleic acid **10**, 3.2 µM β-carotene **1**	2.00-40.00
K_2CO_3	500 µM linoleic acid **10**, 3.2 µM β-carotene **1**	2.00-40.00
KH_2PO_4	500 µM oleic acid **38**	2.00-40.00
K_2CO_3	500 µM oleic acid **38**	2.00-40.00
KH_2PO_4	500 µM steric acid **37**	2.00-40.00
K_2CO_3	500 µM steric acid **37**	2.00-40.00

[a]1% buffer concentration at 30 °C.

Appendix B

Table B1 Initial rates of oxidation of linoleic acid **10** in the presence of LOX1 (050M1910v) from Sigma and surfactant **52** (Tween 20).

pH[b]	Initial Rates (υ, μM min^{-1})[a]			
	υ1	υ2	υ3	υ_{av} ± SD[c]
6.5	2.15	2.15	1.75	2.02 ± 0.23
7	2.17	2.12	2.34	2.21 ± 0.12
7.5	4.19	4.10	4.33	4.21 ± 0.12
8	4.66	4.79	4.66	4.70 ± 0.08
8.5	5.37	5.25	5.24	5.29 ± 0.08
9	4.76	4.76	4.72	4.75 ± 0.02
9.5	4.76	4.96	4.69	4.80 ± 0.14
10	5.15	5.01	4.40	4.85 ± 0.40

[a] Reaction mixtures were maintained at 30 °C and contained LOX1 enzyme from Novozymes (0.33 μg ml^{-1}), linoleic acid **10** (500 μM) and surfactant **52** (Tween 20) (200 μg ml^{-1}). [b] Phosphate or borate buffer (50 mM) were used to maintain pH 6.50-8.00 and 8.50-9.00, respectively. [c] Standard deviation (SD) was calculated using the following formula: $SD = \sqrt{\frac{\sum(x-\mu)^2}{(n-1)}}$ where μ is the mean and n is the number of samples.

Table B2 Initial rates of oxidation of linoleic acid **10** in the presence of LOX1 (050M1910) from Sigma and surfactant **52** (Tween 20).

pH[b]	Initial Rates (υ, μM min^{-1})[a]			
	υ1	υ2	υ3	υ_{av} ± SD[c]
6.50	2.08	2.35	2.03	2.153 ± 0.174
7.00	2.45	4.89	2.72	3.354 ± 1.340
7.50	5.97	5.72	5.28	5.656 ± 0.353
8.00	7.55	7.69	7.05	7.430 ± 0.334
8.50	6.96	6.64	6.18	6.593 ± 0.391
9.00	5.97	6.09	5.82	5.961 ± 0.134
9.50	6.36	6.48	6.28	6.369 ± 0.101
10.00	6.12	6.11	6.28	6.169 ± 0.092

[a] Reaction mixtures were maintained at 30 °C and contained LOX1 enzyme from Novozymes (0.33 μg ml^{-1}), linoleic acid **10** (500 μM) and surfactant **52** (Tween 20) (200 μg ml^{-1}). [b] Phosphate or borate buffer (50 mM) were used to maintain pH 6.50-8.00 and 8.50-9.00, respectively. [c] Standard deviation (SD) was calculated using the following formula: $SD = \sqrt{\frac{\sum(x-\mu)^2}{(n-1)}}$ where μ is the mean and n is the number of samples.

Table B3 Initial rates of oxidation of linoleic acid **10** in the presence of LOX1 from Novozymes and surfactant **52** (Tween 20).

pH[b]	Initial Rates (υ, μM min^{-1})[a]			
	υ1	υ2	υ3	υ_{av} ± SD[c]
6.50	1.94	1.64	1.64	1.75 ± 0.17
7.00	1.12 x 10^{1}	1.16 x 10^{1}	1.16 x 10^{1}	(1.15 ± 0.026) x 10^{1}
7.50	2.31 x 10^{1}	2.40 x 10^{1}	2.49 x 10^{1}	(2.41 ± 0.090) x 10^{1}
8.00	3.46 x 10^{1}	3.48 x 10^{1}	3.64 x 10^{1}	(3.53 ± 0.10) x 10^{1}
8.50	3.87 x 10^{1}	3.63 x 10^{1}	3.60 x 10^{1}	(3.70 ± 0.15) x 10^{1}
9.00	3.74 x 10^{1}	3.76 x 10^{1}	3.77 x 10^{1}	(3.76 ± 0.017) x 10^{1}
9.50	3.72 x 10^{1}	3.70 x 10^{1}	3.80 x 10^{1}	(3.75 ± 0.051) x 10^{1}
10.00	3.78 x 10^{1}	3.43 x 10^{1}	3.56 x 10^{1}	(3.59 ± 0.18) x 10^{1}

[a] Reaction mixtures were maintained at 30 °C and contained LOX1 enzyme from Novozymes (0.33 μg ml^{-1}), linoleic acid **10** (500 μM) and surfactant **47** (Tween 20) (200 μg ml^{-1}). [b] Phosphate or borate buffer (50 mM) were used to maintain pH 6.50-8.00 and 8.50-9.00, respectively. [c] Standard deviation (SD) was calculated using the following formula: $SD = \sqrt{\frac{\sum(x-\mu)^2}{(n-1)}}$ where μ is the mean and n is the number of samples.

Table B4 Initial rates of oxidation of linoleic acid **10** in the presence of LOX3 from Novozymes and surfactant **52** (Tween 20).

pH[b]	Initial Rates (υ, μM min^{-1})[a]			
	υ1	υ2	υ3	υ_{av} ± SD[c]
6.50	1.32 x 10^{1}	1.33 x 10^{1}	1.51 x 10^{1}	(1.39 ± 0.11) x 10^{1}
7.00	4.52	4.67	4.38	4.53 ± 0.14
7.50	3.69	3.37	3.56	3.54 ± 0.16
8.00	3.09	3.25	3.19	3.18 ± 0.083
8.50	3.82 x 10^{-1}	3.73 x 10^{-1}	3.87 x 10^{-1}	(3.81 ± 0.070) x 10^{-1}
9.00	8.40 x 10^{-2}	6.70 x 10^{-2}	8.00 x 10^{-2}	(7.70 ± 0.90) x 10^{-2}
9.50	1.30 x 10^{-2}	1.30 x 10^{-2}	1.30 x 10^{-2}	(1.30 ± 0.00) x 10^{-2}
10.00	9.00 x 10^{-3}	9.00 x 10^{-3}	9.00 x 10^{-3}	(9.00 ± 0.00) x 10^{-3}

[a] Reaction mixtures were maintained at 30 °C and contained LOX1 enzyme from Novozymes (0.33 μg ml^{-1}), linoleic acid **10** (500 μM) and surfactant **47** (Tween 20) (200 μg ml^{-1}). [b] Phosphate or borate buffer (50 mM) were used to maintain pH 6.50-8.00 and 8.50-9.00, respectively. [c] Standard deviation (SD) was calculated using the following formula: $SD = \sqrt{\frac{\sum(x-\mu)^2}{(n-1)}}$ where μ is the mean and n is the number of samples.

Table B5 Initial rates of oxidation of linoleic acid **10** (80 μM) in the presence of LOX1 from Novozymes and surfactant **52** (Tween 20).

pH[b]	Initial Rates (υ, μM min^{-1})[a]		
	υ1	υ2	υ_{av} ± SD[c]
4.5	8.90 x 10^{-2}	1.07 x 10^{-1}	(9.80 ± 1.30) x 10^{-2}
5	2.13 x 10^{-1}	2.09 x 10^{-1}	(2.11 ± 0.030) x 10^{-1}
5.5	4.09 x 10^{-1}	3.56 x 10^{-1}	(3.82 ± 0.38) x 10^{-1}
6	9.42 x 10^{-1}	9.82 x 10^{-1}	(9.62 ± 0.28) x 10^{-1}
6.5	8.71 x 10^{-1}	8.98 x 10^{-1}	(8.84 ± 0.19) x 10^{-1}
7	4.01	3.54	3.78 ± 0.33
7.5	5.02	1.08 x 10^{1}	7.951 ± 4.1
8	1.90 x 10^{1}	1.56 x 10^{1}	(1.73 ± 0.24) x 10^{1}
8.5	2.72 x 10^{1}	2.61 x 10^{1}	(2.67 ± 0.081) x 10^{1}
9	2.69 x 10^{1}	2.57 x 10^{1}	(2.63 ± 0.078) x 10^{1}
9.5	2.60 x 10^{1}	2.78 x 10^{1}	(2.69 ± 0.12) x 10^{1}
10	2.61 x 10^{1}	2.79 x 10^{1}	(2.70 ± 0.12) x 10^{1}

[a] Reaction mixtures were maintained at 30 °C and contained LOX1 enzyme from Novozymes (0.33 μg ml^{-1}), linoleic acid **10** (80 μM) and surfactant **47** (Tween 20) (200 μg ml^{-1}). [b] Phosphate or borate buffer (50 mM) were used to maintain pH 6.50-8.00 and 8.50-9.00, respectively. [c] Standard deviation (SD) was calculated using the following formula: $SD = \sqrt{\frac{\sum(x-\mu)^2}{(n-1)}}$ where μ is the mean and n is the number of samples.

Table B6 Initial rates of oxidation of linoleic acid **10** (80 μM) in the presence of LOX3 from Novozymes and surfactant **52** (Tween 20).

pH[b]	Initial Rates (υ, μM min^{-1})[a]		
	υ1	υ2	υ_{av} ± SD[c]
4.50	6.70 x 10^{-2}	5.80 x 10^{-2}	(6.20 ± 0.60) x 10^{-2}
5.00	6.70 x 10^{-2}	7.60 x 10^{-2}	(7.10 ± 0.60) x 10^{-2}
5.50	7.60 x 10^{-2}	8.00 x 10^{-2}	(7.80 ± 0.30) x 10^{-2}
6.00	8.00 x 10^{-2}	8.40 x 10^{-2}	(8.20 ± 0.30) x 10^{-2}
6.50	4.90 x 10^{-2}	3.10 x 10^{-2}	(4.00 ± 1.3) x 10^{-2}
7.00	1.64 x 10^{-1}	1.29 x 10^{-1}	(1.47 ± 0.25) x 10^{-1}
7.50	1.87 x 10^{-1}	1.69 x 10^{-1}	(1.78 ± 0.13) x 10^{-1}
8.00	3.24 x 10^{-1}	2.09 x 10^{-1}	(2.67 ± 0.82) x 10^{-1}
8.50	4.93 x 10^{-1}	1.78 x 10^{-1}	(3.36 ± 2.2) x 10^{-1}
9.00	8.62 x 10^{-1}	2.04 x 10^{-1}	(5.33 ± 4.7) x 10^{-1}
9.50	2.18 x 10^{-1}	1.60 x 10^{-1}	(1.89 ± 0.41) x 10^{-1}
10.00	1.56 x 10^{-1}	1.60 x 10^{-1}	(1.58 ± 0.030) x 10^{-1}

[a] Reaction mixtures were maintained at 30 °C and contained LOX1 enzyme from Novozymes (0.33 μg ml^{-1}), linoleic acid **10** (80 μM) and surfactant **47** (Tween 20) (200 μg ml^{-1}). [b] Phosphate or borate buffer (50 mM) were used to maintain pH 6.50-8.00 and 8.50-9.00, respectively. [c] Standard deviation (SD) was calculated using the following formula: $SD = \sqrt{\frac{\sum(x-\mu)^2}{(n-1)}}$ where μ is the mean and n is the number of samples.

Table B7 Initial rates of oxidation of linoleic acid **10** (80 μM) in the presence of LOX1 (050M1910v) from Sigma and surfactant **52** (Tween 20).

pH	Initial Rates (υ, μM min^{-1})[a]		
	υ1	υ2	υ_{av} ± SD*
4.50	9.80 x 10^{-2}	3.10 x 10^{-2}	(6.4 ± 4.7) x 10^{-2}
5.00	1.20 x 10^{-1}	5.80 x 10^{-2}	(8.9 ± 4.4) x 10^{-2}
5.50	6.20 x 10^{-2}	1.78 x 10^{-1}	(1.20 ± 0.82) x 10^{-1}
6.00	3.51 x 10^{-1}	7.29 x 10^{-1}	(5.40 ± 2.67) x 10^{-1}
6.50	2.23	7.38 x 10^{-1}	1.484 ± 1.056
7.00	2.23	2.16	2.196 ± 0.050
7.50	1.27 x 10^{1}	7.11	9.909 ± 3.963
8.00	1.29 x 10^{1}	1.34 x 10^{1}	(1.32 ± 0.04) x 10^{1}
8.50	1.35 x 10^{1}	1.38 x 10^{1}	(1.37 ± 0.02) x 10^{1}
9.00	1.48 x 10^{1}	1.39 x 10^{1}	(1.43 ± 0.06) x 10^{1}
9.50	1.42 x 10^{1}	1.40 x 10^{1}	(1.41 ± 0.02) x 10^{1}
10.00	1.30 x 10^{1}	1.34 x 10^{1}	(1.32 ± 0.03) x 10^{1}

[a] Reaction mixtures were maintained at 30 °C and contained LOX1 enzyme from Novozymes (0.33 μg ml^{-1}), linoleic acid **10** (80 μM) and surfactant **52** (Tween 20) (200 μg ml^{-1}). [b] Phosphate or borate buffer (50 mM) were used to maintain pH 6.50-8.00 and 8.50-9.00, respectively. [c] Standard deviation (SD) was calculated using the following formula: $SD = \sqrt{\frac{\sum(x-\mu)^2}{(n-1)}}$ where μ is the mean and n is the number of samples.

[b] Standard deviation (SD) was calculated using the following formula: $SD = \sqrt{\frac{\sum(x-\mu)^2}{(n-1)}}$ where μ is the mean and n is the number of samples.

Table B8 Initial rates of oxidation of linoleic acid **10** in the presence of LOX1 from Novozymes and surfactants **52** (Tween 20), **53** (Tween 80), **54** (AE7) and **55** (AE1S) at pH 6.5.

Surfactant	Concentration (μg mL^{-1})	Initial Rates (υ, μM min^{-1})[a]			
		υ1	υ2	υ3	υ_{av} ± SD[b]
Tween 20	200	1.24	9.60 x 10^{-1}	9.73 x 10^{-1}	1.06 ± 0.16
	400	7.91 x 10^{-1}	7.38 x 10^{-1}	8.49 x 10^{-1}	(7.93 ± 0.56) x 10^{-1}
Tween 80	200	7.51 x 10^{-1}	8.80 x 10^{-1}	9.24 x 10^{-1}	(8.52 ± 0.90) x 10^{-1}
	400	6.36 x 10^{-1}	6.40 x 10^{-1}	4.13 x 10^{-1}	(5.63 ± 1.3) x 10^{-1}
AE7	200	5.56 x 10^{-1}	5.11 x 10^{-1}	6.27 x 10^{-1}	(5.64 ± 0.58) x 10^{-1}
	400	3.87 x 10^{-1}	3.51 x 10^{-1}	4.09 x 10^{-1}	(3.82 ± 0.29) x 10^{-1}
AE1S	200	1.62 x 10^{1}	1.68 x 10^{1}	1.77 x 10^{1}	(1.69 ± 0.072) x 10^{1}
	400	5.85	6.93	6.28	6.36 ± 0.55

[a] Reaction mixtures were maintained at 30 °C and contained LOX1 enzyme from Novozymes (0.33 μg ml^{-1}), linoleic acid **10** (500 μM) and borate buffer (50 mM) to maintain pH 9.00. [b] Standard deviation (SD) was calculated using the following formula: $SD = \sqrt{\frac{\sum(x-\mu)^2}{(n-1)}}$ where μ is the mean and n is the number of samples.

Table B9 Initial rates of oxidation of linoleic acid **10** in the presence of LOX1 from Novozymes and surfactants **52** (Tween 20), **53** (Tween 80), **54** (AE7) and **55** (AE1S) at pH 9.0.

Surfactant	Concentration ($\mu g\ mL^{-1}$)	Initial Rates (υ, $\mu M\ min^{-1}$)[a]			
		$\upsilon 1$	$\upsilon 2$	$\upsilon 3$	$\upsilon_{av} \pm SD$[b]
Tween 20	200	3.23×10^{1}	3.73×10^{1}	4.41×10^{1}	$(3.79 \pm 0.60) \times 10^{1}$
	400	2.63×10^{1}	2.65×10^{1}	2.84×10^{1}	$(2.71 \pm 0.12) \times 10^{1}$
Tween 80	200	3.12×10^{1}	3.46×10^{1}	3.13×10^{1}	$(3.24 \pm 0.19) \times 10^{1}$
	400	2.42×10^{1}	2.80×10^{1}	2.59×10^{1}	$(2.61 \pm 0.19) \times 10^{1}$
AE7	200	3.15×10^{1}	3.09×10^{1}	2.92×10^{1}	$(3.06 \pm 0.12) \times 10^{1}$
	400	2.69×10^{1}	2.63×10^{1}	2.71×10^{1}	$(2.68 \pm 0.040) \times 10^{1}$
AE1S	200	3.19×10^{1}	3.09×10^{1}	2.98×10^{1}	$(3.09 \pm 0.10) \times 10^{1}$
	400	2.85×10^{1}	2.51×10^{1}	2.60×10^{1}	$(2.66 \pm 0.17) \times 10^{1}$

[a] Reaction mixtures were maintained at 30 °C and contained LOX1 enzyme from Novozymes (0.33 $\mu g\ ml^{-1}$), linoleic acid **10** (500 μM) and borate buffer (50 mM) to maintain pH 9.00. [b] Standard deviation (SD) was calculated using the following formula: $SD = \sqrt{\frac{\sum(x-\mu)^2}{(n-1)}}$ where μ is the mean and n is the number of samples.

Table B10 Initial rates of oxidation of linoleic acid **10** in the presence of LOX3 from Novozymes and surfactants **52** (Tween 20), **53** (Tween 80), **54** (AE7) and **55** (AE1S) at pH 6.5.

Surfactant	Concentration ($\mu g\ mL^{-1}$)	Initial Rates (υ, $\mu M\ min^{-1}$)[a]			
		$\upsilon 1$	$\upsilon 2$	$\upsilon 3$	$\upsilon_{av} \pm SD$[b]
Tween 20	200	7.30	6.00	5.63	6.31 ± 0.88
	400	4.44×10^{-1}	3.38×10^{-1}	3.02×10^{-1}	$(3.61 \pm 0.74) \times 10^{-1}$
Tween 80	200	4.87	3.89	4.40	4.39 ± 0.49
	400	1.78×10^{-1}	1.60×10^{-1}	1.51×10^{-1}	$(1.63 \pm 0.14) \times 10^{-1}$
AE7	200	4.22×10^{-1}	4.44×10^{-1}	4.71×10^{-1}	$(4.46 \pm 0.24) \times 10^{-1}$
	400	4.84×10^{-1}	3.73×10^{-1}	3.51×10^{-1}	$(4.03 \pm 0.71) \times 10^{-1}$
AE1S	200	4.40×10^{-1}	3.87×10^{-1}	4.89×10^{-1}	$(4.39 \pm 0.51) \times 10^{-1}$
	400	8.31×10^{-1}	9.96×10^{-1}	9.78×10^{-1}	$(9.35 \pm 0.90) \times 10^{-1}$

[a] Reaction mixtures were maintained at 30 °C and contained LOX1 enzyme from Novozymes (0.33 $\mu g\ ml^{-1}$), linoleic acid **10** (500 μM) and borate buffer (50 mM) to maintain pH 9.00. [b] Standard deviation (SD) was calculated using the following formula: $SD = \sqrt{\frac{\sum(x-\mu)^2}{(n-1)}}$ where μ is the mean and n is the number of samples.

Table B11 Initial rates of oxidation of linoleic acid **10** in the presence of LOX3 from Novozymes and surfactants **52** (Tween 20), **53** (Tween 80), **54** (AE7) and **55** (AE1S) at pH 9.0.

Surfactant	Concentration ($\mu g\ mL^{-1}$)	Initial Rates (υ, $\mu M\ min^{-1}$)[a]			
		$\upsilon 1$	$\upsilon 2$	$\upsilon 3$	$\upsilon_{av} \pm SD$[b]
Tween 20	200	1.80×10^{-2}	9.00×10^{-3}	6.20×10^{-2}	$(3.00 \pm 2.9) \times 10^{-2}$
	400	2.20×10^{-2}	5.80×10^{-2}	5.80×10^{-2}	$(4.60 \pm 2.1) \times 10^{-2}$
Tween 80	200	2.20×10^{-2}	6.70×10^{-2}	5.80×10^{-2}	$(4.90 \pm 2.4) \times 10^{-2}$
	400	5.30×10^{-2}	1.24×10^{-1}	3.96×10^{-1}	$(1.91 \pm 1.8) \times 10^{-1}$
AE7	200	1.80×10^{-2}	1.80×10^{-2}	5.30×10^{-2}	$(3.00 \pm 2.1) \times 10^{-2}$
	400	3.02×10^{-1}	3.38×10^{-1}	7.60×10^{-2}	$(2.39 \pm 1.4) \times 10^{-1}$
AE1S	200	9.00 x 10-3	1.30×10^{-2}	1.30×10^{-2}	$(1.20 \pm 0.30) \times 10^{-2}$
	400	1.80×10^{-2}	2.20×10^{-2}	1.30×10^{-2}	$(1.80 \pm 0.40) \times 10^{-2}$

[a] Reaction mixtures were maintained at 30 °C and contained LOX1 enzyme from Novozymes (0.33 $\mu g\ ml^{-1}$), linoleic acid **10** (500 µM) and borate buffer (50 mM) to maintain pH 9.00. [b] Standard deviation (SD) was calculated using the following formula: $SD = \sqrt{\frac{\sum(x-\mu)^2}{(n-1)}}$ where µ is the mean and n is the number of samples.

Table B12 Initial rates of oxidation of linoleic acid **10** in the presence surfactant **55** (AE1S) at pH 6.5.

AE1S Concentration ($\mu g\ mL^{-1}$)	Initial Rates (υ, $\mu M\ min^{-1}$)[a]			
	$\upsilon 1$	$\upsilon 2$	$\upsilon 3$	$\upsilon_{av} \pm SD$[b]
200	5.33×10^{-1}	4.88×10^{-1}	5.33×10^{-1}	$(5.19 \pm 0.26) \times 10^{-1}$
300	4.44×10^{-1}	4.00×10^{-1}	4.00×10^{-1}	$(4.15 \pm 0.26) \times 10^{-1}$
400	3.55×10^{-1}	4.00×10^{-1}	3.11×10^{-1}	$(3.56 \pm 0.44) \times 10^{-1}$
500	4.88×10^{-1}	3.55×10^{-1}	2.22×10^{-1}	$(3.56 \pm 0.13) \times 10^{-1}$
600	2.66×10^{-1}	6.22×10^{-1}	4.89×10^{-2}	$(3.13 \pm 2.9) \times 10^{-1}$

[a] Reaction mixtures were maintained at 30 °C and contained, linoleic acid **10** (500 µM) and phosphate buffer (50 mM) to maintain pH 6.50. [b] Standard deviation (SD) was calculated using the following formula: $SD = \sqrt{\frac{\sum(x-\mu)^2}{(n-1)}}$ where µ is the mean and n is the number of samples.

Table B13 Initial rates of oxidation of linoleic acid **10** in the presence of LOX1 from Novozymes and surfactant **55** (AE1S) at pH 6.5.

AE1S Concentration ($\mu g\ mL^{-1}$)	Initial Rates (υ, $\mu M\ min^{-1}$)[a]			
	$\upsilon 1$	$\upsilon 2$	$\upsilon 3$	$\upsilon_{av} \pm SD$[b]
200	1.76×10^{1}	2.19×10^{1}	1.71×10^{1}	$(1.89 \pm 0.26) \times 10^{1}$
300	1.32×10^{1}	8.13	1.59×10^{1}	$(1.24 \pm 0.40) \times 10^{1}$
400	1.03×10^{1}	1.09×10^{1}	5.95	9.08 ± 2.7
500	4.04	1.15×10^{1}	8.44	8.02 ± 3.8
600	3.15	4.04	6.57	4.59 ± 1.8

[a] Reaction mixtures were maintained at 30 °C and contained LOX1 enzyme from Novozymes (0.33 $\mu g\ ml^{-1}$), linoleic acid **10** (500 µM) and phosphate buffer (50 mM) to maintain pH 6.50. [b] Standard deviation (SD) was calculated using the following formula: $SD = \sqrt{\frac{\sum(x-\mu)^2}{(n-1)}}$ where µ is the mean and n is the number of samples.

Table B14 β-Carotene bleaching rate constants for combinations of LOX1 and LOX3 from Novozymes with linoleic acid and surfactant **54** (AE7).

Isozyme ratio (LOX1:LOX3)	pH[b]	Initial Rates (υ, μM min^{-1})[a]			
		υ1	υ2	υ3	υ_{av} ± SD[c]
100:0	6.50	2.26×10^{-2}	2.56×10^{-2}	2.64×10^{-2}	$(2.49 \pm 1.6) \times 10^{-2}$
	7.00	6.70×10^{-3}	5.90×10^{-3}	1.28×10^{-2}	$(8.50 \pm 8.0) \times 10^{-3}$
	7.50	9.64×10^{-2}	9.03×10^{-2}	1.00×10^{-1}	$(9.56 \pm 0.77) \times 10^{-2}$
	8.00	1.67×10^{-1}	1.77×10^{-1}	1.87×10^{-1}	$(1.78 \pm 0.16) \times 10^{-1}$
	8.50	1.07×10^{-1}	9.82×10^{-2}	1.58×10^{-1}	$(1.21 \pm 0.34) \times 10^{-1}$
	9.00	8.85×10^{-2}	7.00×10^{-2}	8.38×10^{-2}	$(8.08 \pm 1.6) \times 10^{-2}$
70:30	6.50	2.41×10^{-2}	2.49×10^{-2}	2.56×10^{-2}	$(2.49 \pm 1.5) \times 10^{-2}$
	7.00	1.51×10^{-2}	1.44×10^{-2}	1.36×10^{-2}	$(1.44 \pm 0.50) \times 10^{-2}$
	7.50	7.18×10^{-2}	6.79×10^{-2}	6.26×10^{-2}	$(6.74 \pm 0.73) \times 10^{-2}$
	8.00	1.39×10^{-1}	1.50×10^{-1}	1.54×10^{-1}	$(1.48 \pm 0.13) \times 10^{-1}$
	8.50	7.90×10^{-2}	9.90×10^{-2}	1.08×10^{-1}	$(9.54 \pm 1.7) \times 10^{-2}$
	9.00	7.77×10^{-2}	8.23×10^{-2}	8.62×10^{-2}	$(8.21 \pm 1.0) \times 10^{-2}$
50:50	6.50	2.79×10^{-2}	3.56×10^{-2}	3.10×10^{-2}	$(3.15 \pm 1.8) \times 10^{-2}$
	7.00	1.28×10^{-2}	1.05×10^{-2}	1.82×10^{-2}	$(1.38 \pm 0.82) \times 10^{-2}$
	7.50	6.64×10^{-2}	6.18×10^{-2}	6.79×10^{-2}	$(6.54 \pm 0.59) \times 10^{-2}$
	8.00	1.27×10^{-1}	1.34×10^{-1}	1.42×10^{-1}	$(1.35 \pm 0.13) \times 10^{-1}$
	8.50	4.21×10^{-2}	3.90×10^{-2}	3.82×10^{-2}	$(3.97 \pm 0.38) \times 10^{-1}$
	9.00	1.77×10^{-2}	2.46×10^{-2}	3.00×10^{-2}	$(2.41 \pm 1.2) \times 10^{-2}$
30:70	6.50	3.18×10^{-2}	3.49×10^{-2}	3.64×10^{-2}	$(3.44 \pm 1.6) \times 10^{-2}$
	7.00	1.74×10^{-2}	9.70×10^{-3}	1.82×10^{-2}	$(1.51 \pm 0.89) \times 10^{-2}$
	7.50	5.79×10^{-2}	5.41×10^{-2}	5.18×10^{-2}	$(5.46 \pm 0.58) \times 10^{-2}$
	8.00	9.79×10^{-2}	9.87×10^{-2}	1.07×10^{-1}	$(1.01 \pm 0.11) \times 10^{-1}$
	8.50	2.51×10^{-2}	2.74×10^{-2}	2.74×10^{-2}	$(2.67 \pm 0.31) \times 10^{-2}$
	9.00	9.20×10^{-3}	8.50×10^{-3}	1.85×10^{-2}	$(1.21 \pm 1.2) \times 10^{-2}$
0:100	6.50	7.10×10^{-2}	3.41×10^{-2}	2.95×10^{-2}	$(4.49 \pm 3.7) \times 10^{-2}$
	7.00	1.21×10^{-2}	1.44×10^{-2}	1.36×10^{-2}	$(1.33 \pm 0.54) \times 10^{-2}$
	7.50	1.79×10^{-2}	1.87×10^{-2}	2.03×10^{-2}	$(1.90 \pm 0.39) \times 10^{-2}$
	8.00	3.72×10^{-2}	3.79×10^{-2}	2.95×10^{-2}	$(3.49 \pm 1.0) \times 10^{-2}$
	8.50	-2.56×10^{-4}	1.28×10^{-3}	-2.56×10^{-4}	$(2.56 \pm 27) \times 10^{-4}$
	9.00	-2.08×10^{-2}	-1.54×10^{-2}	-2.08×10^{-2}	$(-1.90 \pm 0.92) \times 10^{-2}$

[a] Reaction mixtures were maintained at 30 °C and contained LOX1 and/or LOX3 enzyme from Novozymes (0.33 μg ml^{-1} total concentration), β-carotene **1** (3.1 μM), linoleic acid **10** (500 μM) and surfactant **54** (AE7) (367 μg ml^{-1}). [b] Phosphate or borate buffer (50 mM) were used to maintain pH 6.50-8.00 and 8.50-9.00, respectively. [c] Standard deviation (SD) was calculated using the following formula: $SD = \sqrt{\frac{\sum(x-\mu)^2}{(n-1)}}$ where μ is the mean and n is the number of samples.

Table B15 β-Carotene bleaching rate constants for combinations of LOX1 and LOX3 from Novozymes with linoleic acid and surfactant **53** (Tween 80).

Isozyme ratio (LOX1:LOX3)	pH[b]	Initial Rates (υ, μM min^{-1})[a]			
		υ1	υ2	υ3	υ_{av} ± SD[c]
100:0	6.50	1.87 x 10^{-2}	2.56 x 10^{-2}	3.03 x 10^{-2}	(2.49 ± 1.4) x 10^{-2}
	7.00	3.64 x 10^{-2}	2.41 x 10^{-2}	3.79 x 10^{-2}	(3.28 ± 0.95) x 10^{-2}
	7.50	2.67 x 10^{-1}	2.59 x 10^{-1}	2.80 x 10^{-1}	(2.69 ± 0.15) x 10^{-1}
	8.00	3.47 x 10^{-1}	3.83 x 10^{-1}	3.58 x 10^{-1}	(3.63 ± 0.21) x 10^{-1}
	8.50	3.20 x 10^{-1}	3.09 x 10^{-1}	2.96 x 10^{-1}	(3.09 ± 0.15) x 10^{-1}
	9.00	3.12 x 10^{-1}	2.99 x 10^{-1}	2.99 x 10^{-1}	(3.04 ± 0.12) x 10^{-1}
70:30	6.50	8.10 x 10^{-2}	6.95 x 10^{-2}	8.10 x 10^{-2}	(7.72 ± 1.1) x 10^{-2}
	7.00	4.26 x 10^{-2}	8.56 x 10^{-2}	3.26 x 10^{-2}	(5.36 ± 3.0) x 10^{-2}
	7.50	2.43 x 10^{-1}	2.25 x 10^{-1}	2.27 x 10^{-1}	(2.32 ± 0.15) x 10^{-1}
	8.00	2.81 x 10^{-1}	2.96 x 10^{-1}	3.05 x 10^{-1}	(2.94 ± 0.15) x 10^{-1}
	8.50	2.71 x 10^{-1}	2.75 x 10^{-1}	2.59 x 10^{-1}	(2.69 ± 0.11) x 10^{-1}
	9.00	2.56 x 10^{-1}	2.75 x 10^{-1}	2.80 x 10^{-1}	(2.71 ± 0.17) x 10^{-1}
50:50	6.50	5.18 x 10^{-2}	8.33 x 10^{-2}	5.41 x 10^{-2}	(6.31 ± 2.5) x 10^{-2}
	7.00	4.79 x 10^{-2}	3.79 x 10^{-2}	3.26 x 10^{-2}	(3.95 ± 0.97) x 10^{-2}
	7.50	2.31 x 10^{-1}	1.98 x 10^{-1}	1.91 x 10^{-1}	(2.07 ± 0.26) x 10^{-1}
	8.00	2.41 x 10^{-1}	2.57 x 10^{-1}	2.87 x 10^{-1}	(2.62 ± 0.26) x 10^{-1}
	8.50	2.18 x 10^{-1}	2.12 x 10^{-1}	2.09 x 10^{-1}	(2.13 ± 0.74) x 10^{-1}
	9.00	2.20 x 10^{-1}	2.22 x 10^{-1}	2.13 x 10^{-1}	(2.19 ± 0.090) x 10^{-1}
30:70	6.50	8.41 x 10^{-2}	5.72 x 10^{-2}	6.33 x 10^{-2}	(6.82 ± 2.2) x 10^{-2}
	7.00	2.26 x 10^{-2}	4.41 x 10^{-2}	4.72 x 10^{-2}	(3.79 ± 1.5) x 10^{-2}
	7.50	1.61 x 10^{-1}	1.64 x 10^{-1}	1.57 x 10^{-1}	(1.61 ± 0.088) x 10^{-1}
	8.00	1.65 x 10^{-1}	1.78 x 10^{-1}	1.81 x 10^{-1}	(1.75 ± 0.11) x 10^{-1}
	8.50	8.67 x 10^{-2}	7.90 x 10^{-2}	7.51 x 10^{-2}	(7.95 ± 0.96) x 10^{-2}
	9.00	7.26 x 10^{-2}	7.87 x 10^{-2}	7.41 x 10^{-2}	(7.21 ± 0.66) x 10^{-2}
0:100	6.50	8.49 x 10^{-2}	9.64 x 10^{-2}	8.64 x 10^{-2}	(8.92 ± 1.4) x 10^{-2}
	7.00	3.10 x 10^{-2}	7.79 x 10^{-2}	2.79 x 10^{-2}	(4.56 ± 3.0) x 10^{-2}
	7.50	5.64 x 10^{-2}	6.18 x 10^{-2}	5.64 x 10^{-2}	(5.82 ± 0.81) x 10^{-2}
	8.00	3.49 x 10^{-2}	3.87 x 10^{-2}	1.87 x 10^{-2}	(3.08 ± 0.13) x 10^{-2}
	8.50	-1.72 x 10^{-2}	-1.64 x 10^{-2}	-1.26 x 10^{-2}	(-1.56 ± 0.55) x 10^{-2}
	9.00	-1.97 x 10^{-2}	-2.05 x 10^{-2}	-1.97 x 10^{-2}	(-1.90 ± 0.70) x 10^{-2}

[a] Reaction mixtures were maintained at 30 °C and contained LOX1 and/or LOX3 enzyme from Novozymes (0.33 μg ml^{-1} total concentration), linoleic acid **10** (500 μM) and surfactant **53** (Tween 80) (367 μg ml^{-1}). [b] Phosphate or borate buffer (50 mM) were used to maintain pH 6.50-8.00 and 8.50-9.00, respectively. [c] Standard deviation (SD) was calculated using the following formula: $SD = \sqrt{\frac{\Sigma(x-\mu)^2}{(n-1)}}$ where μ is the mean and n is the number of samples.

Appendix C

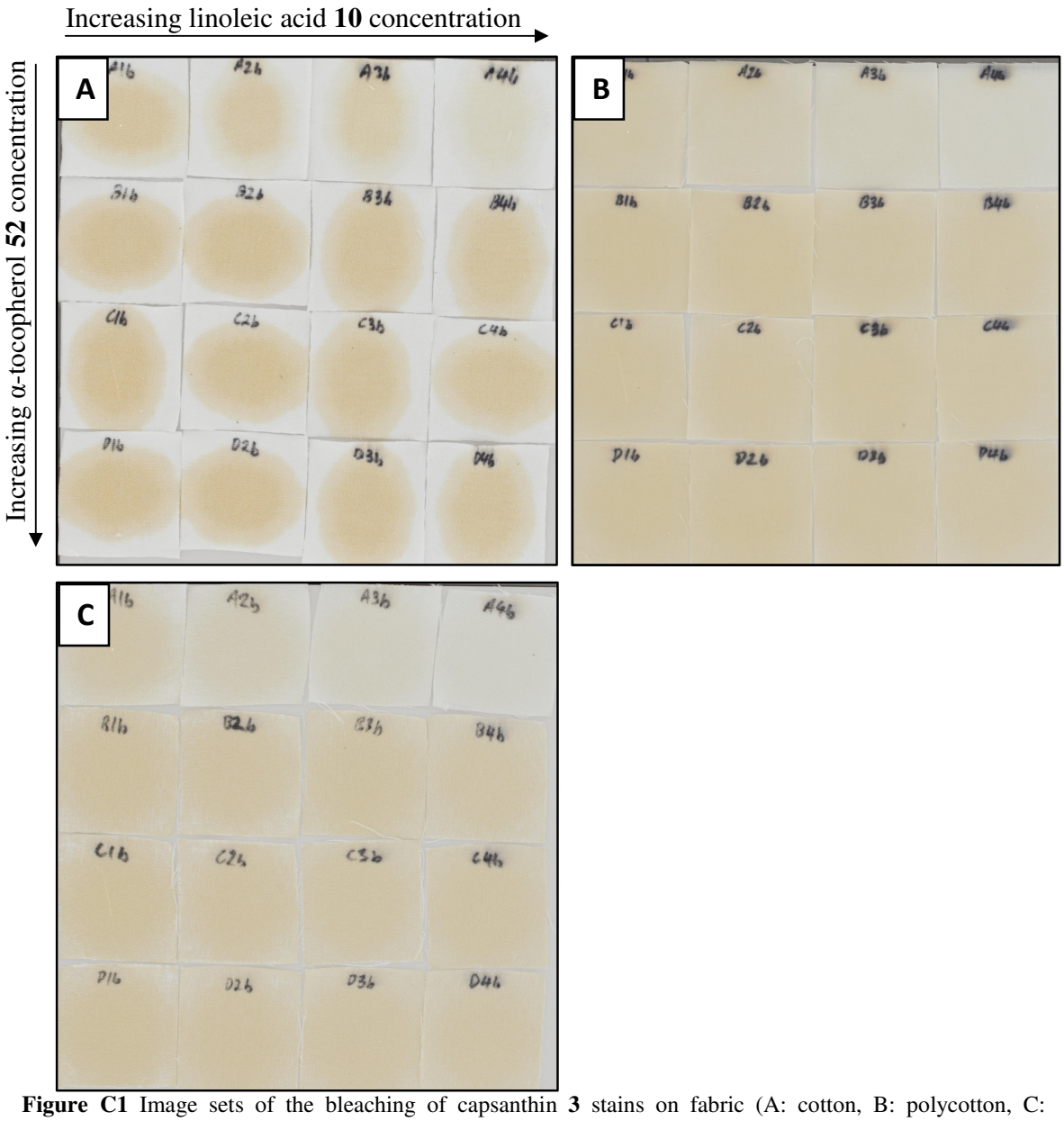

Figure C1 Image sets of the bleaching of capsanthin **3** stains on fabric (A: cotton, B: polycotton, C: polyester) in the presence of different concentrations of linoleic acid **10** and α-tocopherol **58** after a wash cycle and 18 hours drying at 30 °C.

Table C1 SRI values of capsanthin **3** stains on fabrics in the presence of linoleic acid **10** and α-tocopherol **58**.

Fabric	[α-Tocopherol **51**] (w/w%)	[Linoleic acid **10**] (w/w%)	SRI (%)	Fabric	[α-Tocopherol **58**] (w/w%)	[Linoleic acid **10**] (w/w%)	SRI (%)
Knitted Cotton	0	0	29	Polyester	0	0	34
		5	34			5	48
		10	40			10	60
		20	67			20	74
	0.01	0	20		0.01	0	20
		5	19			5	22
		10	24			10	20
		20	23			20	23
	0.05	0	17		0.05	0	21
		5	17			5	22
		10	21			10	22
		20	24			20	18
	0.10	0	19		0.10	0	19
		5	18			5	22
		10	20			10	21
		20	20			20	21
Polycotton	0	0	27				
		5	36				
		10	54				
		20	68				
	0.01	0	11				
		5	11				
		10	10				
		20	12				
	0.05	0	11				
		5	12				
		10	10				
		20	14				
	0.10	0	14				
		5	13				
		10	15				
		20	15				

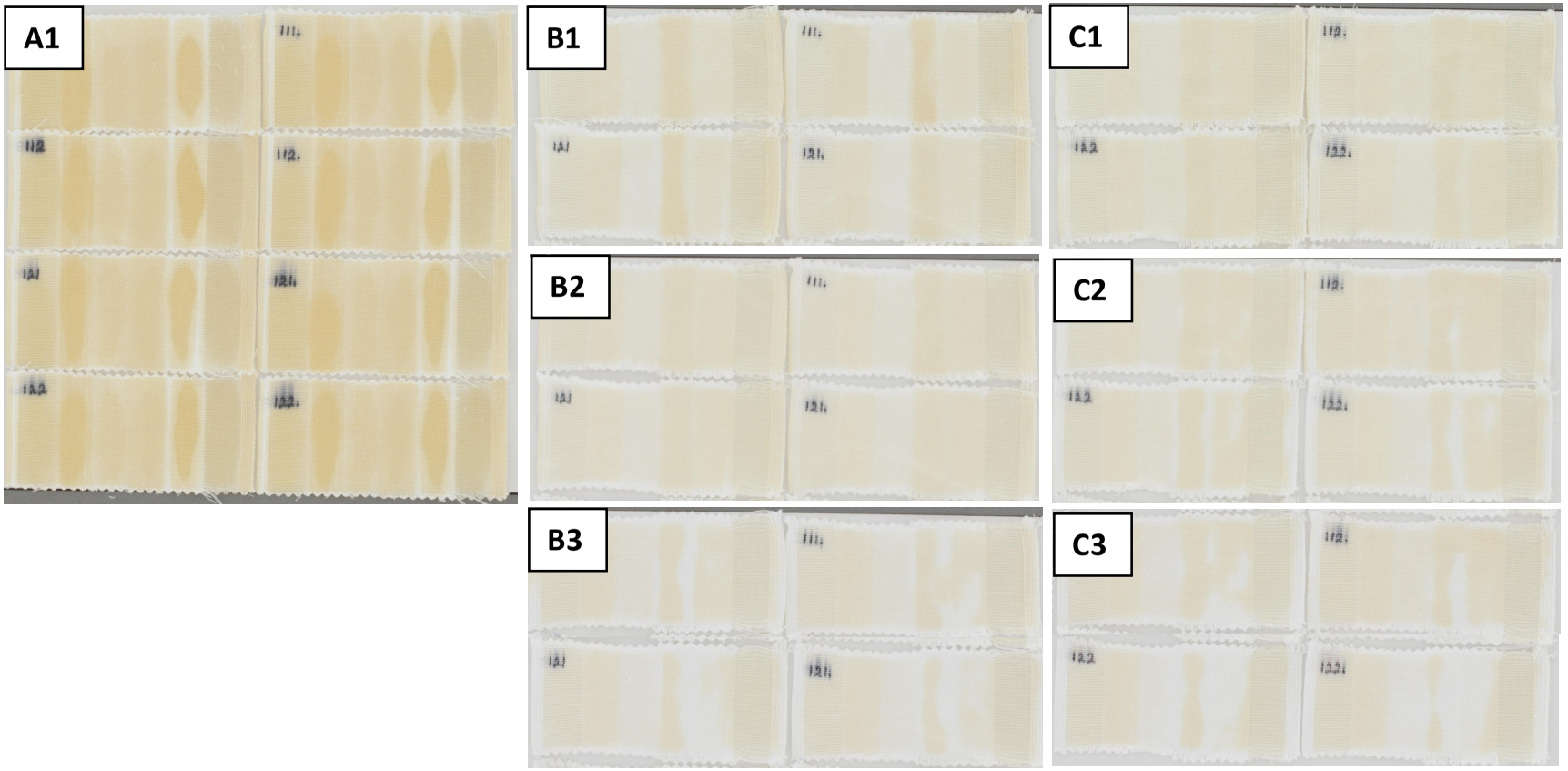

Figure C2 Image sets of the bleaching of capsanthin stains on multifibre (fabrics from left: diacetate, cotton, polyamide, polyester, acrylic and wool) at different time points after a wash cycle. **A1**: immediately after wash, **B1**: 1 h at 20 °C, **B2**: 3 h at 20 °C, **B3**: 48 h at 20 °C, **C1**: 1h at 50 °C, **C2**: 1h at 50 °C then 2 h at 20 °C, **C3**: 1h at 50 °C then 47 h at 20 °C. Multifibre strips were not prewashed.

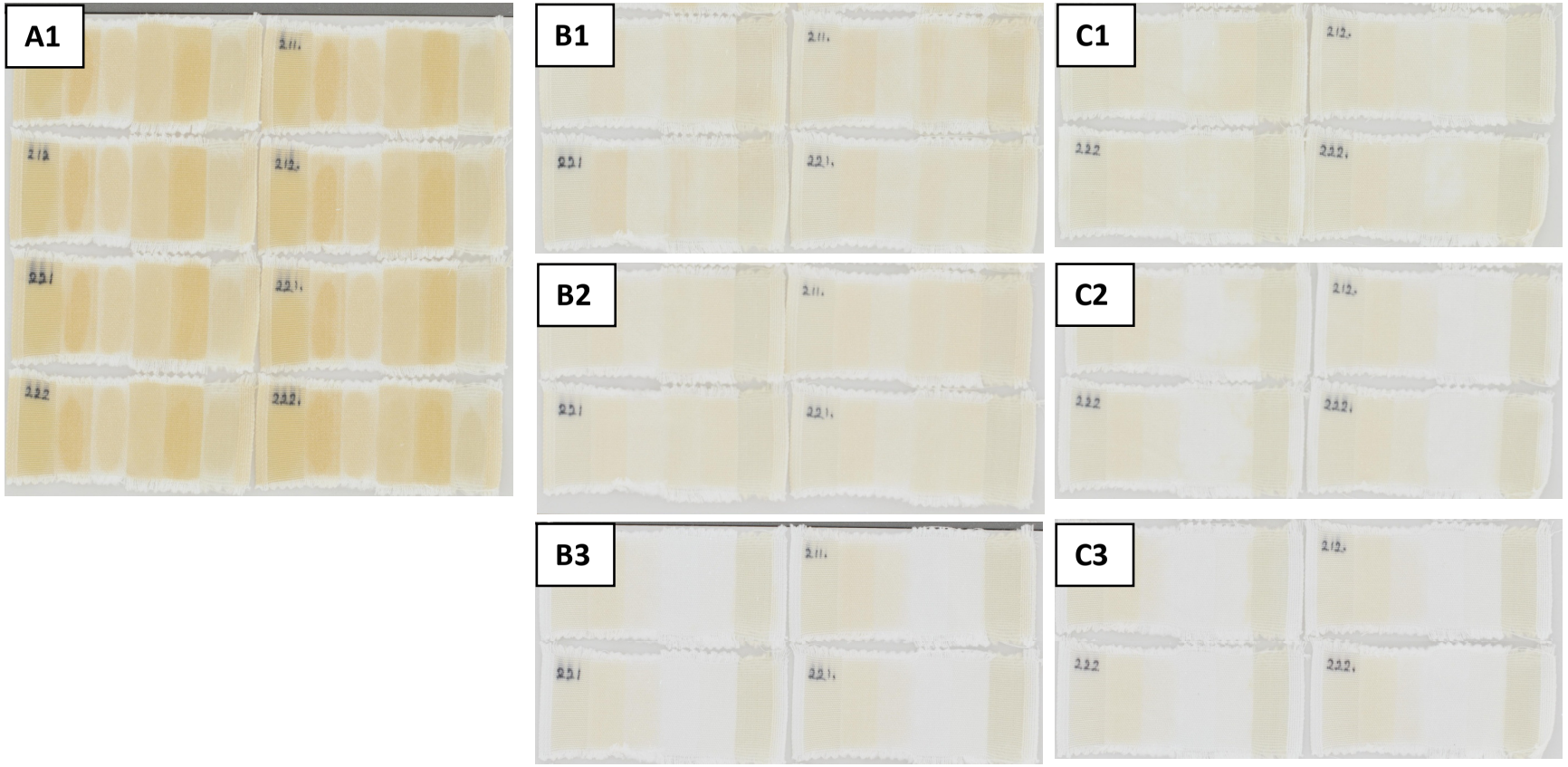

Figure C3 Image sets of the bleaching of capsanthin stains on multifibre (fabrics from left: diacetate, cotton, polyamide, polyester, acrylic and wool) at different time points after a wash cycle. **A1**: immediately after wash, **B1**: 1 h at 20 °C, **B2**: 3 h at 20 °C, **B3**: 48 h at 20 °C, **C1**: 1h at 50 °C, **C2**: 1h at 50 °C then 2 h at 20 °C, **C3**: 1h at 50 °C then 47 h at 20 °C. Multifibre strips were prewashed in capsule formulation before the application of stain material.

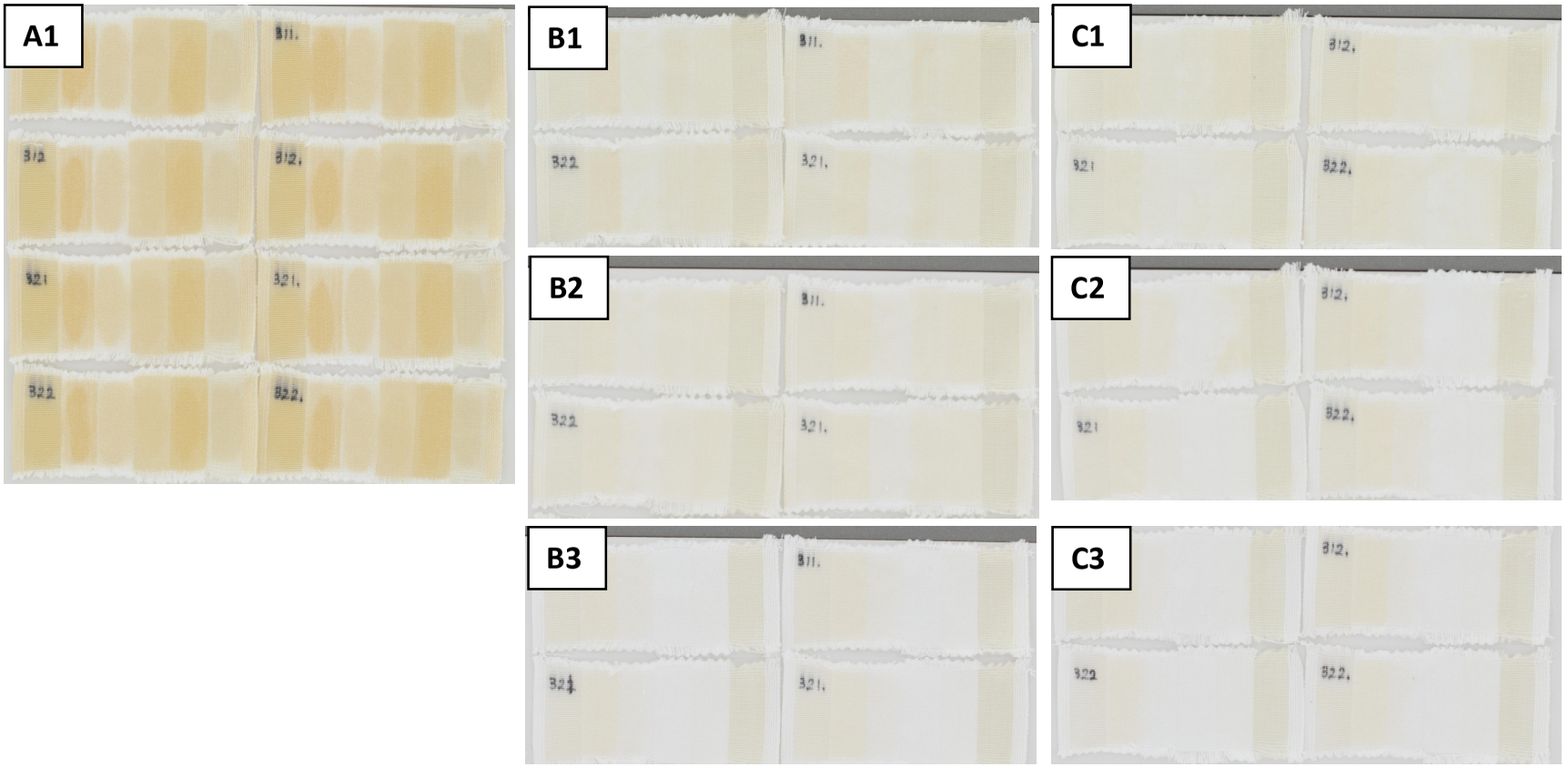

Figure C4 Image sets of the bleaching of capsanthin stains on multifibre (fabrics from left: diacetate, cotton, polyamide, polyester, acrylic and wool) at different time points after a wash cycle. **A1**: immediately after wash, **B1**: 1 h at 20 °C, **B2**: 3 h at 20 °C, **B3**: 48 h at 20 °C, **C1**: 1h at 50 °C, **C2**: 1h at 50 °C then 2 h at 20 °C, **C3**: 1h at 50 °C then 47 h at 20 °C. Multifibre strips were prewashed in capsule formulation in the presence of lipase before the application of stain material.

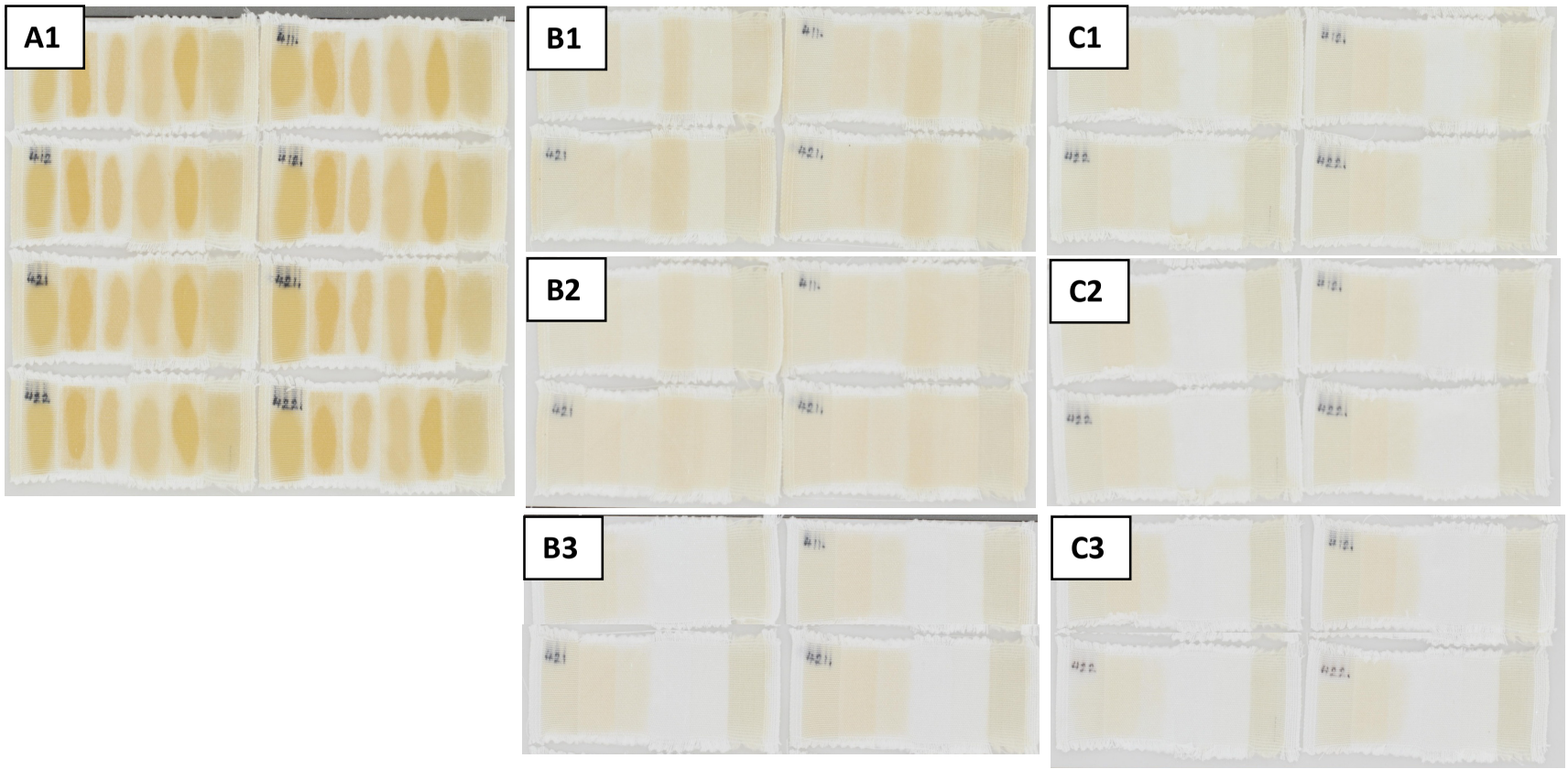

Figure C5 Image sets of the bleaching of capsanthin stains on multifibre (fabrics from left: diacetate, cotton, polyamide, polyester, acrylic and wool) at different time points after a wash cycle. **A1**: immediately after wash, **B1**: 1 h at 20 °C, **B2**: 3 h at 20 °C, **B3**: 48 h at 20 °C, **C1**: 1h at 50 °C, **C2**: 1h at 50 °C then 2 h at 20 °C, **C3**: 1h at 50 °C then 47 h at 20 °C. Multifibre strips were prewashed in capsule formulation in the presence of lipase then rinsed with fabric softener before the application of stain material.

Table C2 SRI values of capsanthin **3** stains on treated diacetate fabrics 1, 3 and 48 h after a wash cycle.

Pretreatment	Lipase in Wash	Drying Temperature	SRI1 1 h	SRI2 1 h	SRI_{av} 1 h ± SD	SRI1 3 h	SRI2 3 h	SRI_{av} 3 h ± SD	SRI1 48 h	SRI2 48 h	SRI_{av} 48 h ± SD
Not pretreated	No	20 °C	62.75	65.62	64.19 ± 2.03	64.26	68.15	66.20 ± 2.75	66.70	68.58	67.64 ± 1.33
		1 h at 50 °C	68.98	58.20	63.59 ± 7.62	69.63	59.10	64.36 ± 7.44	68.81	60.78	64.79 ± 5.68
	Yes	20 °C	64.92	65.29	65.11 ± 0.26	67.38	67.09	67.24 ± 0.20	69.06	68.44	68.75 ± 0.44
		1 h at 50 °C	60.91	62.60	61.76 ± 1.20	63.28	64.50	63.89 ± 0.86	66.65	65.75	66.20 ± 0.64
Prewashed	No	20 °C	74.96	65.51	70.24 ± 6.68	73.75	67.58	70.67 ± 4.36	77.48	70.93	74.20 ± 4.63
		1 h at 50 °C	69.36	71.92	70.64 ± 1.81	71.45	74.97	73.21 ± 2.49	74.62	79.63	77.13 ± 3.54
	Yes	20 °C	67.85	71.73	69.79 ± 2.74	70.54	72.94	71.74 ± 1.69	75.24	76.10	75.67 ± 0.61
		1 h at 50 °C	69.98	71.00	70.49 ± 0.72	73.30	73.72	73.51 ± 0.30	80.97	80.11	80.54 ± 0.60
Prewashed with lipase	No	20 °C	73.54	75.28	74.41 ± 1.23	77.74	79.26	78.50 ± 1.07	83.09	83.51	83.30 ± 0.30
		1 h at 50 °C	77.67	74.11	75.89 ± 2.51	77.05	75.24	76.15 ± 1.28	80.57	79.15	79.86 ± 1.01
	Yes	20 °C	75.29	76.99	76.14 ± 1.20	79.63	80.10	79.87 ± 0.33	84.68	83.52	84.10 ± 0.82
		1 h at 50 °C	81.01	77.79	79.40 ± 2.28	82.73	79.48	81.10 ± 2.30	88.11	85.52	86.81 ± 1.83
Prewashed, rinsed with fabric softener	No	20 °C	74.04	74.36	74.20 ± 0.22	78.16	73.66	75.91 ± 3.18	79.87	75.84	77.85 ± 2.85
		1 h at 50 °C	78.15	75.58	76.87 ± 1.82	78.32	76.32	77.32 ± 1.41	79.46	78.01	78.73 ± 1.02
	Yes	20 °C	71.69	72.22	71.96 ± 0.37	70.96	69.65	70.30 ± 0.93	73.45	72.02	72.73 ± 1.01
		1 h at 50 °C	74.66	73.56	74.11 ± 0.77	76.49	74.13	75.31 ± 1.67	86.85	81.58	84.21 ± 3.72

Table C3 SRI values of capsanthin **3** stains on treated cotton fabrics 1, 3 and 48 h after a wash cycle.

Pretreatment	Lipase in Wash	Drying Temperature	SRI1 1 h	SRI2 1 h	SRI_{av} 1 h ± SD	SRI1 3 h	SRI2 3 h	SRI_{av} 3 h ± SD	SRI1 48 h	SRI2 48 h	SRI_{av} 48 h ± SD
Not pretreated	No	20 °C	60.52	55.83	58.18 ± 3.31	61.75	64.96	63.36 ± 2.27	63.58	65.30	64.44 ± 1.22
		1 h at 50 °C	63.07	59.84	61.45 ± 2.28	63.74	60.51	62.13 ± 2.28	65.01	61.86	63.43 ± 2.23
	Yes	20 °C	58.36	61.28	59.82 ± 2.07	64.73	64.99	64.86 ± 0.18	66.74	65.89	66.31 ± 0.60
		1 h at 50 °C	60.91	63.12	62.02 ± 1.57	62.48	63.75	63.12 ± 0.90	65.41	66.68	66.04 ± 0.90
Prewashed	No	20 °C	59.69	50.84	55.26 ± 6.25	64.07	60.22	62.15 ± 2.72	68.30	63.91	66.11 ± 3.11
		1 h at 50 °C	61.46	63.27	62.37 ± 1.28	63.10	66.03	64.57 ± 2.07	66.40	70.73	68.57 ± 3.06
	Yes	20 °C	51.66	55.95	53.81 ± 3.03	63.81	62.45	63.13 ± 0.96	69.00	67.64	68.32 ± 0.96
		1 h at 50 °C	62.47	62.65	62.56 ± 0.13	65.07	65.50	65.29 ± 0.31	70.61	70.63	70.62 ± 0.01
Prewashed with lipase	No	20 °C	59.81	60.41	60.11 ± 0.42	68.89	70.43	69.66 ± 1.09	74.75	75.12	74.93 ± 0.26
		1 h at 50 °C	67.75	65.25	66.50 ± 1.77	69.07	67.74	68.40 ± 0.94	73.34	71.36	72.35 ± 1.40
	Yes	20 °C	60.17	65.47	62.82 ± 3.75	70.17	71.01	70.59 ± 0.59	76.08	76.00	76.04 ± 0.05
		1 h at 50 °C	72.07	68.32	70.19 ± 2.65	74.18	70.30	72.24 ± 2.74	80.77	77.51	79.14 ± 2.31
Prewashed, rinsed with fabric softener	No	20 °C	67.62	65.89	66.75 ± 1.22	73.21	68.02	70.61 ± 3.67	75.82	70.75	73.29 ± 3.59
		1 h at 50 °C	70.32	69.53	69.92 ± 0.55	71.67	70.16	70.92 ± 1.07	73.26	72.44	72.85 ± 0.59
	Yes	20 °C	66.91	68.66	67.79 ± 1.24	67.47	66.71	67.09 ± 0.54	71.08	69.94	70.51 ± 0.81
		1 h at 50 °C	68.73	68.30	68.51 ± 0.30	70.69	70.01	70.35 ± 0.48	77.85	74.85	76.35 ± 2.12

Table C4 SRI values of capsanthin **3** stains on treated polyamide fabrics 1, 3 and 48 h after a wash cycle.

Pretreatment	Lipase in Wash	Drying Temperature	SRI1 1 h	SRI2 1 h	SRI_{av} 1 h ± SD	SRI1 3 h	SRI2 3 h	SRI_{av} 3 h ± SD	SRI1 48 h	SRI2 48 h	SRI_{av} 48 h ± SD
Not pretreated	No	20 °C	69.87	72.39	71.13 ± 1.79	67.02	70.21	68.62 ± 2.26	72.92	73.54	73.23 ± 0.44
		1 h at 50 °C	68.38	57.52	62.95 ± 7.68	69.33	61.61	65.47 ± 5.46	76.59	66.26	71.43 ± 7.30
	Yes	20 °C	76.08	75.27	75.67 ± 0.58	71.17	72.17	71.67 ± 0.71	77.58	78.18	77.88 ± 0.42
		1 h at 50 °C	62.74	66.82	64.78 ± 2.89	66.76	70.54	68.65 ± 2.67	84.38	86.88	85.63 ± 1.77
Prewashed	No	20 °C	64.18	52.04	58.11 ± 8.58	64.84	57.62	61.23 ± 5.11	76.83	66.73	71.78 ± 7.14
		1 h at 50 °C	61.55	62.25	61.90 ± 0.50	64.58	66.92	65.75 ± 1.65	79.02	76.16	77.59 ± 2.03
	Yes	20 °C	60.64	58.53	59.59 ± 1.49	63.51	63.18	63.35 ± 0.24	73.41	72.98	73.19 ± 0.30
		1 h at 50 °C	62.64	59.83	61.24 ± 1.99	66.78	65.07	65.92 ± 1.21	79.38	81.00	80.19 ± 1.15
Prewashed with lipase	No	20 °C	69.55	70.58	70.06 ± 0.73	72.37	74.27	73.32 ± 1.35	82.71	83.01	82.86 ± 0.21
		1 h at 50 °C	68.00	63.61	65.81 ± 3.11	70.32	68.47	69.40 ± 1.31	85.69	82.09	83.89 ± 2.55
	Yes	20 °C	71.94	76.17	74.05 ± 2.99	74.13	76.38	75.25 ± 1.59	84.83	84.37	84.60 ± 0.32
		1 h at 50 °C	77.73	67.91	72.82 ± 6.95	80.17	72.23	76.20 ± 5.62	93.88	90.46	92.17 ± 2.42
Prewashed, rinsed with fabric softener	No	20 °C	72.15	56.82	64.48 ± 10.84	72.67	64.77	68.72 ± 5.59	80.66	71.10	75.88 ± 6.67
		1 h at 50 °C	67.39	65.07	66.23 ± 1.64	71.04	70.62	70.83 ± 0.30	75.86	77.23	76.54 ± 0.97
	Yes	20 °C	56.81	52.69	54.75 ± 2.92	64.92	61.74	63.33 ± 2.25	72.91	70.56	71.74 ± 1.66
		1 h at 50 °C	68.30	64.78	66.54 ± 2.49	72.50	71.86	72.18 ± 0.45	86.77	85.48	86.13 ± 0.91

Table C5 SRI values of capsanthin **3** stains on treated polyester fabrics 1, 3 and 48 h after a wash cycle.

Pretreatment	Lipase in Wash	Drying Temperature	SRI1 1 h	SRI2 1 h	SRI_{av} 1 h ± SD	SRI1 3 h	SRI2 3 h	SRI_{av} 3 h ± SD	SRI1 48 h	SRI2 48 h	SRI_{av} 48 h ± SD
Not pretreated	No	20 °C	38.18	29.71	33.94 ± 5.99	42.70	44.45	43.57 ± 1.24	62.84	61.44	62.14 ± 0.99
		1 h at 50 °C	43.73	40.02	41.87 ± 2.63	47.20	46.61	46.91 ± 0.41	56.96	59.91	58.44 ± 2.09
	Yes	20 °C	33.96	40.13	37.04 ± 4.37	47.32	48.21	47.76 ± 0.63	67.52	74.49	71.01 ± 4.93
		1 h at 50 °C	40.53	45.26	42.90 ± 3.35	44.60	55.37	49.98 ± 7.62	63.90	79.62	71.76 ± 11.11
Prewashed	No	20 °C	54.73	44.48	49.61 ± 7.25	58.04	50.65	54.34 ± 5.23	95.93	95.79	95.86 ± 0.10
		1 h at 50 °C	73.50	74.79	74.15 ± 0.91	91.78	93.43	92.60 ± 1.16	95.67	95.35	95.51 ± 0.23
	Yes	20 °C	51.05	52.48	51.76 ± 1.01	58.71	57.99	58.35 ± 0.51	95.58	95.61	95.60 ± 0.02
		1 h at 50 °C	68.69	75.16	71.93 ± 4.58	91.68	93.30	92.49 ± 1.15	95.65	94.61	95.13 ± 0.73
Prewashed with lipase	No	20 °C	58.32	59.74	59.03 ± 1.01	68.61	68.68	68.65 ± 0.05	96.51	96.31	96.41 ± 0.14
		1 h at 50 °C	69.94	82.42	76.18 ± 8.82	92.63	95.24	93.94 ± 1.84	96.31	96.43	96.37 ± 0.09
	Yes	20 °C	64.06	60.36	62.21 ± 2.62	72.72	69.58	71.15 ± 2.22	95.82	96.17	95.99 ± 0.25
		1 h at 50 °C	79.97	81.95	80.96 ± 1.40	93.43	94.80	94.11 ± 0.96	95.87	95.31	95.59 ± 0.39
Prewashed, rinsed with fabric softener	No	20 °C	37.61	37.40	37.50 ± 0.15	52.66	47.08	49.87 ± 3.94	97.07	96.49	96.78 ± 0.41
		1 h at 50 °C	91.31	91.31	91.31 ± 0.00	95.07	95.05	95.06 ± 0.02	96.66	96.67	96.67 ± 0.01
	Yes	20 °C	34.17	36.27	35.22 ± 1.48	49.36	47.46	48.41 ± 1.34	96.16	96.26	96.21 ± 0.07
		1 h at 50 °C	90.66	91.68	91.17 ± 0.72	95.23	95.07	95.15 ± 0.12	96.33	95.54	95.94 ± 0.56

Table C6 SRI values of capsanthin **3** stains on treated acrylic fabrics 1, 3 and 48 h after a wash cycle.

Pretreatment	Lipase in Wash	Drying Temperature	SRI1 1 h	SRI2 1 h	SRI_{av} 1 h ± SD	SRI1 3 h	SRI2 3 h	SRI_{av} 3 h ± SD	SRI1 48 h	SRI2 48 h	SRI_{av} 48 h ± SD
Not pretreated	No	20 °C	64.22	60.71	62.46 ± 2.48	56.44	57.42	56.93 ± 0.69	67.67	75.77	71.72 ± 5.73
		1 h at 50 °C	59.60	52.74	56.17 ± 4.86	64.46	55.83	60.15 ± 6.11	76.18	61.21	68.69 ± 10.59
	Yes	20 °C	63.59	65.46	64.52 ± 1.33	58.42	59.39	58.91 ± 0.68	80.10	78.50	79.30 ± 1.13
		1 h at 50 °C	57.06	54.38	55.72 ± 1.89	64.61	63.45	64.03 ± 0.82	83.14	83.02	83.08 ± 0.09
Prewashed	No	20 °C	65.41	61.44	63.42 ± 2.81	62.86	57.58	60.22 ± 3.74	94.85	93.70	94.27 ± 0.81
		1 h at 50 °C	60.67	70.24	65.46 ± 6.77	80.26	92.01	86.14 ± 8.31	94.60	94.73	94.66 ± 0.09
	Yes	20 °C	62.15	67.22	64.68 ± 3.59	64.57	66.07	65.32 ± 1.06	94.46	93.99	94.22 ± 0.33
		1 h at 50 °C	68.92	68.00	68.46 ± 0.66	87.49	89.60	88.54 ± 1.49	94.16	92.77	93.46 ± 0.98
Prewashed with lipase	No	20 °C	70.73	67.73	69.23 ± 2.13	74.37	72.44	73.40 ± 1.36	95.41	94.51	94.96 ± 0.64
		1 h at 50 °C	66.13	70.46	68.29 ± 3.06	79.92	92.20	86.06 ± 8.69	94.89	94.46	94.68 ± 0.31
	Yes	20 °C	68.45	74.04	71.25 ± 3.95	73.90	75.11	74.50 ± 0.86	94.99	94.37	94.68 ± 0.44
		1 h at 50 °C	79.77	79.96	79.86 ± 0.13	92.39	92.09	92.24 ± 0.21	94.66	93.44	94.05 ± 0.87
Prewashed, rinsed with fabric softener	No	20 °C	76.31	73.16	74.74 ± 2.22	74.16	68.51	71.33 ± 3.99	95.96	94.96	95.46 ± 0.71
		1 h at 50 °C	80.53	82.78	81.65 ± 1.59	93.99	94.32	94.16 ± 0.23	95.80	95.25	95.52 ± 0.39
	Yes	20 °C	77.30	73.49	75.39 ± 2.69	69.05	67.69	68.37 ± 0.96	95.31	94.88	95.10 ± 0.31
		1 h at 50 °C	85.58	86.30	85.94 ± 0.51	93.04	95.05	94.05 ± 1.42	95.28	94.46	94.87 ± 0.58

Table C7 SRI values of capsanthin **3** stains on treated wool fabrics 1, 3 and 48 h after a wash cycle.

Pretreatment	Lipase in Wash	Drying Temperature	SRI1 1 h	SRI2 1 h	SRI_{av} 1 h ± SD	SRI1 3 h	SRI2 3 h	SRI_{av} 3 h ± SD	SRI1 48 h	SRI2 48 h	SRI_{av} 48 h ± SD
Not pretreated	No	20 °C	55.61	51.11	53.36 ± 3.18	65.16	66.06	65.61 ± 0.64	77.49	76.62	77.06 ± 0.61
		1 h at 50 °C	64.90	60.23	62.57 ± 3.30	71.69	70.14	70.91 ± 1.10	80.17	77.40	78.78 ± 1.96
	Yes	20 °C	57.69	58.72	58.21 ± 0.73	64.78	68.96	66.87 ± 2.96	78.82	78.32	78.57 ± 0.35
		1 h at 50 °C	63.91	61.20	62.56 ± 1.91	68.54	70.76	69.65 ± 1.57	81.12	79.33	80.23 ± 1.27
Prewashed	No	20 °C	53.50	38.35	45.93 ± 10.71	67.13	63.41	65.27 ± 2.63	83.44	77.63	80.53 ± 4.11
		1 h at 50 °C	62.12	72.14	67.13 ± 7.08	69.43	80.04	74.73 ± 7.50	87.28	87.98	87.63 ± 0.50
	Yes	20 °C	57.11	63.93	60.52 ± 4.82	73.16	74.98	74.07 ± 1.29	83.62	85.91	84.77 ± 1.62
		1 h at 50 °C	71.87	63.68	67.78 ± 5.79	78.80	76.47	77.64 ± 1.65	87.73	86.76	87.25 ± 0.68
Prewashed with lipase	No	20 °C	72.27	68.83	70.55 ± 2.43	79.60	80.52	80.06 ± 0.64	90.58	90.40	90.49 ± 0.13
		1 h at 50 °C	72.53	71.51	72.02 ± 0.72	78.49	80.64	79.57 ± 1.52	90.80	93.48	92.14 ± 1.90
	Yes	20 °C	71.83	73.93	72.88 ± 1.48	78.97	83.12	81.05 ± 2.94	90.47	93.07	91.77 ± 1.84
		1 h at 50 °C	77.32	75.38	76.35 ± 1.37	82.11	84.59	83.35 ± 1.75	92.05	94.09	93.07 ± 1.44
Prewashed, rinsed with fabric softener	No	20 °C	64.90	67.54	66.22 ± 1.87	77.70	77.17	77.44 ± 0.37	89.51	85.32	87.41 ± 2.96
		1 h at 50 °C	78.48	74.25	76.36 ± 2.99	82.33	81.67	82.00 ± 0.47	88.63	89.15	88.89 ± 0.37
	Yes	20 °C	69.60	68.41	69.00 ± 0.84	78.06	75.74	76.90 ± 1.64	85.96	85.35	85.65 ± 0.43
		1 h at 50 °C	78.43	75.42	76.92 ± 2.13	84.19	84.10	84.15 ± 0.06	92.64	91.38	92.01 ± 0.90

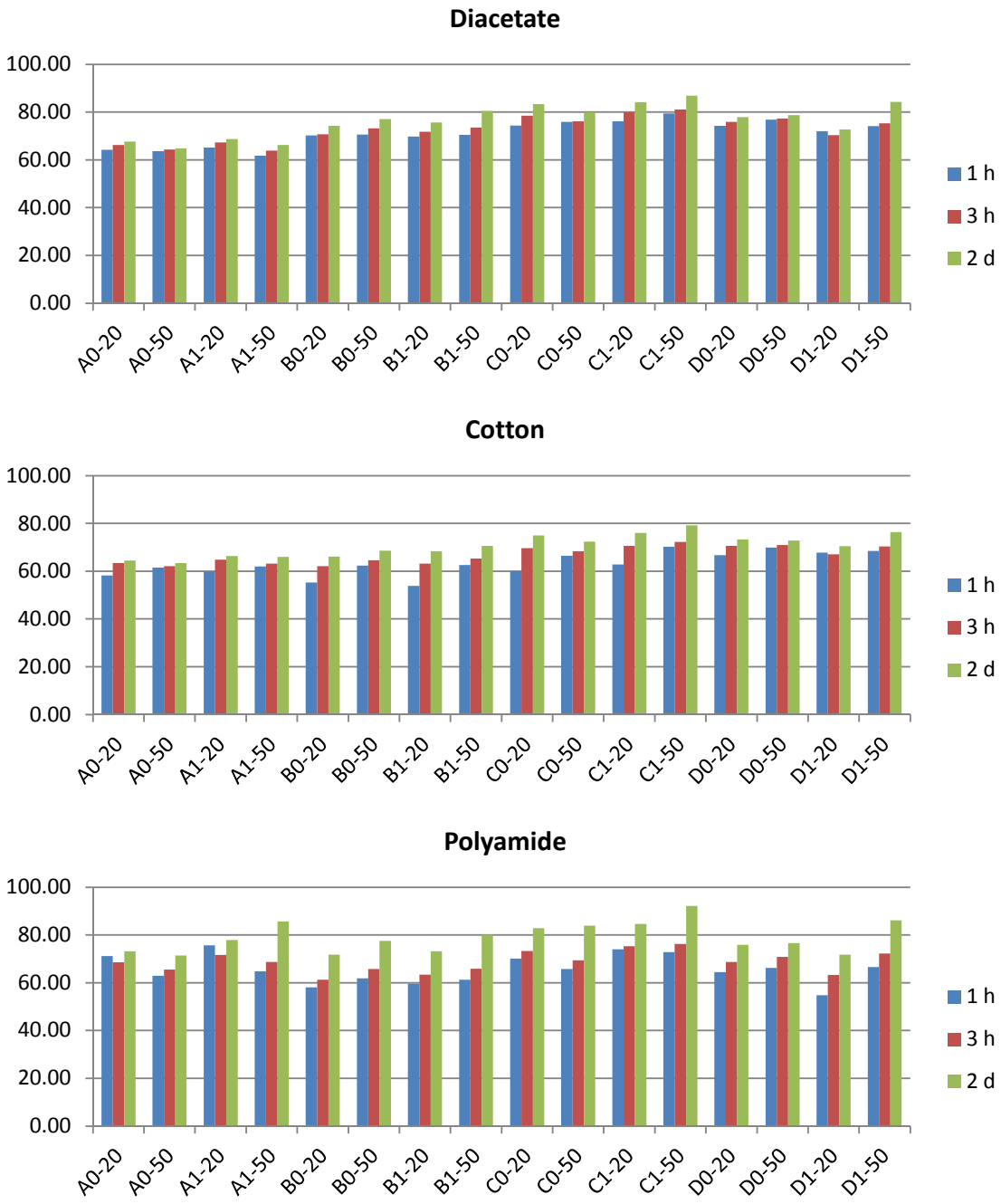

Figure C6 SRI values of capsanthin **3** stains on treated fabrics. Initial treatment code: (A) untreated, (B) prewashed, (C) prewashed with lipase, (D) prewashed with lipase and rinsed with fabric softener. Wash treatment code: (0) no lipase in wash, (1) lipase in wash. Drying treatment code: (20) dried at 20 °C, (50) dried at 50 °C for 1 h then dried at 20 °C.

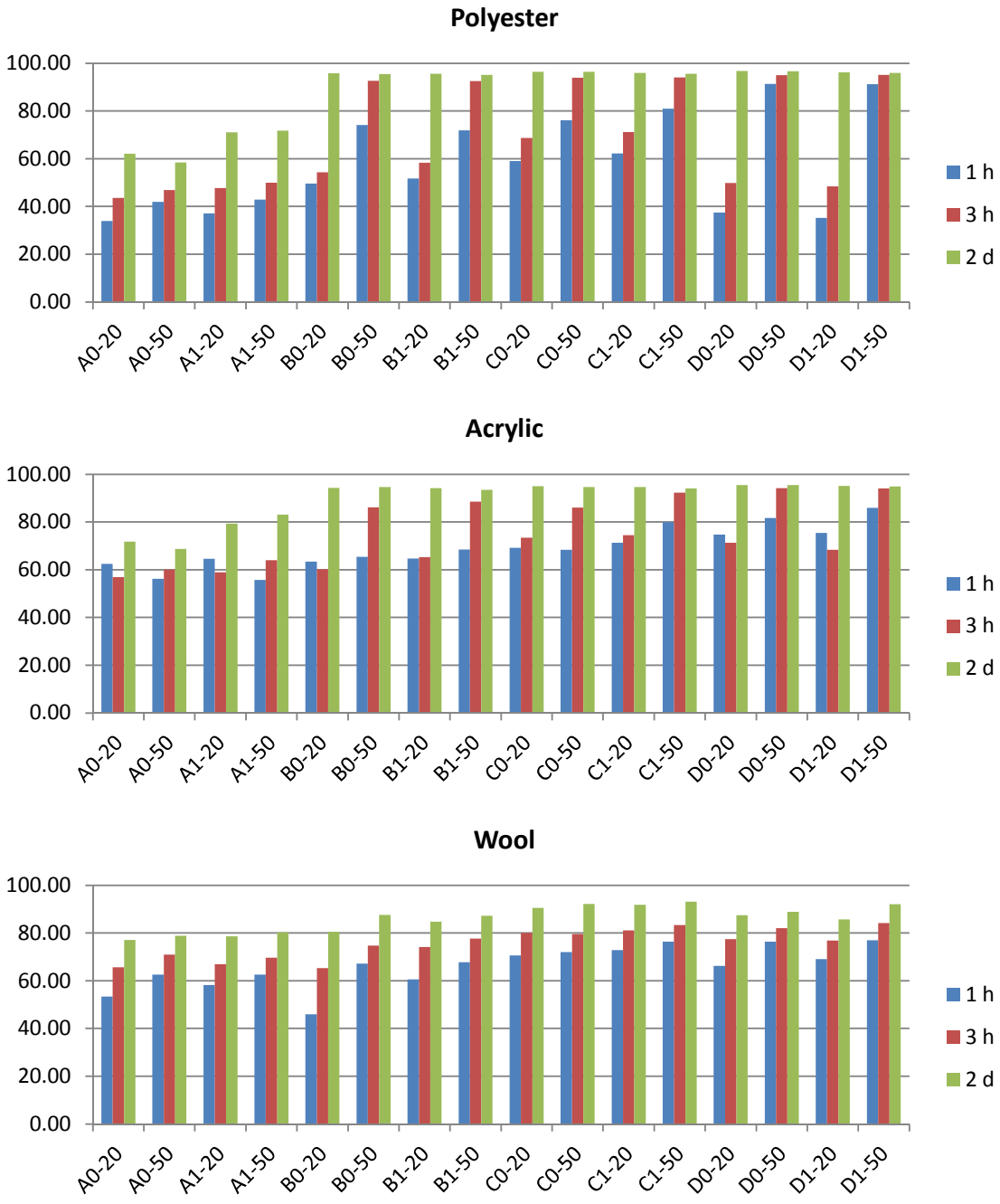

Figure C7 SRI values of capsanthin **3** stains on treated fabrics. Initial treatment code: (A) untreated, (B) prewashed, (C) prewashed with lipase, (D) prewashed with lipase and rinsed with fabric softener. Wash treatment code: (0) no lipase in wash, (1) lipase in wash. Drying treatment code: (20) dried at 20 °C, (50) dried at 50 °C for 1 h then dried at 20 °C.

Table C8 First order rate constants and extent of bleaching of β-carotene solutions in the presence of linoleic acid **10**, surfactant **53** (Tween 80) and untreated fabrics.

Fabric	First order bleaching rate constants (s^{-1})				Extent of bleaching (%)			
	$k_{obs}1$	$k_{obs}2$	$k_{obs}3$	k_{obs} ave ± SD	$x1$	$x2$	$x3$	$\bar{x}$
None	9.64×10^{-1}	1.33	1.23	1.17 ± 0.19	100	99	99	99 ± 1
Cotton	2.41×10^{-1}	5.52×10^{-2}	5.12×10^{-2}	$1.16 \pm 1.09 \times 10^{-1}$	39	48	43	43 ± 4
Polycotton	5.01×10^{-2}	6.68×10^{-2}	6.84×10^{-2}	$6.17 \pm 1.01 \times 10^{-2}$	40	47	47	45 ± 4
Polyester	4.12×10^{-1}	4.28×10^{-1}	4.91×10^{-1}	$4.44 \pm 0.41 \times 10^{-1}$	97	98	97	97 ± 1

Table C9 First order rate constants and extent of bleaching of β-carotene solutions in the presence of linoleic acid **10**, surfactant **54** (AE7) and untreated fabrics.

Fabric	First order bleaching rate constants (s^{-1})				Extent of bleaching (%)			
	$k_{obs}1$	$k_{obs}2$	$k_{obs}3$	k_{obs} ave ± SD	$x1$	$x2$	$x3$	$\bar{x}$
None	1.32	1.32	1.29	1.31 ± 0.02	98	99	98	98 ± 0
Cotton	1.09×10^{-1}	1.12×10^{-1}	1.61×10^{-1}	$1.27 \pm 0.29 \times 10^{-1}$	43	44	53	47 ± 5
Polycotton	2.03×10^{-1}	2.28×10^{-1}	2.57×10^{-1}	$2.29 \pm 0.27 \times 10^{-1}$	28	29	29	29 ± 1
Polyester	4.47×10^{-1}	5.68×10^{-1}	5.72×10^{-1}	$5.29 \pm 0.71 \times 10^{-1}$	94	96	94	95 ± 1

Table C10 First order rate constants and extent of bleaching of β-carotene solutions in the presence of oleic acid **33**, surfactant **53** (Tween 80) and untreated fabrics.

Fabric	First order bleaching rate constants (s^{-1})				Extent of bleaching (%)			
	$k_{obs}1$	$k_{obs}2$	$k_{obs}3$	k_{obs} ave ± SD	$x1$	$x2$	$x3$	$\bar{x}$
None	4.33×10^{-1}	4.40×10^{-1}	4.29×10^{-1}	$4.34 \pm 0.06 \times 10^{-1}$	98	97	97	97 ± 0
Cotton	1.54×10^{-1}	2.00×10^{-1}	1.70×10^{-1}	$1.75 \pm 0.24 \times 10^{-1}$	38	39	37	38 ± 1
Polycotton	1.07×10^{-1}	9.16×10^{-2}	7.50×10^{-2}	$9.13 \pm 1.62 \times 10^{-2}$	43	45	42	43 ± 1
Polyester	1.20×10^{-1}	9.26×10^{-2}	1.31×10^{-1}	$1.15 \pm 0.20 \times 10^{-1}$	64	88	88	80 ± 14

Table C11 First order rate constants and extent of bleaching of β-carotene solutions in the presence of linoleic acid **10**, surfactant **53** (Tween 80) and untreated fabrics (0.50 g).

Fabric	First order bleaching rate constants (s^{-1})				Extent of bleaching (%)			
	$k_{obs}1$	$k_{obs}2$	$k_{obs}3$	k_{obs} ave ± SD	$x1$	$x2$	$x3$	$\bar{x}$
None	8.94×10^{-1}	1.11	4.61×10^{-1}	$8.22 \pm 3.30 \times 10^{-1}$	99	99	98	98 ± 0
Cotton	1.64×10^{-1}	1.48×10^{-1}	1.42×10^{-1}	$1.52 \pm 0.12 \times 10^{-1}$	29	37	39	35 ± 5
Polycotton	1.59×10^{-1}	1.06×10^{-1}	3.71×10^{-2}	$1.00 \pm 0.61 \times 10^{-1}$	25	33	45	34 ± 10
Polyester	4.27×10^{-1}	2.89×10^{-1}	2.27×10^{-1}	$3.14 \pm 1.02 \times 10^{-1}$	97	96	92	95 ± 3

Appendix D

Table D1 Observed rate constants for the hydrolysis of triethyloxonium tetrafluoroborate.

Buffer	pH	Concentration (M)	k_{obs}1,2,3 (s^{-1})	k_{obs} (s^{-1})
0.1-1.0 M HCO_2H/HCO_2K 10% FB	2.57	0.100	1.57×10^{-3}	1.56×10^{-3}
			1.65×10^{-3}	
			1.94×10^{-3}	
		0.400	2.17×10^{-3}	
			1.36×10^{-3}	
			1.68×10^{-3}	
		0.700	2.15×10^{-3}	
			1.27×10^{-3}	
			1.32×10^{-3}	
		1.000	7.81×10^{-4}	
			1.67×10^{-3}	
			1.21×10^{-3}	
0.1-1.0 M HCO_2H/HCO_2K 90% FB	4.67	0.100	2.25×10^{-3}	1.46×10^{-3}
			1.32×10^{-3}	
			1.99×10^{-3}	
		0.400	2.14×10^{-3}	
			2.27×10^{-3}	
			1.24×10^{-3}	
		0.700	3.43×10^{-4}	
			1.75×10^{-3}	
			7.11×10^{-4}	
		1.000	1.51×10^{-3}	
			7.08×10^{-4}	
			1.32×10^{-3}	

0.05-0.5 M KH_2PO_4/K_2HPO_4 50% FB	6.67	0.050	2.77×10^{-3}	2.55×10^{-3}
			3.11×10^{-3}	
			2.39×10^{-3}	
		0.200	2.49×10^{-3}	
			2.29×10^{-3}	
			2.87×10^{-3}	
		0.350	1.67×10^{-3}	
			2.28×10^{-3}	
			1.68×10^{-3}	
		0.500	4.58×10^{-3}	
			2.25×10^{-3}	
			2.20×10^{-3}	
0.035-0.35 M KH_2PO_4/K_2HPO_4 90% FB	7.72	0.035	2.73×10^{-3}	2.71×10^{-3}
			2.82×10^{-3}	
			2.57×10^{-3}	
		0.140	3.07×10^{-3}	
			2.34×10^{-3}	
			2.83×10^{-3}	
		0.245	2.82×10^{-3}	
			2.10×10^{-3}	
			2.44×10^{-3}	
		0.350	3.86×10^{-3}	
			2.65×10^{-3}	
			2.26×10^{-3}	
0.025-0.25 M H_3PO_4/NaH_2PO_4 50% FB	1.99	0.025	1.28×10^{-3}	1.29×10^{-3}
			1.30×10^{-3}	
			1.28×10^{-3}	
		0.100	1.53×10^{-3}	
			1.24×10^{-3}	

			1.25×10^{-3}	
		0.175	1.21×10^{-3}	
			1.41×10^{-3}	
			1.33×10^{-3}	
		0.250	1.60×10^{-3}	
			8.32×10^{-4}	
			1.38×10^{-3}	
0.025-0.25 M H_3PO_4/NaH_2PO_4 90% FB	3.01	0.025	1.28×10^{-3}	1.32×10^{-3}
			1.30×10^{-3}	
			1.38×10^{-3}	
		0.100	1.35×10^{-3}	
			1.15×10^{-3}	
			1.17×10^{-3}	
		0.175	1.18×10^{-3}	
			1.71×10^{-3}	
			1.68×10^{-3}	
		0.250	1.26×10^{-3}	
			1.22×10^{-3}	
			1.12×10^{-3}	
0.025-0.25 M CH_3CO_2H/CH_3CO_2Na 50% FB	4.52	0.025	2.07×10^{-3}	1.32×10^{-3}
			2.15×10^{-3}	
			2.00×10^{-3}	
		0.100	9.27×10^{-4}	
			1.01×10^{-3}	
			9.73×10^{-4}	
		0.175	9.25×10^{-4}	
			9.64×10^{-4}	
			1.08×10^{-3}	
		0.250	1.20×10^{-3}	

			1.26×10^{-3}	
			1.24×10^{-3}	
0.025-0.25 M CH_3CO_2H/CH_3CO_2Na 90% FB	5.20	0.025	2.28×10^{-3}	1.55×10^{-3}
			2.50×10^{-3}	
			2.47×10^{-3}	
		0.100	1.03×10^{-3}	
			9.93×10^{-4}	
			1.09×10^{-3}	
		0.175	1.25×10^{-3}	
			1.22×10^{-3}	
			1.44×10^{-3}	
		0.250	1.46×10^{-3}	
			1.36×10^{-3}	
			1.46×10^{-3}	
0.05-0.50 M NaH_2PO_4/Na_2HPO_4 50% FB	6.61	0.050	1.90×10^{-3}	3.37×10^{-3}
			1.89×10^{-3}	
			1.88×10^{-4}	
		0.200	3.85×10^{-3}	
			3.25×10^{-4}	
			1.93×10^{-3}	
		0.350	4.13×10^{-3}	
			4.86×10^{-3}	
			4.92×10^{-3}	
		0.500	5.93×10^{-3}	
			5.89×10^{-3}	
			4.60×10^{-3}	
0.035-0.35 M NaH_2PO_4/Na_2HPO_4 90% FB	7.40	0.035	1.48×10^{-3}	5.52×10^{-3}
			1.67×10^{-3}	

			1.81×10^{-3}	
		0.140	4.70×10^{-3}	
			4.32×10^{-3}	
			2.41×10^{-3}	
		0.245	1.04×10^{-2}	
			4.78×10^{-3}	
			5.04×10^{-3}	
		0.350	7.11×10^{-3}	
			7.31×10^{-3}	
			1.53×10^{-2}	
0.02-0.2 M Tricine/Tricine$^-$ 90% FB	8.64	0.080	1.70×10^{-3}	1.89×10^{-3}
			1.67×10^{-3}	
			1.60×10^{-3}	
		0.140	1.80×10^{-3}	
			1.92×10^{-3}	
			1.71×10^{-3}	
		0.200	2.21×10^{-3}	
			2.18×10^{-3}	
			2.20×10^{-3}	
0.05-0.50 M $NaHCO_3$/Na_2CO3 50% FB	10.30	0.050	5.80×10^{-3}	2.57×10^{-2}
			1.25×10^{-2}	
			1.11×10^{-2}	
		0.200	1.15×10^{-2}	
			1.02×10^{-2}	
			8.96×10^{-3}	
		0.350	9.47×10^{-3}	
			1.27×10^{-2}	
			1.20×10^{-2}	
		0.500	2.69×10^{-2}	

			5.75×10^{-2}	
			2.46×10^{-2}	
0.035-0.35 M $NaHCO_3/Na_2CO_3$ 90% FB	11.30	0.035	7.78×10^{-3}	2.82×10^{-2}
			1.09×10^{-2}	
			1.12×10^{-2}	
		0.140	5.90×10^{-3}	
			5.60×10^{-3}	
			6.15×10^{-3}	
		0.245	1.91×10^{-2}	
			1.25×10^{-2}	
			1.27×10^{-2}	
		0.350	2.45×10^{-2}	
			2.91×10^{-2}	
			3.09×10^{-2}	

Table D2 Observed rate constants for the hydrolysis of triethyloxonium tetrafluoroborate.

Buffer	pH	Concentration (M)	$k_{obs}1,2,3$ (s^{-1})	k_{obs} (s^{-1})
0.0125-0.0500 M H_3PO_4/NaH_2PO_4 50% FB	2.60	0.025	1.64×10^{-3}	1.02×10^{-3}
			2.34×10^{-3}	
			1.06×10^{-3}	
		0.100	1.14×10^{-3}	
			8.90×10^{-4}	
			1.01×10^{-3}	
0.0125-0.0500 M H_3PO_4/NaH_2PO_4 90% FB	3.37	0.025	1.31×10^{-3}	1.66×10^{-3}
			1.29×10^{-3}	
			9.92×10^{-4}	
		0.100	1.57×10^{-3}	
			1.70×10^{-3}	
			1.71×10^{-3}	
		0.175	1.79×10^{-3}	
			1.49×10^{-2}	
			1.59×10^{-3}	
		0.250	1.70×10^{-3}	
			3.36×10^{-3}	
			1.65×10^{-3}	
0.0125-0.0500M CH_3CO_2H/CH_3CO_2Na 50% FB	5.24	0.025	2.37×10^{-3}	3.16×10^{-3}
			2.05×10^{-3}	
			1.98×10^{-3}	
		0.100	3.00×10^{-3}	
			3.27×10^{-3}	
			3.20×10^{-3}	
0.0125-0.0500 M CH_3CO_2H/CH_3CO_2Na	5.48	0.025	2.38×10^{-3}	4.42×10^{-3}

90% FB				
			2.34×10^{-3}	
			2.40×10^{-3}	
		0.100	4.53×10^{-3}	
			5.09×10^{-3}	
			3.63×10^{-3}	
0.025 M NaH_2PO_4/Na_2HPO_4 50% FB	7.57	0.050	5.06×10^{-3}	5.35×10^{-3}
			5.55×10^{-3}	
			5.44×10^{-3}	
0.0175 M NaH_2PO_4/Na_2HPO_4 90% FB	7.59	0.0350	6.05×10^{-3}	6.06×10^{-3}
			6.02×10^{-3}	
			6.11×10^{-3}	
0.025-0.100 M $NaHCO_3/Na_2CO3$ 50% FB	10.18	0.050	1.06×10^{-2}	1.75×10^{-2}
			1.12×10^{-2}	
			1.17×10^{-2}	
		0.200	1.97×10^{-2}	
			1.57×10^{-2}	
			1.72×10^{-2}	
0.0175-0.0700 M $NaHCO_3/Na_2CO_3$ 90% FB	11.17	0.035	1.26×10^{-2}	2.15×10^{-2}
			1.26×10^{-2}	
			1.28×10^{-2}	
		0.140	2.96×10^{-2}	
			1.75×10^{-2}	
			1.74×10^{-2}	